A Pd-catalysed Decarboxylative Route to Functionalized Nitrogen Heterocycles

Jiaxin Han

A thesis submitted in partial fulfilment of the requirements for the degree of
Doctor of Philosophy

The University of Sheffield
Department of chemistry

July 2023

Abstract

This thesis describes the synthesis of a pool of 5- and 6-membered sp^3-rich *N*-heterocyclic compounds bearing orthogonal functionality via a Pd-catalysed decarboxylative allylation strategy. An easily prepared trimethylene carbamate bearing different substituents at nitrogen reacted with Pd-catalysts for the *in situ* generation of a 1,4-dipole reagent that can react with α-fluoro-β-keto esters and sulfonium ylides to provide piperidines and pyrrolidines after cyclization.

The use of chiral catalysts or chiral auxiliaries provided a platform to access enantiomerically enriched products. In addition, we successfully employed stereochemical models in order to explain the stereochemical outcome in each case.

The potential of their downstream functionalization was fully showcased, and synthetic value was also proved by gram-scale reactions.

- Proposed sequence to enantioenriched 3-fluoropiperidines
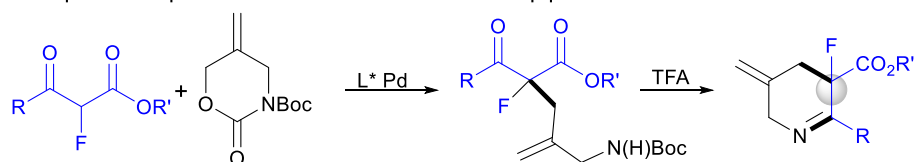
- Proposed sequence to pyrrolidines
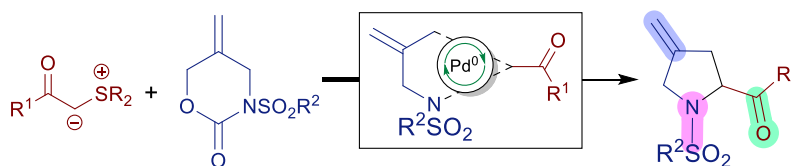
Acknowledgement

I enjoy the 'tough' academic period during which I become more independent, stronger, and never flinch from facing up to trouble. This period allows me to have a better understanding of life. With time going, I gradually realized that besides the praise from outside, I need to pursue something meaningful in the corner to realize my value and inner peace. Although an individual is always negligible, he can still contribute to his academic area someday who knows.

First, I will show sincere gratitude to my supervisor: Prof. Joseph. P. A. Harrity. It is under your guidance and strict criteria that I can enjoy every thrilling moment of a new discovery as a young chemist. During this period, I grasped not only the knowledge, but also presentation and writing skills under your assistance. To be honest, I have never seen such a patient professor as you especially when I made many silly mistakes. Besides, I am grateful that you continuously provided me with continuous opportunities of 'showing' my project to other professors. My gratitude is out of expression!

Wenzheng: You are a hardworking and optimistic man. When I was depressed, you were always the first person to encourage me and offered some advice which was usually useful to me. It was you who can always feel my happiness and sadness. I know how much effort you endeavoured for becoming an outstanding chemist. I hope you can always keep motivated and realize your dream in the future.

Fernando: I have never seen such a helpful person. Your experimental suggestions were always helpful which made my experiments more efficient. Besides, you always encouraged me like an elder brother (although we are almost at the same age) when I was puzzled and taught me everything unknown. Anyway, good luck with your future.

Larry: Even when you were busy with your thesis, you helped me purify my compounds. You shared your experience without hesitation.

Dan: Thanks for your contributions to our lab and coordinated the lab well. When the lab was out of use, you were still able to ensure everybody can work as normal.

Other group members: Thanks for your encouragement and contribution to our lab.

Yunsong, Xiaotian, Wenhao and Kavya: Thanks for the experience of becoming a mentor. The coolest thing was I can feel your amazing improvement even before you knew. You were hardworking and worked late everyday like PhD. Your efforts deserved the ideal results and I was proud of all of you.

Dad and Mom: The most significant families in my life. I still remember during childhood, you always brought me to your lab and I recognized many amazing things (microscope, HPLC, some vials containing unknown compounds, etc.). From that time, I determined to become an academic. Mom, you are a hardworking person: in the last century, English was not popular and you learn it just from a heavy dictionary and video. Until now, you still sometimes stayed up late to work, which was out of imagination because you are not as young as before. You always tell me to be strict on my academic life and keep learning no matter how elder you are. I hope one day, you can be proud of me just like I take pride in you. When I was sad, Dad just told me 'This is your life' and I need to grow up to become an independent person. Thanks for providing such a harmonious family environment and numerous cares during my life.

Abbreviations

ACN	acetonitrile		MeOH	methanol
Boc	*tert*-butoxycarbonyl		min	minutes
^{n}Bu	*n*-butyl		mol	moles
^{t}Bu	*tert*-butyl		Ms	methanesulfonyl
dba	dibenzylideneacetone		Ns	nitrobenzenesulfonyl
DBU	1,8-Diazabicyclo[5.4.0]undec-7-ene		Nu	generic nucleophile
DIPEA	N,N-Diisopropylethylamine		Ph	phenyl
DMAP	dimethylaminopyridine		PHOX	Phosphinooxazolines
DMSO	dimethyl sulfoxide		^{i}Pr	isopropyl
dr	diastereomeric ratio		R	generic carbon-containing group
EDG	electron donating group		rt	room temperature
ee	enantiomeric excess		TEA	triethylamine
eq	equivalent(s)		THF	tetrahydrofuran
er	enantiomeric ratio		TFA	trifluoroacetic acid
et al.	*et alia*		t	time
Et$_2$O	diethyl ether		Ts	4-methylbenzenesulfonyl
EWG	electron withdrawing group			
FCC	flash column chromatography			
h	hour(s)			
HRMS	high resolution mass spectrometry			
Hz	Hertz			
J	coupling constant			
LG	leaving group			
M	molar			

Contents

Chapter 1: Introduction

1.0 The Tsuji-Trost reaction

Transition-metal catalysed reactions have been an active area in organic chemistry because they provide an accessible platform for the elaboration of complex compounds, typically involving carbon-carbon bond or carbon-heteroatom bond formation.[1] It is noteworthy that these methods often exploit readily available substrates via an atom-economic route.[2]

The synthetic value of transition-metal catalysed allylic alkylation reactions (Scheme 1.0.1) has been known since the last century because of relatively high stereoselectivity and chemo selectivity compared to non-transition metal catalysed process. The overall transformation can be promoted by a range of transition metal catalysts, e.g., Pd, Ni, Pt, Rh, Fe, Ru, Mo, Cu and W. For example, Ni catalysed allylic alkylation has mainly involved hard nucleophiles (Grignard reagent); Ir and W catalysts as a complementary catalyst for Pd, substitutions dominate in more substituted allylic terminal. Overall, other transition metal catalysts have been less explored for their induction of asymmetry and synthetic value in comparison with Pd catalytic system. [3]
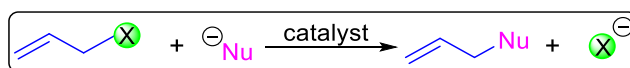
Scheme 1.0.1 General route for a transition-metal catalysed allylic reaction.

Transition metal complexes based on Pd offer an efficient and reliable means for the asymmetric allylic alkylation (AAA) reaction, and this has largely been established by the Trost group. Indeed, very few transition-metal catalysts can form such a variety of carbon-heteroatom bonds (Figure 1.0.1).[4]

Nu=CH$_3$, SO$_2^t$Bu, NH$_2$, halide, OH, PPh$_2$
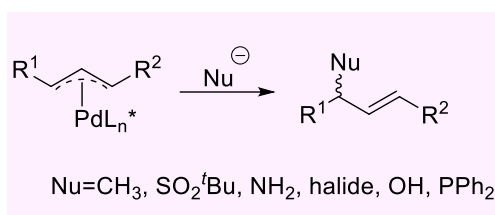
Figure 1.0.1 Examples of Pd-catalysed AAA.

In the case of the Trost reaction, the commonly agreed mechanism is shown in Figure 1.0.2: i) the Pd(0)-ligand complex associates with olefin moiety to form π-complex; ii) Pd(0) undergoes oxidative insertion into allylic C-X bond leading to ionization. Substitution for X by Pd occurs with inversion and in concert with nucleophilic attack; iii) finally, new product is delivered and Pd(0) is regenerated. Typically, leaving groups (X) such as OAc OCO$_2$R, OPO(OR)$_2$, halides are chosen because they participate efficiently in the alkylation process.[5]
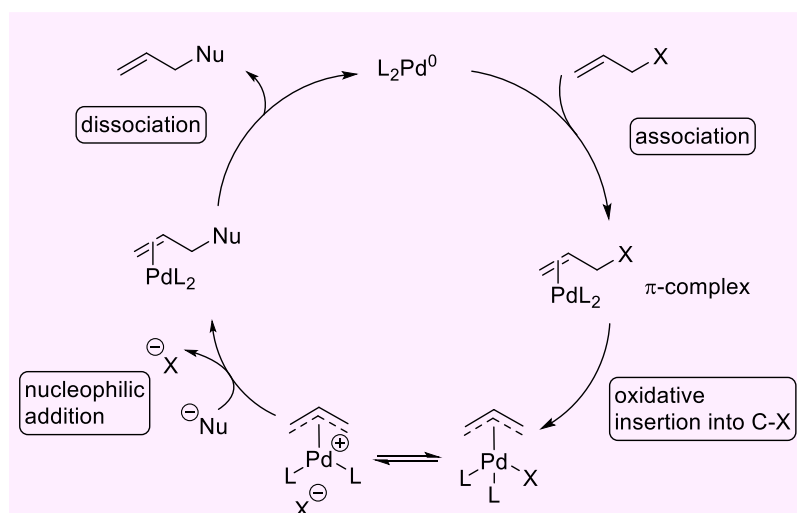
Figure 1.0.2 Trost alkylation reaction mechanism.

It is noteworthy that the mechanism of the nucleophilic addition step is determined by the nature of the nucleophile's pK_a.[3] An inner-sphere nucleophilic attack is the most common process for hard nucleophiles (pK_a >25) which attach to the Pd directly followed by reductive elimination. On the other hand, the reaction involving soft nucleophiles (pK_a <25) proceeds via a different course:

nucleophilic attack is outside of Pd and on the face of π-allyl moiety opposite of Pd-ligand complex, therefore, the stereochemistry of the allylation product is retained overall (Scheme 1.0.2).[4]

a) **Hard** nucleophile AAA (**net inversion**)

Inner sphere

b) **Soft** nucleophile AAA (**net retention**)
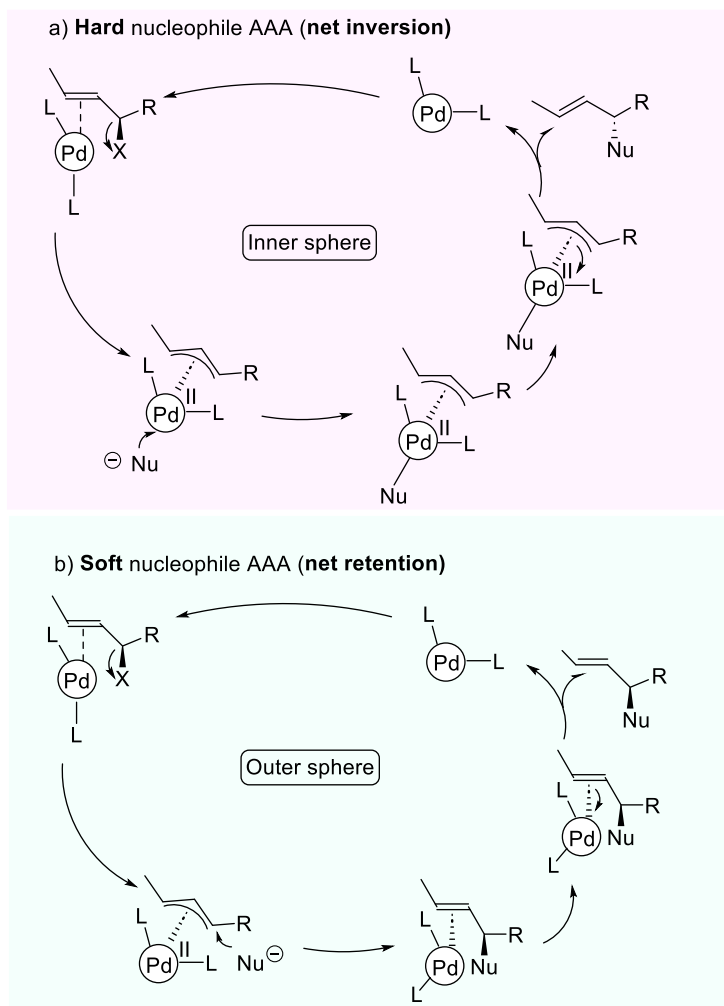
Outer sphere

Scheme 1.0.2 Introduction of different stereochemistry during outer-sphere and inner-sphere mechanisms.

1,3-Symmetrically substituted substrates listed in Figure 1.0.3 whose allylic intermediate is enantiotopic have been prevalent in Pd-AAA reactions since its introduction, because the allyl termini are chemical equivalent so that the enantiocontrol is transformed to regioselectivity of enantiotopic carbon of the allyl terminus.[6]
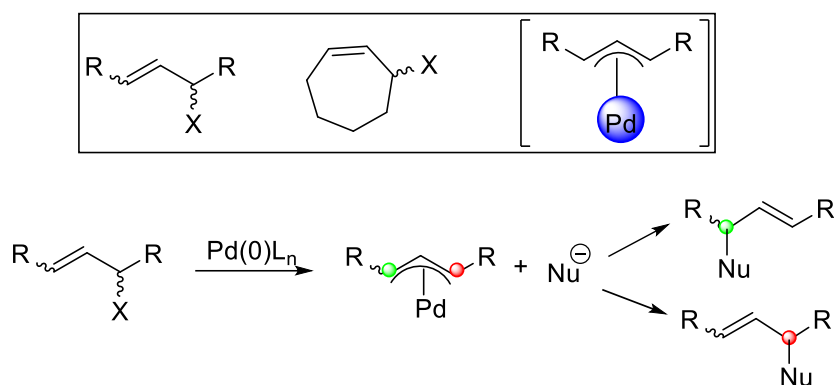
Figure 1.0.3 1,3-Symmetrically substituted substrates.

In contrast, 1-monosubstituted substrates which have no symmetry plane are much more challenging. The nature of the nucleophilic addition step is quite complex: here, the two terminal carbons are different and different factors will influence the reaction regioselectivity (Scheme 1.0.3). Nucleophilic attack towards the primary carbon stems from steric influences (path b), which is highlighted by bulkier nucleophile. For example, methyl benzenesulfonylacetate prefers to attack on the least substituted allyl terminus due to the ibduction of bulky sulfone moiety compared to sterically less demanding dimethyl malonate; in addition, there is an exclusive attack at exocyclic position for five- and seven- member rings in terms of less sterically congested approach. On the other hand, considering electronic effects, reaction at the secondary carbon can be more favourable (path a and c).[6]
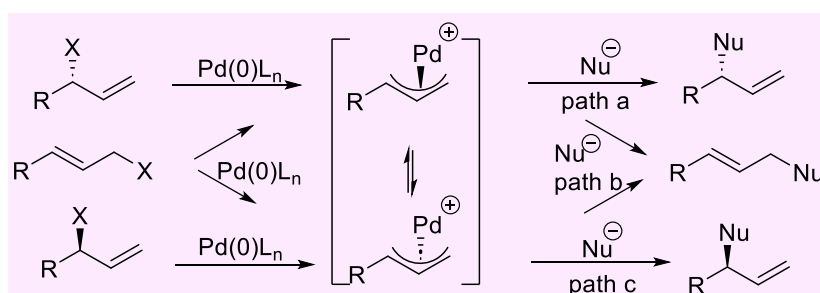
Scheme 1.0.3 1-Monosubstituted π-allyl intermediate.

1.1 Pd π-allyl complexes in decarboxylative asymmetric reactions

Since Tsuji and Saegusa reported the Pd-catalysed decarboxylative asymmetric allylic alkylation (DAAA) (Scheme 1.1.1) forty years ago, this process has become an active area of research and has been widely utilized as a powerful strategy for the enantioselective formation of heterocyclic compounds.[7] Many of the derivatives arising from these transformations have played a pivotal role in lead-like drug development.[8]
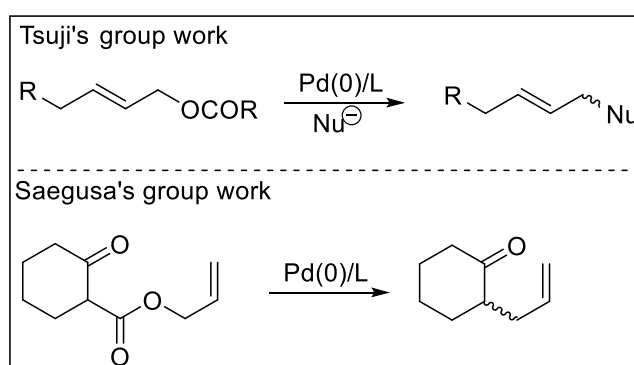
Scheme 1.1.1 First two examples of DAAA developed by Tsuji's and Saegusa's groups.

In general, there have been three prevalent kinds of Pd π-allyl complex intermediates involved in DAAA that have been exploited in heterocycle formation and these are shown in Figure 1.1.1.[9]
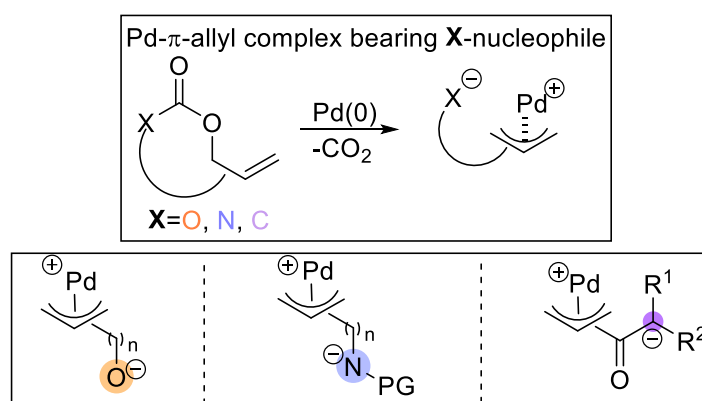
Figure 1.1.1 Common Pd π-allyl complex intermediates in decarboxylative asymmetric reactions.

The distinctive merits of decarboxylative asymmetric reactions lie in the fact that 1) carbon dioxide is the only by-product; 2) the substrates are readily available; 3) the reaction conditions are mild; 4) the π-allyl intermediate is readily captured by its partner.

1.1.1 Dipole reagents bearing a *N*-nucleophile

Our group designed a precursor to a Pd π–allyl complex bearing a *N*-nucleophile, and this has been widely used in DAAA since 2015.[10] We commenced our DAAA studies in the enantioselective synthesis of piperidine analogues. Spirocyclic compounds were successfully synthesized in a two-step sequence under Pd catalysis with a series of chiral phosphoramidite ligands (Scheme 1.1.2). We also found enantioselectivity was sensitive to temperature: the best enantiocontrols for different substrate **1** was obtained under different temperatures. This finding was helpful in future enantioselectivity investigations. The product was endowed with high functionality by downstream application and protentional biological significance (acetyl-CoA carboxylase inhibitor).[10a]
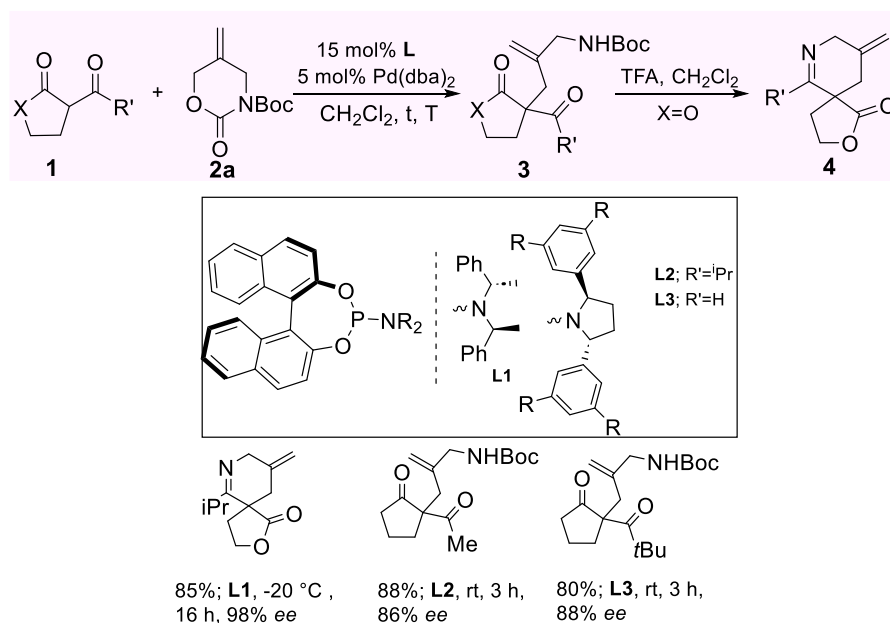
Scheme 1.1.2 Our **first** example of asymmetric synthesis of piperidine **4**.

In addition, the exploitation of the DAAA strategy for the synthesis of constrained peptides proved the robustness and versatility of carbamate **2a** again.[10b] The incorporation of azlactone **5** as a nucleophilic reagent to Pd dipole reagent derived from **2a** allowed the assembly of lactam monomer readily. The route showed good generality and lactam mimics were generated with both polar and hydrophobic side chains (Scheme 1.1.3).
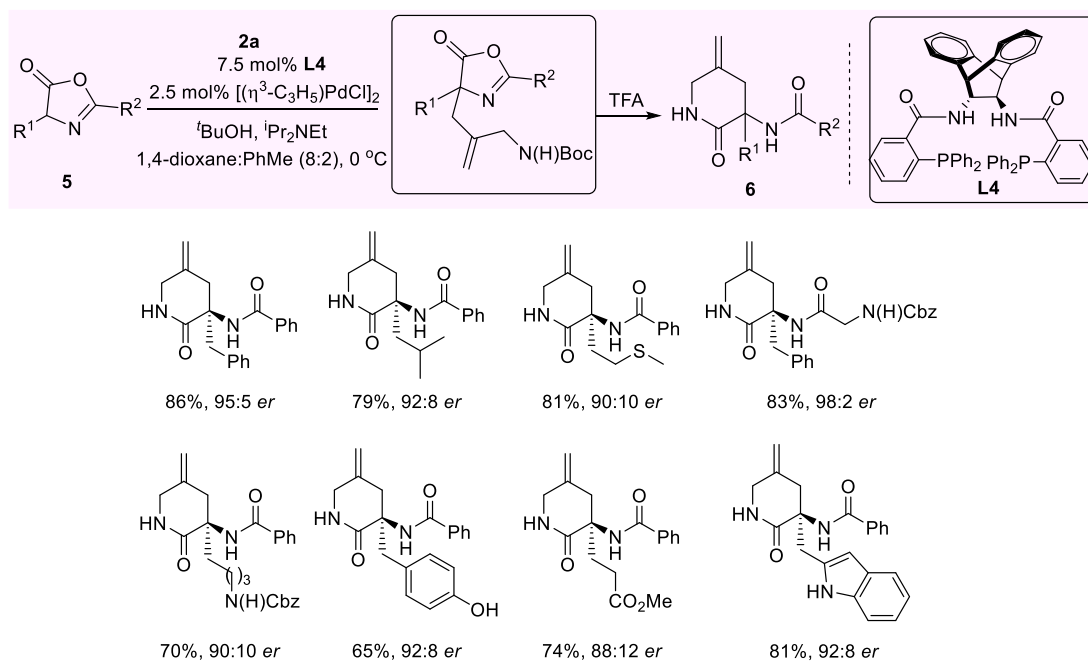
Scheme 1.1.3 Our asymmetric synthesis of constrained lactams **6**.

To prove the versatility of asymmetric reaction conditions, for example, nucleophilic reagent 1-substitued-2-indanone **7** was employed to in situ Pd zwitterion in the enantioselective allylation /condensation consequence for the construction of another series of tricyclic compounds **8** (Scheme 1.1.4) and the generality of this approach is in progress in our group.[10c]
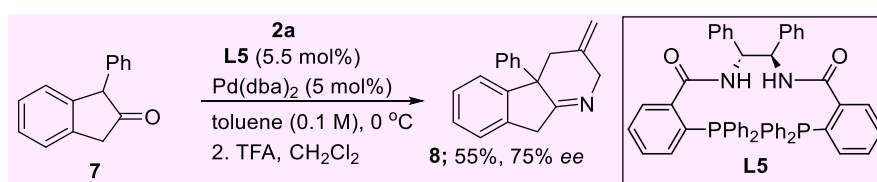
Scheme 1.1.4 Our asymmetric synthesis of tricyclic compounds.

Other researchers have used a similar carbamate in an effort to expand the scope of decarboxylative stereoselective reactions for the synthesis of heterocyclic compounds. For example, Guo's group reported a decarboxylative cyclization reaction for the synthesis of spirodihydropyrazolones (Scheme 1.1.5).[11] Unfortunately, they failed to uncover an asymmetric variant after screening chiral ligands, but they proved the yield and diastereoselectivity of the reaction was not influenced by the position and electronic effects of substituents on the aromatic group (R^1 and R^2) of **9** when using Xantphos ligand **L6**. Finally, spirodihydropyrazolone **10** was endowed with excellent functionality by downstream derivatization, affording pharmacologically active spirodihydroprazolone analogues.
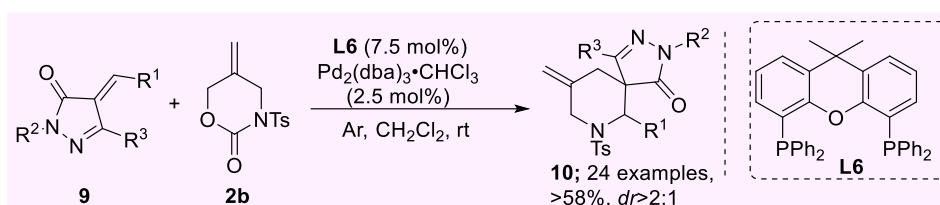
Scheme 1.1.5 Guo's work on the diastereoselective synthesis of spirodihydropyrazolone **10**.

Carbamate **2b** was also exploited by Yuan and co-workers in a synthetic strategy for the synthesis of enantiopure 2-piperidones **12** (Scheme 1.1.6).[12] An array of such products was accessed using phosphoramidite ligand **L7** with high yield and excellent enantioselectivity. It was noteworthy that the formation of final product **12** proceeded via intramolecular aminolysis from precursor **12'**.
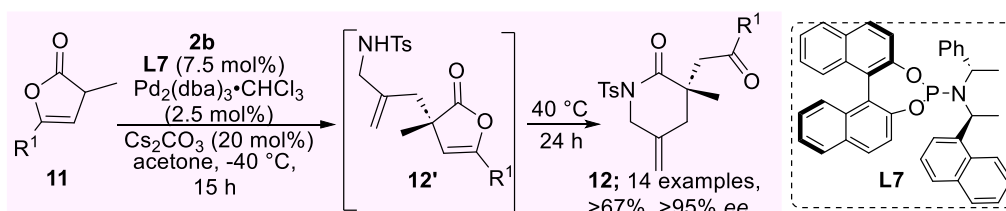
Scheme 1.1.6 Yuan's work on the asymmetric synthesis of 2-piperidones **12**.

A related dipolar Pd-complex aza-*ortho*-xylene **13'** is a versatile intermediate that can be generated from vinyl benzoxazinanone **13** (Figure 1.1.2).[13] The key carbamate **13** can be accessed in a 5-step sequence from *ortho*-amino benzyl alcohol (Scheme 1.1.7). Each step proceeded smoothly in the course of merely 2-4 hours with full conversion from commercial available reactants, alebit the yield has been unknown based on literature.[14]
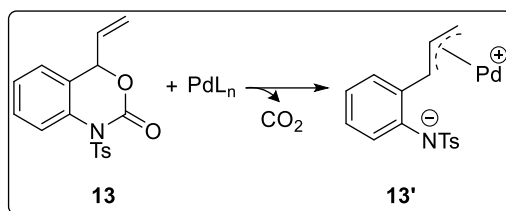
Figure 1.1.2 Formation of 1,4-dipole reagent **13.**
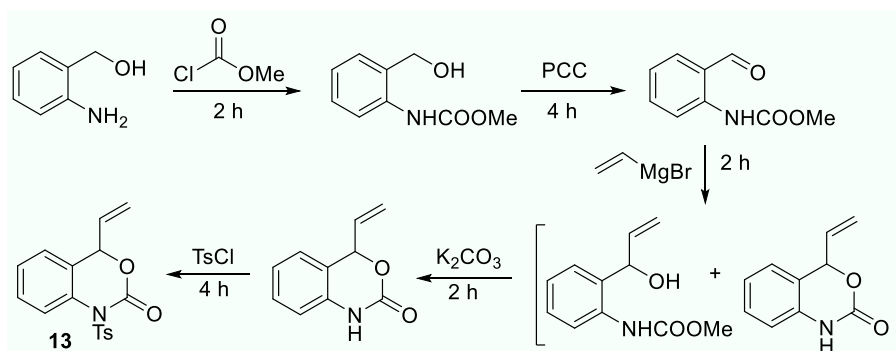
Scheme 1.1.7 Synthesis of **13** with full conversion in each step.

Huang's group unveiled the asymmetric decarboxylative synthesis of spirobenzoxazine analogues using **14** as a dipole reagent precursor, and 4,5-diones as its partner.[15] Under the optimized conditions, a broad range of substrates bearing different functional groups successfully underwent cyclization with up to 72% yield and 96% *ee* (Scheme 1.1.8). Additionally, the nucleus of benzo[*d*][1,3]oxazine highlighted in Scheme 1.1.8 has anticancer bioactivity.[16]
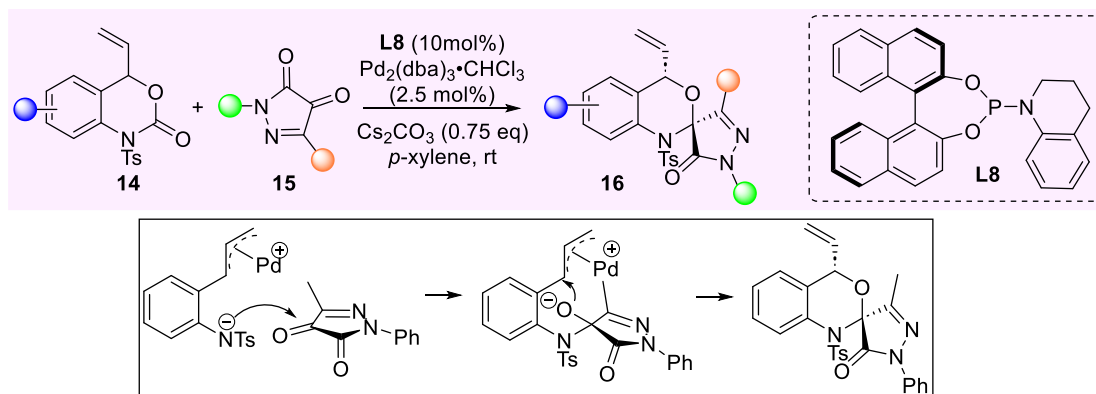
Scheme 1.1.8 Huang's work on the asymmetric synthesis of spirobenzoxazine **16**.

Shi's group reported the first example of an asymmetric decarboxylative synthesis of the tryptanthrin motif **19** which is widely found in natural alkaloids.[17] The combination of **17** bearing a free N-H and isatin **18** produced a panel of enantioenriched tryptanthrin skeleta **19** with high yields (Scheme 1.1.9). Most strikingly, the enantioselectivity is determined during the C-N bond forming step in this case, as opposed to addition to the C=O bond, as described in Scheme 1.1.8.
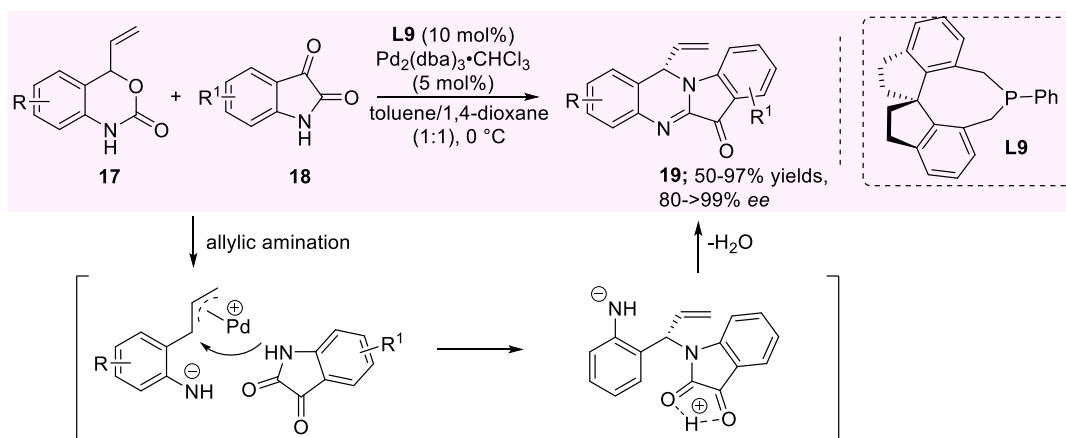
Scheme 1.1.9 Shi's work on the asymmetric synthesis of tryptanthrin **19**.

1.1.2 Dipole reagents bearing an *O*-nucleophile.

Oxygen containing heterocycles can be produced by the generation of analogous *O*-based dipolar reagents. Towards this end, carbonate **20** was accessed in a three-step sequence with 64% overall yield, thus delivering a useful precursor for the formation of the key Pd-zwitterionic intermediate (Scheme 1.1.10).[18]
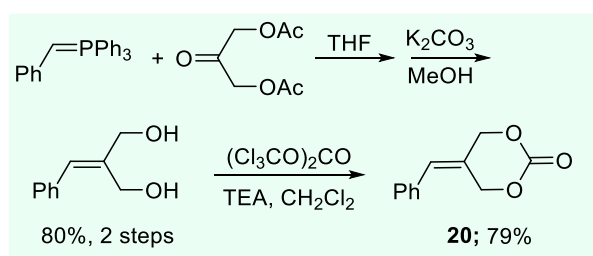
Scheme 1.1.10 Total synthesis of carbonate **20.**

Pd-catalysed decarboxylative cyclization of carbonate **20**, and reaction with isocyanate **21** was achieved by Hayashi's group in 2011.[18a] A proposed mechanism is illustrated below: Pd π-allyl carbonate **I** is delivered by oxidative addition of allyl carbonate **20** to Pd(0). Decarboxylation occurs to form Pd π-allyl alkoxide **II** as a nucleophile attacking isocyanate **21**. Palladacyclobutane **IV** is accessed as a consequence of nucleophilic attack from the nitrogen atom of **21** to the central carbon of Pd π-allyl component of intermediate **III** via 5-*exo*-trig pathway. Reductive elimination released final product **22** and regenerated Pd(0). On the other hand, **23** is obtained by a common ring condensation through nucleophilic attack towards the terminal carbon of Pd π-allyl moiety followed by reductive elimination.

They used a Pd/PAr$_3$ catalyst system and found different triarylphosphine ligands with different electronic nature gave different selectivity for formation of compounds **22** and **23** (Table 1.1.1). The complicated reactivity difference can be explained as follows. Due to electron-withdrawing nature of ligand, the reaction pathway is more kinetically controlled and HOMO of **21** overlaps better with π*-derived empty orbital of Pd π-allyl moiety, which can facilitate the formation of **22**.

Oppositely, under the use of electron-rich phosphine ligands, the nucleophilic attack will be slow, leading to a thermodynamically more favourable product **23**. Overall, the influence of electronic nature of phosphine ligands can be briefly concluded to kinetic control and orbital interaction.[18b-18c]

Table 1.1.1 Ligand effects on the reaction of carbonate **20**.
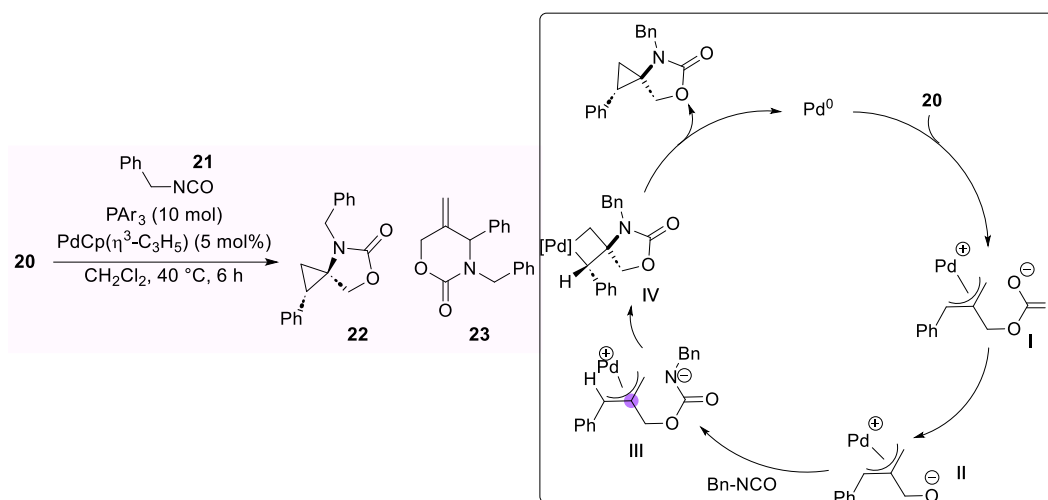
Entry	Ar	Yield (%)	22/23	*dr* of 22
1	4-MeOC$_6$H$_4$	0%	--	--
2	Ph	27%	< 1/99	--
3	4-FC$_6$H$_4$	41%	34/66	>99/1
4	4-CF$_3$C$_6$H$_4$ (**L10**)	84%	92/8	96/4

The first asymmetric decarboxylative reaction under Pd catalysis between carbonate **24** and trisubstituted electron-deficient olefin **25** was reported by Guo's group.[19] The derived chiral spirocyclic tetrahydropyran skeleton **26** was accessed in excellent enantioselectivity (up to 99% *ee*), (Scheme 1.1.11) and with useful functionality including hydroboration, epoxidation, etc.
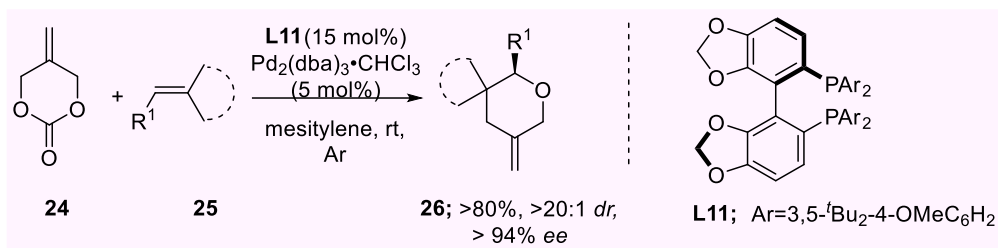
Scheme 1.1.11 Guo's work on the asymmetric synthesis of spirocyclic tetrahydropyrans **26**.

1.1.3 Dipole reagents bearing a *C*-nucleophile.

Hayashi's group introduced a new zwitterionic precursor **27** in 2017, which has become a versatile four-carbon motif in asymmetric decarboxylative reactions. Lactone **27** was prepared from readily available substrates in two-steps with high yield (Scheme 1.1.12).[20]
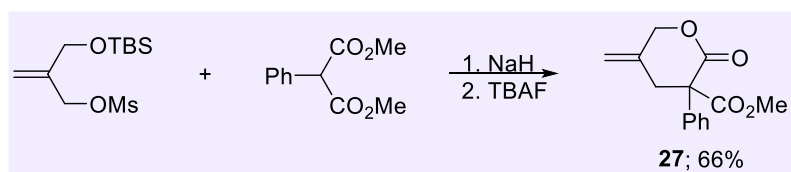
Scheme 1.1.12 Synthesis of lactone **27**.

Lactone **28** was combined with nitrones **29** in the presence of a Pd catalyst and the reaction proceed smoothly. The tolerance of substrate functional groups was high, besides, high yield and enantioselectivity were obtained under the optimal catalytic conditions (Scheme 1.1.13a). In addition, azomethine ylide **31** was applied as a surrogate of **29** and high diastereocontrol was obtained under the employment of achiral phosphoramidite ligand **L13** (Scheme 1.1.13b).[20]
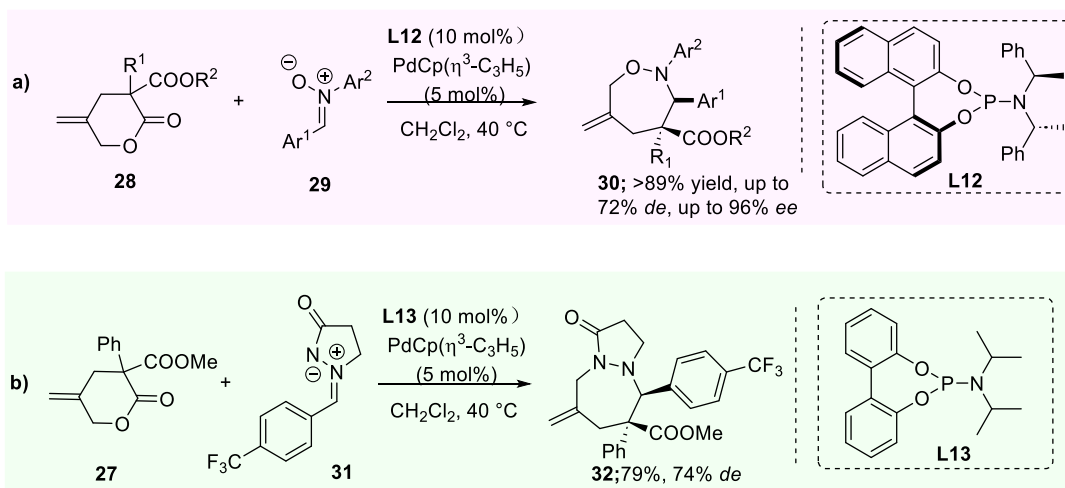
Scheme 1.1.13 Hayashi's work on the asymmetric synthesis of **30** and diastereoselective synthesis of **32**.

Hayashi's group also constructed alternative seven-membered carbo- and heterocycles under the employment of **27** and three-membered ring containing partners: dicyanocyclopropane **33** and aziridine **35** (Scheme 1.1.14a).[21] Surprisingly, switching from 3-Ph lactone **27** to the 3-Me analogue **37** led to a different medium-sized ring **38** (Scheme 1.1.14b). They attributed this to a slower decarboxylation step because the alkyl group cannot stabilize the adjacent anion, and so the formation of the *C*-centred dipole reagent was not favourable in that case.
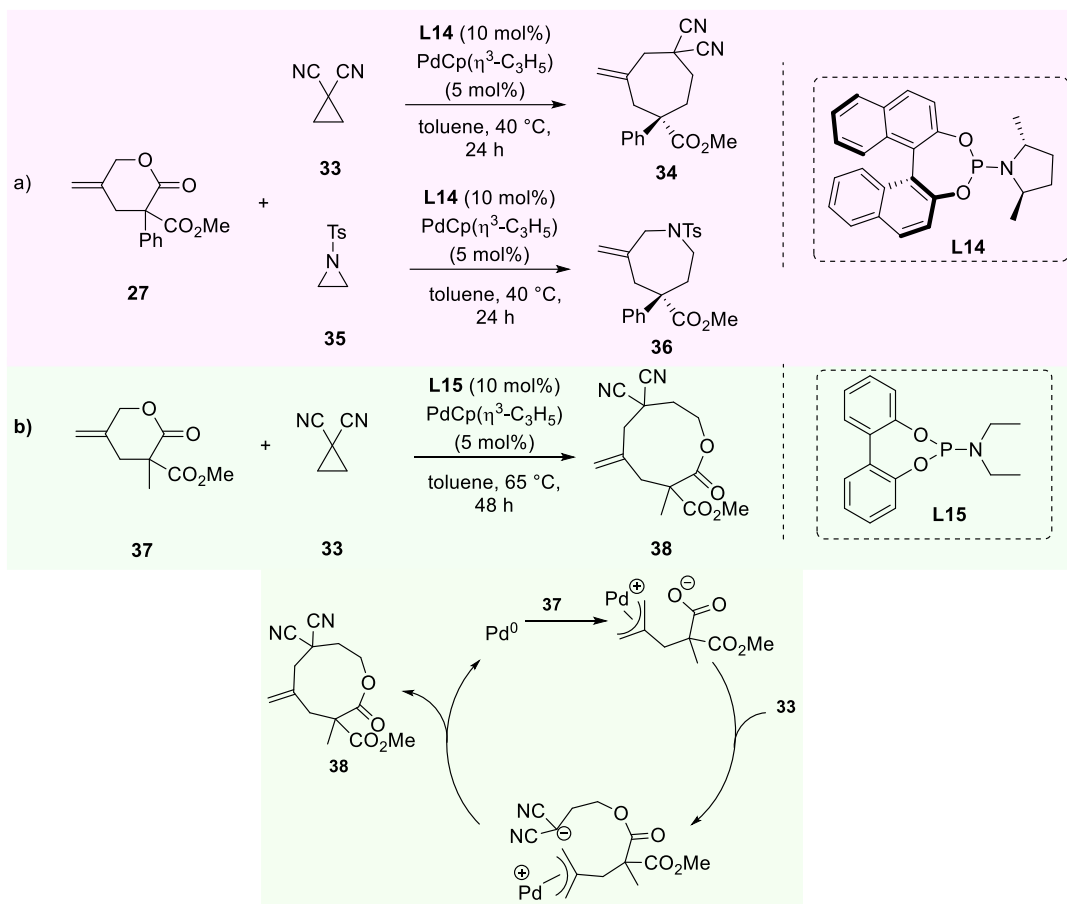
Scheme 1.1.14 Hayashi's work on the asymmetric synthesis of medium-sized rings.

Besides **27**, Zi and co-workers envisioned **39** as a precursor to an oxyallyl cation which can function as a carbon-centered zwitterion species (Scheme 1.1.15).[22]
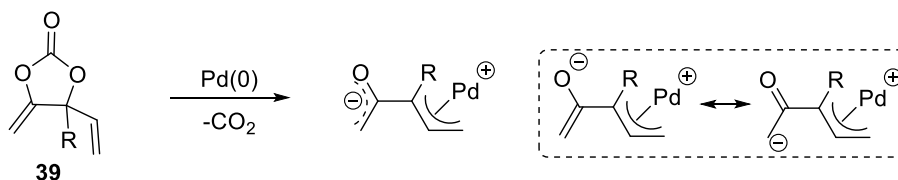
Scheme 1.1.15 Guo's design of new precursor **39**.

The vinyl pentanone derivatives **41** were delivered from **39** and its acceptor **40** in highly diastereoselective fashion with high functional group tolerance (Scheme 1.1.16).[23]
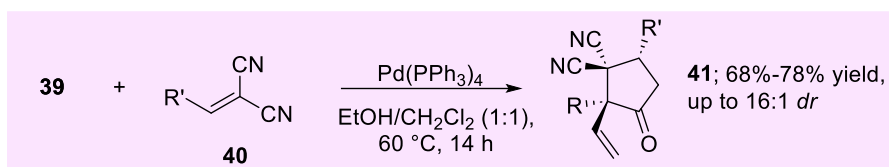
Scheme 1.1.16 Guo's work on the synthesis and application of new dipole reagent bearing C nucleophile **39**.

1.2 Rationalizing the high selectivity of the Trost ligand series in asymmetric allylic alkylation reactions

Since the Trost ligand series was introduced in the last century, many different researchers have contributed reports of the high enantioselectivity enabled by Trost's modular ligand scaffold to a plethora of allylic alkylation reactions.[24] To-date, two different models have become popular for rationalizing the stereoselectivity of these processes, and these will be discussed in this section.

The chiral space surrounding the allyl moiety has been carefully designed to have a large P-Pd-P angle in order to ensure close contact between the ligand structure and the allyl fragment (Figure 1.2.1).[25]
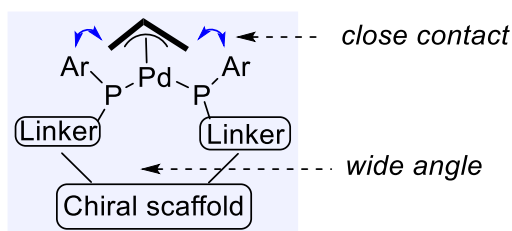
Figure 1.2.1 Model for Trost ligand design.

There is general agreement that there are two synergistic effects influencing chiral ligand performance: a steric interaction between the ligand and allyl moiety; and selective nucleophilic attack at the favorable allylic terminus.[26] In 1999, Trost and Toste proposed a simple cartoon

22

model for elucidation of the Trost ligand performance. In this model, the four phenyl rings play a vital role in stereoselectivity; the "wall" that determines the pathway of the incoming nucleophile while the allyl fragment is in a plane that runs parallel to raised "flap" (Figure 1.2.2).[24a]
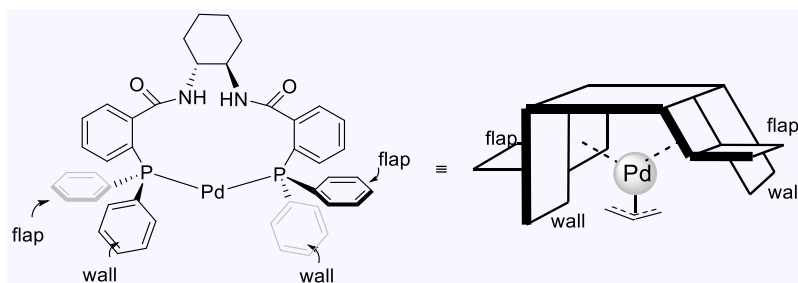
Figure 1.2.2 Wall-and-flap cartoon model.

The model has been widely used in the explanation of desymmetrization stereochemistry of intermediates such as **42**. There are two possible transition states of *exo*-nucleophilic attack. In *exo*-**43**, the nucleophile approaches from an open space where the flap is upwards, however, in *exo*-**44**, there is a steric clash between nucleophile and lowered flap together with the fact that the R group is towards the 'wall' (Figure 1.2.3). Therefore, *exo*-**43** should be the major enantiomer in the Trost reaction.[6]
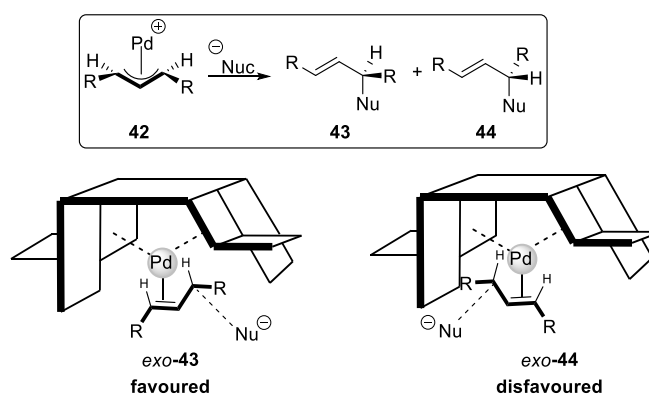
Figure 1.2.3 Two enantiomers formation via *exo*-nucleophilic attack.

To get a better understanding of wall-and-flap cartoon model, here we will introduce two examples [27] which featured the steric interaction between wall of the ligand and the substrate that leads to

23

stereocontrol. For example, an asymmetric decarboxylative reaction of 2-methyl-1 tetralone **45** was conducted under mild conditions as shown in Figure 1.2.4. In terms of naked enolate, *Si* attack was more favourable to avoid undesired steric clash between the 'wall' and phenyl group.
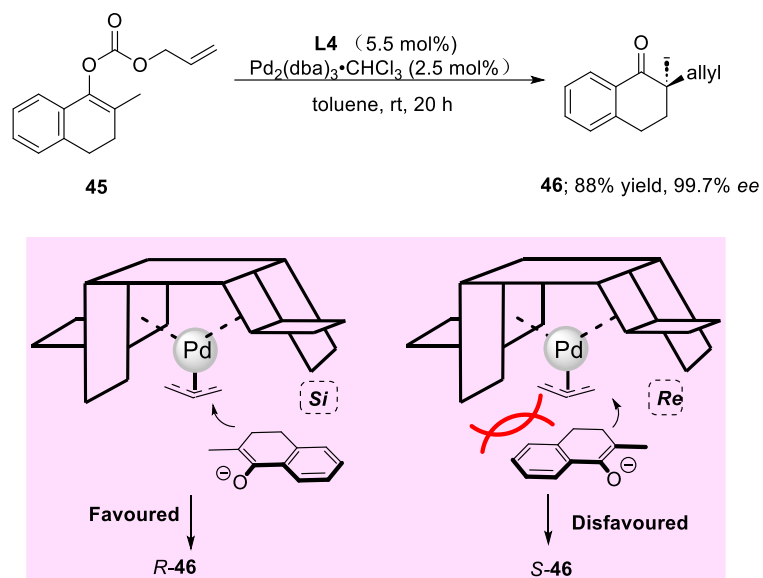
Figure 1.2.4 'Wall-and-flap' cartoon example of decarboxylative reaction of **45**.

However, Trost and Schmide observed an opposite enantioselectivity of the same reaction when conducted in the presence of 2 equivalents of LDA, as well as higher levels of enantioselectivity according to their preliminary results.[28] LDA aggregation was proposed to make the oxygen bulkier than the phenyl ring, therefore, *Re*-attack can diminish steric clash between 'wall' and oxygen terminus (Figure 1.2.5). Hence, the enantioselectivity observed in the Pd catalysed allylic reaction was quite sensitive to enolate structure.
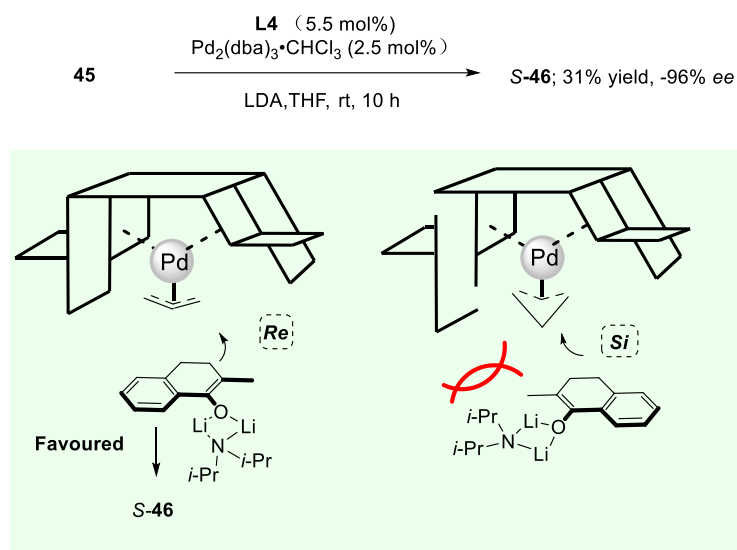
Figure 1.2.5 LDA enol nucleophile **45** gave contradictory enantioselectivity of **46**.

The influence of double bond geometry on enantioselectivity and reaction rate was also explained from this model. Regarding the *Z*-enolate of **47** (Figure 1.2.6b), although *Re*-face nucleophilic attack can avoid the steric clash between cyclohexane and 'wall' of Trost ligand, the Me group has a steric clash with the 'wall' to some extent. On the other hand, the corresponding *Si*-face addition also approaches the wall. In contrast, addition of the *E*-enolate (Figure 1.2.6a) can undergo addition through the *Si*-face quite easily, which rationalized why the enantioselectivity from the *Z*-enolate was lower.
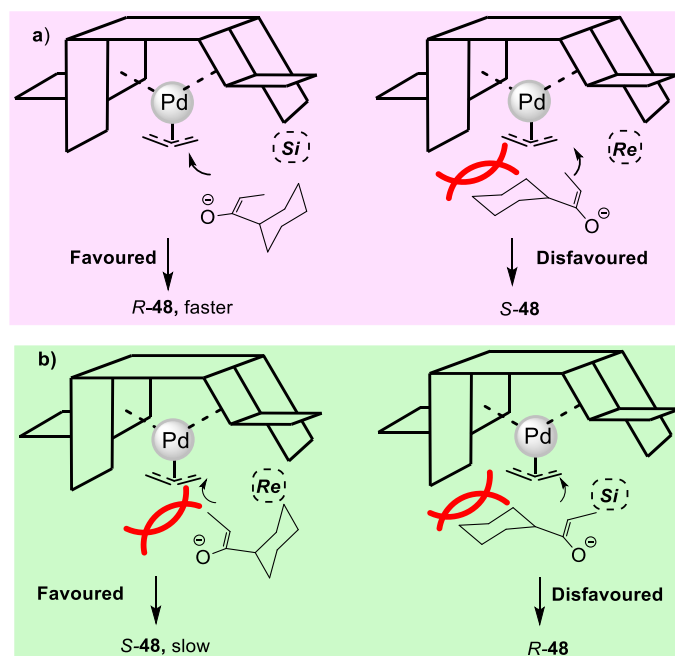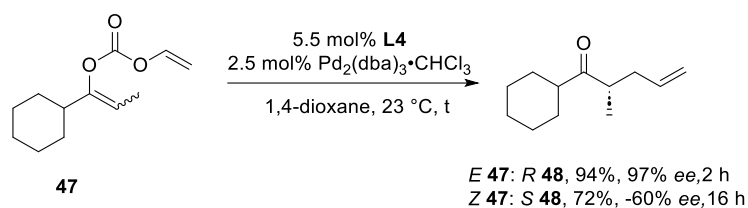
Figure 1.2.6 'Wall-and-flap' cartoon in the DAAA.

Overall, the 'wall-and-flap' model focuses on minimizing steric interactions between nucleophile and the 'wall' of Trost model. Where possible, bulky fragments should be positioned at the 'flap' side of ligand.

Lloyd-Jones and Norrby have proposed an alternative model based on solution phase NMR studies of the Pd-Trost ligand series. They found there were two distinct monomeric species during preparation of Pd-**49** and **49'** complexes of the Trost ligand. As shown in Figure 1.2.7, **49a** and **49b** can interconvert, whereas for **49'**, the *exo* conformer **49'a** predominates because there is an induced steric strain in **49'b** with clash of cyclohexane backbone. In addition, in both *exo* conformers, only the allylic terminus trans to P donors in the ligand framework without steric repulsion is more activated.[29]
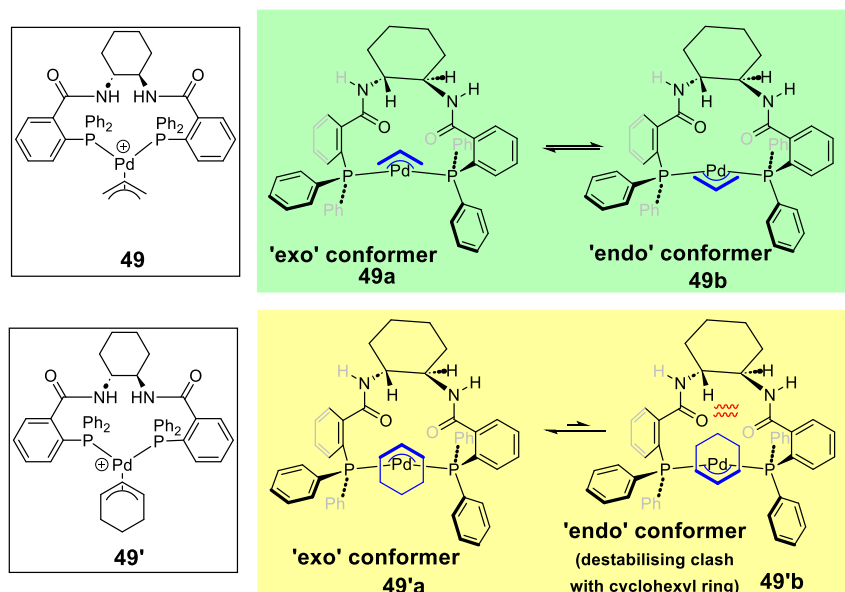
Figure 1.2.7 Lloyd-Jones and Norrby model.

Guiry's group adopted the Lloyd-Jones and Norrby model to explain the high enantioselectivity observed in a Pd-catalysed decarboxylative allylic reaction of lactone **50**.[30] With regard to pathway a, a steric clash between a bulky aromatic group and the Trost ligand backbone resulted in a favourable addition mode where the aromatic group was orientated away from the backbone benzene rings (Figure 1.2.8).
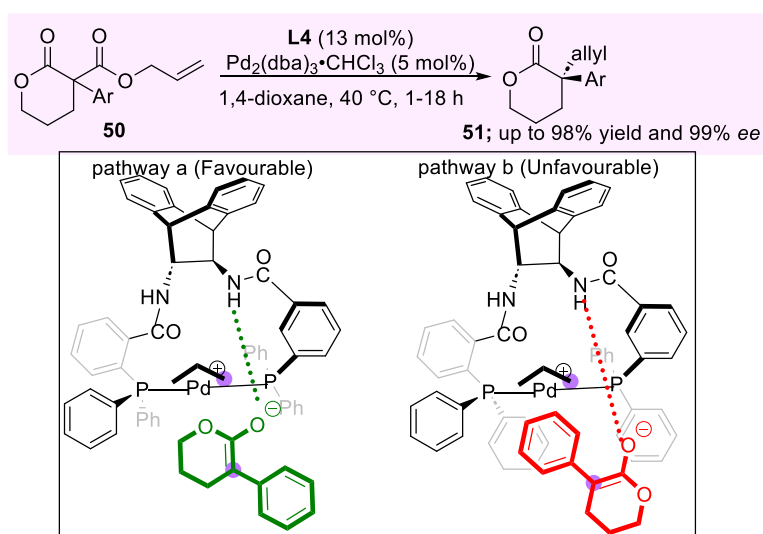
Figure 1.2.8 Explanation of stereochemistry by Lloyd and Norrby model.

1.3 Pd-catalysed reactions of ylides and related compounds

Pd-catalysed tandem reactions using carbene equivalents for the construction of heterocyclic compounds has been a dynamic area of research in organic chemistry.[31] Carbene-type reactivity can be accessed by the loss of stable small molecules from their corresponding ylide precursors.[32]

1.3.1 Diazo compounds as a carbene synthon in Pd-catalysed reactions

Diazo compounds have been commonly used as a carbene source despite their instability and explosive potential.[33] Here, we will focus on several examples for the synthesis of heterocyclic compounds via Pd-catalysed decarboxylative annulation from a series of diazo compounds.

Xiao's group reported the asymmetric synthesis of quinolinone **54** by the Pd-catalysed decarboxylative annulation reaction of **14** and *in situ* generated ketene **53** from α-diazoketone **52** (Scheme 1.3.1).[34] The photoactivation of **52** provided a direct route for the synthesis of **54** with a loss of N_2 gas. A series of quinolinone analogues were produced under mild conditions with high yield and stereoselectivity. Importantly, the synthetic practicality of the method was achieved by a gram-scale (1 g) reaction under sunlight without resorting to blue light.
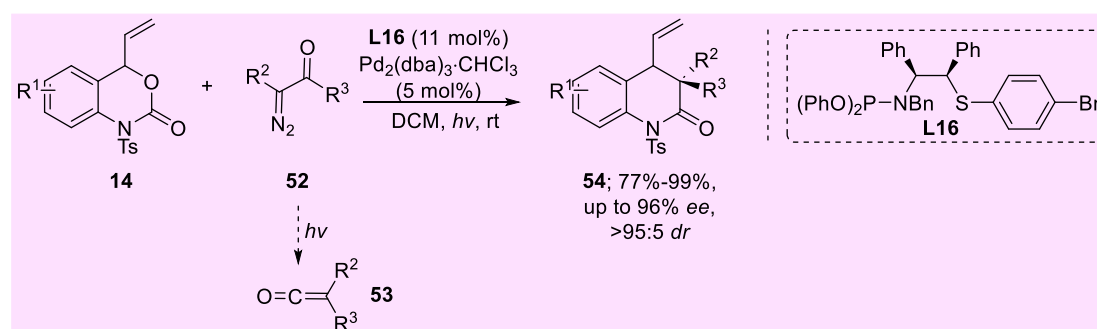
Scheme 1.3.1 Xiao's work on the asymmetric synthesis of **54.**

Yang's group reported an unprecedented Pd-catalysed synthesis of seven-membered ring **57** from three-modular allylic reactions of **17** (Scheme 1.3.2). This methodology endowed sodium sulfinate

55 with diverse substitution. Dipole reagent intermediate **I** reacts with sodium sulfonate **55** to deliver intermediate **II** with a successive reductive elimination step to regenerate Pd(0) and affords product **i**. Pd(0) enables decomposition of diazo ester **56** to form Pd carbene intermediate **III**. Besides, they found that in the presence of DBU and air, oxidation to an imine took place to generate the final product.[35]
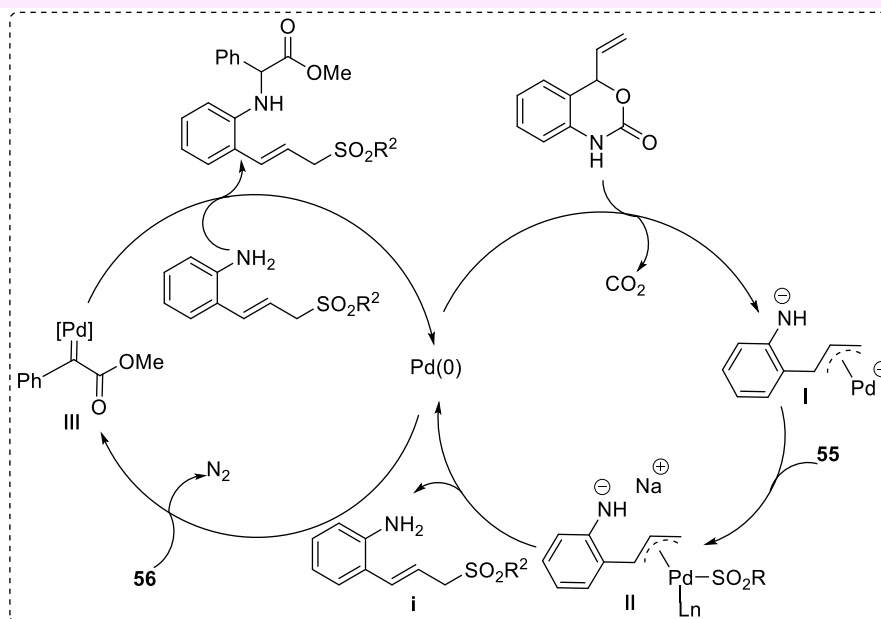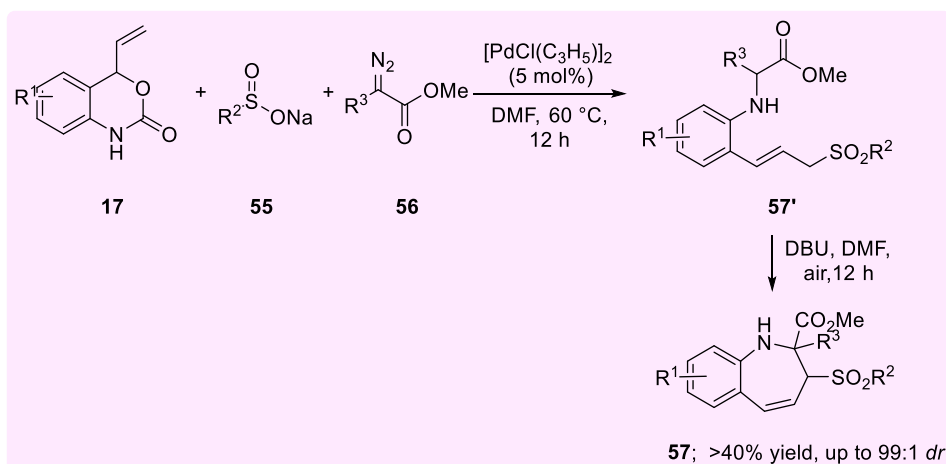
Scheme 1.3.2 Yang's work on the synthesis of **57**.

N-Sulfonyl hydrazone **58** is a stable precursor of a diazo compound under basic conditions. Ashfeld's group reported that the transformation of **58** and **14** in the presence of Pd catalyst gave dihydroindole **59** with exceptional diastereoselectivity rationalized in Scheme 1.3.3. In addition,

they also concluded that a key intermediate contained a Pd^{II}-carbene complexed with a π-allyl ligand after a series of unsuccessful chiral ligands were investigated.[36]
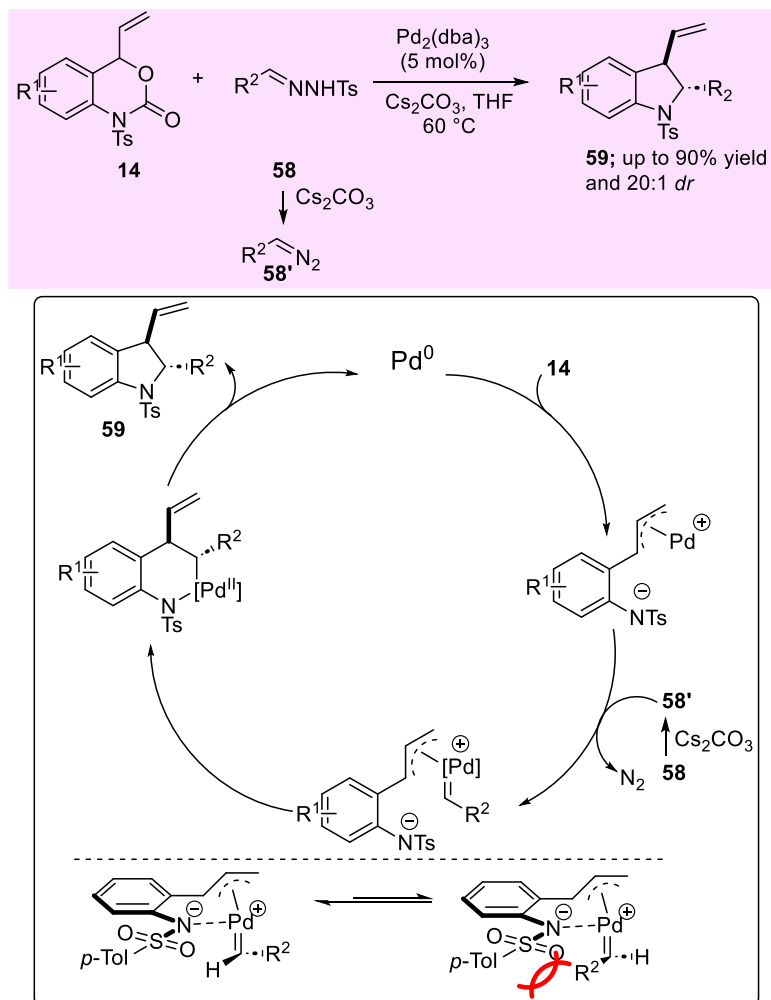
Scheme 1.3.3 Ashfeld's work on the synthesis of **59.**

Meanwhile, they evaluated this transformation in the absence of Cs$_2$CO$_3$ and **60** was formed via reductive elimination which highlighted the importance of base for generating the carbene (Scheme 1.3.4).
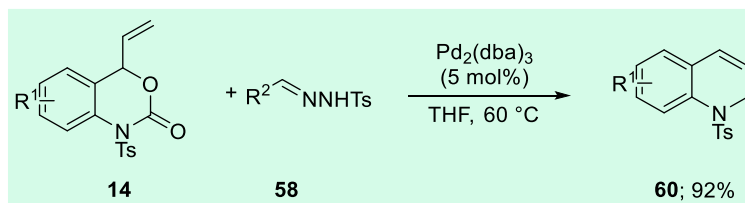
Scheme 1.3.4 Side reaction in the absence of base.

1.3.2 Sulfur ylides in Pd-catalysed reactions

Besides diazo compounds, sulfur ylides have become a popular class of carbene equivalents since 1970, and they have been widely used in metal mediated cyclization (which will be discussed in Chapter 3). Here, we will discuss some recent examples about Pd catalysed reactions of sulfur ylides.

For instance, Xiao and co-workers exploited a dearomatization-rearomatization reaction of benzoxazinones **61** with aza-sulfur ylides **62** under Pd-catalysis for the synthesis of dibenzodiazepine **63**.[37] The functional groups (aromatic substituents: R^1 and R^2) were tolerated well in the synthetic route, giving **63** in moderate to high yields (Scheme 1.3.5).
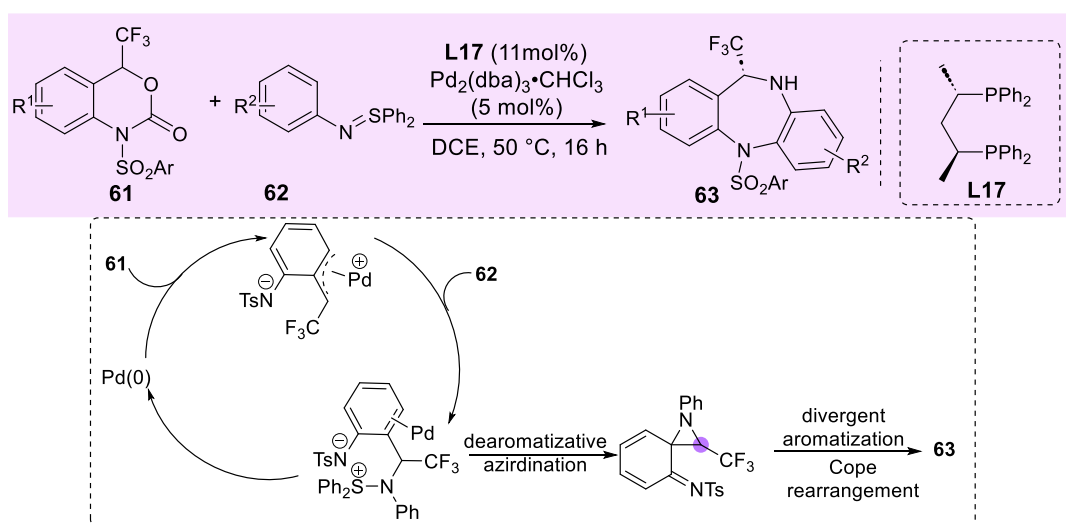
Scheme 1.3.5 Xiao's work on the synthesis of **63**.

Jiang's group reported a new strategy for the construction of **66** by Pd-catalysed cyclization/C-C bond formation via sulfoxonium ylide **65**.[38] This synthetic route generated α,β-unsaturated compounds **66** with high functional group tolerance, high yield and excellent diastereoselectivity (Scheme 1.3.6).
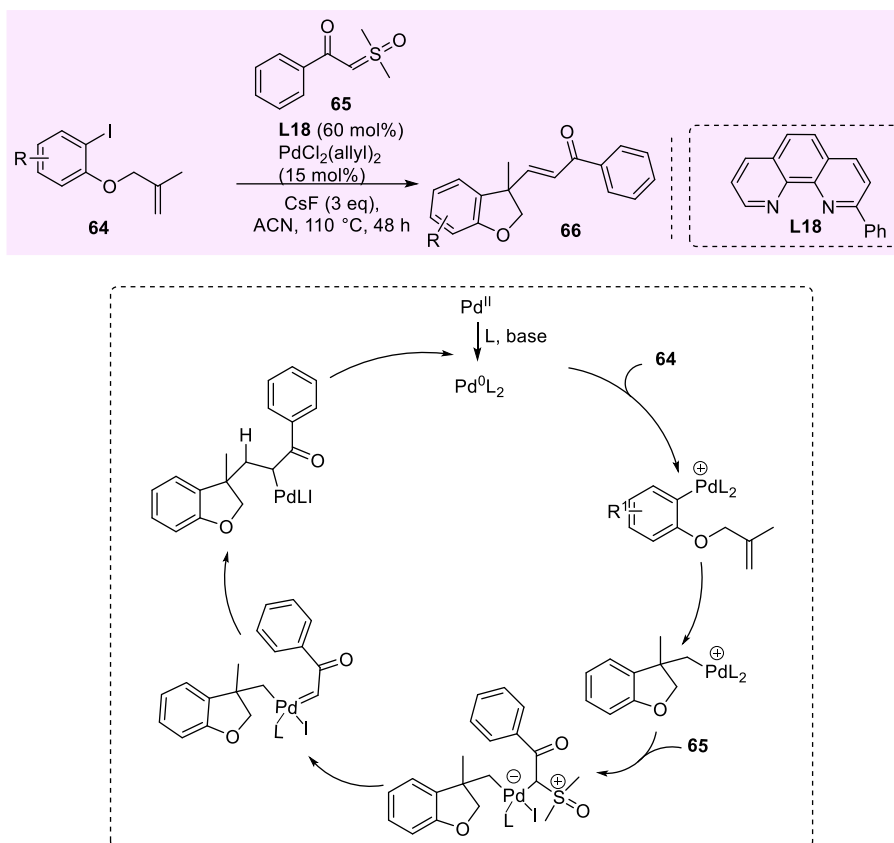
Scheme 1.3.6 Jiang's work on the synthesis of **66**.

Chen's group reported the Pd-catalysed [3+2] cyclization for the synthesis of 2,4-diarylthiazole analogues **68** (Scheme 1.3.7). The functional group compatibility was high and **68** was accessed in moderate to high yields.[39]
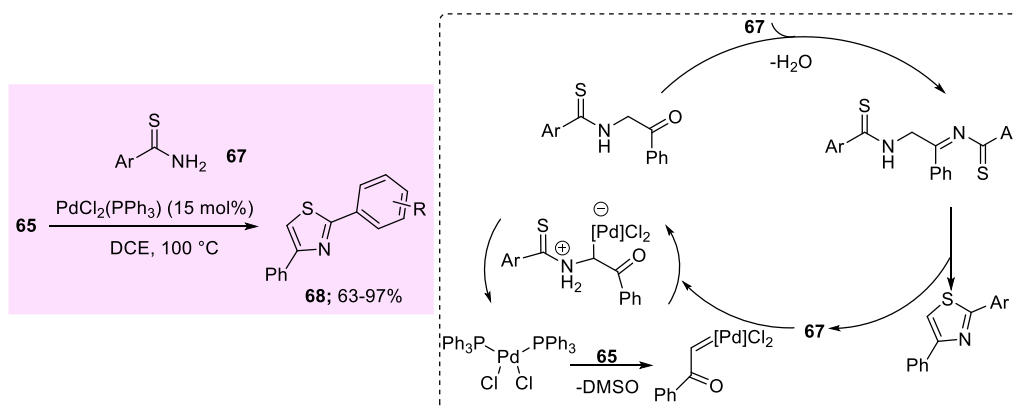
Scheme 1.3.7 Chen's work on the synthesis of **68**.

1.3.3 Phosphorus ylides in Pd-catalysed cyclization reactions

The strong binding capacity of phosphorous ylides with transition-metals has impeded their widespread use in transition metal catalysed reactions as they tend to promote catalyst deactivation.[40] However, some examples are beginning to emerge and will be covered here.

Carbonyl stabilized phosphonium ylides have been applied in the recent synthetic studies due to their stability and easy preparation.[41] Xiao and co-workers reported a novel Pd-catalysed Ullmann-type annulation of carbonyl stabilized phosphonium ylides (Scheme 1.3.8). This synthetic route provided a promising platform for synthesis of novel phosphorous heterocycles **71.**
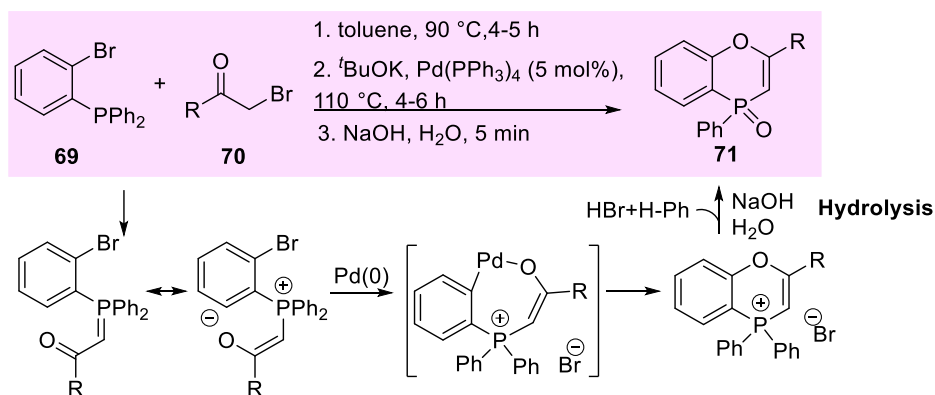
Scheme 1.3.8 Xiao's work on the synthesis of **71**.

Considering phosphorous ylides have not been widely applied in Pd-catalysed reactions, here, we will introduce other transition-metal catalysed reactions of phosphorous ylides. In general, transition-metal catalysed reactions associated with phosphorous ylides have involved γ-*O*-coordination of metal and subsequent intramolecular Wittig reaction for construction of an alkene moiety.

For example, Li's group disclosed the Rh-catalysed annulation of readily available α-diazo carbonyl compounds **73** and *in situ* generated phosphonium ylide to access 1-naphthol **74** and isocoumarin **76** (Scheme 1.3.9).[43a] Most strikingly, **76** was formed in a *6-exo*-trig cyclization from enol precursor as a result of C-O bond formation [43b] and C-C bond cleavage.
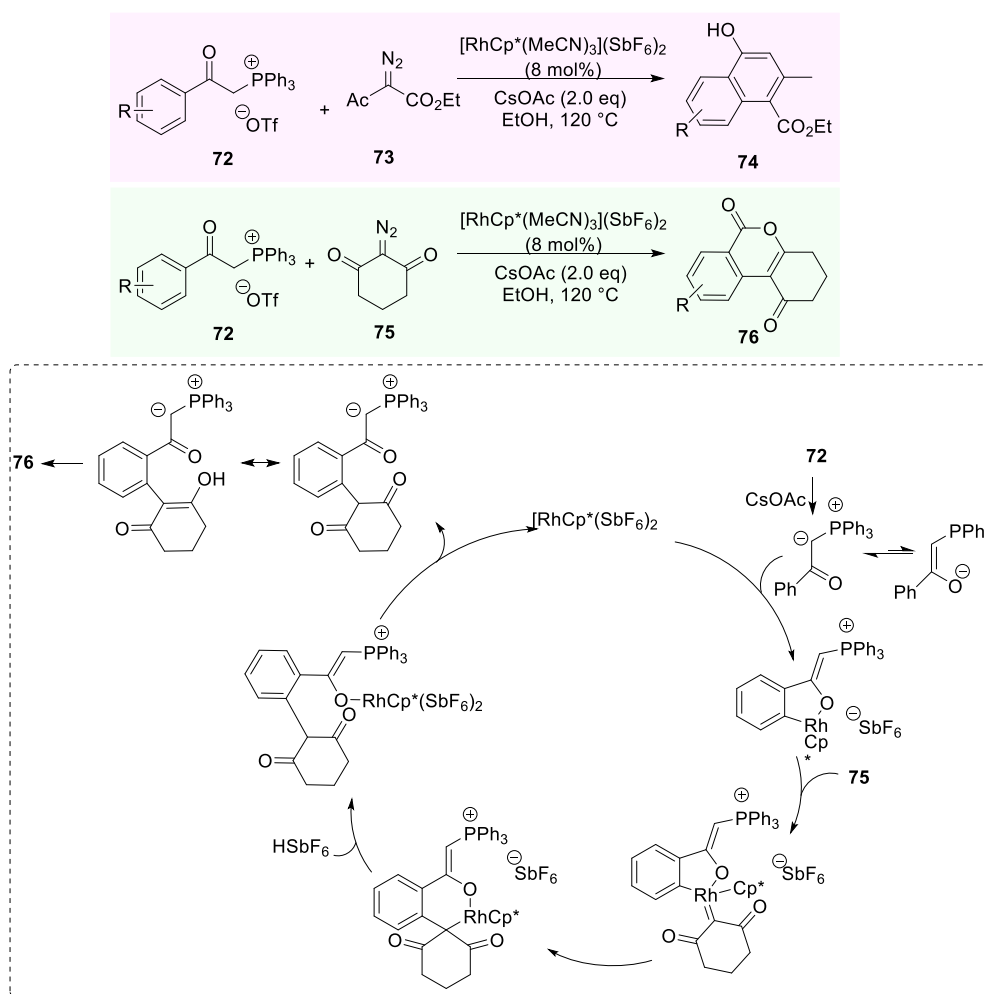
Scheme 1.3.9 Li's work on the synthesis of **76**.

Besides diazo compounds, sulfonium ylides are a common partner for phosphorous ylides in transition-metal catalysed reactions. Indeed, these can be coupled in a Ru-catalysed reaction for the synthesis of 1-naphthols **77**.[44] The typical processes incorporating Ru-carbene insertion, and Wittig reaction were involved as shown in Scheme 1.3.10. A broad range of substrates were tolerated with up to 94% yield.
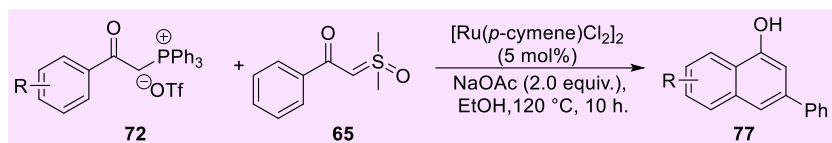
Scheme 1.3.10 Chen's work on the synthesis of **77**.

Chapter 2: Studies Towards the Synthesis of Enantiomerically Enriched 3-Fluoropiperidines

2.0 Introduction

Nitrogen-containing heterocyclic frameworks are widely present in nature products and drug candidates and have been an active goal for synthetic chemists. In particular, it is noteworthy that piperidine holds the most predominant role in FDA approved drugs.[45] Fluorinated piperidines that offer favourable pharmacokinetic and pharmacodynamic properties have been successfully introduced to the market.[46]

Within this specific class, in theory, there are three possible positions that a fluorine atom can be incorporated, however, 3-fluorinated piperidines have emerged as prevalent motifs in small molecule pharmaceuticals (Figure 2.0.1).[47]
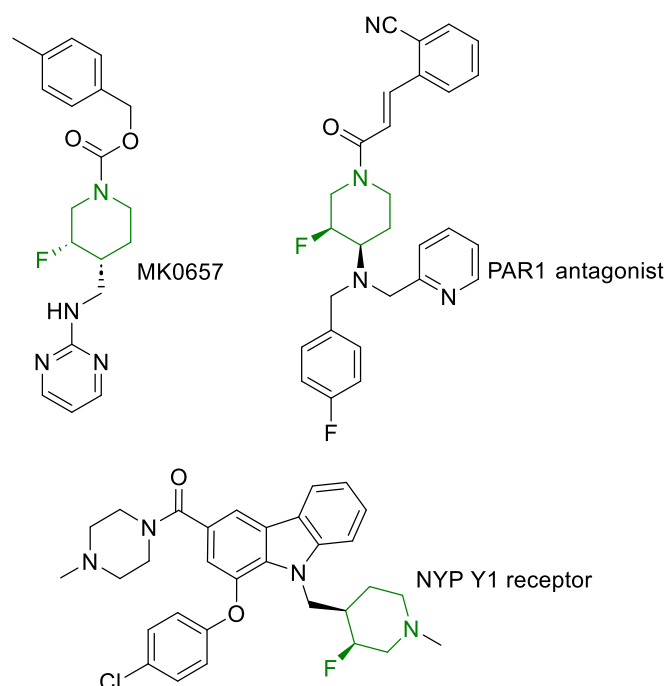
Figure 2.0.1 Bioactive compounds featuring 3-fluoropiperidine fragments.

The reason for this is that 2-fluoropiperidines are chemically unstable while 4-fluoropiperidines are unable to exert a strong influence on piperidine basicity (Figure 2.0.2).
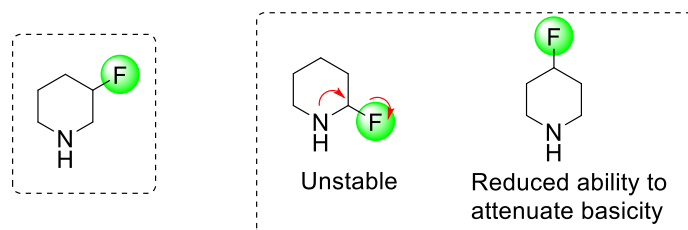
Figure 2.0.2 Influence of fluorine position.

The synthesis of 3-fluorinated piperidines is an active area due to their importance in drug development. The most commonly used strategy is functionalization of accessible fluorinated compounds. However, this strategy is not general and these approaches suffer from inherent drawbacks.[48] For example, Nairoukh *et al*. have reported that hydrogenation of fluorinated unsaturated cyclic compounds proceeds with high diastereocontrol under rhodium catalysis.[49] This approach requires an elaborate Rh-catalyst and a high pressure hydrogen reactor necessitating specialised equipment.
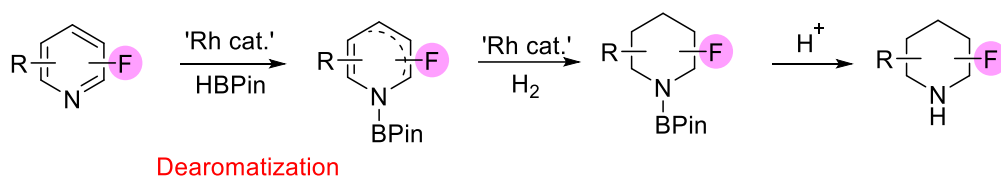
Scheme 2.0.1 One-pot dearomatization-hydrogenation for the synthesis of fluorinated piperidines.

Another common strategy is the introduction of a fluorine atom to a piperidine precursor using a reagent such as DAST or Deoxofluor.[50] Low atom economy and strict anhydrous conditions are unappealing aspects of this method. The example shown in Scheme 2.0.2 also highlights that side reactions can occur that result in low product yields.

Scheme 2.0.2 Fluorination of precursor.

4-Piperidone is also a common precursor of 3-fluorinated piperidines via the fluorination of an intermediate enolate. The example in Scheme 2.0.3 shows the synthesis of an *N*-alkylpiperidine which is an important moiety for the treatment of neurological conditions.[51] However, the methodology takes many steps and requires NaN_3 which is a hazardous reagent (Scheme 2.0.3).

Scheme 2.0.3 Total synthesis of 3-fluorinated *N*-alkylpiperidine framework.

The introduction of a fluorine atom into ethyl 3-chloropropyl-2-cyanoacetate also provides a platform for the synthesis of 3-fluorinated piperidines.[52] The disadvantages of this approach lie in the fact that the synthetic route is linear and the fluorinating agent (NFSI) is expensive (Scheme 2.0.4).

Scheme 2.0.4 Fluorination of ethyl 3-chloropropyl-2-cyanoacetate and intramolecular reaction.

Our group succeeded in the synthesis of 3-fluorinated piperidine analogues in a one-pot reaction (palladium catalysed-decarboxylative allylic alkylation followed with condensation).[53] The starting materials are readily available, and the products are endowed with versatile functionality that make them useful scaffolds for heterocycle synthesis (Scheme 2.0.5).
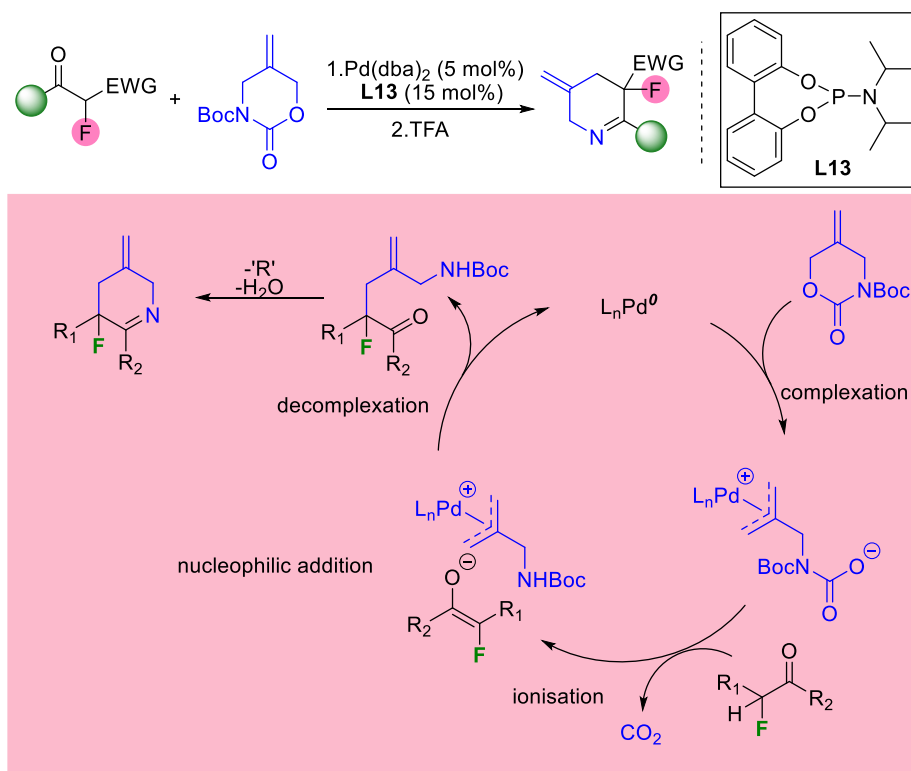
Scheme 2.0.5 Palladium catalysis of 3-fluorinated piperidine analogues.

In addition, our group members also explored a pool of chiral ligands in order to access high enantioselectivity. Unfortunately, the enantiocontrol was found to be very poor, albeit full

conversion was achieved (Table 2.0.1).

Table 2.0.1 Preliminary screening of chiral phosphoramidite ligands.
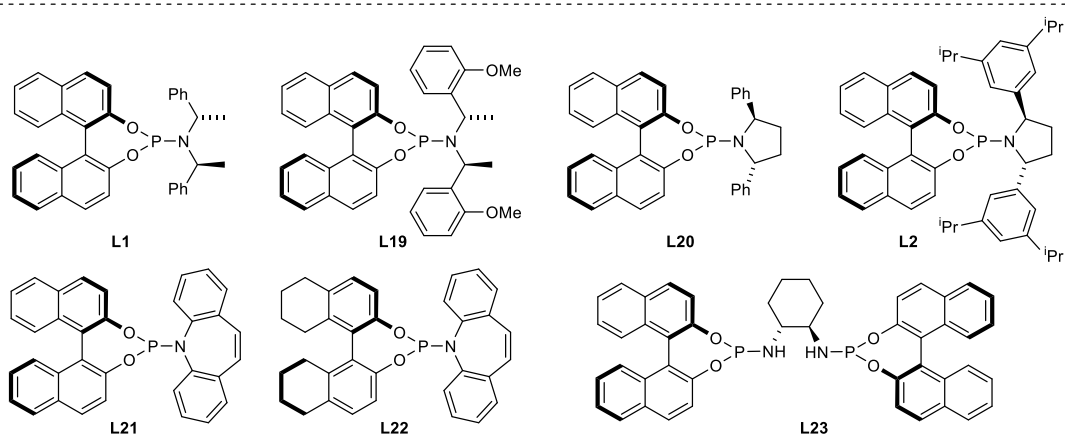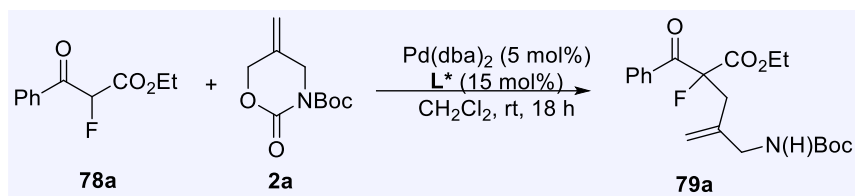
Entry	Ligand	Conv. (%)	*ee* (%)
1	**L1**	100%	<5%
2	**L29**	100%	6%
3	**L20**	100%	<5%
4	**L2**	100%	<5%
5	**L21**	100%	8%
6	**L22**	100%	<5%
7	**L23**	0%	--

It was assumed that the low enantioselectivity resulted from an acyclic ketone which can form an *E/Z* enolate mixture that leads to opposite enantiomers after allylation (Figure 2.0.3).
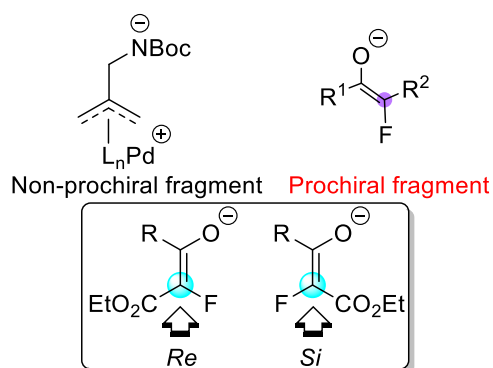
Figure 2.0.3 Hypothesis of reason resulting in low enantioselectivity.

The influence of enolate configuration on allylic alkylation enantioselectivity has been explored. Nakamura and co-workers carried out the investigation of the allylation of cyclic and acyclic α-fluoroketones, and they found the enantioselecitvity of the latter substrate to be moderate (Scheme 2.0.6). He attributed this observation to the in situ generation of an *E/Z* mixture of the palladium enolate. [27]
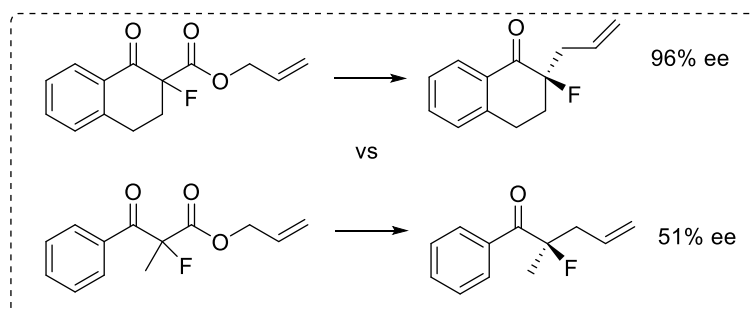
Scheme 2.0.6 Comparision of fluorinated acyclic and cyclic ketones.

Trost and co-workers reported the double bond geometry influences not only the enantioselectivity performance but also the reaction rate, which is explained in Figure 1.2.6. Notably, *E-* and *Z*-enolates do produce opposite enantiomers of the allylation product (Scheme 2.0.7).
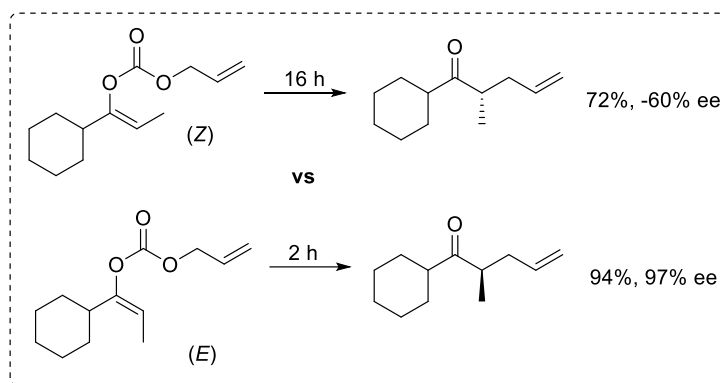
Scheme 2.0.7 *E/Z* geometry influences reaction rate and enantiomeric excess.

Guo's group also subjected fluorinated ketones to different bases to control the *E/Z* ratio of the intermediate enolate, and also found the enantioselectivity to vary with different *E/Z* ratios (Scheme 2.0.8).[55]
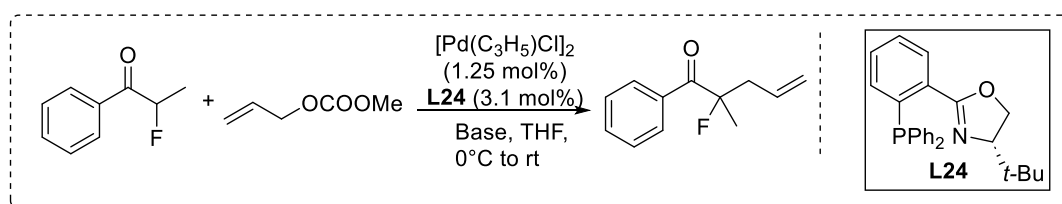
Entry	Base	*Z/E ratio*	Yield (%)	*ee* (%)
1	LiHMDS	>20:1	60%	84%
2	NaHMDS	<20:1	77%	75%
3	KHMDS	<20:1	80%	69%

Scheme 2.0.8 Highest *E/Z* ratio under the base of LiHMDS resulted in highest enantioselectivity.

Based on the literature, we can conclude that the main challenge to achieving high enantioselectivities in the asymmetric allylic alkylation of acyclic ketones derives from control of the double bond geometry of the intermediate enolate.

2.1 Aim

The aim of this project was to react carbamate **2a** with a series of acyclic α-fluoro-β-ketoesters **78** under asymmetric Pd catalysis in order to establish the influence of the *E/Z* enolate geometry on enantioselectivity of **79a**. In addition, we also wanted to demonstrate the selective functionalisation of the piperidine products.
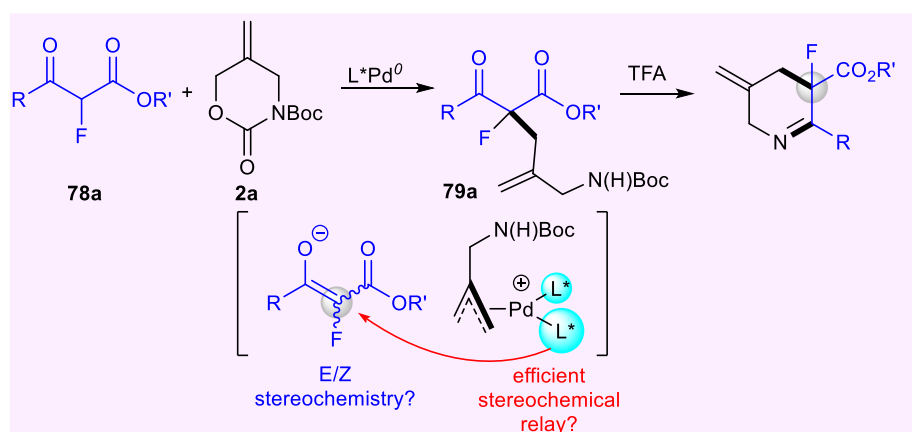
Scheme 2.1.1 Pd-catalysed asymmetric allylic alkylation of α-fluoro-β-ketoesters **78**.

2.2 Results and Discussion

2.2.0 Synthesis of α-fluoro-β-keto ethyl esters

Three approaches were used to access the required α-fluoro-β-keto esters **78**. Broadly speaking we used the Claisen condensation followed by trapping the enolate product with Selectfluor, or the condensation of α-fluoroacetate itself (Scheme 2.2.1). Broadly speaking, direct fluorination (**route c**) gave the highest yield. It was assumed that the low efficiency of both **route a and route b** was trigged from product loss during purification.
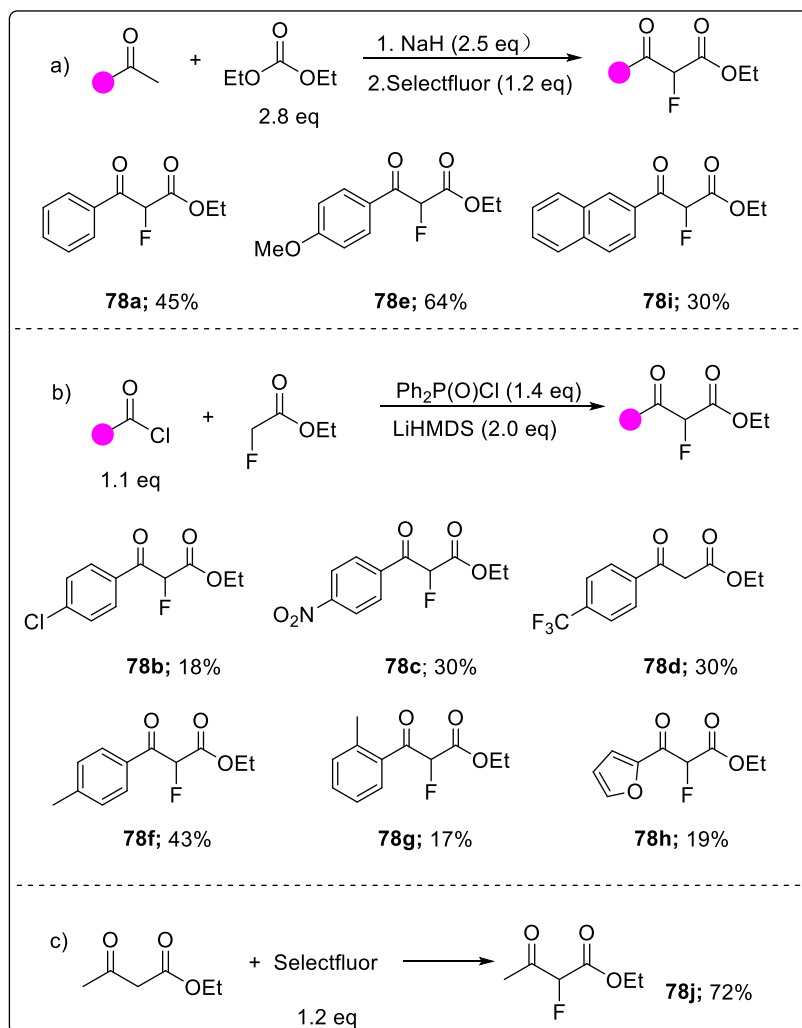
Scheme 2.2.1 Synthesis of α-fluoro-β-ketoesters **78**.

2.2.1 Synthesis of carbamate

We commenced with the synthesis of the cyclic carbamate, the key precursor to the dipolar Pd-intermediate. Desymmetrisation of diol **80** (typically carried out on 25 g scale) by iodination proceeded in modest yield due to the formation of di-iodination product (**81'**). This by-product formation could not be avoided, even when a stoichiometric amount of iodine was added portion wise. The carbamate framework was accessed from cyclization using AgOCN and the intermediate was protected by a Boc group, which is an easily removable nitrogen protecting group (Scheme 2.2.2).
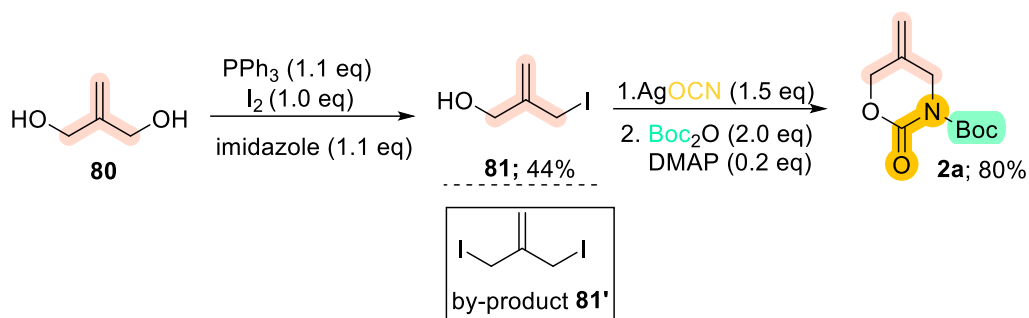
Scheme 2.2.2 Synthesis of carbamate **2a**.

2.2.2 Asymmetric allylic alkylation study

The enantioselectivity determining step is the allylation of the enolate intermediate. There are two possibilities: a) inner-sphere nucleophilic attack: in this pathway, Pd directly coordinates to oxygen and there is a close contact between chiral ligands and substrate; b) outer-sphere route: where the substrate attacks the π-allyl framework externally (Figure 2.2.1). The latter model has been used to explain the outcome of our reactions, as will be explained later.
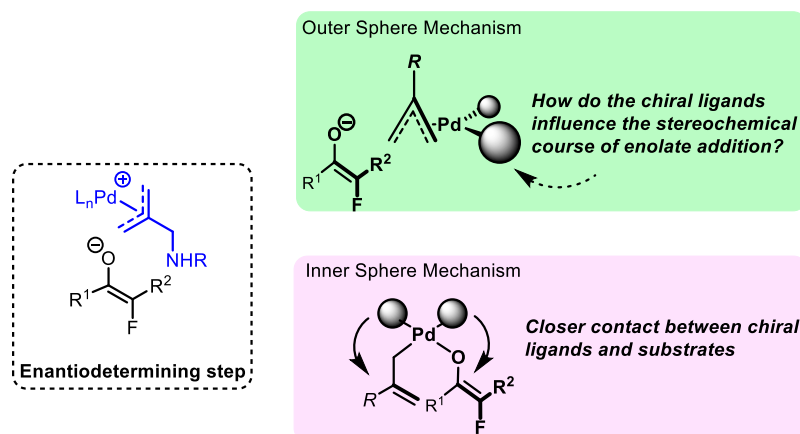
Figure 2.2.1 Enantioselectivity determining step.

We used **78a** as a model substrate for asymmetric allylation investigation (Table 2.2.1). Different classes of chiral ligands were examined using a 3 h reaction period in NMP at rt. The four Trost ligands (**L4, L15, L25 and L27**) gave excellent yields and encouraging enantioselectivities, with **L27**

exhibiting the highest enantiocontrol (entry 7).

Table. 2.2.1 General screening of different chiral ligands **L***.
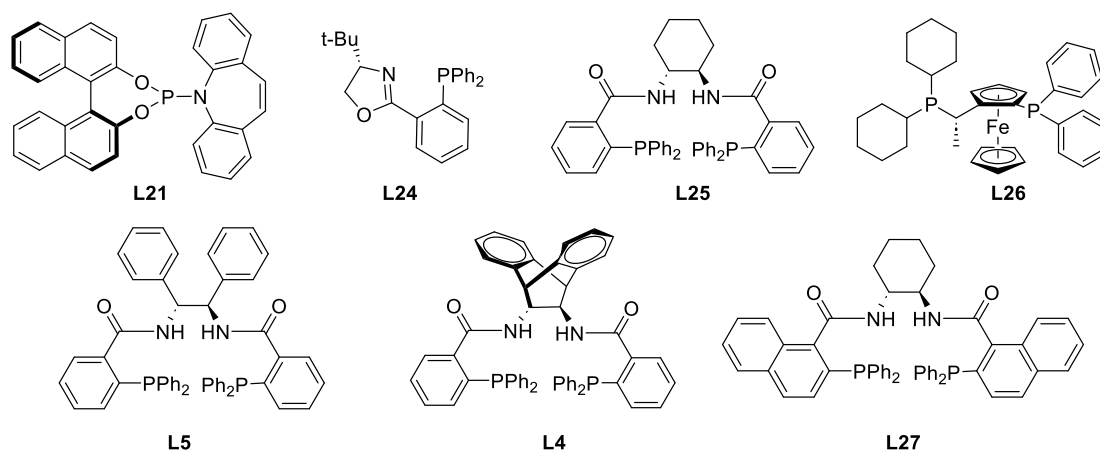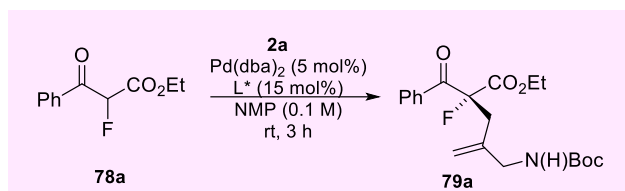
Entry	Ligand	Yield (%)	*ee* (%)
1	**L21**	70%	-8%
2	**L24**	73%	-10%
3	**L25**	70%	34%
4	**L26**	80%	<5%
5	**L5**	99%	41%
6	**L4**	79%	25%
7	**L27**	99%	48%

Next, **L27** was subjected to different solvents at rt. Indeed, solvent effects were noticeable (Table 2.2.2). Disappointingly however, we could not get a good balance between yield and enantioselectivity. The use of CH_2Cl_2 (entry 2) gave a similar result to the original NMP conditions, while the use of THF and dioxane (entries 3 and 4) resulted in a distinct improvement in

enantiocontrol, but the conversions were very low, even after leaving the reactions overnight. We were surprised to find that no product was obtained in toluene (entry 5). We can simply conclude that while the use of polar solvents can facilitate the allylation step, these exhibit very poor enantioselectivities (except 1,4-dioxane).

Table. 2.2.2 Investigation of solvents effects.
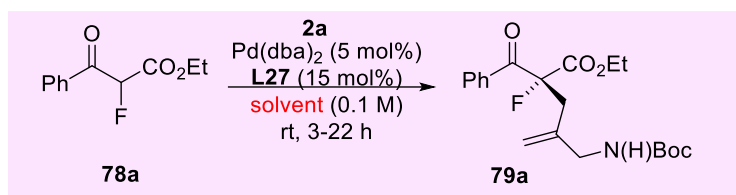
Entry	solvent	t (h)	Yield (%)	*ee* (%)
1	NMP	3 h	99%	48%
2	CH$_2$Cl$_2$	3 h	75%	42%
3	1,4-Dioxane	22 h	20%	62%
4	THF	22 h	10%	60%
5	PhMe	22 h	<5%	--

We envisioned that the conversion could be improved by promoting enolate formation [56] and so different bases were introduced to toluene where the base effect should be more distinctive (Table 2.2.3). Pleasingly, the addition of only a catalytic amount of TEA could promote the conversion in toluene (entry 2). Meanwhile, the use of inorganic base Cs$_2$CO$_3$ in conjunction with **L27** in toluene also gave a similar result (entry 3). Switching TEA to the more basic DBU, however, failed to improve the yield (entry 4). Returning to TEA, we noted an increase in conversion by the addition of 1.2 equivalents, and the enantioselectivity performance was not altered (entry 5). The use of TEA in THF and dioxane maintained similar levels of enantiocontrol, but with lower conversion.

Table. 2.2.3 Base screening.
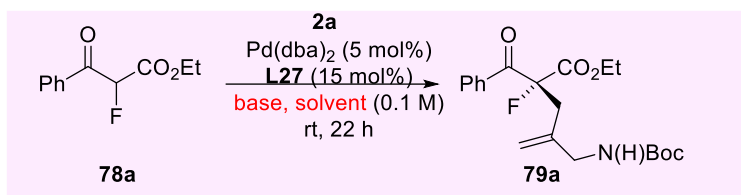
Entry	Solvent	Base	Yield (%)	ee (%)
1	PhMe	--	<5%	--
2	PhMe	TEA (0.1 eq)	35%	65%
3	PhMe	Cs_2CO_3 (0.1 eq)	29%	62%
4	PhMe	DBU (0.1 eq)	30%	63%
5	PhMe	TEA (1.2 eq)	42%	65%
6	THF	TEA (1.2 eq)	30%	62%
7	1,4-Dioxane	TEA (1.2 eq)	15%	60%

As keto ester **78a** can tautomerize to the corresponding enol, it seemed reasonable to speculate whether this could function as a nucleophile. Trost and co-workers have exploited this idea through the combination of toluene/ ^{t}BuOH which is proposed to promote enol formation by induction of hydrogen bonding from its donor ^{t}BuOH and can afford high enantioselectivities.[56] After many experiments, we found that an addition of excess ^{t}BuOH played an indispensable role in the improvement of enantioselectivity (Scheme 2.2.3).
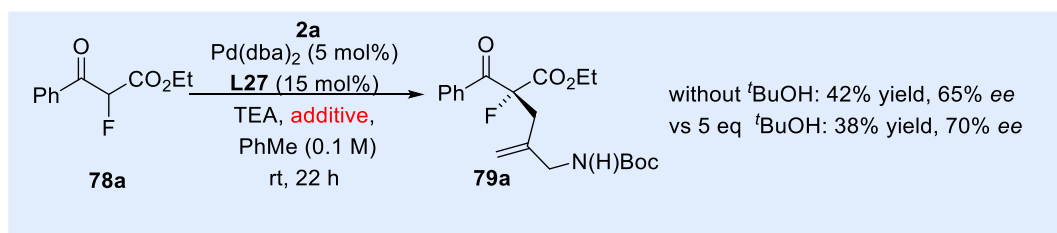
Scheme 2.2.3 Addition of ^{t}BuOH promotes enantioselectivity.

Overall, we concluded that toluene is a good solvent for the asymmetric allylation reaction, and both exogenous base and ^{t}BuOH served two different roles in improving enantiocontrol and conversion. Meanwhile, work ongoing elsewhere in the group separately proved the use of a combination of base and ^{t}BuOH could offer optimal yields and selectivity under the employment of Trost ligands.

Different palladium pre-catalysts were also examined, unfortunately, the reaction proceeded sluggishly in the presence of other Pd salts such as $[(\eta^3\text{-}C_3H_5)PdCl]_2$.

We next decided to explore the reactivity and selectivity of a fully formed enolate. Therefore, we conducted the enolization of **78a** by LiHMDS, which was shown to provide a higher *E/Z* ratio in comparison with other strong bases (KHMDS or NaHMDS), albeit on ketones rather than keto esters.[55] In the event, this strong base showed an increase in conversion and enantioselectivity (Scheme 2.2.4).
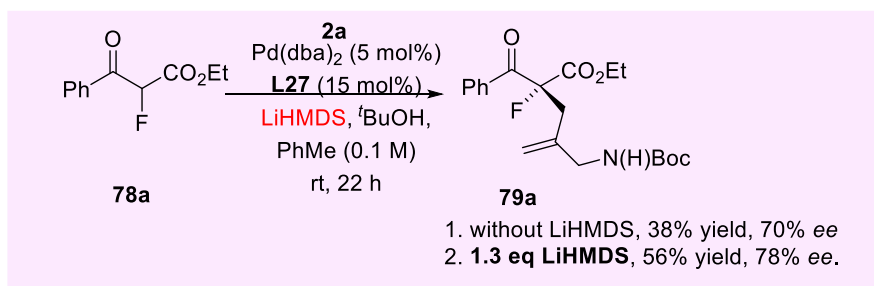
Scheme 2.2.4 Addition of LiHMDS accelerated reaction progress.

In order to understand the significance of this result, we wanted to further explore the influence of enolate *E/Z* ratio on reaction performance. Previous work carried out in the group initially showed that the introduction of bulky silyl protecting group could deliver the corresponding silyl enol ether **83** with a high *E/Z* ratio (Figure 2.2.2).[57]

49
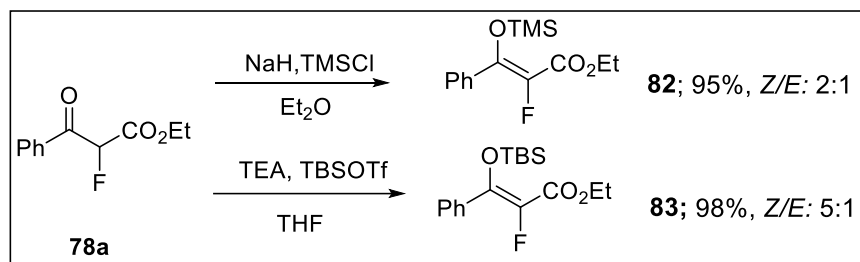
Figure 2.2.2 Hoteite's studies on silyl enol ether formation.

The different *Z/E* enolate mixtures influenced by purification were subjected to the asymmetric allylic alkylation reaction (Scheme 2.2.5). It was interesting that the enantioselectivity and conversion were not influenced by the *Z/E* ratio under the employment of **L27**. It was also notable that silyl enol ether **83** gave better enantioselectivity than keto ester **78a** (entry 1, Table 2.1.1).
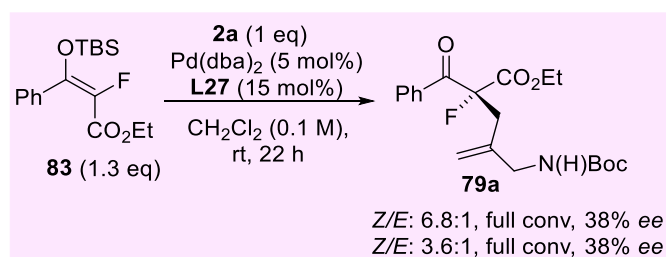
Scheme 2.2.5 Influence of silyl enol ether on *ee* value.

Trost ligand **L27** was replaced by **L25** and **L5** in the hope that these less hindered systems might improve reactivity. Trost ligands **L25** and **L5** were employed under the optimal conditions for conversion and selectivity, and the result provided further data on the influence of the *Z/E* enolate ratio (Table 2.2.4). Inspection of conversion versus *Z/E* ratio suggests that the major isomer reacted faster (entry 1). Interestingly however, similar product *ee* values were obtained irrespective of *Z/E* ratio (entries 1 and 2), a result that supported Hoteite's earlier work.[57] Meanwhile, **L5** exhibited similar enantioselectivity performance but the yield was disappointing (entry 3).

Table 2.2.4 Influence of TBS protecting group on *ee* value and yield.
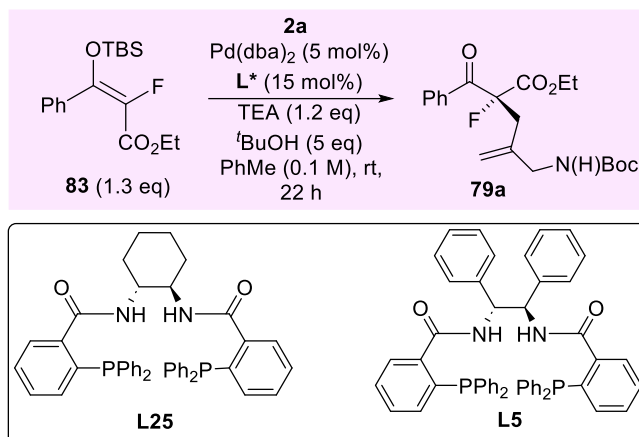
Entry	Z/E ratio	L*	Yield (%)	ee (%)	Z/E RSM
1	16.0:1	**L25**	78%	56%	3.2:1
2	3.3:1	**L25**	75%	56%	--
3	16.0:1	**L5**	8%	57%	--

We endeavoured to purify the *E/Z* enolate mixture (see page 116) to know the geometry of the major isomer from **83**. We envisaged that it would be easiest to analyse the NOE interactions of reduction product **84** and proceeded to generate this compound. DIBAL-H reacted rapidly with **83** to give the reduction product **84** with excellent yield (Scheme 2.2.6).
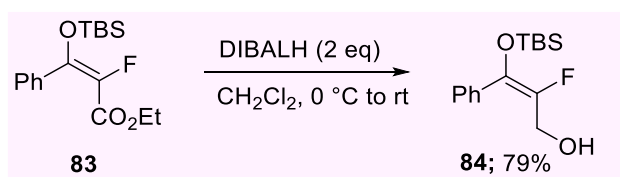
Scheme 2.2.6 Reduction of **83** by DIBAL-H.

Next, **84** was subjected to NOE analysis. According to the NOE data, we can conclude that the CH$_2$OH moiety was closer in space to the phenyl group and distant from TBS protecting group

(Figure 2.2.3). Therefore, the major isomer was assigned as the *Z* isomer, which is in line with literature reports of the stereochemistry of enolate formation in aryl ketones.[11]
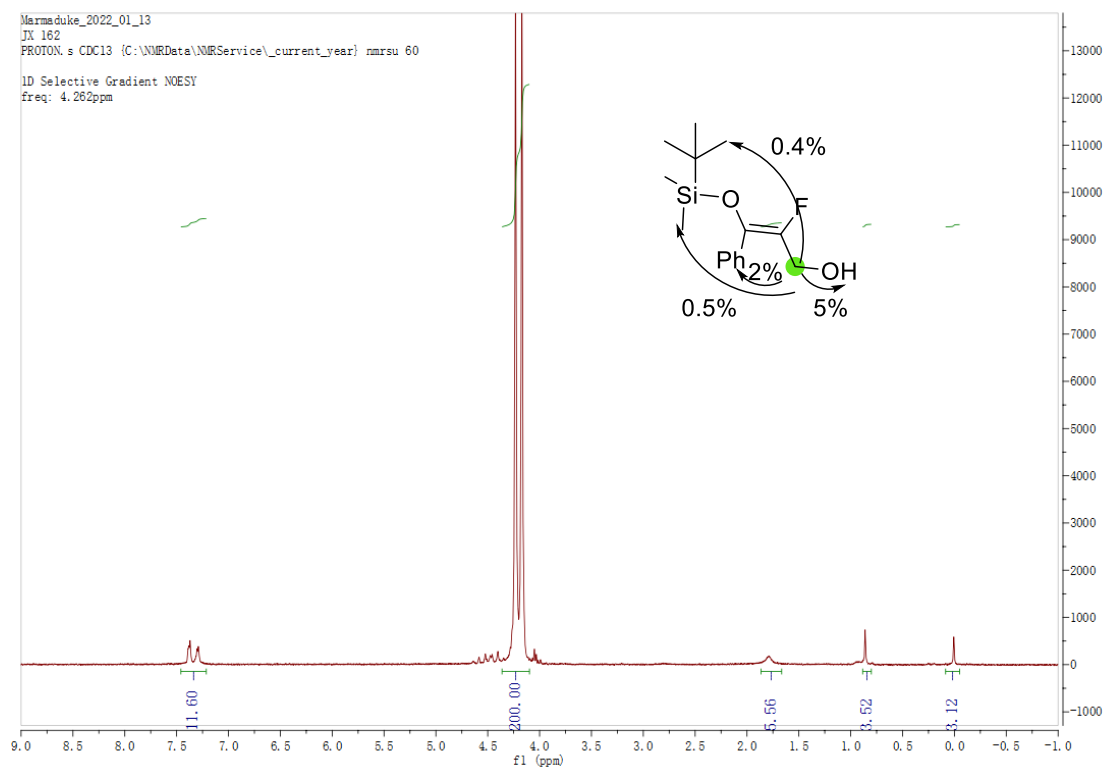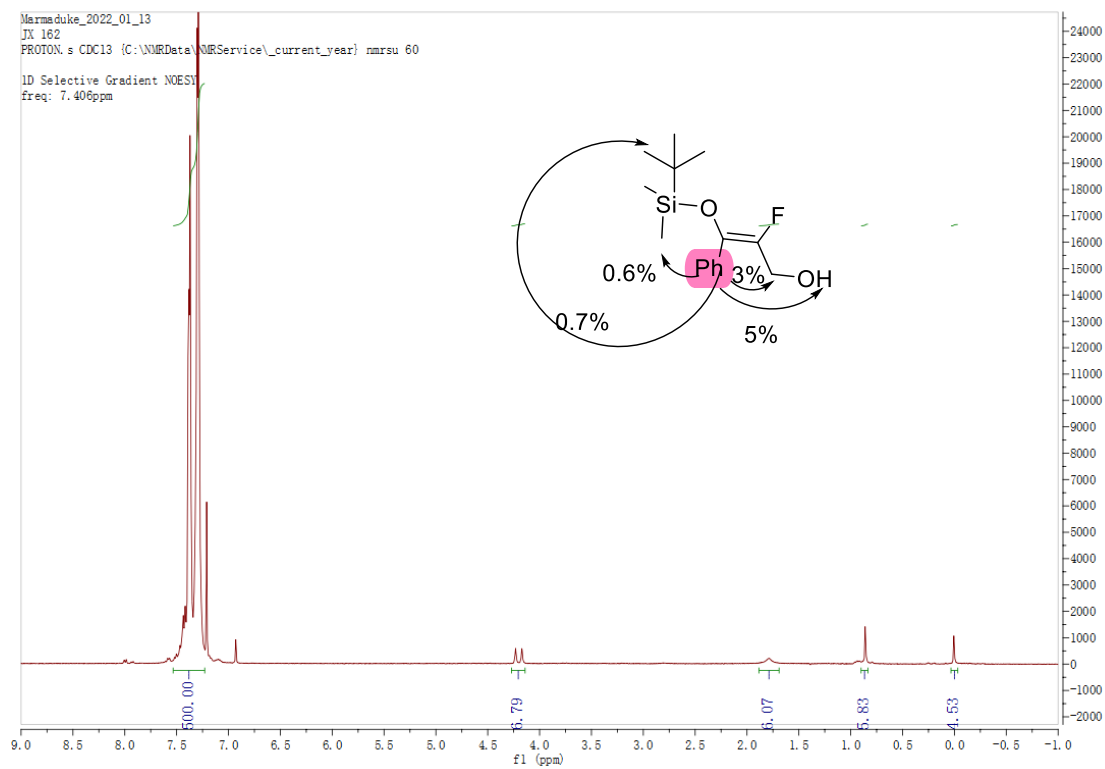
Figure 2.2.3 NOE results of **84**.

We continued our further asymmetric investigations with **L25** which showcased the best balance between conversion and enantioselectivity (entry 1, Table 2.2.4). It was assumed that the reaction temperature could play a pivotal role in the enantioselectivity of this reaction (Table 2.2.5). Therefore, **L25** was employed in the allylation of **83** at 0 °C in toluene. Pleasingly, the enantioselectivity was improved a lot without diminishing the yield (entry 2). Next, the temperature was adjusted to -20 °C, surprisingly however, both the enantioselectivity and conversion were significantly reduced (entry 3). It was concluded that 0 °C was the optimal temperature for reaction efficiency and enantiocontrol, while offering a simple experimental set-up requiring only an ice bath.

Table 2.2.5 Influence of temperature on reaction performance.
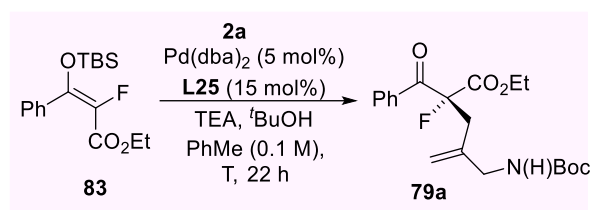
Entry	*Z/E* ratio	T	Yield (%)	*ee* (%)
1	3.3:1	rt	75%	56%
2	3.3:1	0°C	73%	73%
3	3.3:1	-20°C	22%	40%

Considering fluorinated keto ester as a standard substrate rather than silyl enol ether **83**, we still researched on the optimal conditions for **78a** on the basis of entry 2, Table 2.2.5.

Lloyd-Jones and co-workers have shown that the enantioselectivity of asymmetric allylic alkylation reactions is highly sensitive to the concentration of Trost ligand used.[58] Complex monomeric cationic **[85]⁺** readily undergoes polymerisation to generate oligomer species **{[85]⁺}ₙ** (Figure 2.2.4). There will be a competition between **[85]⁺** and **{[85]⁺}ₙ** in promoting the alkylation step, but only

[85]+ was identified to be capable of high asymmetric induction. Therefore, oligomeric cationic {[85]+}n is prone to eroding the high enantioselectivty in these reactions. Indeed, Paquin and co-workers highlighted the importance of the ratio between Pd and ligand in their studies, especially when using fluorinated substrates.[30]
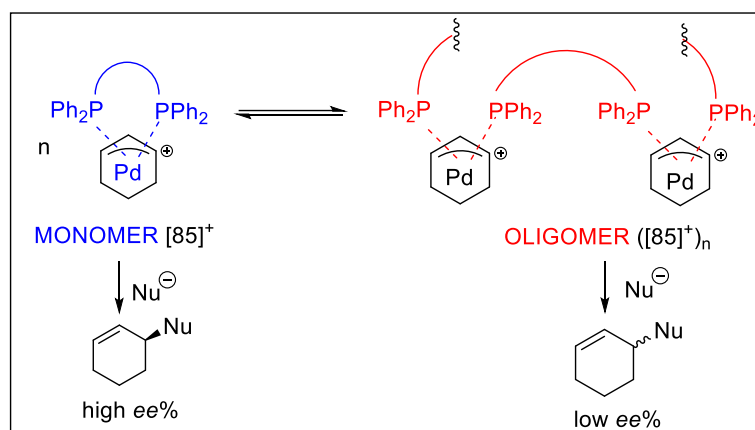
Figure 2.2.4 Influence of the ratio between Pd and ligand.

Therefore, we investigated the influence of Pd and ligand ratio on enantioselectivity (Table 2.2.6). The ratio between Pd(dba)$_2$ and **L25** was reduced from 1:3 to 1:1.1, unfortunately however, the reaction conversion was impeded although a small improvement on enantioselectivity was witnessed (entry 2). As mentioned earlier, the introduction of external base (TEA) can accelerate the reaction progress. Hünig's base was used in place of TEA in an attempt to improve conversion. The yield was found to increase to our satisfaction, and enantioselectivity was maintained (entry 3). We speculated whether better enantioselectivity could be achieved by the introduction of a chiral base or replacement of toluene by xylene. However, neither gave an improvement in *ee* but instead reduced the product yields (entries 4 and 5).

Table. 2.2.6 Optimized conditions for asymmetric synthesis of **79a**.
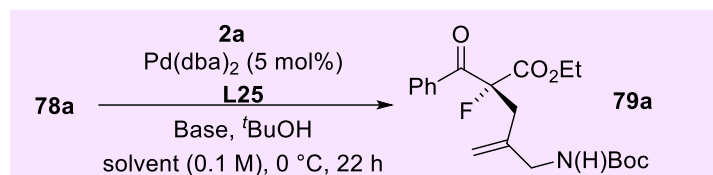
Entry	Solvent	Base (1.2 eq)	L25 (mmol%)	Yield (%)	*ee* (%)
1	PhMe	TEA	15	73%	73%
2	PhMe	TEA	5.5	42%	78%
3	PhMe	DIPEA	5.5	78%	75%
4	PhMe	quinine	5.5	52%	78%
5	xylene	DIPEA	5.5	50%	75%

2.2.3 Asymmetric synthesis of 3-fluorinated piperidine intermediates 79a-79j

With a reasonably effective set of conditions (entry 3, Table 2.2.6) in hand, we next expanded the scope of the enantioselective allylic alkylation of α-fluoro-β-ketoesters **(78a-78j).**

79a; 78%, 75% *ee* **79b;** 50% (conv 64%), 81% *ee* **79c;** 77%, 80% *ee* **79d;** 82%, 81% *ee*

79e; 68% (conv 81%), 75% *ee* **79f;** 47% (conv 72%), 77% *ee* **79g;** 83%, 86% *ee*

79h; 80%, 76% *ee* **79i;** 80%, 82% *ee* **79j;** 65%, 61% *ee*
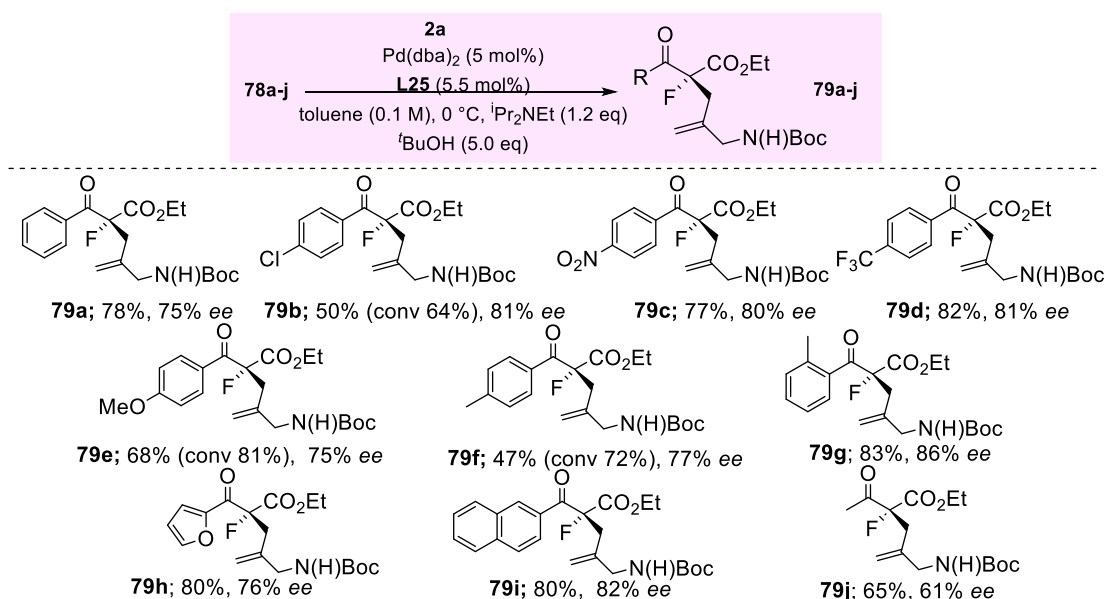
Figure 2.2.5 Scope of asymmetric allylic alkylation.

To our satisfaction, the enantiocontrol was not influenced by electronic effects and steric size of aromatic substituents (Figure 2.2.5). Introduction of weak and strong electron-withdrawing groups (**79b-79d**) into the *para* position led to enantioselectivities above 80%, although the conversion of **79b** was moderate. *Para*-methoxy and methyl (**79e and 79f**) gave a similar level of enantiocontrol. It was surprising to us that an *ortho*-methyl substituted aryl group offered the highest enantiomeric excess. In addition, the performance of the chiral catalyst with different aromatic rings was maintained with *ee* values around 80% (**79h and 79i**). In comparison with aromatic rings, **L25** did not provide products derived from keto esters bearing aliphatic substituent with the same level of enantioselectivity (**79j**).

Next, we tried to establish the absolute stereochemistry of a selection of products from asymmetric reactions of **78a-78j**. Recrystallization of **79b, 79f and 79i** from the solvent mixture of PhMe/CH$_2$Cl$_2$ gave the enantioenriched product (>95% *ee*, same enantiomer from HPLC data). The crystal structure clearly depicted the configuration of the asymmetric product and showed the major enantiomer to consistently have (*R*)-stereochemistry (Figure 2.2.6). The configuration of the products **79a-79j** were all assigned as (*R*) by inference.
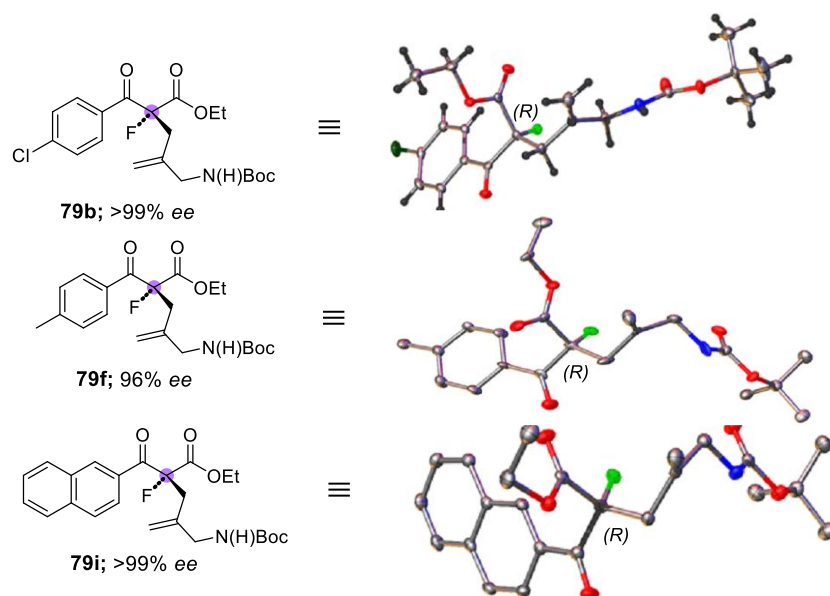
Figure 2.2.6 X-ray crystal structures of **79b, 79f and 79i**.

2.2.4 Model for the explanation of enantioselectivity

Based on the assumption that the *Z*-enolate predominates, we wanted to devise a model that could explain the stereochemical outcome of the allylation step. We first considered the conventional 'wall and flap' model designed by Trost.[24a] The nucleophile **78a** should approach the Pd π-allyl complex by its *Re* face to avoid the disfavoured steric clash between the backbone of **L25** and aromatic moiety of **2a** (Figure 2.2.7). However, the application of this model (as the *Z*-enolate) predicted the formation of the (*S*)-enantiomer thereby contradicting the X-ray crystal structure data.
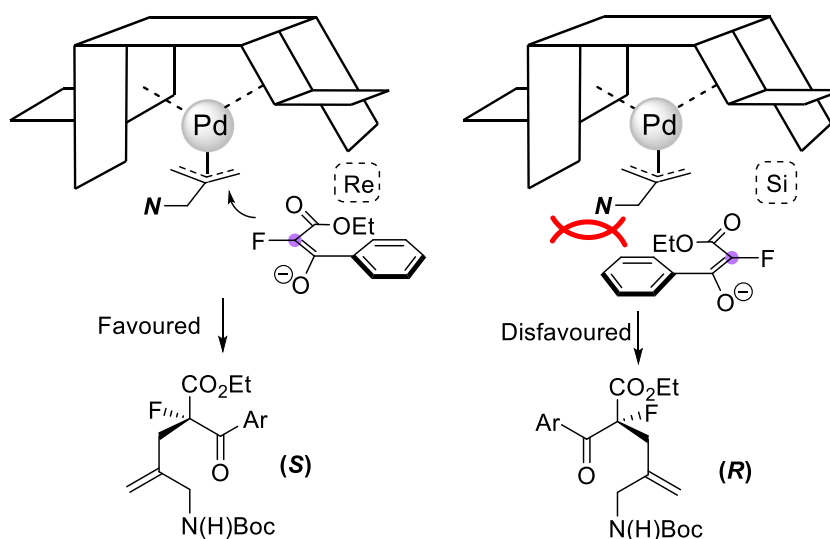
Figure 2.2.7 Application of the Trost model cartoon.

As an alternative to the 'wall and flap' model, Lloyd-Jones and Norrby devised a picture that focuses on two different binding locations (NH and CO) from the Trost-modular ligand series. We attempted to use this model for the elucidation of the origin of the stereoselectivity in **78a** (Figure 2.2.8). We assumed the reactive π-allyl complex adopted an *endo* conformation which was distant from amino group in **L25**. This model could explain the better enantiocontrol in non-polar solvents, where there was a strong hydrogen bonding between **L25** and substrate **78a** (Figure 2.2.8). However, on first inspection, there still appeared to be a key influence of *E/Z* enolate geometry of on the asymmetric allylic alkylation.

'*exo*' conformer   '*endo*' conformer

Model design elements

large '*cis*' groups may destabilise binding

Non-polar solvents may aid catalyst-substrate H-bonding

need to control enolate geometry

Figure 2.2.8 Model design.

In principle, in compound **78a**, there were two hydrogen-bonding acceptors: the ketone and ester groups, and each has been considered in turn. Figure 2.2.9 describes the possible addition modes and they are classified as 'Favoured' or 'Disfavoured' depending on whether they generate the observed major (*R*) enantiomer of product, or not. Regarding H-bonding at the ester, a strong steric clash between the aromatic ring of substrate **78a** and benzene ring from **L25** destabilized **86c** and **86d** conformers, this is alleviated by reaction through **86a/b**. Regarding binding via the ketone, in each case **86'a-86'd** there is a close contact between the keto ester aromatic ring and the ligand framework in **L25**.

Figure 2.2.9 Ester and keto hydrogen bonding to **L25**.

Thus, we assumed that **L25** coordinated to substrate **78a** via the ester group. Next, we considered the possibility of keto-enolate isomers adopting *s-cis* and *s-trans* conformations, respectively. This analysis revealed that the observed (*R*)-enantiomer derived from the corresponding *s-cis* conformation, regardless of the nature of the enolate configuration (Figure 2.2.10).
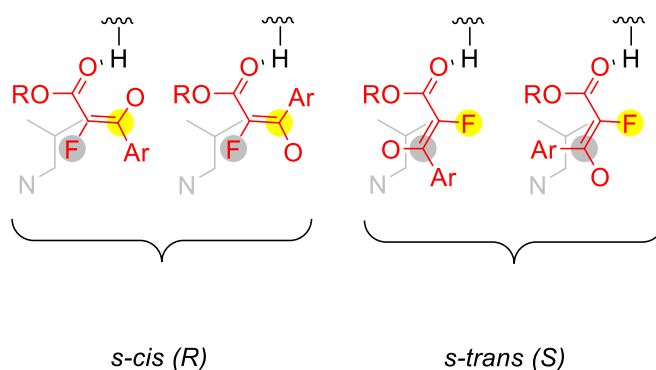
Figure 2.2.10 *S-cis* and *s-trans* conformation of **78a.**

As discussed earlier, we found that the use of different *E/Z*-silyl enol ether mixture **83** led to the similar enantioselectivity (Scheme 2.2.26). To probe this issue further, we generated both *E*-**83** and *Z*-**83** isomers in pure form as single geometric isomers accessed from cautious flash column purification and subjected these to our optimal allylation conditions. Interestingly, both reactions gave the same level of enantioselectivity in the product, albeit with quite different yields. This result is in line with our earlier finding that the major isomer *Z* enolate reacted faster than the *E* isomer (entry 1, Scheme 2.2.6). The difference in reaction rates from the two different isomers and favourable production of the (*R*)-enantiomer in both cases could originate from the steric clash between aromatic ring **78a** and benzene rings in **L25** (cf **87b, d**). Regardless, this result provided evidence that the enolate *E/Z* geometry was not necessarily responsible for enantiodivergence in the allylation of acyclic enolates (Figure 2.2.11).
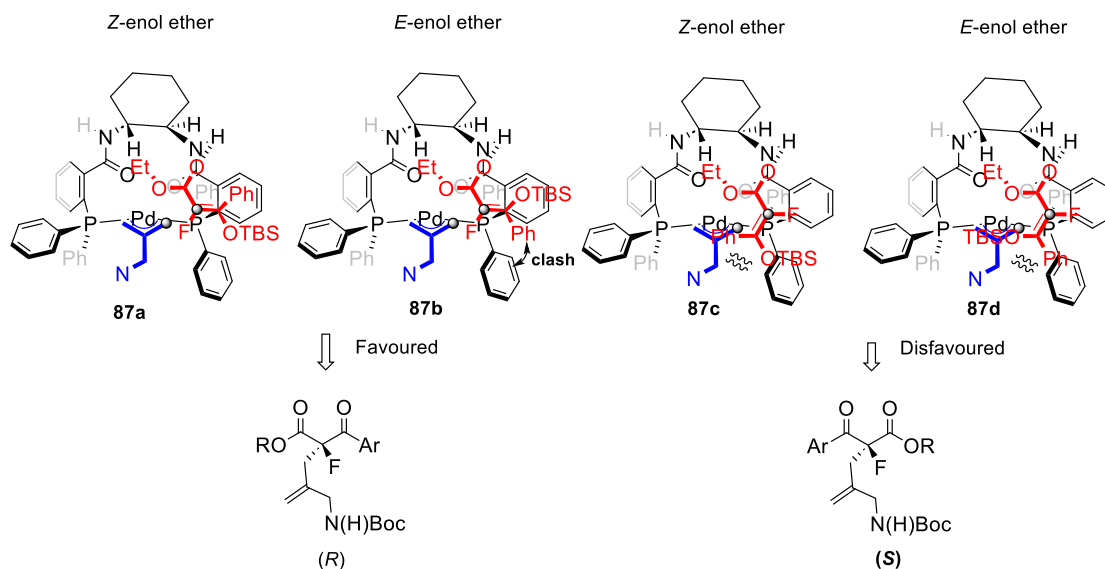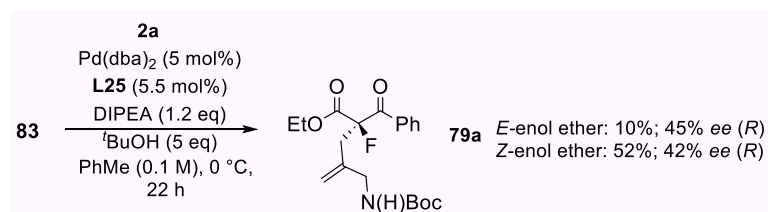
Figure 2.2.11 Reaction of *E/Z*-silyl enol ether **83**.

If the *s-cis* conformation is indeed responsible for the formation of the major enantiomer, it is reasonable to assume that induction of bulky ester group could further encourage this conformation, favouring the production of (*R*)-enantiomer through an ester 'gearing effect' (Figure 2.2.12).
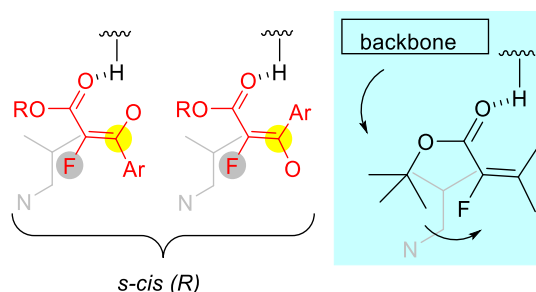
Figure 2.2.12 *t*-Butyl group encourages the formation of *s-cis* conformation.

2.2.5 Asymmetric allylic alkylation of α-fluoro-β-keto *tert*-butyl esters 89a-89f

We commenced our studies on the synthesis of **89a-14f**, which can be generally accessed in a three-step sequence (Scheme 2.2.7). Intermediates of **88a-88e** were formed by the aldol reaction between *t*-butyl acetate and aldehyde derivatives in the presence of base. Manganese (IV) oxide generated keto esters **89a-89e** and these were fluorinated by selectfluor™. The sequence was telescoped without need for purification of intermediates. As the substrate for **88f** is commercially available, it was fluorinated directly.
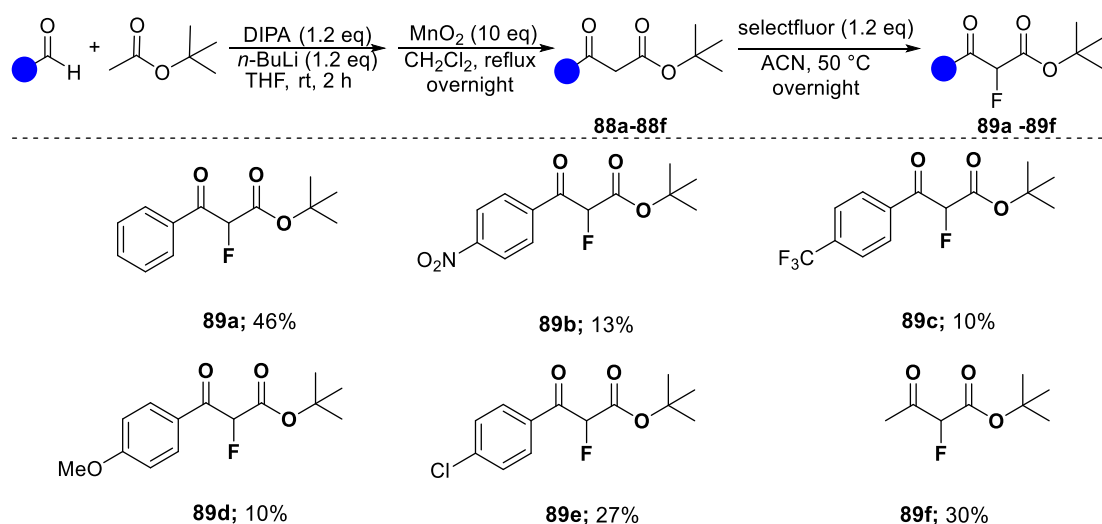
Scheme 2.2.7 Synthesis of **89a-89f.**

We conducted the asymmetric allylic alkylation of the α-fluoro-β-keto *tert*-butyl esters **89a-89f** under the optimized conditions to investigate the hypothesized 'gearing effect' (Scheme 2.2.8). In general, *t*-butyl esters **89a-89f** all showed an improvement in terms of enantioselectivity in comparison to their ethyl ester analogues. Pleasingly, the enantiomeric excess of **90f** showed a significant improvement, a leap from 61% to 81%.
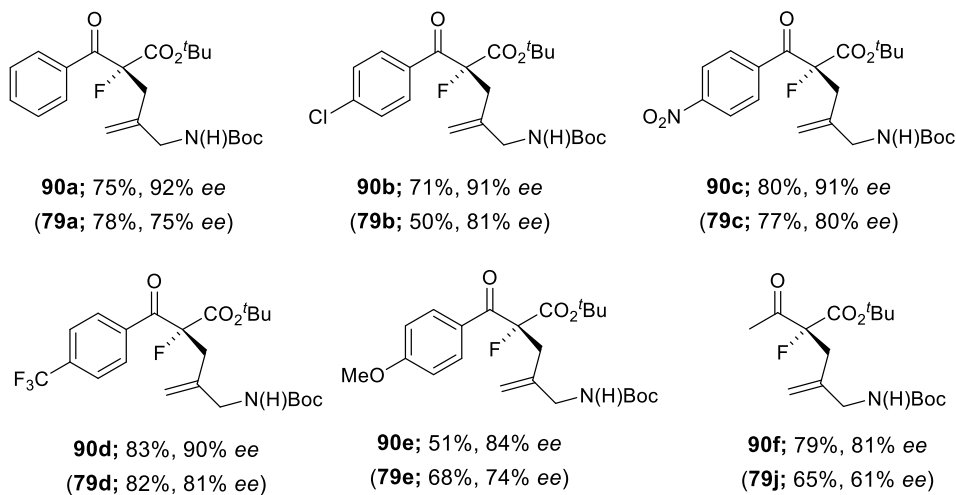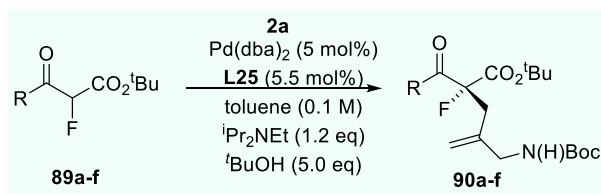
Scheme 2.2.8 Improved enantioselectivity using *tert*-butyl esters (notice: compounds in brackets are ethyl ester products).

In order to establish the absolute stereochemistry of these products, we converted enriched sample **79e** to **90e** under refluxing conditions with NaH and excess ^{t}BuOH (Scheme 2.2.9) and found the HPLC trace of this product to show the same major enantiomer as that derived from the asymmetric allylation step, indicating that the *tert*-butyl esters give the same product configuration.
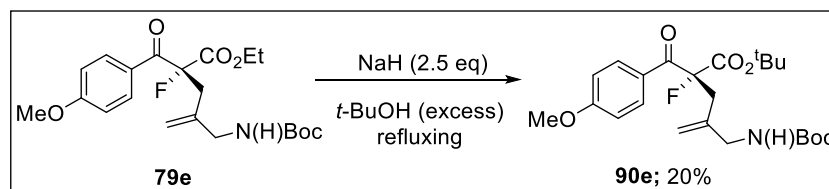
Scheme 2.2.9 Transesterification of **79e.**

2.2.6 Cyclization of 90a and downstream functionalization of 91

Treatment of **90a** with TFA led to the expected 3-fluorinated piperidine **91** (Table 2.2.7). We found that an excess amount of TFA (75 equivalents) resulted in the hydrolysis of the *t*-butyl ester group (entry 1), leading to a low yield of **91**. Surprisingly, **90a** under the refluxing conditions with hydrochloric acid, was fully converted to the enamine **92** (entry 2). We found it tricky to determine the conversion using TLC analysis because of the tailing effect triggered by TFA. Pleasingly however, diluting the reaction, shortening the time period and reduction of TFA to 50 equivalents mitigated ester hydrolysis, giving the desired product in high yield (entry 3).

Table 2.2.7 Cyclization of **90a** under TFA.
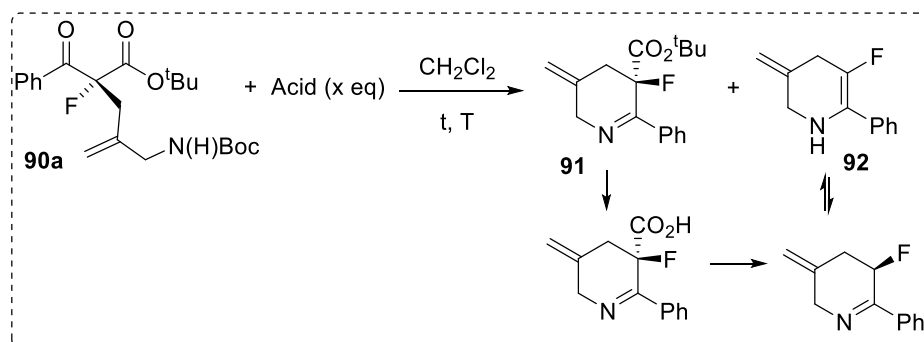
Entry	Acid	conc (M)	t (h)	T (°C)	Yield of 91
1	TFA (75 eq)	0.1	1.5 h	rt	29%
2	HCl (75 eq)	0.1	1.5 h	100 °C	--
3	TFA (50 eq)	0.05	0.5 h	rt	81%

The synthetic value of the asymmetric synthesis of **90a** was demonstrated by a gram-scale reaction. Considering **L25** is expensive, it was prepared from readily available substrates via a DMAP catalysed Steglich reaction (Scheme 2.2.10).
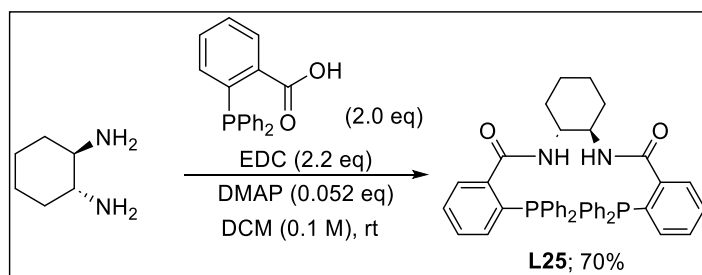
Scheme 2.2.10 Preparation of **L25**.

A scale up reaction for the synthesis of **91** was conducted in two-step sequence giving over 1 g of product in an overall yield of 71% (Scheme 2.2.11).
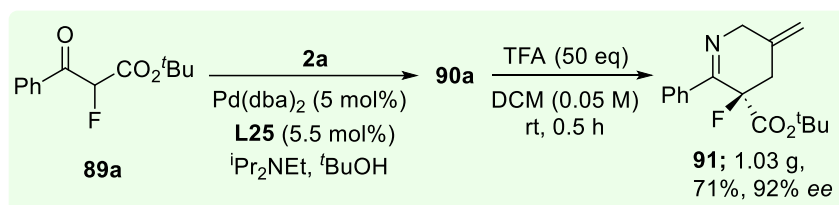
Scheme 2.2.11 Total synthesis of **91** in gram-scale.

The imine moiety of **91** was reduced by NaBH$_4$ to access piperidine skeleton **93** with high diastereoselectivity (Scheme 2.2.12). The reduction proceeded smoothly under mild conditions and gave a satisfactory yield. The stereochemistry of **93** was assigned on the basis of a related compound (**96;** discussed later).
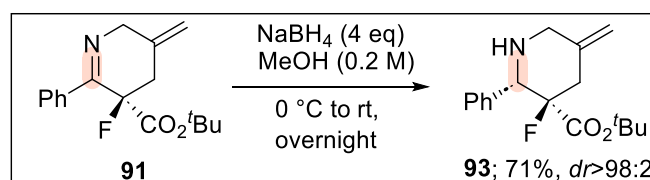
Scheme 2.2.12 Reduction of **91**.

Unfortunately, attempts to conduct an acid catalysed hydrolysis of **93** failed (Scheme 2.2.13). It is possible that the product of ester hydrolysis was not stable or the water solubility of the product prevented its isolation after work up.
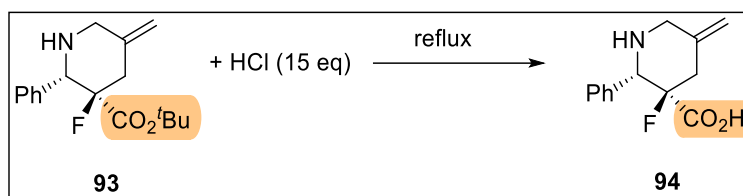
Scheme 2.2.13 Ester hydrolysis of **93**.

As hydrolysis was unsuccessful, we attempted the reduction of the ester group by DIBALH to afford the corresponding alcohol. Surprisingly however, this reaction instead gave an epoxide group as the outcome of S_N2-like reaction (Scheme 2.2.14) even through fluoride is not normally considered a good leaving group in this process. Compared to other potential route (H-F elimination followed with conjugate addition), it seems faster intramolecular S_N2 reaction is more favourable which also determines the stereochemistry of **95**.
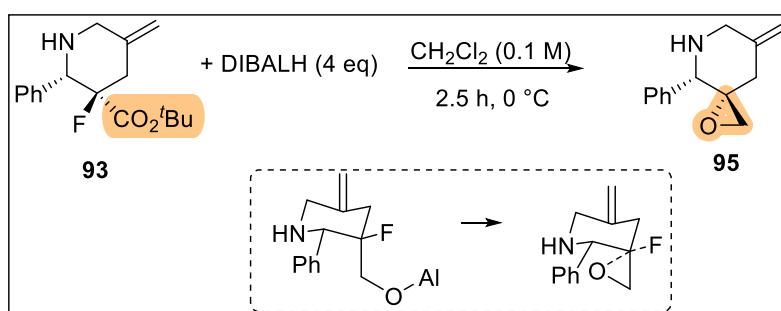
Scheme 2.2.14 Ester reduction of **93.**

Next, we attempted to introduce Boc as a protecting group for **93** and were pleased to find that this proceeded smoothly under standard conditions (Scheme 2.2.15). The stereochemistry of **96** was determined previously in our group by X-ray crystallography (albeit on a racemate). As well as acting as a protecting group, the Boc group offers a defined conformation that can help control

the stereochemistry of subsequent transformations. Specifically, the planar sp^2 nitrogen [59] results in A (1,3) allylic strain which encourages the 2-substituent to adopt a pseudoaxial orientation.
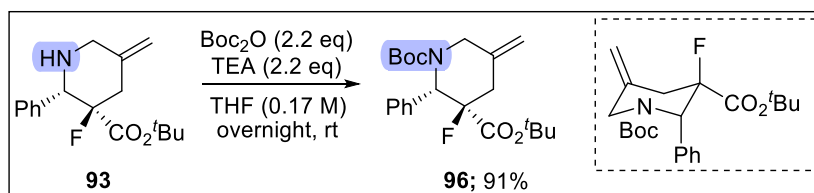
Scheme 2.2.15 Boc protection of **93.**

Ester reduction of **96** proceeded successfully without the previously observed epoxide forming side reaction, offering an effective method for introducing alcohol functionality (Scheme 2.2.16). Careful control of the stoichiometry of reducing reagent also inhibited further reduction of Boc.
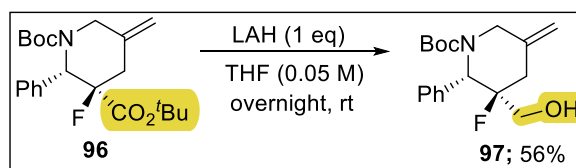
Scheme 2.2.16 Ester reduction of **96.**

We next turned our attention to functionalization of the alkene. Different methods for epoxidation of the alkene gave distinctive results (Table 2.2.8): there was no epoxidation product upon treatment with oxone. Therefore, epoxidation was conducted using an excess amount of *m*-CPBA, which gave the product in 54% yield. However, the diastereoselectivity was disappointing, which can be concluded that there is no stereoselective difference on epoxidation of *exo*-alkene moiety from behind or in front in this case.

Table 2.2.8 Epoxidation of **96**.
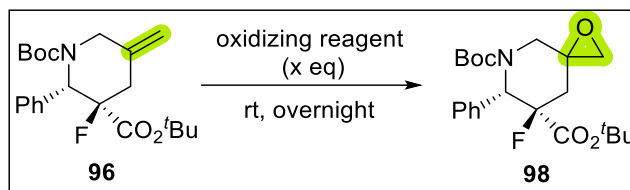
Entry	Oxidizing reagent	X (eq)	Y (%)	*dr*
1	oxone	26.0	--	--
2	*m*-CPBA	5.0	54%	3:2

The exocyclic olefin in heterocyclic compound **96** also provided a convenient platform for the formation of a difluorocyclopropane. The stereocontrol of this reaction was high with 50% yield (Scheme 2.2.17) although the configuration of the major diastereomer could not be established.
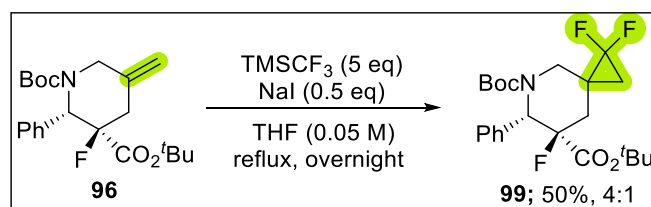
Scheme 2.2.17 Difluorocyclopropanation of **96**.

Continuing with our investigations into alkene cyclopropanation, in principle, combination of a transitional metal catalyst and a diazo compound can produce carbene equivalents, serving as a robust and versatile tool for cyclopropane synthesis. However, after subjecting **96** to TMS diazomethane in the presence of Pd(OAc)$_2$ overnight, only led to starting material being recovered (Scheme 2.2.18).
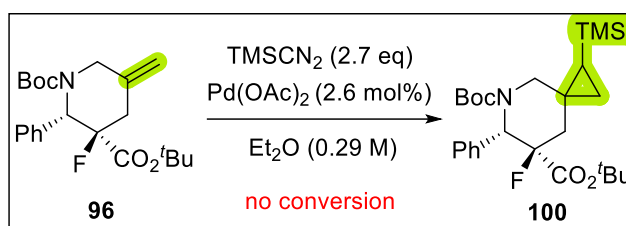
Scheme 2.2.18 TMS cyclopropanation of **96**.

We next explored the hydroboration of **96** using two different borane sources. Surprisingly, BH$_3$ and 9-BBN gave contrasting diastereoselectivity with 9-BBN more prone to attack the top face of the alkene (Figure 2.2.13).
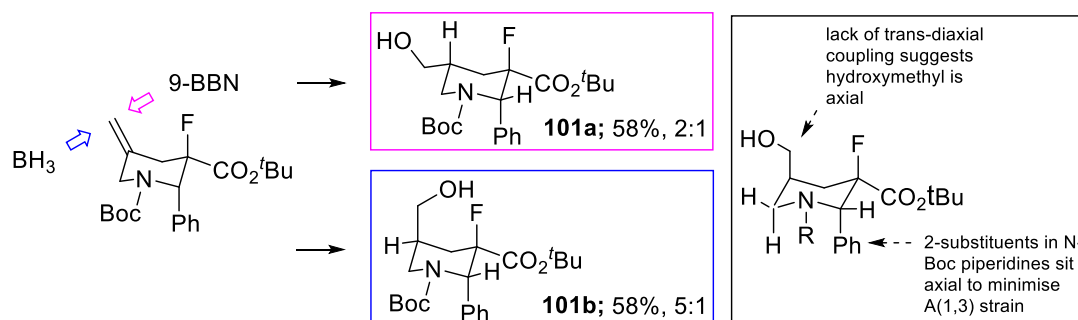
Figure 2.2.13 Hydroboration of **96**.

We assigned the diastereoisomer **101b** using peaks at 4.0 ppm and 3.0 ppm that were assigned to C^{5}H$_2$-NBoc (see page 156 and 157). Both peaks had only one large doublet coupling (J = 14.5 Hz) with the absence of *trans*-diaxial coupling indicating that the C^{4}H was in an equatorial orientation (Figure 2.2.22). Besides, the *geminal* coupling constant of the axial 2-alkyl piperidines with Boc protecting group is always around 15 Hz, which is similar to our data. Overall, the stereochemistry of the diastereomers of **101b** were tentatively assigned on the basis of similar shift and splitting patterns present in *cis/trans*-2-methyl 5-hydroxymethyl N-Boc piperidines.[60]

2.3 Conclusion

We have developed the first highly enantioselective allylic alkylation of acyclic α-fluoro-β-ketoesters, which are widely regarded as a challenging class of substrates with respect to stereoselectivity. Based on experimental evidence, we challenge the traditional ideas about the influence of *Z/E* enolate isomerisation as the origin of low enantiocontrol. Meanwhile, we put forward a rationale based on Lloyd-Jones and Norrby's model and explain the importance of *s-cis/trans* conformational mobility. This methodology allows easy preparation of useful 3-fluoropiperidine intermediates, and we demonstrate that these scaffolds are versatile in further chemoselective functionalization leading to useful building blocks for lead-like drug discovery.

Chapter 3: Studies Towards the Synthesis of Functionalized Pyrrolidines

3.0 Introduction

Since the Corey-Chaykovsky reaction was presented in the last century, organosulfur chemistry has been an active area of research in organic synthesis with their widespread application in synthetic small ring building blocks, such as epoxides, cyclopropanes, aziridines, etc. (Scheme 3.0.1).[61]

X= O, CH$_2$, NR^2, S, CHCOR^3, CHCO$_2$R^3, CHCONR$_2$, CHCN
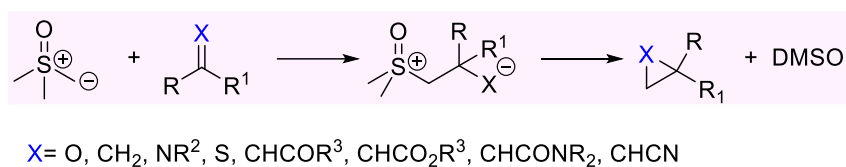
Scheme 3.0.1 Corey-Chaykovsky reaction.

Due to the pioneering work of Corey and his co-workers, sulfur ylides have become established reagents due to their stability, easy preparation, and low toxicity.[62] Their stability relies on delocalization of the electrons on the *α*-carbanion and substituents on the sulfur atom.[63] In particular, those bearing a carbonyl group at *α*-carbon are especially attractive as they are more stable in comparison with other general sulfonium or sulfoxonium ylides (Figure 3.0.1).[64]

INCREASED STABILITY   **INCREASED NUCLEOPHILICITY**
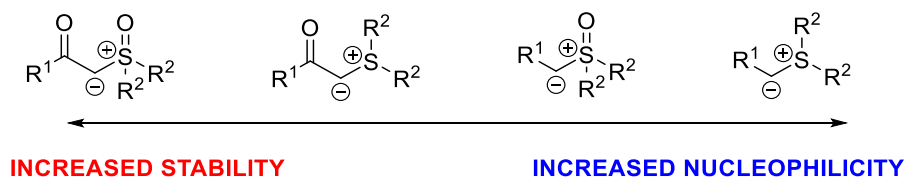
Figure 3.0.1 Stability and reactivity of sulfur ylides.

Aggarwal's group has demonstrated the potential of sulfur ylide chemistry for the synthesis of complex heterocycles. For instance, (-)-balanol was generated by the employment of vinyl sulfonium salts as a precursor (Scheme 3.0.2).[65]

71
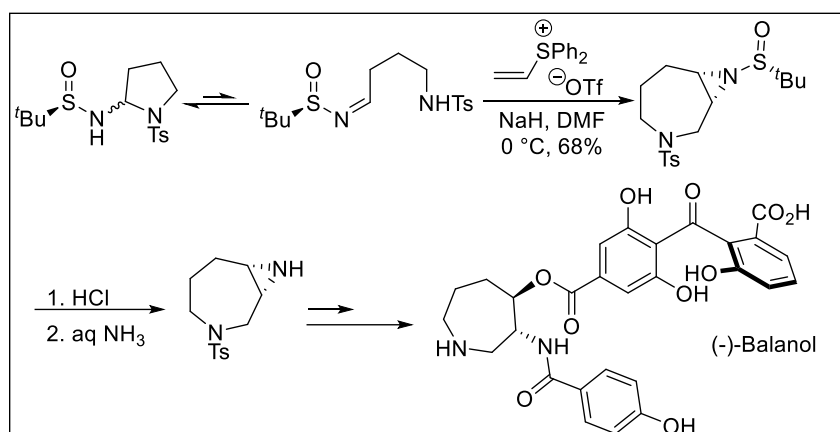
Scheme 3.0.2 Aggarwal's work on the synthesis of balanol via a vinyl sulfonium salt.

It is noteworthy that there has been limited success in the development of an asymmetric [4+1] cyclization using sulfonium ylides. However, in 2014, Li *et al.* disclosed the enantioselective trapping of a Pd dipole reagent with sulfonium ylides, affording a series of indole derivatives with excellent enantioselectivities and yields (Scheme 3.0.3).[66]
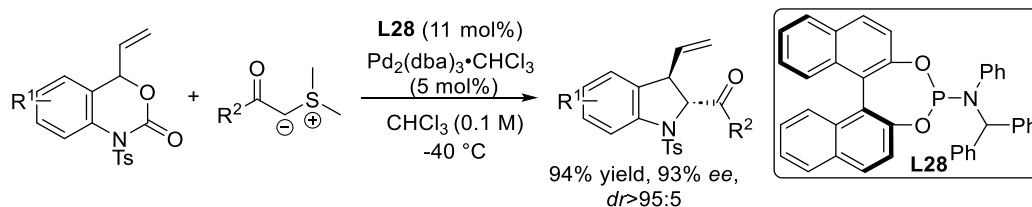
Scheme 3.0.3 Asymmetric synthesis of indole by sulfonium ylide.

This encouraging result stimulated other groups to further extend the allylation reaction of sulfur ylides for the synthesis of N-heterocyclic compounds towards a robust and versatile methodology. For example, under the employment of non-vinyl benzoxazinanones with the installation of a CF_3 moiety, a series of substituted trifluoromethyl indolones have been successfully prepared with high diastereocontrol (Scheme 3.0.4).[67]
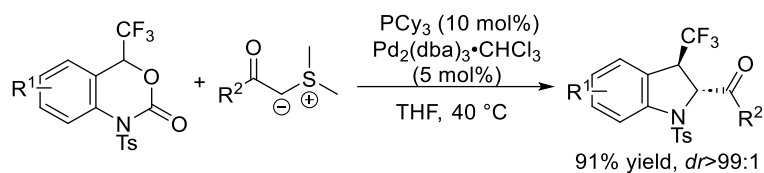
Scheme 3.0.4 Diastereoselective synthesis of CF₃-indole by sulfonium ylides.

With the aim of expanding the scope of sulfonium ylides in Pd-catalysed cyclization reactions for the construction of heterocycles, we targeted the synthesis of pyrrolidine derivatives as this motif is ranked amongst the top 5 nitrogen heterocyclic compounds in FDA approved pharmaceuticals. In addition, it is also established as a key residue in protein folding.[68]

Within the particular class, 4-methyleneproline is an important lead-like moiety in drug discovery. Although this fragment has limited occurrence in nature, its significance in enzymatic inhibitors and drugs is well known, such as inhibitors of proline dehydrogenase and tomaymycin analogues (Figure 3.0.2).[69]

inhibitors of proline   **dehydrogenase**

tomaymycin
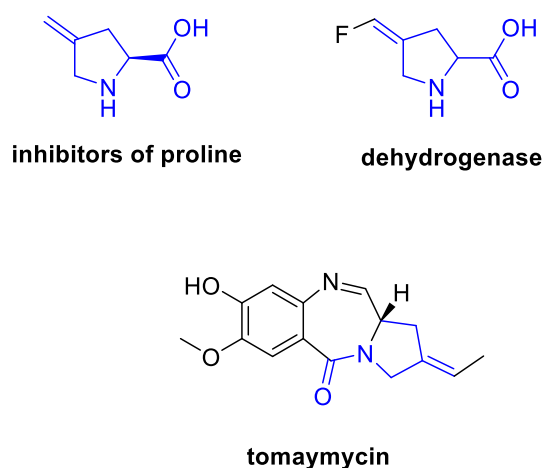
Figure 3.0.2 Bioactive compounds featuring the 4-methylene proline fragment.

Despite the pharmaceutical importance of 4-methylene prolines, relatively few methods for their synthesis exist. In the past, the synthetic methods were mostly limited to the Wittig reaction of 4-oxoproline.[70] Indeed, attempts to perform this transformation during the course of this project

using ^{t}BuOK showed that the Wittig reaction was slow and resulted in the oxidation of the ylide to Ph$_2$P(O)CH$_3$. The use of a stronger base was successful, albeit with a low yield of product. These studies highlighted that the Wittig approach to these products is not straightforward (Figure 3.0.3).
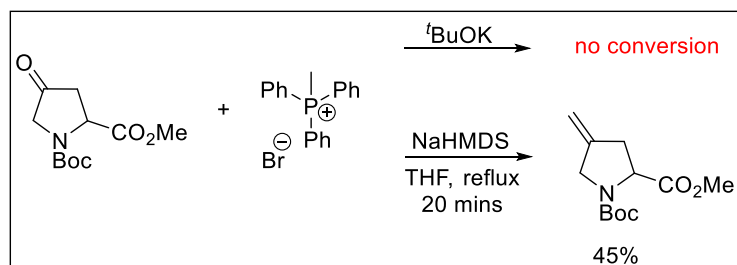
Figure 3.0.3 Wittig reaction for the production of 4-methylene proline.

Besides, [3+2] cyclization offered an alternative synthetic route as shown in Scheme 3.0.5. The intermediate was finally hydrolysed with a cation exchange resin under acidic condition. However, the substrate scope was limited, and no downstream functionalization was reported.[71]
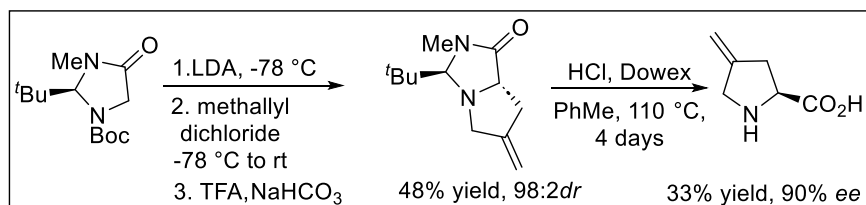
Scheme 3.0.4 [3+2] cyclization towards 4-methylene proline**.**

Motivated by these cyclization strategies, a new [4+1] cyclization based on metal catalysis was put forward recently (Scheme 3.0.6).[72] Compared to the previous methods, this approach had many advantages: straightforward synthetic route with a one-step sequence, a wide pool of substrates and useful downstream functionality. However, this method does also have drawbacks: the diazo compounds are hazardous, and rhodium is a relatively expensive metal catalyst. In addition, the authors failed to devise an asymmetric method for the synthesis 4-methylene proline analogues.
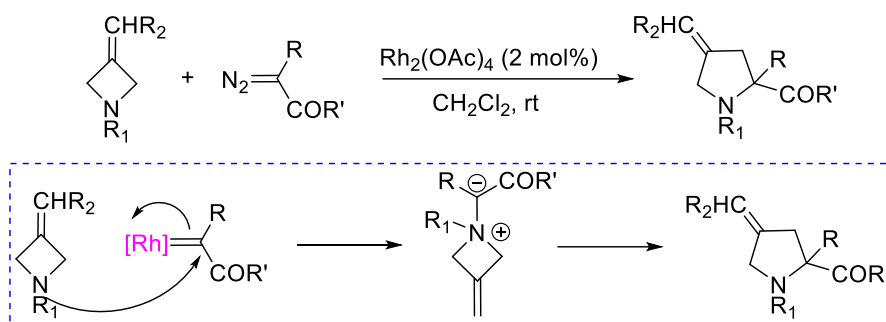
Scheme 3.0.6 [4+1] cyclization towards 4-methylene prolines.

3.1 Aim

Inspired by previous progress on palladium catalysed reactions of sulfur ylides, and asymmetric synthesis of N-heterocycles using zwitterionic reagents discussed in the previous chapter, we envisioned an efficient and simple methodology for the synthesis of 4-methyleneproline analogues through a Pd-catalysed decarboxylative [4+1] cycloaddition reaction (Figure 3.1.1).
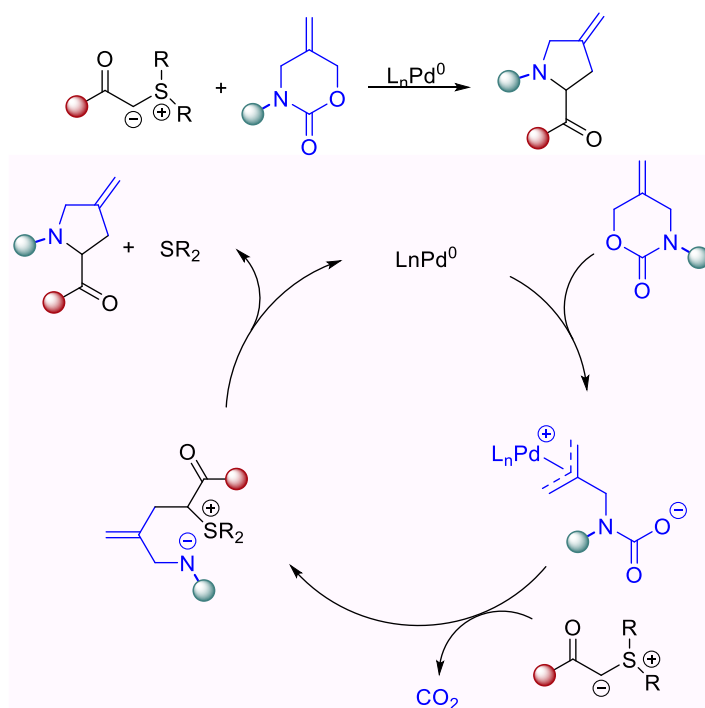
Figure 3.1.1 Proposed synthetic route towards 4-methylene proline via sulfur ylides.

The reaction is proposed to proceed via palladium coordination to the alkene of carbamate, which activates the allylic oxygen, resulting in the cleavage of the C-O bond, thus leading to the formation of Pd-π-allyl complex. The carbamate anion undergoes the decarboxylation and forms the zwitterionic reagent. Then, the α-keto-stabilized sulfur ylide acts as a soft nucleophile to react with Pd-π-allyl system, in situ generating Pd (0), followed by the nucleophilic substitution at the α carbon of keto sulfur ylide, releasing dimethyl sulfide. The route suggests that we can access 4-methylene proline derivatives in a one-pot reaction, which is simple and convenient. The success of the mechanism depends on two key steps: 1) α-keto-stabilized sulfur ylides attacking the Pd-π-allyl system; 2) 5-*exo*-tet cyclization releasing dimethyl sulfide.

3.2 Results and Discussion

3.2.0 Synthesis of α-keto-stabilized sulfur ylides

We prepared a panel of α-keto-stabilized sulfur ylides (**102a-102o**) from their corresponding α-bromoketones in a two-step sequence without any purification (Scheme 3.2.1a).
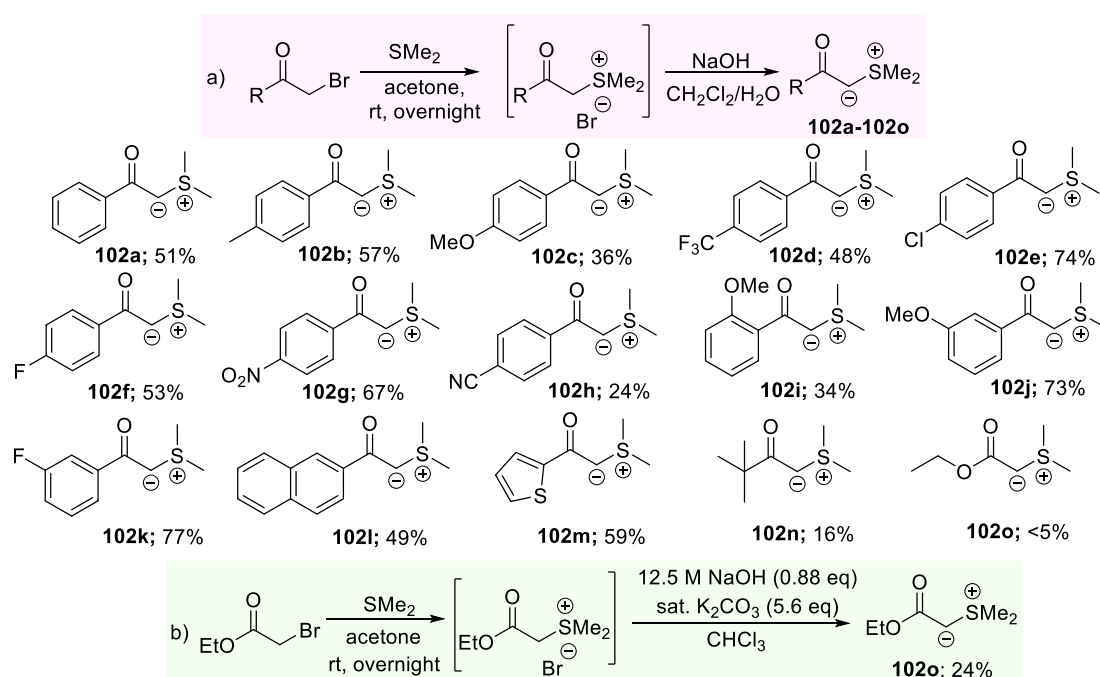
Scheme 3.2.1 Synthesis of sulfur ylide **102a-102o.**

Surprisingly, the ester sulfonium ylide **102o** could not be delivered by this route and instead, a mixture of NaOH (12.5 M) and sat. K_2CO_3 was employed to generate the ylide 24% yield (Scheme 3.2.1b).

3.2.1 Synthesis of the carbamate protected by a sulfonyl group

With a selection of sulfur ylides in hand, a series of sulfonyl substituted carbamates (**2b-2d**) were synthesized from the free N-H precursor using *n*-BuLi (Scheme 3.2.2).

2b; -NTs, 35%, 2 h
2c; -NNs, 52%, overnight
2d; -NMs, 42%, 4 h
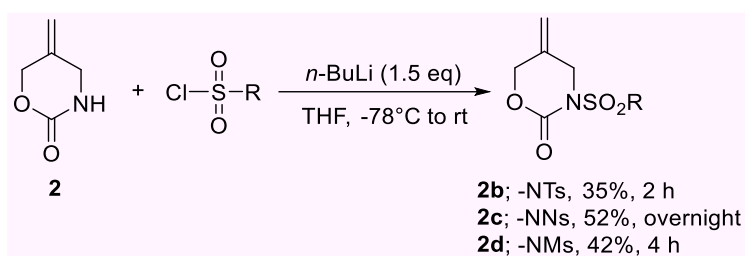
Scheme 3.2.2 Synthesis of carbamates **2b-2d**.

3.2.2 Investigation of the [4+1] cyclization reaction

We began our studies by screening different ligands and Pd sources which are commonly used in Pd alkylation by using sulfonium ylide **102a** as a standard substrate, and selected results are highlighted in Table 3.2.1. To our surprise, Pd(PPh$_3$)$_4$ did not exhibit the expected catalytic reactivity (entry 1, Table 3.2.1). Next, we turned our attention to general screen of ligands under the employment of Pd(dba)$_2$ and found **L13** to show better conversion than **L29** and **L30** (entries 2-4, Table 3.2.1). We speculated that there was perhaps a side reaction between sulfonium ylide and dba (Scheme 3.2.3). To avoid the Michael reaction, we changed Pd pre-catalyst from Pd(dba)$_2$ to [(η^3-C$_3$H$_5$)PdCl]$_2$, however, there was very little improvement on the yield (entry 5, Table 3.2.1).

To promote [4+1] cyclization, the temperature was raised to 50 °C in CH$_2$Cl$_2$ (entries 6 and 7, Table 3.2.1). Surprisingly, there was a pronounced difference between Pd(dba)$_2$ and [(η^3-C$_3$H$_5$)PdCl]$_2$

under these conditions and the yield was improved to 61% using the latter pre-catalyst (entry 7, Table 3.2.1).

Table 3.2.1. Ligand and Pd source screening and optimization.
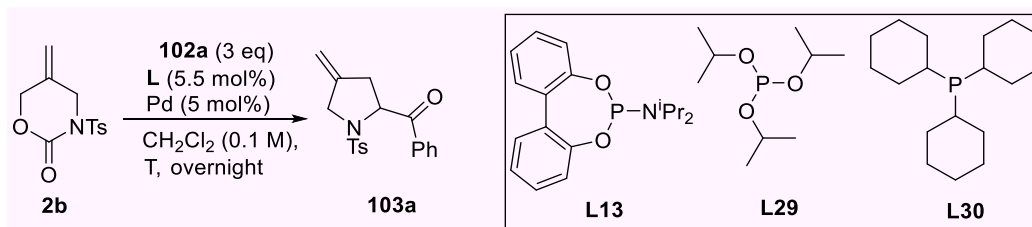
Entry	Pd source	Ligand	T (°C)	Yield (%)
1	Pd(PPh$_3$)$_4$	\	rt	0%
2	Pd(dba)$_2$	**L29**	rt	10%
3	Pd(dba)$_2$	**L29**	rt	0%
4	Pd(dba)$_2$	**L30**	rt	0%
5	[(η^3-C$_3$H$_5$)PdCl]$_2$	**L13**	rt	12%
6	Pd(dba)$_2$	**L13**	50 °C	48%
7	[(η^3-C$_3$H$_5$)PdCl]$_2$	**L13**	50 °C	61%
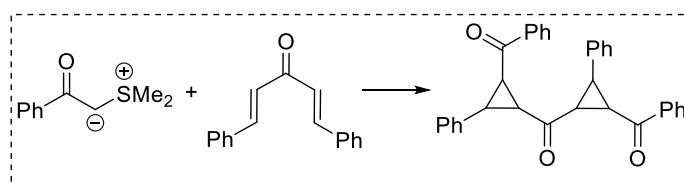
Scheme 3.2.3 Potential 1,4-addition reaction between α-keto-stabilized sulfur ylide and dba.

Given that an increase in temperature offered an improvement in the yield, we screened alternative higher boiling solvents, disappointingly however, these failed to give any conversion to product under refluxing conditions (Table 3.2.2).

Table 3.2.2. Investigation of solvents.
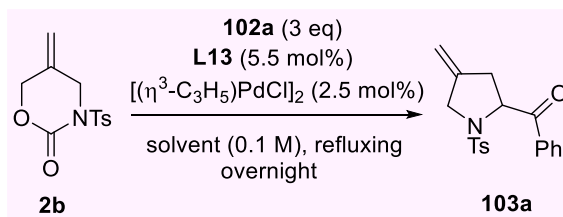
Entry	Solvent	Yield (%)
1	CH_2Cl_2	61%
2	DCE	0%
3	PhMe	0%
4	DMF	0%
5	NMP	0%
6	MeOH	0%
7[a]	CH_2Cl_2	48%

[a] 1.5 eq of sulfur ylide **102a** used in this case.

The sensitivity of this reaction towards solvent is surprising and while origin is unclear, it is known that sulfur ylides can decompose via a Wolff rearrangement (Scheme 3.2.4).[73] Regardless, the solvent screening results indicated that CH_2Cl_2 was the most effective. Considering economy, the sulfonium ylide **102a** was reduced to half amount but with a loss of conversion in this case (entry 7, Table 3.2.2).
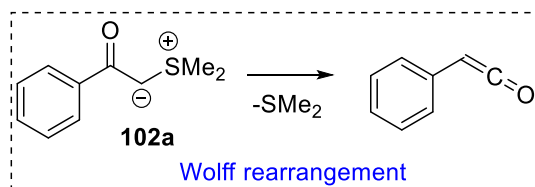
Scheme 3.2.4 Potential side reaction from Wolff rearrangement.

3.2.3 The scope of dimethyl sulfonium ylides reacting with carbamates

Next, we conducted the cyclization reaction between sulfur ylide **102a** and a series of carbamates (Scheme 3.2.5). Surprisingly, we only observed products when using sulfonyl protected carbamates (**2a-2d**). The Boc-carbamate was ineffective, and we also employed the carbamate bearing a free NH **2**, however, there was no conversion in this case either. Therefore, we can conclude that the sulfonamide played a pivotal role in the reaction and propose that stronger electron withdrawing effect of protecting group can stabilize the nitrogen anion of the decarboxylative intermediate.
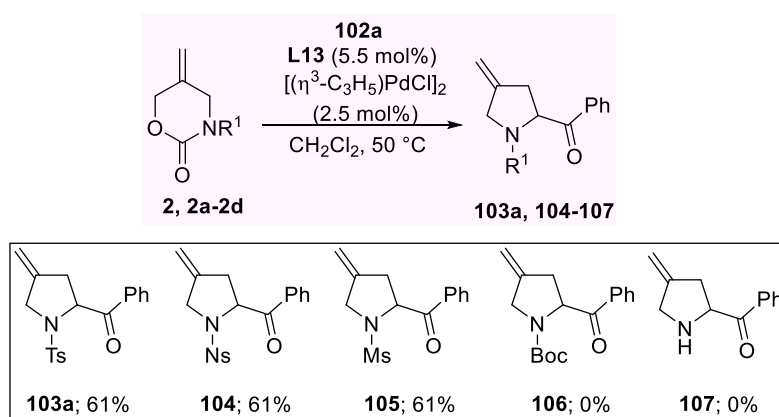
Scheme 3.2.5 Cyclization reaction of dimethyl sulfonium ylide **102a** and different carbamates.

Next, with the optimal reaction conditions in hand, we investigated the scope of the Pd catalysed cyclization of the carbamate **2b** and sulfur ylides **102b-102o** (Scheme 3.2.6). A range of sulfur ylides reacted smoothly to form the corresponding 4-methylene pyrrolidines. To be more specific, reactions of *para* substituted aromatic sulfur ylides containing electron-donating groups, Me and OMe gave high yields (**103b-103c**). In addition, weakly electron-withdrawing groups, CF$_3$, Cl and F were successful, giving similar levels of yields (60%-79%). When the aromatic ketone sulfur ylides are substituted by stronger electron-withdrawing groups, for example, NO$_2$ and CN, the yields are diminished to 10-27% with low conversions. Surprisingly, the aromatic ylide substituted by *ortho*-methoxy **102i** was not tolerated well in spite of the fact that the *meta-analogue* furnishing the corresponding product **103j** with 61% yield. In the same way, the ylide with a *meta*-F substituted phenyl group showed a similar yield (**103k**). To conclude, both the electronic nature and the

position of the substituents on the aromatic group had a remarkable effect on the reactivities. Satisfactorily, different aromatic sulfur ylides delivered desired products **103l-103m** in 57%-60% yields. Finally, and to our disappointment, alkyl and ester functionalized products **103n-103o** did not provide satisfactory yields under these conditions because of low conversion of the carbamate.
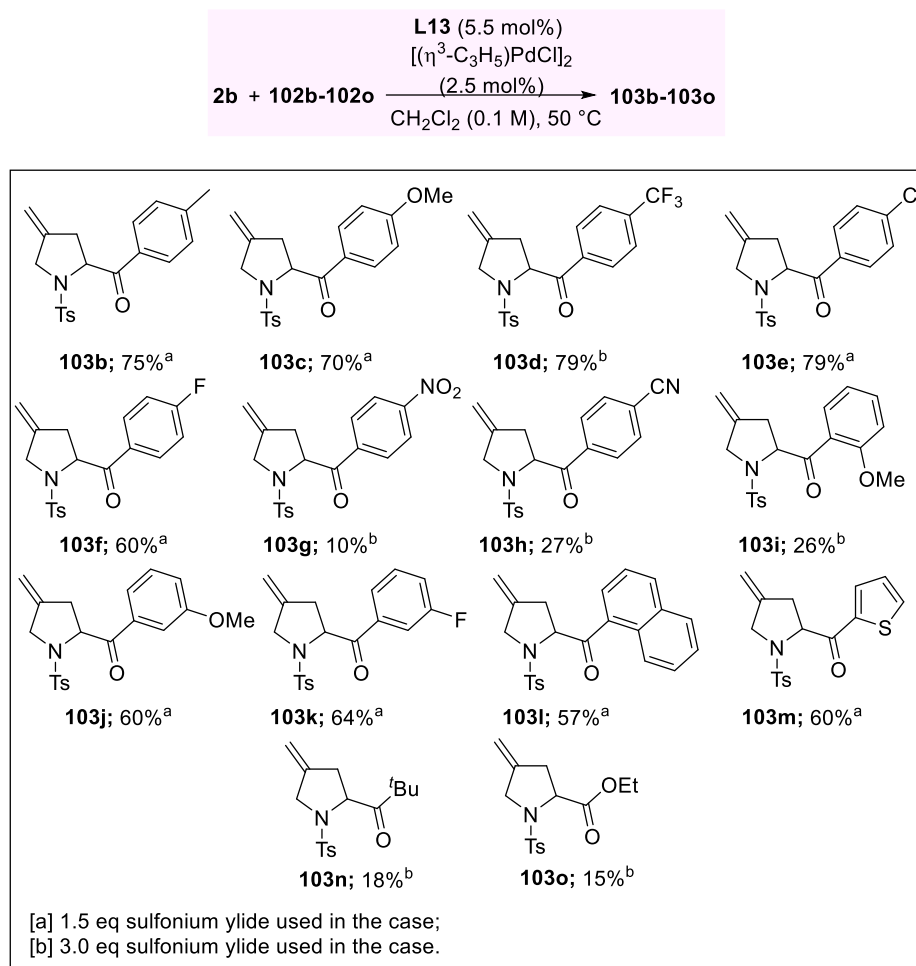
Scheme 3.2.6 Scope of [4+1] annulation.

Initially, it was hypothesized that low yields may arise due to a side reaction between the product and excess sulfonium ylide in the presence of the Pd catalyst (Scheme 3.2.7). However, it was found that the substrate was not consumed when exposed to sulfur ylide and catalyst. Therefore, we can conclude that different sulfonium ylides reacted with the carbamate with different levels of efficiency.
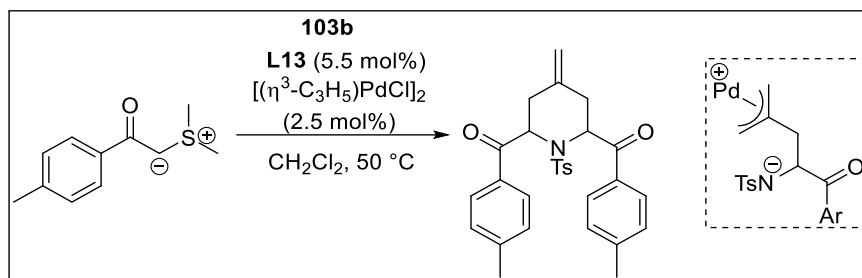
Scheme 3.2.7 Potential [5+1] side reaction between 4-methylene pyrrolidine and excess sulfonium ylide.

3.2.4 The scope of diphenyl sulfonium ylides in the cyclization reaction

With the aim of resolving the issue of low conversion between carbamate and the ylides bearing an ester or ketone group, we endeavored to utilize a series of ylides bearing different sulfonium groups, as well as a variation of our ylide generation method (Table 3.2.3).

First, we tried the sulfonium salt in the hope that ylide **102o** would be generated in situ, however, there was no conversion in this case (entry 1, Table 3.2.3). Instead, still using the sulfonium salt as the reactant, we performed the reaction with triethylamine but disappointingly, no product was delivered (entry 2, Table 3.2.3). Sulfoxonium ylide **102o.ii** is a more electron deficient analogue of the dimethyl sulfonium ylide. Disappointingly however, when used in the cyclization, the conversion was still low (entry 3, Table 3.2.3). Müller and co-workers reported that there was decomposition of **102o** during transition-metal catalysed reaction of styrene.[74] We explored the sulfonium salt **102o.iii** and were pleased to find that this significantly improved conversion (entry 4, Table 3.2.3).

Table 3.2.3 Screening different sulfur ylides for the production of 4-methylene proline **103o.**
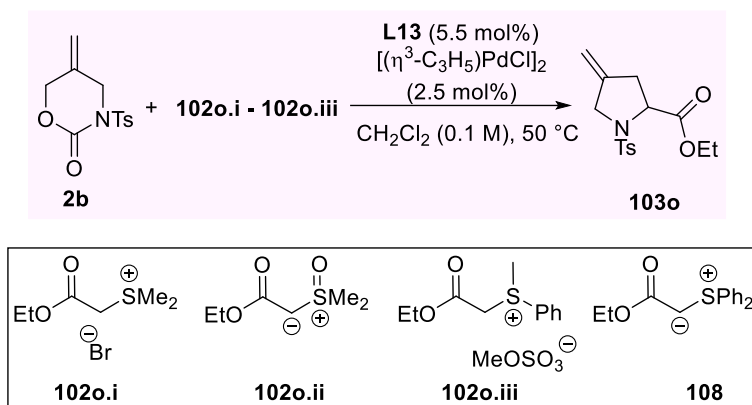
Entry	Ylide	Additive	Conv. (%)	Yield (%)
1	**102o.i**	--	--	--
2	**102o.i**	TEA	--	--
3	**102o.ii**	--	<20%	13%
4	**102o.iii**	--	<40%	26%

This promising result (entry 4, Table 3.2.3) pointed us in the direction of making the diphenyl sulfonium ylide. The precursor of **108** was prepared from the reaction of diphenyl sulfide with ethyl bromoacetate in the presence of $AgBF_4$. When the salt was deprotonated by TEA in EtOH, a side reaction occurred with the production of an *E/Z* mixture of ethyl maleate (which could be confirmed from diagnostic peaks on the ^1H NMR spectrum: δ 6.87 and 6.24) and its precursor ylide (which could be detected by LC-MS analysis $[M+H]^+$: 359.1319). Alternatively, NaH in anhydrous media was applied to the production of the diphenyl sulfonium ylide **108**, this was successful and there were almost no impurities detected (Scheme 3.2.8).
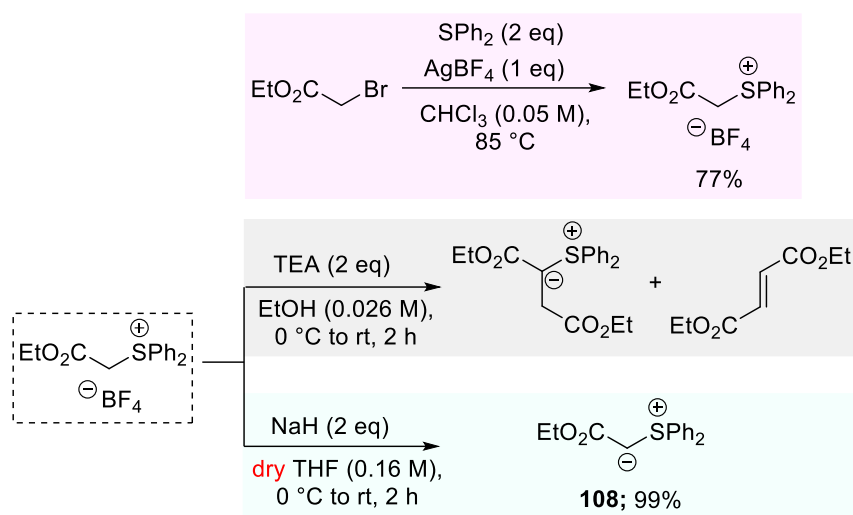
Scheme 3.2.8 Synthesis of diphenyl sulfonium ylide **108.**

Subjection of sulfonium ylide **108** to the cyclization led to full conversion, albeit the yield of product was only 46%. Analysis of the reaction mixture showed that products arising from carbamate dimerization and ylide dimerization were also present (entry 1, Table 3.2.4). To alleviate these side reactions, we added sulfonium ylide portionwise or added more equivalents of carbamate. Unfortunately, the yields were not improved in either case (entries 2-3, Table 3.2.4). Notably, there was an instant production of ethyl maleate upon the addition of ylide to the reaction mixture (as judged by TLC analysis) indicating that this is a decomposition pathway for the ylide. Next, the temperature was lowered to room temperature to resolve the issue of carbamate dimerization, it was pleasing to find the yield was 57% (entry 4, Table 3.2.4). However, the reaction proceeded slowly when conducted at 0 °C with almost no desired product (entry 5, Table 3.2.4). Encouragingly, the yield was improved to 65% when **108** was prepared freshly and used immediately (entry 6, Table 3.2.4).

Table 3.2.4 Optimal conditions for the reaction between **2b** and **108**.
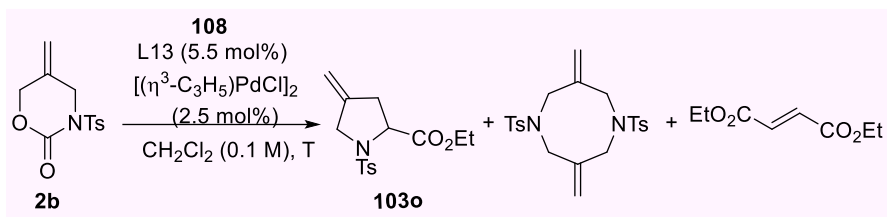
Entry	108:2b	T (°C)	Yield (%)
1	1.5:1	50 °C	46%
2	0.75+0.75:1	50 °C	40%
3	1:1.3	50 °C	50%
4	1.5:1	rt	57%
5	1.5:1	0 °C	17%
6	1.5:1 (fresh)	rt	65%

To ensure that the diphenyl sulfonium ylides are generally applicable in our cyclization reaction, we briefly explored the scope of their reaction with carbamate **2b**. Pleasingly, the use of diphenyl sulfur ylide **109** also delivered **110** with an enhancement of the overall yield (Scheme 3.2.9).
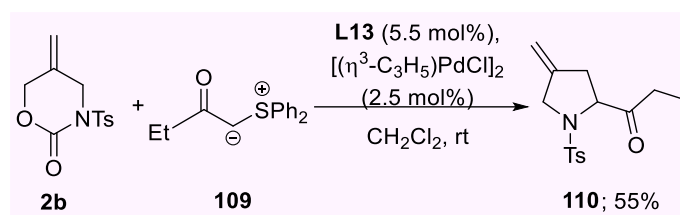
Scheme 3.2.9 Cyclization reaction of diphenyl sulfonium ylide **109** and carbamate **2b**.

Meanwhile, **103g** bearing an aromatic electron-withdrawing group was produced in moderate yield at 50 °C (Scheme 3.2.10).
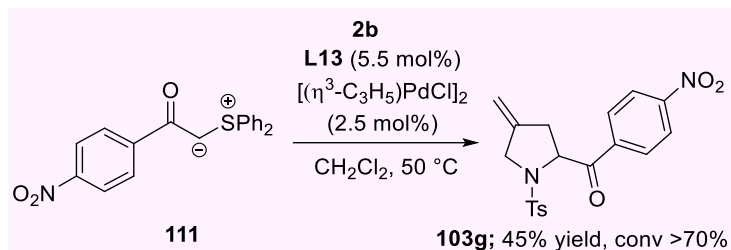
Scheme 3.2.10 Cyclization reaction of diphenyl sulfonium ylide **111** and carbamate **2b**.

On the basis of better reaction performance of a series of diphenyl sulfonium ylides, the decomposition of diphenyl sulfonium ylide is harder than dimethyl sulfonium ylide in terms of stability. On other hand, the annulation step will be facilitated with readily loss of diphenyl sulfide.

3.2.5 Synthesis of enantiopure 4-methylene pyrrolidine

We endeavoured to find an optimal chiral ligand for the synthesis of enantiopure 4-methylene pyrrolidine. Encouraged by the Li's result as mentioned in Scheme 3.0.3, **L1** was investigated first. Unfortunately, however, there was no enantioselectivity (entry 1, Table 3.2.5). Next, we turned our attention to Trost ligand **L25** which gave high enantiomeric excess in the formation of fluorinated piperidine at 0 °C, however, no product was observed in this case, even after the addition of base (entries 2-3, Table 3.2.5). Although a low conversion was achieved at reflux, the enantioselectivity was still 0% (entry 4, Table 3.2.5). From these results, we can conclude that neither BINOL-derived chiral phosphoramidite or Trost ligands exhibited any enantioselectivity in the formation of the 4-methylene pyrrolidine product **103a**.

Table 3.2.5 Asymmetric synthesis of 4-methylene pyrrolidine **103a** by using different chiral
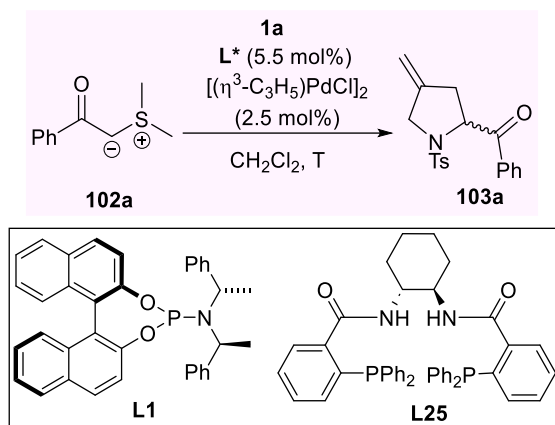
ligands.

Entry	Ligand	T (°C)	Conv. (%)	Yield (%)	*ee* (%)	Additive
1	L1	50 °C	100%	69%	0%	--
2	L25	0 °C	--	--	--	--
3	L25	0 °C	--	--	--	piperidine
4	L25	50 °C	Not determined	20%	0%	--

Inspired the work of Gordillo regarding the highly diastereoselective epoxidation by using chiral

oxazolidinone sulfonium ylides,[75] we envisioned that chiral oxazolidinone sulfur ylides could also

be efficient chiral auxiliaries for an asymmetric variant of our cyclization reaction. Oxazolidinone

sulfur ylide **112** was delivered smoothly in two-step sequence, giving 57% yield as shown in Scheme

3.2.11.
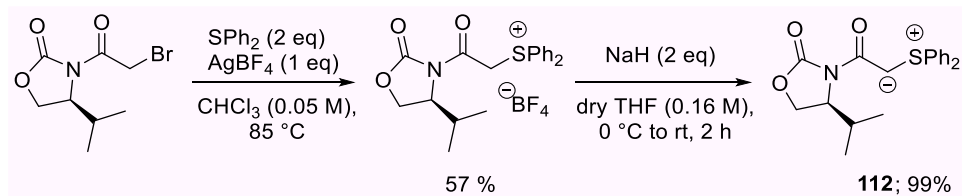
Scheme 3.2.11 Synthesis of chiral oxazolidinone sulfur ylide **112**.

Indeed, by employing oxazolidinone substituted sulfonium ylide, the desired product **113** was

isolated in 76% yield with high diastereocontrol. The diastereoselectivity was estimated from LC-MS analysis initially (Scheme 3.2.12).
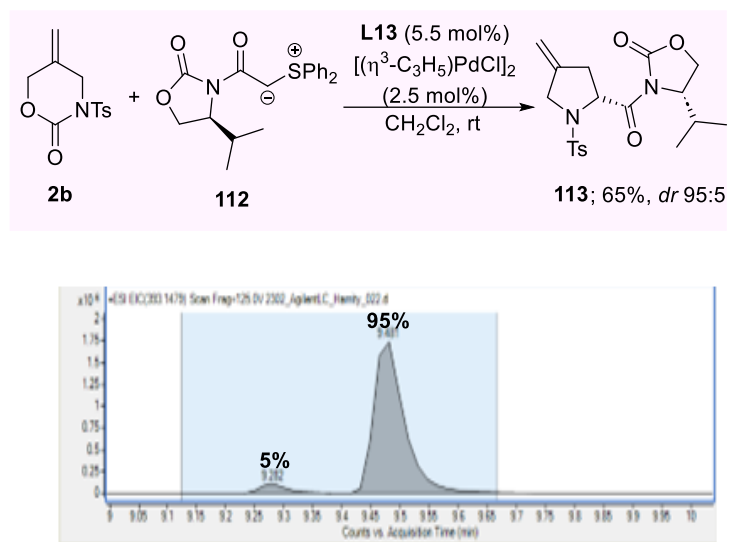
Scheme 3.2.12 Asymmetric synthesis of 4-methylene pyrrolidine **113**.

3.2.6 Employing substituted carbamates in the cyclization reaction

The methodology for the synthesis of 4-methylene pyrrolidine derivatives containing an exocyclic alkene is robust and versatile. However, we wanted to expand the scope of carbamates that participated in this process, in particular with the goal of obtaining more substituted proline derivatives (Scheme 3.2.13). Using alkene substituted carbamates leads to two possibilities of sulfonium ylide insertion: if path a is operative, there is the potential to produce more substituted alkene products. In this case, *E/Z* mixtures ($R_2 \neq R_3$) could arise; in contrast, path b leads to branched products, and in this case we might expect to observe diastereoisomers.
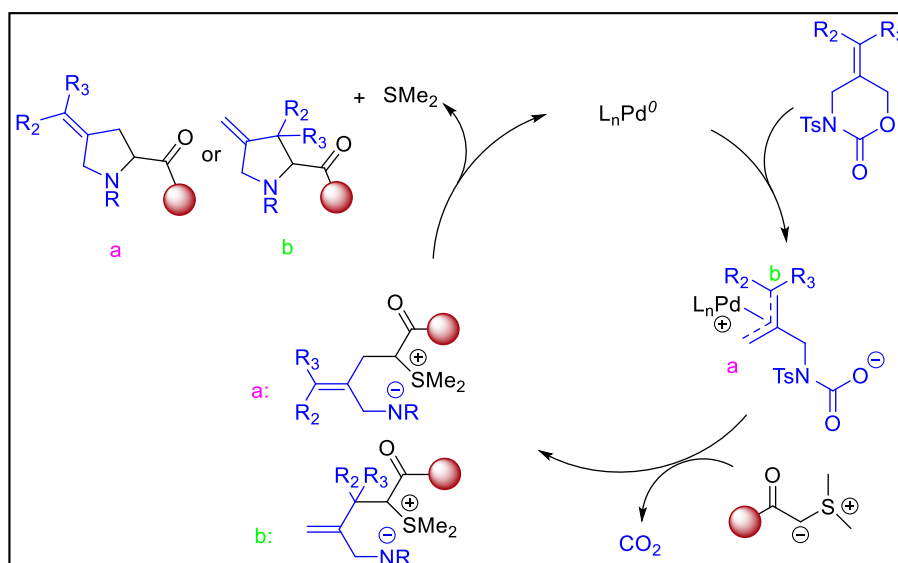
Scheme 3.2.13 Proposed mechanism for the employment of substituted carbamates.

In the past, our group synthesized phenyl substituted carbamate **118** in a 5-step sequence with an overall yield of 7% (Scheme 3.2.14).[76] Diol **115** was synthesized in two steps: Baylis-Hillman adduct **114** was produced from benzaldehyde and methyl acrylate in the presence of the tertiary amine DABCO for 3 days, followed by the ester reduction with LiAlH$_4$ to generate **116**. However, there was a 1,2-reduction by-product in this last step, which impacted the efficiency of this sequence. In general, this route is time-consuming and doesn't allow the efficient generation of substituted carbamate analogues.
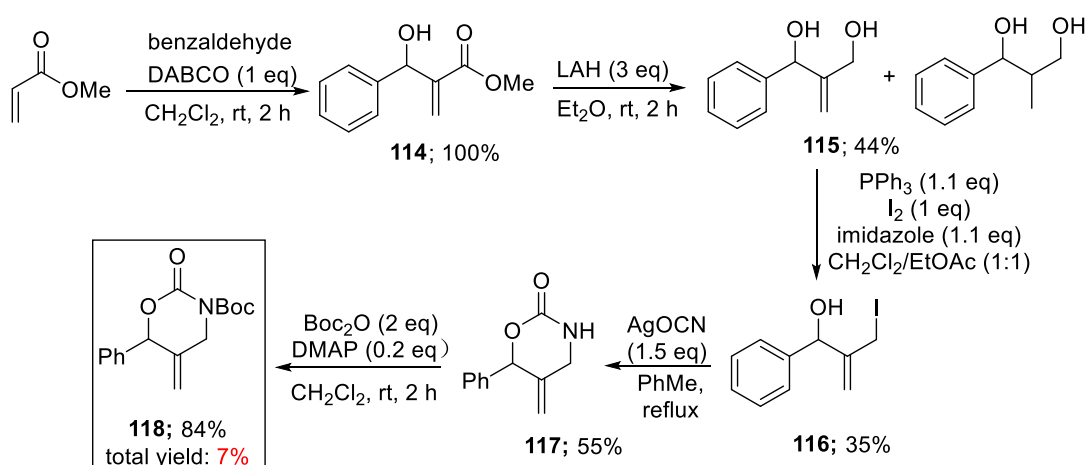
Scheme 3.2.14 Our group's previous synthesis of substituted carbamate **118.**

The privileged choice for the synthesis of substituted alkenes is cross-metathesis under the employment of Grubbs catalyst. In an effort to minimize steric effects in the nucleophilic attack from the sulfonium ylide towards the intermediate Pd π-allyl complex, we decided to synthesize the methyl substituted carbamate rather than the phenyl substituted derivative. In order to avoid the coordination between Ru catalyst and polar functional groups in the carbamate, Ti(OiPr)$_4$ was added as a co-catalyst. 2-Methyl-2-butene is a commercial source of methyl substituted alkene fragments in Grubbs metathesis reaction and so we investigated the cross metathesis of this substrate. In the event, the reaction proceeded but we found both 1,1-dimethyl substituted carbamate **119** and mono-methyl analogue **120** were formed in similar yields (Scheme 3.2.15).
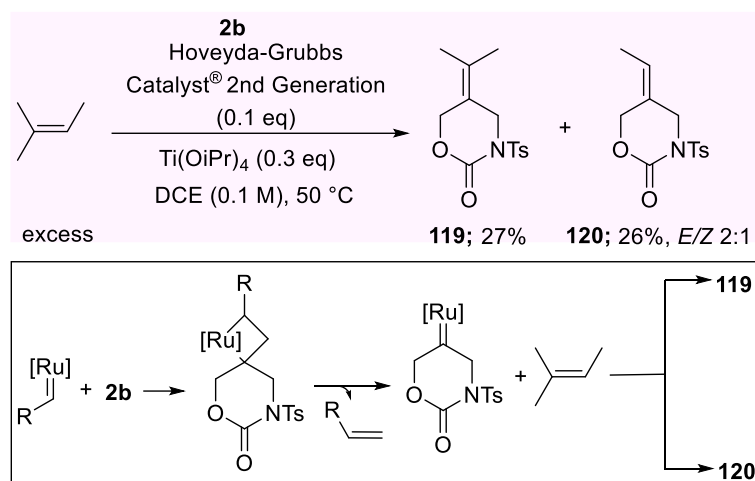
Scheme 3.2.15 Grubbs metathesis of carbamate **2b**.

We next explored the performance of the substituted carbamates **119** and **120** in the [4+1] cyclization reaction. Subjection of the carbamates to the optimized conditions for ester sulfonium ylide **108** led to no conversion in either case. It therefore appears that the alkene substituted carbamates do not react with low valent Pd catalysts (Scheme 3.2.16). It is assumed that steric hindrance of Pd π-substituted allyl moiety impeded nucleophilic attack from α-carbon of keto-sulfonium ylide **108**.
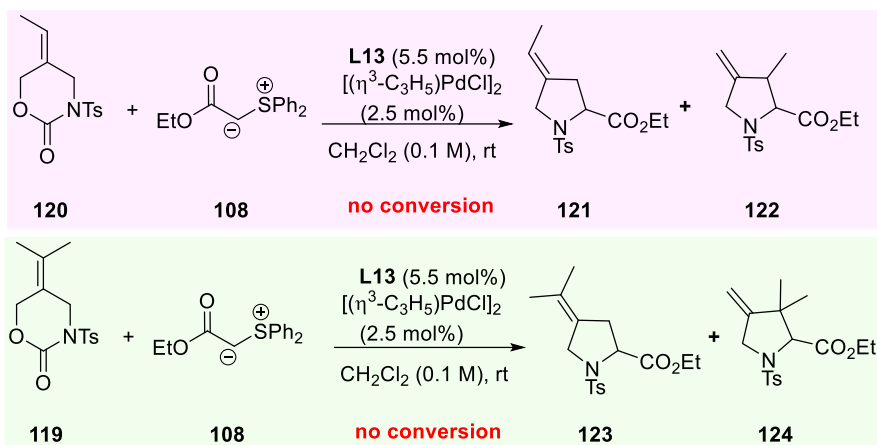
Scheme 3.2.16 Application of substituted carbamates **119** and **120** in the cyclization reaction.

3.2.7 Investigation of substituted sulfonium ylides in the [4+1] cyclization reaction

α-Substituted sulfonium keto ylides provided an opportunity to access more heavily substituted pyrrolidine products, and so we turned our attention to investigating the cyclization of these compounds. As shown in Scheme 3.2.17, methyl substituted ester ylide **125** was successfully obtained in excellent yield. However, the corresponding phenyl substituted ylide could only be prepared in very low yield. In contrast, the corresponding keto-substituted ylide **127** was synthesized smoothly.
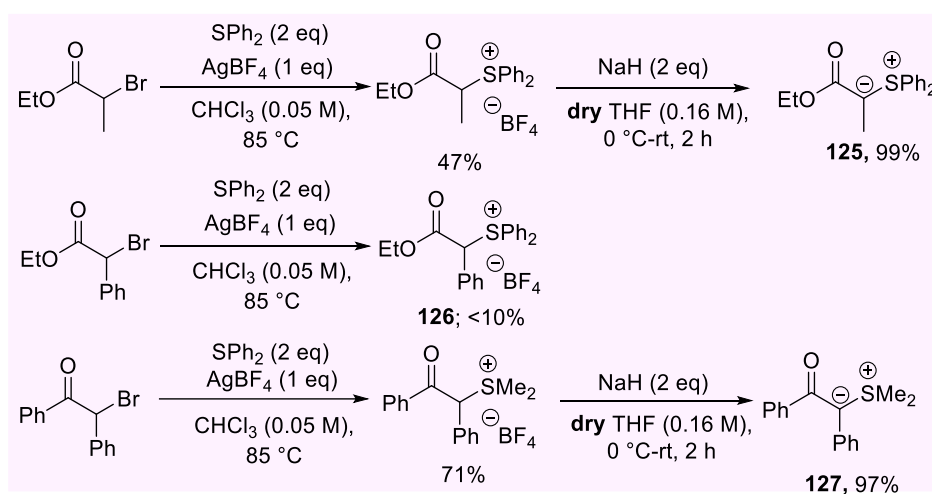
Scheme 3.2.17 Synthesis of substituted sulfonium ylides **125-127**.

With **125** and **127** in hand, we next explored the Pd-catalysed reaction with carbamate **2b**. In principle, the α-carbanion from **125** should be more nucleophilic than **127** because the methyl group is a mild electron-donating group while the aromatic ring can stabilize the anion making it less reactive. Surprisingly, neither **125** nor **127** underwent significant conversion under the standard reaction conditions (Scheme 3.2.18). Based on this result, we believe that the low reactivity is due to steric congestion.
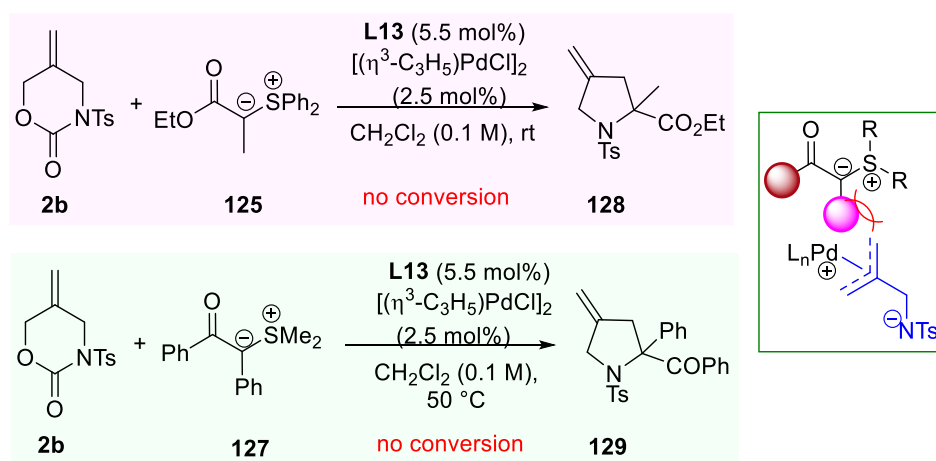
Scheme 3.2.18 Application of substituted sulfonium ylide **125** and **127** in the cyclization reaction.

3.2.8 Functionalization of 4-methylene proline 103o

The synthetic value of this methodology was exemplified by the functionalization of **103o** to produce modified derivatives. As shown in Scheme 3.2.19, cyclopropanation of **103o** with the carbene generated from diiodomethane showed no conversion even after leaving the reaction for one week.
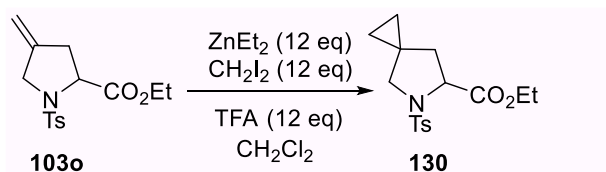
Scheme 3.2.19 Attempted cyclopropanation of **103o**.

Since the cyclopropane represents an important motif in drug compounds, we continued our research on the generation of cyclopropane derivatives. Diazo compounds bearing ester groups are an effective tool for the cyclopropanation of alkenes as the intermediate carbene equivalent can be generated under metal catalysis. In the event, addition of ethyl diazo acetate to **103o** in the presence of a rhodium catalyst was successful in producing cyclopropane derivative **131**, albeit with poor diastereocontrol. Deconvolution of the stereochemistry across the three possible isomers was difficult and so this reaction was ultimately abandoned (Scheme 3.2.20). However, compared with the conditions of the classical Simmons Smith reaction, this methodology is simpler.
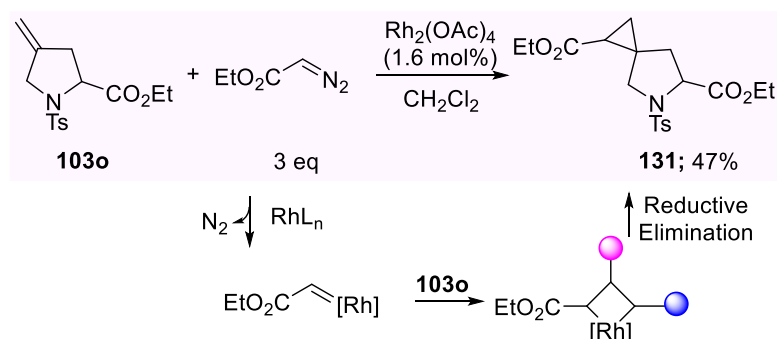
Scheme 3.2.20 Cyclopropanation of **103o**.

Epoxidation of the alkene in **103o** was readily achieved in one step, albeit with poor diastereocontrol (Scheme 3.2.21).
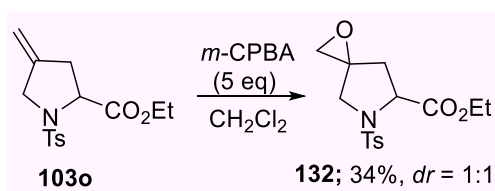
Scheme 3.2.21 Epoxidation of **103o.**

Since fluorinated proline analogues have emerged as important building blocks for ^{19}F NMR labelling in peptide conformational analysis, and as an important moiety in drug design,[77] we introduced fluorine into the alkene in the form of a difluorocyclopropane **133** (Scheme 3.2.22).
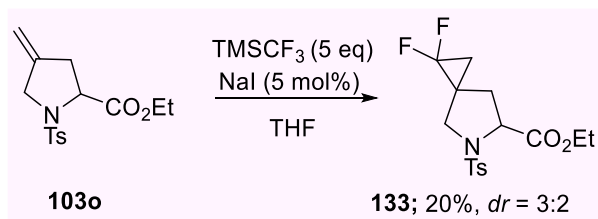
Scheme 3.2.22 Difluoro cyclopropanation of **103o.**

Considering the yields and diastereoselectivities for both **132** and **133** are not ideal, we decided to modify the alkene moiety using cross-metathesis. As shown in Scheme 3.2.23, under the previously employed metathesis conditions (c.f. Scheme 3.2.15), we obtained almost exclusively a single metathesis product **134** with 84% yield.
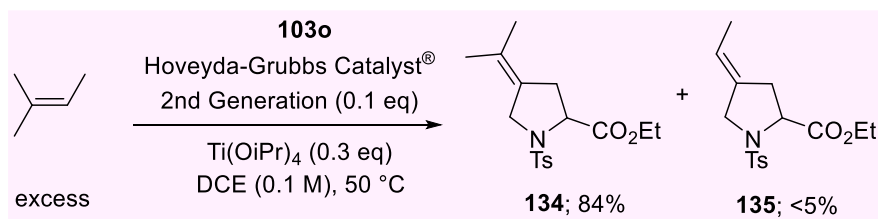
Scheme 3.2.23 Metathesis reaction of **103o**.

The oxidative cleavage of the alkene in **103o** proceeded smoothly as shown in Scheme 3.2.24. In comparison with traditional methodologies, this route is more environmentally friendly and more economical as only a catalytic amount of ruthenium reagent is needed because $RuCl_3$ can be oxidized to RuO_4 by $NaIO_4$ in a recyclable way. In addition, the advantage of the dual phase solvent system is quite distinctive: after consumption of RuO_4 in the organic phase, the by-product RuO_2 can be transferred to aqueous layer where it is oxidized to RuO_4. Notably, compounds with the general structure **137** have proved to be inhibitors of HCV 25 (hepatitis C virus) and NS3 (non-structural 3) protease, which can be produced after suitable modification of **136**.[78]
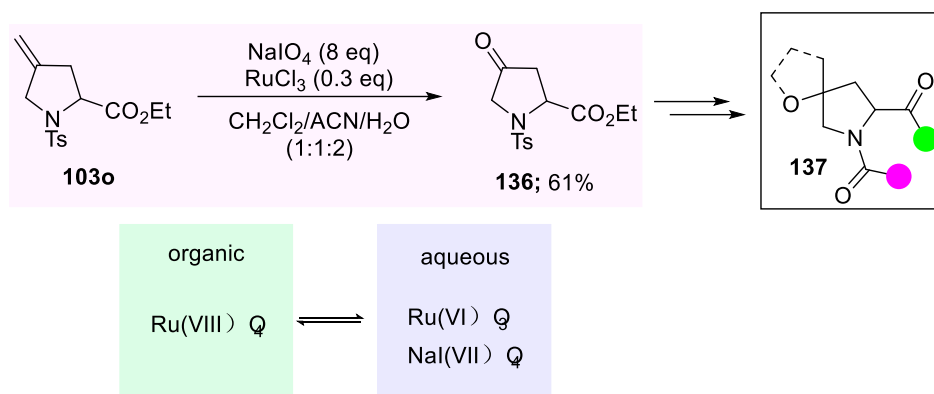
Scheme 3.2.24 Oxidative Cleavage of **103o.**

Reduction of the ester group in **103o** provided alcohol **138** as shown Scheme 3.2.25. Surprisingly, **138** was accompanied by the alkene reduction product **139** (as judged by LC-MS, ^{1}H NMR analysis) in the presence of 2 equivalents LiAlH$_4$, resulting in disappointing yield of alcohol **138**. It was assumed that excess reducing reagent and high temperature caused this side reaction. Indeed, the production of **138** proceeds more selectively at 0 °C with 1 equivalent LiAlH$_4$ in 1 h.
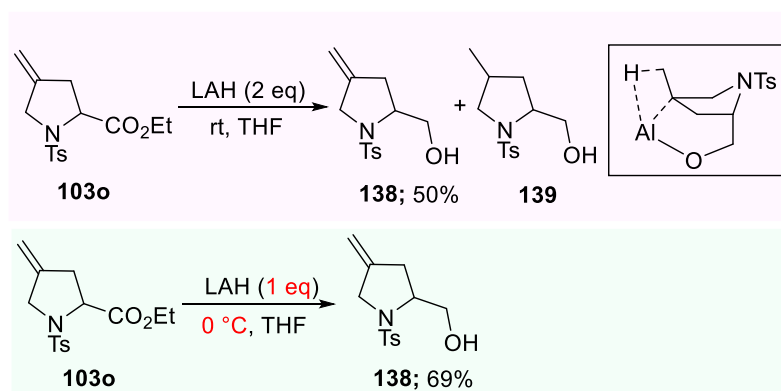
Scheme 3.2.25 Ester reduction of **103o.**

3.2.9 Investigation of Ts deprotection and stereochemistry proof

We further exploited enantioenriched product **113** to examine *dr* ratio from LC-MS analysis (c.f. Scheme 3.2.12). The Ts group is notoriously difficult to remove and can require harsh conditions to

cleave from an amine. Dissolving metal reduction is the most widely used approach and we began our investigation on Ts-dprotection using sodium naphthalenide. Unfortunately, we were unable to detect the deprotected product although **113** was completely consumed (Scheme 3.2.26a).

We next investigated the treatment of **113** with magnesium in MeOH; simply stirring the mixture did not afford the deprotected product, however, under ultrasonic conditions, deprotection proceeded successfully, delivering **149** in low yield around 10% (Scheme 3.2.26 b). In addition to Ts removal, a transesterification to the methyl ester was also observed. The operative mechanism is associate with SET: an electron from magnesium transfers to substrate **113** following a second SET to the radical.
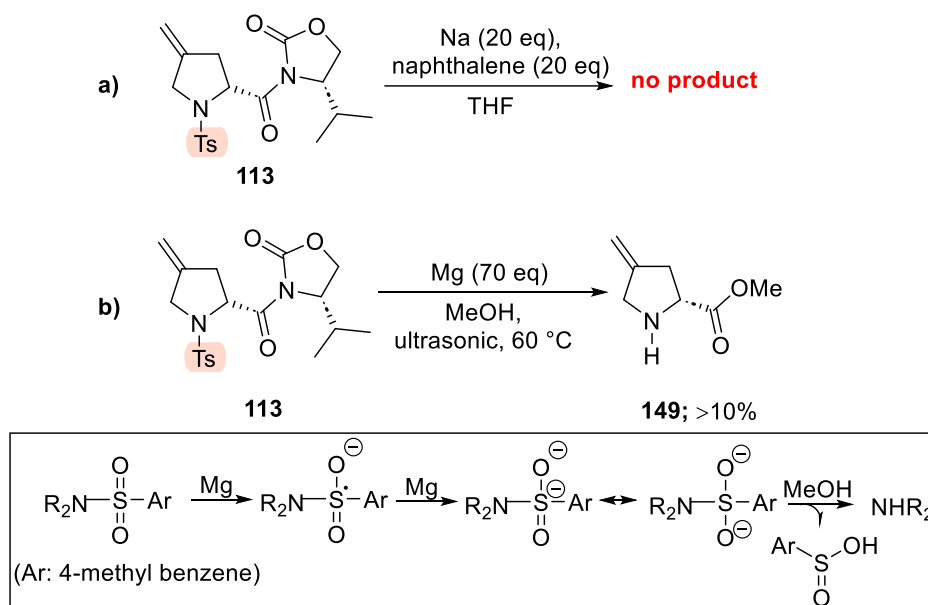
Scheme 3.2.26 Deprotection of **113.**

We assumed the low yield of deprotected product **149** was contingent on decomposition during purification, therefore, Boc protection of **113** proceeded in one-pot reaction, giving **150** with low yield in a 2-step sequence (Scheme 3.2.27).
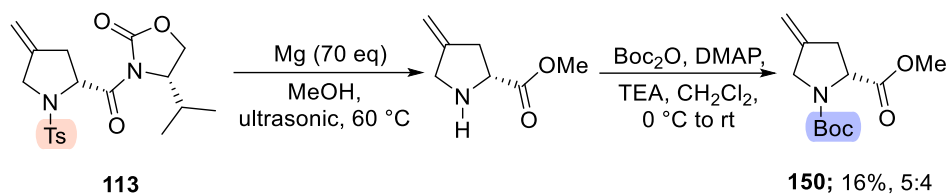
Scheme 3.2.27 Boc protection of **113** in one-pot reaction**.**

Upon checking the enantiopurity of **150** we were surprised to find that all enantioselectivity had been lost, indicating that enolization had taken place during Ts removal resulting in racemization. To avoid the undesirable racemization, the chiral oxazolidinone auxiliary was reduced to alcohol **151** by LiAlH₄ (Scheme 3.2.28). The alcohol moiety was initially protected as the TBDPS ether, but **152** was difficult to separate from TBDPSOH (the by-product from hydrolysis of TBDPSCl). Pleasingly however, TBS protected **153** was synthesized successfully with high yield.
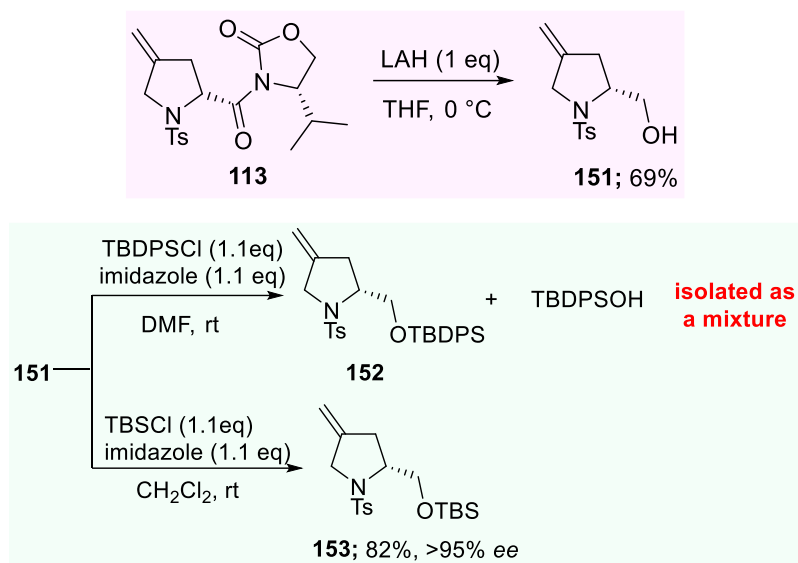
Scheme 3.2.28 Oxazolidinone reduction and alcohol **151** protection.

Under the optimal Ts deprotection conditions mentioned in 3.2.24, **153** was smoothly converted to **154** with higher yield. To our delight, the enantioselectivity was maintained in the final product in this case (Scheme 3.2.29).
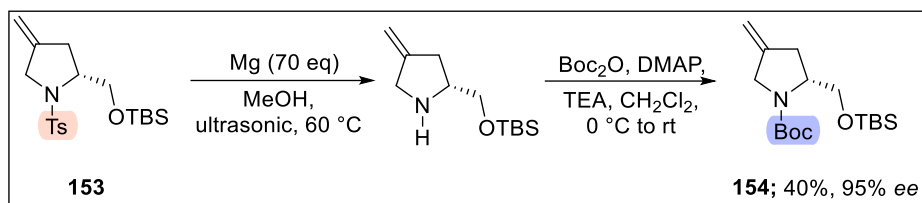
Scheme 3.2.29 Ts cleavage of **153** and Boc protection.

The *S* enantiomer of **154** is commercially available allowing us to directly compare their HPLC traces. In the event, we were able to assign **154** as the (*R*) enantiomer.

Finally, we put forward a model to explain the origin of the cyclization stereochemistry. We expect the ylide to prefer the *s-cis* conformation to minimize steric repulsion between the auxiliary and the sulfonium group. To minimize dipole-dipole repulsion, the auxiliary adopts a conformation whereby the two carbonyl groups point in opposite directions. Our working hypothesis is that the diastereocontrol originates from addition of the Pd π-allyl complex to the open face of the enolate, followed by cyclization (Scheme 3.2.30).
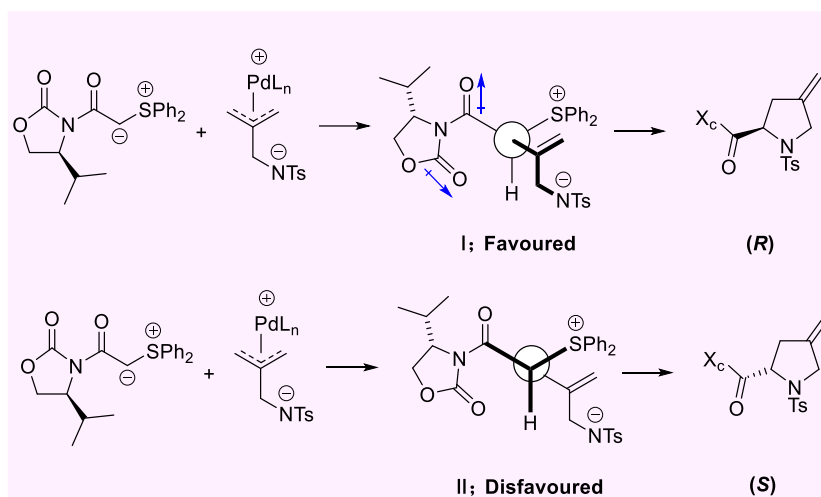
Scheme 3.2.30 Model for explanation of stereochemistry from *s-cis* isomer.

3.3 Conclusion

In summary, we have reported a new palladium catalysed annulation with a series of sulfonium ylides for the synthesis of 4-methylene proline derivatives. High enantioselectivity was obtained by the use of an oxazolidinone-based chiral auxiliary and we successfully elucidated the stereochemistry of the product, allowing us to put forward a stereochemical model. Most importantly, these compounds have the potential for orthogonal functionalization.

4.0 Conclusions

Extensive efforts have been made towards the investigation on the asymmetric synthesis of 3-fluorinated piperidine. A screening of different chiral ligands, additive and other reactions conditions was performed to access enantioenriched 3-fluorinated piperidines. Lloyd-Jones model was employed to explain the origin of stereochemistry. On the basis of the model, better enantiocontrol was obtained under the employment of **89a-89f**. Functionality of our target product **93** was proved by further modification (epoxidation, ester reduction, hydroboration, etc.)

In addition, the compatibility of Pd-catalysed decarboxylative allylation route was proved by the synthesis of pyrrolidine derivatives. In addition, induction of chiral auxiliary oxazolidinone successfully deliver enantioenriched product **113**.

Experimental Section

General Considerations

All reactions were carried out in flame-dried glassware equipped with a magnetic stir bar under nitrogen atmosphere, unless stated otherwise. Solvents were purified using a PureSolv MD purification system and transferred under nitrogen. A DrySyn block combined with a temperature probe was used as the heating source, where required. Infrared (IR) spectra were recorded on a Perkin Elmer Paragon FTIR spectrometer (v_{max} in cm^{-1}). Samples were recorded neat as thin films. ^{1}H NMR spectra were recorded on a Bruker AVIII HD 400 (400 MHz), Bruker AVI 400 (400 MHz) or Bruker AMX400 (400 MHz). Chemical shifts are reported in parts per million (ppm) from tetramethylsilane, using the residual protic solvent resonance as the internal reference: (CHCl$_3$: δ 7.26) unless otherwise stated. Data are reported as follows: chemical shift (integration, multiplicity (s = singlet, d = doublet, t = triplet, q = quartet, br = broad, m = multiplet), coupling constant (Hz)). ^{13}C NMR spectra were recorded on a Bruker AVIII HD 400 (101 MHz), Bruker AVI 400 (101 MHz) or Bruker AMX-400 (101 MHz) with broadband proton decoupling. Chemical shifts are reported in ppm from trimethylsilane with the solvent as the internal reference (CDCl$_3$: δ 77.36). ^{19}F NMR spectra were recorded on a Bruker AV III HD 400 (377 MHz) and are uncorrected. High resolution mass spectra (HRMS) recorded for accurate mass analysis, were performed on either a Micromass LCT operating in electrospray mode (TOF, ES$^+$) or a Micromass Prospec operating in FAB (FAB$^+$), EI (EI$^+$) or CI (CI$^+$) mode. Thin layer chromatography (TLC) was performed on aluminium-backed plates pre coated with silica (0.2 mm, Merck 60 F$_{254}$) which were developed using standard visualizing agents: UV light or potassium permanganate. Flash chromatography was performed on silica gel (Merck 40-63 μm). Melting points were recorded on Gallenkamp melting point apparatus and are uncorrected.

General Procedures

General Procedure A (GPA)
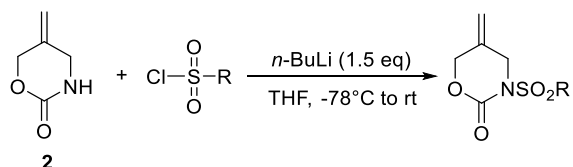
To a stirring solution of 5-methylene-1,3-oxazinan-2-one (1.0 equiv.) in THF (0.22M) at -78 °C was added ^{n}BuLi (1.5 equiv.) dropwise, followed by careful addition of sulfonyl chloride (2 equiv.) and the mixture left to stir for 10 mins. The cold bath was removed, and the reaction mixture was allowed to stir at rt until 5-methylene-1,3-oxazinan-2-one was consumed. The reaction was quenched by the addition of sat. NH$_4$Cl and water. The resulting mixture was extracted with EtOAc and the combined organic layers were then dried over anhydrous magnesium sulfate and concentrated under vacuum. Purification by flash silica column chromatography (FCC) afforded the target carbamate.

General Procedure B (GPB)
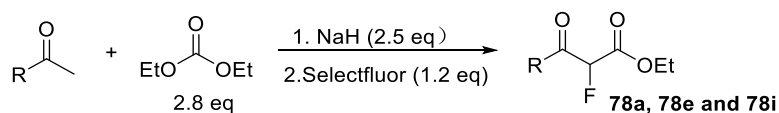
To a suspension of sodium hydride (60% dispersion in mineral oil, 2.5 equiv.) in THF (0.5 M) under nitrogen was added ketone (1 equiv.) and diethyl carbonate (2.8 equiv.) and the resulting suspension heated at reflux until complete consumption of the ketone substrate. The mixture was then cooled to room temperature, diluted with AcOH (0.1 mL per mmol) and water (4 mL per mmol) and extracted with CH$_2$Cl$_2$ (3 x 4 mL per mmol). The combined organic layers were then dried over anhydrous magnesium sulfate and concentrated under vacuum. The crude oil was dissolved in acetonitrile (0.5 M) under nitrogen and selectfluor (1.2 equiv.) was added and the resulting mixture heated at 50 °C overnight. After cooling to room temperature, the mixture was diluted with water (4 mL per mmol) and extracted with ethyl acetate (3 x 4 mL per mmol). The combined organic layers

were then dried over anhydrous magnesium sulfate and concentrated under vacuum. Purification by flash silica column chromatography (FCC) afforded the target fluorinated ketoesters.

General Procedure C (GPC)
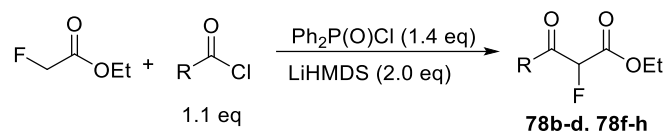
To a solution of ethyl fluoroacetate (1 equiv.) and diphenylphosphinic chloride (1.4 equiv.) in dry THF (0.125 M) at -78 °C was added dropwise a solution of lithium bis(trimethylsilyl)amide (1.0 M in hexanes, 2 equiv.). After 10 minutes, the corresponding acyl chloride (1.1 equiv.) was added dropwise. The mixture was then stirred overnight at RT. After completion, the reaction was diluted with a saturated solution of ammonium chloride (4 mL per mmol) and extracted with ethyl acetate (3x 4 mL per mmol). The combined organic layers were then dried over anhydrous magnesium sulfate and concentrated under vacuum. Purification by flash silica column chromatography (FCC) afforded the target fluorinated ketoesters.

General Procedure D (GPD)
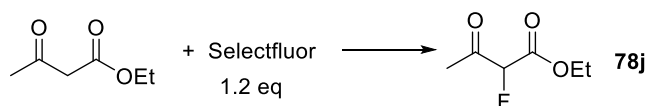
To a solution of the corresponding β-ketoester (1 equiv.) in MeCN (0.5 M) under nitrogen was added selectfluor (1.2 equiv.) and the resulting mixture heated to 50 °C overnight. After cooling to room temperature the reaction was diluted with water (4 mL per mmol) and extracted with ethyl acetate (3 x 4 mL per mmol). The combined organic layers were then dried over anhydrous magnesium sulfate and concentrated under vacuum. Purification by flash silica column chromatography (FCC) afforded the target fluorinated ketoesters.

General Procedure E (GPE)
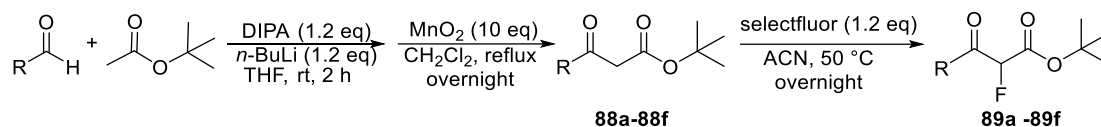
A solution of *n*-butyl lithium in 2.5 M hexane (1.2 equiv.) was added to a stirred solution of diisopropyl amine (1.2 equiv.) in THF (0.8 M) at 0 °C. The solution was stirred at 0 °C for 15 min. Then, *t*-butyl acetate (1 equiv.) was added dropwise at −78 °C. After stirring for 30 min, the aldehyde (1 equiv.) was added, and the reaction mixture was stirred until complete consumption of the aldehyde substrate (as judged by TLC analysis). The reaction mixture was diluted with a saturated solution of ammonium chloride (1.3 mL per mmol) and extracted with CH_2Cl_2 (3 x 1.3 mL per mmol). The combined organic layers were then dried over anhydrous magnesium sulfate and concentrated under vacuum. Activated manganese (IV) oxide (10 equiv.) was added to the crude mixture in dichloromethane (0.8 M). The reaction mixture was heated at reflux overnight, then filtered. The filtrate was concentrated under vacuum. Selectfluor (1.2 equiv.) was added to a solution of the corresponding β-ketoester (1 equiv.) in MeCN (0.5 M) under nitrogen and the reaction mixture was heated at 50 °C overnight. After cooling to room temperature, the mixture was diluted with water (4 mL per mmol) and extracted with ethyl acetate (3 x 4 mL per mmol). The combined organic layers were then dried over anhydrous magnesium sulfate and concentrated under vacuum. Purification by flash silica column chromatography (FCC) afforded the target fluorinated keto esters.

General Procedure F (GPF)
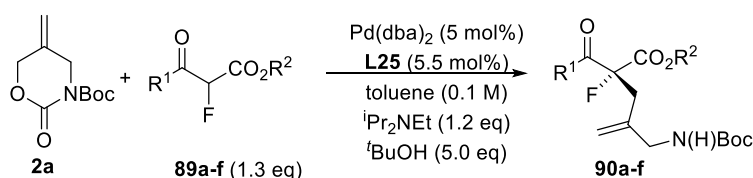
A flame-dried test-tube was charged with *tert*-butyl 5-methylene-2-oxo-1,3-oxazinane-3-carboxylate (1 equiv.), (*R,R*)-Dach-phenyl Trost ligand (5.5 mol%), Pd(dba)₂ (5 mol%), ᵗBuOH (5 equiv.) and DIPEA (1.2 equiv.) under nitrogen. Anhydrous toluene (5 mL per mmol) was then added

and the mixture stirred at 0 °C for 30 minutes. Fluorinated keto ester (1.3 equiv.) in toluene (5 mL per mmol) was added to the mixture and the reaction mixture was stirred overnight at 0 °C. The resulting mixture was then concentrated under vacuum and purified by flash silica column chromatography.

General Procedure G (GPG)
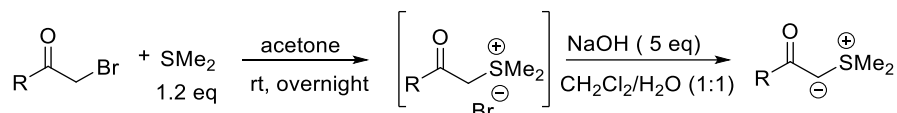
To a solution of bromoketone (1.0 equiv.) in acetone (0.5 M), dimethyl sulfide (1.2 equiv.) was added, and the mixture was stirred for 48 h at rt. Then, the sulfonium salt was collected by filtration, washed with acetone, and dried under high vacuum to afford the product salt that was used without further purification.

To a suspension of sulfonium salt (1.0 equiv.) in CH_2Cl_2 (0.3 M) was added a solution of NaOH (5.0 equiv.) in H_2O (0.3 M) and the mixture was vigorously stirred for 1 h at room temperature. The product was extracted with EtOAc, the extract dried over anhydrous $MgSO_4$, filtered, and concentrated under high vacuum to afford the sulfur ylide that was used without further purification.

General Procedure H (GPH)
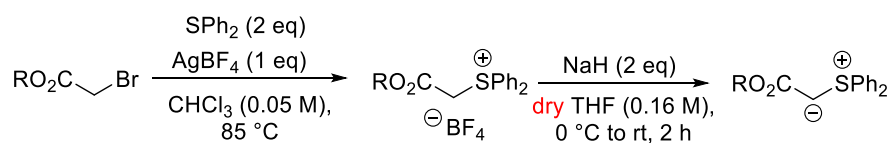
A flamed dried flask was charged with bromide (1.0 equiv.), diphenyl sulfide (2.0 equiv.) and $AgBF_4$ (1.0 equiv). Anhydrous $CHCl_3$ (0.5 M) was added and the reaction mixture was stirred at 85 °C overnight. The resulting mixture was then filtered through celite and washed with CH_2Cl_2. The filtrate was concentrated, and the residue was purified by flash column chromatography to afford the desired sulfonium salt.

To a solution of sulfonium salt (1.0 equiv) in anhydrous THF (0.2 M) was added NaH (2.0 equiv, 60

wt% in mineral oil) portionwise at 0 °C. The resulting suspension was slowly warmed to room temperature and stirred for 2 hours. Then, the reaction mixture was filtered through celite and washed with CH_2Cl_2. The desired product was afforded after evaporation and used without further purification.

Note: The use of anhydrous THF is essential for the generation of pure diphenyl sulfonium ylide products. In addition, the diphenyl sulfonium ylides decompose at room temperature and should be stored in a freezer. It's also important to check the quality of ylide by NMR spectroscopy before its use.

General Procedure I (GPI)
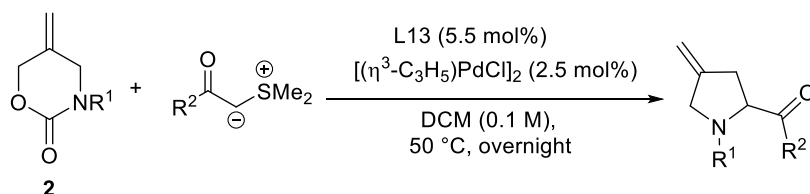
A flame-dried flask was charged with carbamate (1.0 equiv.), *N,N*-diisopropyldibenzo[d,f][1,3,2]dioxaphosphepin-6-amine (5.5 mol%), $[(\eta^3\text{-}C_3H_5)PdCl]_2$ (2.5 mol%), under nitrogen. Anhydrous CH_2Cl_2 (0.5 mL per mmol of carbamate) was then added and the mixture stirred at rt for 15 minutes. Dimethyl sulfur ylide (1.5 equiv. or 3 equiv.) in CH_2Cl_2 (0.5 mL per mmol of carbamate) was added to the mixture and the reaction mixture was stirred overnight at 50 °C. The resulting mixture was then concentrated under vacuum and purified by flash column chromatography.

General Procedure J (GPJ)

A flame-dried flask was charged with 5-methylene-3-tosyl-1,3-oxazinan-2-one (1.0 equiv.), *N,N*-diisopropyldibenzo[d,f][1,3,2]dioxaphosphepin-6-amine (5.5 mol%) and $[(\eta^3\text{-}C_3H_5)PdCl]_2$ (2.5 mol%) under nitrogen. Anhydrous CH_2Cl_2 (0.5 mL per mmol of carbamate) was then added, and the mixture stirred at rt for 15 minutes. Diphenyl sulfur ylide (1.5 equiv.) in CH_2Cl_2 (0.5 mL per mmol of ylide) was added to the mixture and the reaction mixture was stirred overnight at rt or 50 °C. If incomplete conversion was observed, a further portion of *N,N*-

106

diisopropyldibenzo[d,f][1,3,2]dioxaphosphepin-6-amine (5.5 mol%), [(η^3-C_3H_5)PdCl]$_2$ (2.5 mol%) and diphenyl sulfur ylide (0.5 equiv.) were added and the reaction mixture was stirred for another 2 h at rt or 50 °C. The resulting mixture was then concentrated under vacuum and purified by flash silica column chromatography.

NMR Data of Compounds

2-(Iodomethyl)-prop-2-en-1-ol (81)[53]
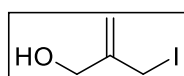
To a solution of 2-methylene-1,3-propanediol (25.0 g, 283 mmol), triphenylphosphine (79.3 g, 312 mmol) and imidazole (21.2 g, 312 mmol) in a mixture of CH_2Cl_2 (370 mL) and EtOAc (370 mL) at 0 °C under nitrogen was added iodine (72.1 g, 59.0 mmol) portionwise and the resulting mixture stirred at room temperature in the dark for 24 hours. The solvent was then removed under vacuum and the residue purified by FCC (gradient from 10-20% EtOAc in 40-60 petroleum ether) to afford 2- (iodomethyl)prop-2-en-1-ol (**81**) as a yellow oil (24.6 g, 44%).

^{1}H NMR (400 MHz, CDCl$_3$) δ 5.38 (dd, J= 1.5, 1.0 Hz, 1H), 5.23 (dd, J= 2.5, 1.5 Hz, 1H), 4.34 (d, J= 5.5 Hz, 2H), 4.00 (d, J= 1.0 Hz, 2H), 2.14 (t, J= 5.5 Hz, 1H); **^{13}C NMR (101 MHz, CDCl$_3$)** δ 145.8, 114.2, 63.9, 5.8.

5-methylene-1,3-oxazinan-2-one (2a)[53]
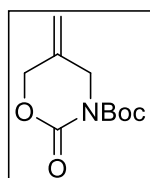
To a suspension of silver cyanate (28.5 g, 190 mmol) in toluene (356 mL) under nitrogen was added 2-(iodomethyl)prop-2-en-1-ol (24.6 g, 124.5 mmol) and the resulting mixture heated at reflux overnight. After cooling to room temperature the mixture was filtered through celite, the filter pad washed with Et_2O and the combined filtrates concentrated under vacuum. The crude solid and 4-dimethylaminopyridine (3.20 g, 249 mmol) were then dissolved in CH_2Cl_2 (189 mL) under nitrogen and the resulting mixture cooled to 0 °C. Di-*tert*-butyl dicarbonate (54.4 g, 249 mmol) was then added slowly and the resulting mixture stirred at room temperature for 24 hours. Removal of the solvent under vacuum and purification by FCC (gradient from 10-20% EtOAc in 40-60 petroleum ether) afforded *tert*-butyl

5-methylene-2-oxo-1,3-oxazinane-3-carboxylate as a colourless oil which converted to an amorphous white solid (**2**) upon standing in the freezer (21.2 g, 80%).

^{1}H NMR (400 MHz, CDCl$_3$) δ 5.28 (s, 2H), 4.72 (s, 2H), 4.36 (t, *J*= 2.0 Hz, 2H), 1.56 (s, 9H); **^{13}C NMR (100 MHz, CDCl$_3$)** δ151.5, 150.1, 134.7, 112.2, 82.2, 69.3, 48.2, 27.3.

N,N-diisopropyldibenzo[d,f][1,3,2]dioxaphosphepin-6-amine (L13)[53]
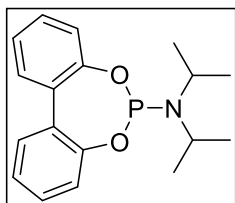
To a flame-dried round bottom flask containing THF (168 mL) at 0 °C under nitrogen was added PCl$_3$ (2.4 mL, 27 mmol) dropwise over 15 minutes. Et$_3$N (19.4 mL 134 mmol) was then added dropwise over 15 minutes followed by the addition of diisopropylamine (3.7 mL, 27 mmol) dropwise over 30 minutes. The resulting mixture was then warmed to room temperature and stirred for 3 hours before cooling to 0 °C. 2,2'-Biphenol (5.0 g, 27 mmol) was then added portionwise and the reaction mixture stirred at room temperature overnight. The volatiles were then removed under vacuum and the resulting residue purified by FCC (gradient from 0-20% CH$_2$Cl$_2$ in 40-60 petroleum ether) to afford *N,N*- diisopropyldibenzo[d,f][1,3,2]dioxaphosphepin-6-amine (**L13**) as a white solid (7.8 g, 68%).

^{1}H NMR (400 MHz, CDCl$_3$) δ 7.57 (dd, *J* = 7.5, 1.5 Hz, 2H), 7.43 (td, *J*= 7.0, 1.5 Hz, 2H), 7.32 −7.28 (m, 4H), 3.71-3.58 (m, 2H), 1.35 (d, *J* = 6.5 Hz, 12H); **^{13}C NMR (101 MHz, CDCl$_3$)** δ 152.1 (d, *J* = 5.5 Hz), 131.0 (d, *J* = 3.5 Hz), 129.8, 129.0, 124.3, 122.2, 44.7 (d, *J* = 13.0 Hz), 24.6 (d, *J* =8.0 Hz); **^{31}P NMR (162 MHz, CDCl$_3$)** δ 152.2 – 151.8 (m).

5-methylene-3-tosyl-1,3-oxazinan-2-one (2b)[76]
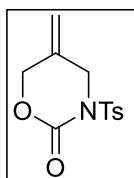
Following GPA using (**2**) (566 mg, 5 mmol), *^{n}*BuLi (3.0 mL, 2.5 M in hexane, 7.5 mmol) and *p*-tolylsulfonyl chloride (1.90 g, 10 mmol) with FCC (20% EtOAc in 40-60 petroleum ether) afforded 5-methylene-3-tosyl-1,3-oxazinan-2-one (**2b**) as a white solid (467 mg, 35%).

^{1}H NMR (400 MHz, CDCl$_3$): δ 7.94 (d, *J* = 8.5 Hz, 2H), 7.34 (d, *J* = 8.5 Hz, 2H), 5.29 (d, *J* = 18.5 Hz, 2H), 4.67 (s, 2H), 4.51 (s, 2H), 2.44 (s, 3H); **^{13}C NMR (101 MHz, CDCl$_3$):** δ 149.6, 145.5, 134.7, 132.6,

129.7, 129.1, 115.3, 70.5, 49.9, 21.6.

5-methylene-3-((4-nitrophenyl)sulfonyl)-1,3-oxazinan-2-one (2c)
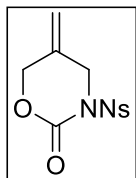
Following GPA using (2) (566 mg, 5 mmol), ^{n}BuLi (3.0 mL, 2.5 M in hexane, 7.5 mmol) and p-tolylsulfonyl chloride (2.21 g, 10 mmol) with FCC (10% EtOAc in 40-60 petroleum ether) afforded 5-methylene-3-tosyl-1,3-oxazinan-2-one (2c) as a white solid (776 mg, 52%).

^{1}H NMR (400 MHz, CDCl$_3$): δ 8.37 (d, J = 9.0 Hz, 2H), 8.25 (d, J = 9.0 Hz, 2H), 5.37 (d, J = 17.0 Hz, 2H), 4.72 (s, 2H), 4.55 (s, 2H); **^{13}C NMR (101 MHz, CDCl$_3$):** δ 151.2, 149.5, 143.4, 131.8, 130.8, 124.4, 116.6, 71.0, 50.4; **FTIR: v_{max}/cm^{-1} (neat):** 3115, 2985, 1735, 1372, 1235, 1044, 740; **HRMS (ESI$^+$):** calculated for C$_{11}$H$_{12}$N$_2$O$_6$S (ES$^+$)(+H$^+$): 299.0260, found: 299.0341.

5-methylene-3-(methylsulfonyl)-1,3-oxazinan-2-one (2d)
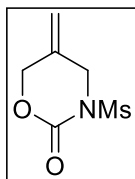
Following GPA using (2) (566 mg, 5 mmol), ^{n}BuLi (3.0 mL, 2.5 M in hexane, 7.5 mmol) and mesyl chloride (1.14 g, 10 mmol) with FCC (25% Et$_2$O in 40-60 petroleum ether) afforded 5-methylene-3-tosyl-1,3-oxazinan-2-one (2d) as a colourless oil (161 mg, 42%).

^{1}H NMR (400 MHz, CDCl$_3$)： δ 5.33 (d, J = 6.5 Hz, 2H), 4.72 (m, 2H), 4.38 (s, 2H), 3.36 (s, 3H); **^{13}C NMR (101 MHz, CDCl$_3$):** δ 150.7, 132.0, 116.2, 71.0, 49.5, 41.1; **FTIR: v_{max}/cm^{-1} (neat):** 3019, 2934, 1726, 1348, 1170, 1143; **HRMS (ESI$^+$):** calculated for C$_6$H$_{10}$NO$_4$S (ES$^+$)(+H$^+$): 192.0252, found: 192.0335.

ethyl 2-fluoro-3-oxo-3-phenylpropanoate (78a)[53]
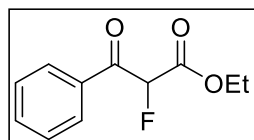
Following GPB using acetophenone (5.05 g, 42 mmol), diethylcarbonate (13.9 g, 118 mmol), sodium hydride (60% dispersion in mineral oil, 4.2 g, 105 mmol), Selectfluor (17.9 g, 50 mmol) and acetic acid (4.2 mL) with FCC (10% EtOAc in 40-60 petroleum ether) afforded ethyl 2-fluoro-3-oxo-3-phenylpropanoate (78a) as a yellow oil (4.0 g, 45%).

1H NMR (400 MHz, CDCl₃) δ 8.05 – 8.03 (m, 2H), 7.66 – 7.59 (m, 1H), 7.52 – 7.46 (m, 2H), 5.87 (d, J = 49.0 Hz, 1H), 4.34 – 4.21 (m, 2H), 1.23 (t, J = 7.0 Hz, 3H); **13C NMR (101 MHz, CDCl₃)** δ 189.1 (d, J = 19.0 Hz), 164.4 (d, J = 23.0 Hz), 134.1, 133.3 (d, J = 1.5 Hz), 129.0 (d, J = 3.0 Hz), 128.4, 89.3 (d, J = 197.0 Hz), 62.1, 13.2; **19F NMR (377 MHz, CDCl₃)** δ -191.9 (d, J = 48.5 Hz).

ethyl 2-fluoro-3-(4-chlorophenyl)-3-oxopropanoate (78b)[53]
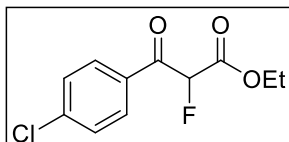
Following GPC using ethyl fluoroacetate (0.53 g, 5 mmol), diphenylphosphinic chloride (1.7 g, 7 mmol), lithium bis(trimethylsilyl)amide (1 M solution in hexane, 10 mL, 10 mmol) and 4-chlorobenzoyl chloride (0.96 g, 5.5 mmol) with FCC (gradient from 10- 20% EtOAc in 40-60 petroleum ether) afforded ethyl 2-fluoro-3-(4- chlorophenyl)-3-oxopropanoate (**78b**) as a pale yellow oil (0.20 g, 18%).

1H NMR (400 MHz, CDCl₃) δ 8.01 – 7.9 (m, 2H), 7.49– 7.45 (m, 2H), 5.91 (d, J = 48.5 Hz, 1H), 4.35 – 4.24 (m, 2H), 1.26 (t, J = 7.0 Hz, 3H); **13C NMR (101 MHz, CDCl₃)** δ 188.6 (d, J = 22.0 Hz), 164.8 (d, J = 24.5 Hz), 141.3, 131.7, 131.0 (d, J = 3.5 Hz), 129.6, 90.3 (d, J = 200.5 Hz), 63.2, 14.2; **19F NMR (377 MHz, CDCl₃):** δ -190.3 (d, J = 49.5 Hz).

ethyl 2-fluoro-3-(4-nitrophenyl)-3-oxopropanoate (78c)[53]
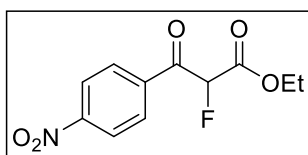
Following GPC using ethyl fluoroacetate (0.53 g, 5 mmol), diphenylphosphinic chloride (1.7 g, 7 mmol), lithium bis(trimethylsilyl)amide (1 M solution in hexane, 10 mL, 10 mmol) and 4-nitrobenzoyl chloride (1.0 g, 5.5 mmol) with FCC (gradient from 10-20% EtOAc in 40-60 petroleum ether) afforded ethyl 2-fluoro-3-(4-nitrophenyl)-3-oxopropanoate (**78c**) as an orange oil (0.39 g, 30%).

1H NMR (400 MHz, CDCl₃): δ 8.28 (d, J = 9.0 Hz, 2H), 8.17 (d, J = 9.0 Hz, 2H), 5.97 (d, J = 48.5 Hz, 1H), 4.30-4.22 (m, 2H), 1.20 (t, J = 7.0 Hz, 3H); **13C NMR (101 MHz, CDCl₃)** δ 188.7 (d, J = 21.5 Hz), 164.2 (d, J = 24.0 Hz), 150.9, 137.7 (d, J = 2.0 Hz), 130.7 (d, J = 3.5 Hz), 123.9, 90.2 (d, J = 200.0 Hz), 63.1, 13.9; **19F NMR (377 MHz, CDCl₃):** δ -191.4 (d, J = 48.5 Hz).

ethyl 2-fluoro-3-(4-trifluoromethylphenyl)-3-oxopropanoate (78d)[53]
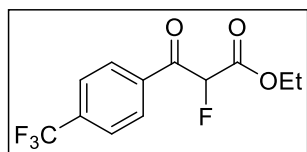
Following GPC using ethyl fluoroacetate (0.53 g, 5 mmol), diphenylphosphinic chloride (1.70 g, 7 mmol), lithium bis(trimethylsilyl)amide (1 M solution in hexane, 10 mL, 10 mmol) and 4-trifluoromethylbenzoyl chloride (1.15 g, 5.5 mmol) with FCC (gradient from 10-20% EtOAc in 40-60 petroleum ether) afforded ethyl 2-fluoro-3-(4-trifluoromethylphenyl)-3-oxopropanoate (**78d**) as a yellow oil (0.42 g, 30%).

^{1}H NMR (400 MHz, CDCl$_3$): δ 8.11 (d, J = 8.5 Hz, 2H), 7.71 (d, J = 8.5 Hz, 2H), 5.90 (d, J = 48.0 Hz, 1H), 4.30 – 4.19 (m, 2H), 1.19 (t, J = 7.0 Hz, 3H); **^{13}C NMR (101 MHz, CDCl$_3$)** δ 189.1 (d, J = 20.5 Hz), 164.5 (d, J = 24.0 Hz), 135.9, 135.6, 129.9 (d, J = 3.5 Hz), 125.8 (dd, J = 7.0, 3.5 Hz), 123.4 (q, J = 272.5 Hz), 90.1 (d, J = 200.5 Hz), 63.1, 14.0; **^{19}F NMR (376 MHz, CDCl$_3$)**: δ -63.6, -191.2 (d, J = 48.5 Hz).

ethyl 2-fluoro-3-(4-methoxyphenyl)-3-oxopropanoate (78e)[53]
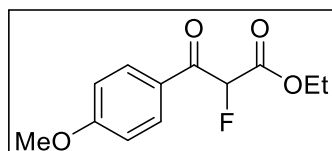
Following GPB using 4-methoxyacetophenone (1.5 g, 10 mmol), diethylcarbonate (3.3 g, 28 mmol), sodium hydride (60% dispersion in mineral oil, 1.0 g, 25 mmol), selectfluor (4.3 g, 12 mmol) and acetic acid (1 mL) with FCC (gradient from 0-10% EtOAc in 40-60 petroleum ether) afforded ethyl 2-fluoro-3-(4-methoxyphenyl)-3- oxopropanoate (**78e**) as an orange oil (1.5 g, 64%).

^{1}H NMR (400 MHz, CDCl$_3$) δ 7.86 – 7.83 (m, 2H), 6.79 – 6.77 (m, 2H), 5.80 (d, J = 48.5 Hz, 1H), 4.11 – 4.05 (m, 2H), 3.67 (s, 3H), 1.04 (t, J = 7.0 Hz, 3H); **^{13}C NMR (101 MHz, CDCl$_3$)** δ 187.9 (d, J = 20.5 Hz), 165.3 (d, J = 24.5 Hz), 164.7, 132.1 (d, J = 3.5 Hz), 126.4 (d, J = 2.5 Hz), 114.2, 90.2 (d, J = 194.5 Hz), 62.7, 55.7, 14.2; **^{19}F NMR (376 MHz, CDCl$_3$)** δ -190.7 (d, J = 48.5 Hz).

ethyl 2-fluoro-3-(4-methylphenyl)-3-oxopropanoate (78f)[53]
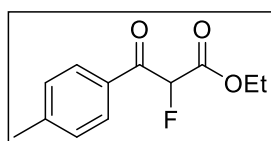
Following GPC using ethyl fluoroacetate (0.53 g, 5 mmol), diphenylphosphinic chloride (1.7 g, 7 mmol), lithium bis(trimethylsilyl)amide (1 M solution in hexane, 10 mL, 10 mmol) and

4-methylbenzoyl chloride (0.85 g, 5.5 mmol) with FCC (gradient from 10-20% EtOAc in 40-60 petroleum ether) afforded ethyl 2-fluoro-3-(4-methylphenyl)-3-oxopropanoate (**78f**) as a colourless oil (0.47 g, 43%).

1H NMR (400 MHz, CDCl3): δ 7.95 (d, *J* =8.0 Hz, 2H), 7.30 (d, *J* = 8.0 Hz, 2H), 5.91 (d, *J* = 49.0 Hz, 1H), 4.34 – 4.23 (m, 2H), 2.42 (s, 3H), 1.25 (t, *J* = 7.5 Hz, 3H); **13C NMR (101 MHz, CDCl3)** δ 189.1 (d, *J* = 20.0 Hz), 165.2 (d, *J* = 23.0 Hz), 145.8, 131.0, 129.6 (d, *J* = 3.0 Hz), 129.5, 89.9 (d, *J* = 196.0 Hz), 62.6, 21.8, 13.9; **19F NMR (377 MHz, CDCl3):** δ -190.6 (d, *J* = 49.0 Hz).

ethyl 2-fluoro-3-(2-methylphenyl)-3-oxopropanoate (78g)[53]
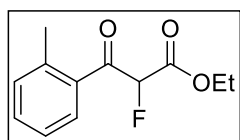
Following GPC using ethyl fluoroacetate (0.8 g, 7.5 mmol), diphenylphosphinic chloride (2.6 g, 10.5 mmol), lithium bis(trimethylsilyl)amide (1 M solution in hexane, 15 mL, 15 mmol) and 2-methylbenzoyl chloride (1.28 g, 6.1 mmol) with FCC (gradient from 10-20% EtOAc in 40-60 petroleum ether) afforded ethyl 2-fluoro-3-(2-methylphenyl)-3-oxopropanoate (**78g**) as a colourless oil (0.29 g, 17%).

1H NMR (400 MHz, CDCl3) δ 7.75 – 7.72 (m, 1H), 7.43 – 7.39 (m, 1H), 7.29 – 7.25 (m, 2H), 5.80 (d, *J* = 49.0 Hz, 1H), 4.30 – 4.18 (m, 2H), 2.48 (s, 3H), 1.20 (t, *J* = 6.5 Hz, 3H); **13C NMR (101 MHz, CDCl3)**: δ 192.1 (d, *J* = 19.0 Hz), 164.5 (d, *J* = 23.5 Hz), 139.6, 133.0, 132.4, 131.8, 129.4 (d, *J* = 4.5 Hz), 125.3, 90.3 (d, *J* = 200.0 Hz), 62.1, 20.7, 13.5; **19F NMR (377 MHz, CDCl3)**: δ -189.4 (d, *J* = 49.0, 2.0 Hz).

ethyl 2-fluoro-3-oxo-3-(furan-2-yl)propanoate (78h)[53]
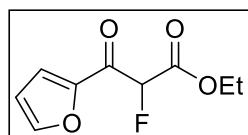
Following GPC using ethyl fluoroacetate (0.53 g, 5 mmol), diphenylphosphinic chloride (1.7 g, 7 mmol), lithium bis(trimethylsilyl)amide (1 M solution in hexane, 10 mL 10 mmol) and furan-2-carbonyl chloride (0.72 g, 5.5 mmol) with FCC (20% EtOAc in 40-60 petroleum ether) afforded ethyl 2-fluoro-3-(furan-2-yl)-3-oxopropanoate (**78h**) as a yellow oil (0.19 g, 19%).

1H NMR (400 MHz, CDCl3) δ 7.73 (s,1H), 7.49 (dd, *J* = 3.5, 2.0 Hz, 1H), 6.63 (d, *J* = 3.5 Hz, 1H), 5.73 (d, *J* = 48.5 Hz, 1H), 4.34 – 4.22 (m, 2H), 1.25 (t, *J* = 7.0 Hz, 3H); **13C NMR (101 MHz, CDCl3)** δ 177.5

(d, *J* = 21.5 Hz), 164.4 (d, *J* = 24.5 Hz), 149.2, 148.6, 122.0 (d, *J* = 6.0 Hz), 112.9, 89.1 (d, *J* = 197.0 Hz), 62.7, 13.9; **^{19}F NMR (377 MHz, CDCl₃)** δ -193.5 (d, *J* = 48.0 Hz).

ethyl 2-fluoro-3-(naphthalen-2-yl)-3-oxopropanoate (78i)[53]
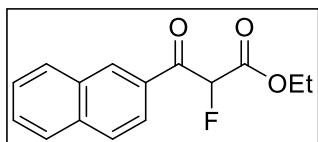
Following GPB using 2-acetylnaphthalene (0.85 g, 5 mmol), diethylcarbonate (1.7 g, 14 mmol), sodium hydride (60% dispersion in mineral oil, 0.50 g, 13 mmol), selectfluor (2.1 g, 6 mmol) and acetic acid (0.5 mL) with FCC (gradient from 20-50% CH_2Cl_2 in 40-60 petroleum ether) afforded ethyl 2-fluoro-3-(naphthalen-2-yl)-3-oxopropanoate (**78i**) as a yellow oil (0.38 g, 30%).

^{1}H NMR (400 MHz, CDCl₃) δ 8.64 (s, 1H), 8.06 (dd, *J* = 8.5, 1.5 Hz, 1H), 7.99 (dd, *J* = 8.0, 0.5 Hz, 1H), 7.92 – 7.86 (m, 2H), 7.64 (ddd, *J* = 8.0, 7.0, 1.5 Hz, 1H), 7.59 (ddd, *J* = 8.0, 7.0, 1.0 Hz, 1H), 6.08 (d, *J* = 49.0 Hz, 1H), 4.38 – 4.27 (m, 2H), 1.26 (t, *J* = 7.5 Hz, 3H); **^{13}C NMR (101 MHz, CDCl₃)** δ 189.4 (d, *J* = 20.0 Hz), 165.0 (d, *J* = 24.5 Hz), 136.1, 132.4 , 132.3, 130.6 (d, *J* = 1.5 Hz), 130.0, 129.4, 128.7, 127.8, 127.1, 124.1, 90.0 (d, *J* = 197.0 Hz), 62.7, 13.9; **^{19}F NMR (376 MHz, CDCl₃)** δ -189.6 (d, *J* = 49.0 Hz)

ethyl 2-fluoro-3-oxobutanoate (78j)[53]
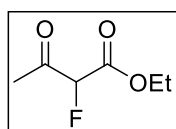
Following GPD using ethyl 3-oxobutanoate (0.65 g, 5 mmol) and selectfluor (2.13 g, 6 mmol) with FCC (gradient from 10-20% EtOAc in 40-60 petroleum ether) afforded ethyl 2-fluoro-3-oxobutanoate (**78j**) as a colourless oil (0.47 g, 72%).

^{1}H NMR (400 MHz, CDCl₃) δ 5.15 (d, *J* = 49.5 Hz, 1H), 4.27 – 4.10 (m, 2H), 2.20 (d, *J* = 4.0 Hz, 3H), 1.19 (t, *J* = 7.0 Hz, 3H); **^{13}C NMR (101 MHz, CDCl₃)** δ 198.7 (d, *J* = 23.0 Hz), 163.9 (d, *J* = 24.5 Hz), 91.3 (d, *J* = 198.0 Hz), 62.5, 26.8, 13.5; **^{19}F NMR (377 MHz, CDCl₃):** δ -193.8 (dq, *J* = 50.0, 4.0 Hz).

tert-butyl 2-fluoro-3-oxo-3-phenylpropanoate (89a)[79]
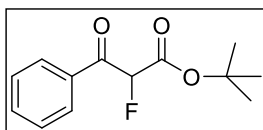
Following GPE using diisopropyl amine (1.7 mL, 12 mmol) *n*-butyl lithium in 2.5 M hexane (4.8 mL, 12 mmol), *tert*-butyl acetate (1.16 g, 10 mmol), benzaldehyde (1.06 g 10 mmol), activated manganese (IV) oxide (8.7 g, 100 mmol) and Selectfluor (4.25 g, 12 mmol) with FCC (gradient from 2.5-5% Et_2O in 40-60

petroleum ether) afforded *tert*-butyl 2-fluoro-3-oxo-3-phenylpropanoate (**89a**) as a colourless oil (1.10 g, 46%).

¹H NMR (400 MHz, CDCl₃) δ 8.01 (d, *J* = 7.5 Hz, 2H), 7.61 (t, *J* = 7.5 Hz, 1H),7.48 (t, *J* = 7.5 Hz, 2H), 5.75 (d, *J* = 49.0 Hz, 1H), 1.41 (s, *9*H); **¹³C NMR (101 MHz, CDCl₃)** δ 190.4 (d, *J* = 20.0 Hz), 164.2 (d, *J* = 24.5 Hz), 134.6, 134.0 (d, *J* = 2.0 Hz), 129.8 (d, *J* = 3.0 Hz), 129.2, 90.5 (d, *J* = 196.5 Hz), 84.9, 28.2; **¹⁹F NMR (377 MHz, CDCl₃):** δ -189.4 (d, *J* = 49.0 Hz).

tert-butyl 2-fluoro-3-(4-nitrophenyl)-3-oxopropanoate (89b)
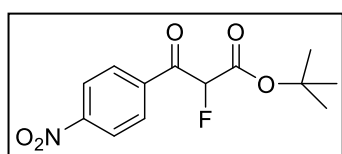
Following GPE using diisopropyl amine (1.7 mL, 12 mmol) *n*-butyl lithium in 2.5 M hexane (4.8 mL, 12 mmol), *tert*-butyl acetate (1.16 g, 10 mmol), 4-nitrobenzaldehyde (1.52 g, 10 mmol), activated manganese (IV) oxide (8.7 g, 100 mmol) and selectfluor (4.25 g, 12 mmol) with FCC (gradient from 5-10% EtOAc in 40-60 petroleum ether) afforded *tert*-butyl 2-fluoro-3-(4-nitrophenyl)-3-oxopropanoate (**89b**) as a white solid (0.35 g, 13%).

¹H NMR (400 MHz, CDCl₃) δ 8.32 (d, *J* =8.5 Hz, 2H), 8.19 (d, *J* = 8.5 Hz, 2H), 5.74 (d, *J* = 49.0 Hz, 1H), 1.41 (s, 9H); **¹³C NMR (101 MHz, CDCl₃)** δ 188.9 (d, *J* = 21.5 Hz), 163.1 (d, *J* = 24.0 Hz), 150.8, 138.0 (d, *J* = 3.0 Hz), 130.6 (d, *J* = 3.5 Hz), 123.9, 90.3 (d, *J* = 198.0 Hz), 85.3, 27.8; **¹⁹F NMR (377 MHz, CDCl₃):** δ -189.4 (d, *J* = 49.0Hz). **FTIR:** v$_{max}$/cm^{-1} (neat) 3018, 1709, 1530, 1356, 1220, 1155, 751; **HRMS (ESI⁺):**   calculated for $C_{13}H_{14}FNO_5Na$ (ES⁺)(+Na⁺): 306.0748. Found: 306.0749.

tert-butyl 2-fluoro-3-oxo-3-(4-(trifluoromethyl)phenyl)propanoate (89c)
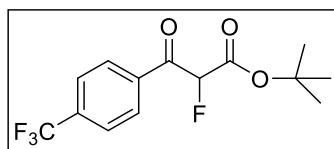
Following GPE using diisopropyl amine (1.7 mL, 12 mmol) *n*-butyl lithium in 2.5 M hexane (4.8 mL, 12 mmol), *tert*-butyl acetate (1.16 g, 10 mmol), 4-(trifluoromethyl)benzaldehyde (1.74 g, 10 mmol), activated manganese (IV) oxide (8.7 g, 100 mmol) and selectfluor (4.25 g, 12 mmol) with FCC (gradient from 5-10% EtOAc in 40-60 petroleum ether) afforded *tert*-butyl 2-fluoro-3-oxo-3-(4-(trifluoromethyl)phenyl)propanoate (**89c**) as a yellow oil (0.3 g, 10%).

¹H NMR (400 MHz, CDCl₃) δ 8.14 (d, *J* = 8.5 Hz, 2H), 7.75 (d, *J* = 8.5 Hz, 2H), 5.72 (d, *J* = 49.0 Hz, 1H), 1.42 (s, *9*H); **¹³C NMR (101 MHz, CDCl₃)** δ 189.5 (d, *J* = 21.0 Hz), 163.6 (d, *J* = 24.1 Hz), 136.5, 135.6 (d, *J* = 33.0 Hz), 130.0 (d, *J* = 3.5 Hz), 125.9 (d, *J* =3.5 Hz), 123.6 (q, *J* = 276.0 Hz), 90.6 (d, *J* = 197.5 Hz), 85.2, 28.0; **¹⁹F NMR (377 MHz, CDCl₃):** δ -63.4, -189.3 (d, *J* = 49.0 Hz). **FTIR:** v_{max}/cm⁻¹ (neat) 3019, 1756, 1710, 1412, 1325, 1230, 1134, 1068, 752, 667; HRMS (ESI⁺): calculated for C₁₄H₁₄F₄O₃Na (ES⁺)(+Na⁺): 329.0771. Found: 329.0774.

tert-butyl 2-fluoro-3-(4-methoxyphenyl)-3-oxopropanoate (89d)
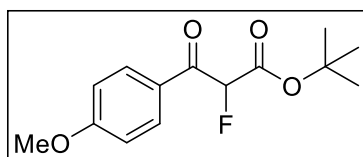
Following GPE using diisopropyl amine (1.7 mL, 12 mmol) *n*-butyl lithium in 2.5 M hexane (4.8 mL, 12 mmol), *tert*-butyl acetate (1.16 g, 10 mmol), 4-methoxybenzaldehyde (1.36 g, 10 mmol), activated manganese (IV) oxide (8.7 g, 100 mmol) and selectfluor (4.25 g, 12 mmol) with FCC (10% EtOAc in 40-60 petroleum ether) afforded *tert*-butyl 2-fluoro-3-(4-methoxyphenyl)-3-oxopropanoate (**89d**) as a white solid (0.25 g, 10%).

¹H NMR (400 MHz, CDCl₃) δ 7.96 (d, *J* = 8.5 Hz, 2H), 6.90 (d, *J* = 9.0 Hz, 2H), 5.69 (d, *J* = 49.0 Hz, 1H), 3.81 (s, 3H), 1.37 (s, 9H); **¹³C NMR (101 MHz, CDCl₃)** δ 188.2 (d, *J* = 20.0 Hz), 164.5, 164.1 (d, *J* = 24.5 Hz), 131.9, 126.5, 114.0, 89.9 (d, *J* = 196.0 Hz), 84.2, 55.5, 27.7 ; **¹⁹F NMR (377 MHz, CDCl₃):** δ -188.9 (d, *J* = 49.0 Hz). **FTIR:** v_{max}/cm⁻¹ (neat) 3056, 1754, 1600, 1264, 734, 705; HRMS (ESI⁺): calculated for C₁₄H₁₇FO₄ (ES⁺)(+Na⁺): 291.1009. Found: 291.1022.

tert-butyl 2-fluoro-3-(4-chlorophenyl)-3-oxopropanoate (89e)
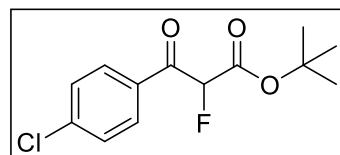
Following GPE using diisopropyl amine (1.7 mL ,12 mmol) *n*-butyl lithium in 2.5 M hexane (4.8 mL, 12 mmol), *tert*-butyl acetate (1.16 g, 10 mmol), 4-chlorobenzaldehyde (1.36 g, 10 mmol), activated manganese (IV) oxide (8.7 g, 100 mmol) and selectfluor (4.25 g, 12 mmol) with FCC (5% Et₂O in 40-60 petroleum ether) afforded *tert*-butyl 2-fluoro-3-(4-chlorophenyl)-3-oxopropanoate (**89e**) as a pale orange oil (0.74 g, 27%)

¹H NMR (400 MHz, CDCl₃) δ 7.94 (d, *J* = 8.5 Hz, 2H), 7.43 (d, *J* = 8.5 Hz, 2H), 5.72 (d, *J* = 49.0 Hz, 1H), 1.39 (s, 9H); **¹³C NMR (101 MHz, CDCl₃)** δ 189.0 (d, *J* = 20.5 Hz), 163.7 (d, *J* = 24.5 Hz), 141.1, 132.1

(d, J = 2.5 Hz), 131.0 (d, J = 3.5 Hz), 129.3, 90.2 (d, J = 197.0 Hz), 84.9, 27.9 ; **^{19}F NMR (377 MHz,**

CDCl$_3$): δ -189.5 (d, J = 49.0 Hz). **FTIR:** v_{max}/cm^{-1} (neat) 2981, 1756, 1589, 1249, 771, 729; HRMS

(ESI$^+$): calculated for C$_{14}$H$_{14}$^{35}ClFO$_3$Na (ES$^+$)(+Na$^+$): 295.0513. Found: 295.0708.

ethyl 3-((*tert*-butyldimethylsilyl)oxy)-2-fluoro-3-phenylacrylate (83)
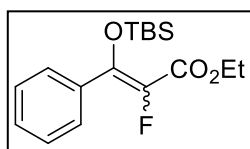
Ethyl 2-fluoro-3-oxo-3-phenylpropanoate (0.4 g, 1.9 mmol) was dissolved in CH$_2$Cl$_2$ (4 mL) and cooled to 0 °C. *tert*-Butyldimethylsilyl trifluoromethanesulfonate (1.0 g, 3.8 mmol) followed by Et$_3$N (0.68 g, 4.8 mmol) were each added dropwise and the reaction was allowed to warm to rt. and stirred under nitrogen overnight. After solvent removal under reduced pressure, the crude material was subjected to silica gel flash column chromatography (2% Et$_2$O in 40-60 petroleum ether) to give silyl enol ether (**83**) as a colourless oil (0.38 g, 62%). Careful purification allowed each isomer to be separated; (*Z*)-isomer: 0.330 g, 87%; (*E*)-minor isomer: 0.050 g, 13%).

(*Z*)-isomer: **^{1}H NMR (400 MHz, CDCl$_3$)** δ 7.42 - 7.32 (m, 5H), 4.09 (q, J = 7.0 Hz, 2H), 1.10 (t, J = 7.0 Hz, 3H), 0.90 (s, 9H), 0.07 (d, J = 1.5 Hz, 6H); **^{13}C NMR (101 MHz, CDCl$_3$)** δ 161.7 (d, J = 30.0 Hz), 149.6 (d, J = 14.5 Hz), 139.3, 134.8, 129.5, 129.1 (d, J = 2.5 Hz), 127.7, 60.7, 25.4, 18.4, 13.9, -4.5 (d, J = 3.0 Hz); **^{19}F NMR (377 MHz, CDCl$_3$)** δ -148.2.

(*E*)- isomer: **^{1}H NMR (400 MHz, CDCl$_3$)** δ 7.57 - 7.49 (m, 2H), 7.43 - 7.34 (m, 3H), 4.34 (q, J = 7.0 Hz, 2H), 1.36 (t, J = 7.0 Hz, 3H), 0.92 (s, 9H), -0.05 (s, 6H); **^{13}C NMR (101 MHz, CDCl$_3$)** δ 161.7 (d, J = 30.0 Hz), 149.6 (d, J = 14.5 Hz), 136.9, 134.8, 129.9, 128.3 (d, J = 5.5 Hz), 128.1, 60.7, 25.7, 18.5, 14.5, -4.3; **^{19}F NMR (377 MHz, CDCl$_3$)** δ -158.7.

(*Z*)-3-((*tert*-butyldimethylsilyl)oxy)-2-fluoro-3-phenylprop-2-en-1-ol (84)
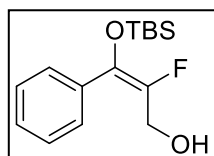
(*Z*)-ethyl 3-((*tert*-butyldimethylsilyl)oxy)-2-fluoro-3-phenylacrylate (**83**) (65 mg, 0.2 mmol) was dissolved in CH$_2$Cl$_2$ (2 mL) and cooled to 0 °C. -H (0.21 mL, 0.42 mmol) was added dropwise and the reaction mixture was stirred under nitrogen for 1 h. The reaction was quenched by the addition of MeOH (2 mL) at 0 °C, diluted with water (20 mL) and extracted with diethyl ether (3 x 20 mL). The combined organic layers were then

dried over anhydrous magnesium sulfate and concentrated under vacuum to give (*Z*)-3-((*tert*-butyldimethylsilyl)oxy)-2-fluoro-3-phenylprop-2-en-1-ol (**84**) as a colourless oil (44 mg, 79%).

1H NMR (400 MHz, CDCl₃) δ 7.38-7.29 (m, 5H), 4.25 (d, *J* = 24.5 Hz, 2H), 1.84 (s, 1H), 0.91 (s, 9H), 0.06 (s, 6H); **13C NMR (101 MHz, CDCl₃)** δ 148.1, 145.7, 135.3 (d, *J* = 3.5 Hz), 128.9, 128.5 (d, *J* = 2.5Hz), 128.3, 59.6 (d, *J* = 27.0 Hz), 29.8, 25.7, -4.5 (d, *J* = 2.5 Hz); **19F NMR (377 MHz, CDCl₃):** δ -137.8 (t, *J* = 24.5 Hz). **FTIR:** v_{max}/cm^{-1} (neat) 3003, 1420, 1359, 1220, 1092, 1047, 784, 616; HRMS (ESI⁺): calculated for $C_{15}H_{23}F\ O_2SiNa$ (ES⁺)(+Na⁺): 305.1349. Found: 305.1345.

ethyl (*R*) 2-benzoyl-4-{[(*tert*-butoxycarbonyl)amino]methyl}-2-fluoropent-4-enoate (79a)[53]
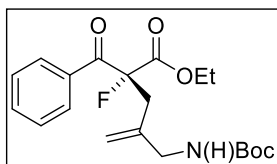
Following GPF with ethyl 2-fluoro-3-oxo-3-phenylpropanoate (**78a**) (27 mg, 0.13 mmol), *tert*-butyl 5-methylene-2-oxo-1,3-oxazinane-3-carboxylate (**2a**) (22 mg, 0.1 mmol), Pd(dba)₂ (2.9 mg, 0.005 mmol) , *(R,R)*-Dach-phenyl Trost ligand (3.8 mg, 0.0055 mmol), *t*-BuOH (0.048 mL, 0.5 mmol) and DIPEA (0.021 mL, 0.12 mmol) in PhMe (1 mL) with FCC (gradient from 20-30% Et₂O in 40-60 petroleum ether) afforded ethyl (*R*) 2-benzoyl-4-{[(*tert*-butoxycarbonyl)amino]methyl}-2-fluoropent-4-enoate(**79a**) as a pale yellow oil (33 mg, 78%).

1H NMR (400 MHz, CDCl₃): δ 8.02 (d, *J* = 8.0 Hz, 2H, CH_Ar), 7.58 (t, *J* = 7.5 Hz, 1H, CH_Ar), 7.44 (t, *J* = 8.0 Hz, 2H, CH_Ar), 5.13 (s, 1H, C=CH), 5.03 (s, 1H, C=CH), 4.79 (br, 1H, NH), 4.30 – 4.15 (m, 2H, CH₂CH₃), 3.76 (d, *J* = 4.0 Hz, 2H, CH₂), 3.13 (dd, *J* = 33.0, 15.0 Hz, 1H, CH₂), 2.96 (dd, *J* = 18.5, 15.5 Hz, 1H, CH₂), 1.43 (s, 9H, C(CH₃)₃), 1.19 (t, *J* = 7.0 Hz, 3H, CH₃CH₂); **13C NMR (101 MHz, CDCl₃)** δ 191.3 (d, *J* = 30.0 Hz), 167.0 (d, *J* = 26.0 Hz), 155.9, 139.8, 134.1, 133.8 (d, *J* = 3.0 Hz), 129.9 (d, *J*= 5.5 Hz), 128.8, 116.2, 100.0 (d, *J*= 200.0 Hz), 79.5, 62.9, 45.8, 38.2 (d, *J* = 20.5 Hz), 28.5, 14.1; **19F NMR (377 MHz, CDCl₃):** δ -160.1 (dd, *J* = 33.0, 18.5 Hz). **HPLC** (Cellulose-1, hexane: ⁱPrOH 90:10, flow rate 1.0 mL/min, λ = 254 nm, 25 °C) t_R(major) = 6.730 min, t_R(minor) = 9.393 min, *ee* = 75%.

ethyl (*R*) 4-{[(*tert*-butoxycarbonyl)amino]methyl}-2-fluoro-2-(4-chloromethylbenzoyl)pent-4-enoate (79b)[53]
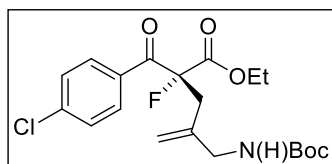
Following GPF with ethyl 2-fluoro-3-(4-chloromethylphenyl)-3-oxopropanoate (**78b**) (32 mg, 0.13 mmol), *tert*-butyl 5-methylene-2-oxo-1,3-oxazinane-3-carboxylate (**2a**) (22 mg, 0.1 mmol), Pd(dba)$_2$ (2.9 mg, 0.005 mmol) , *(R,R)*-Dach-phenyl Trost ligand (3.8 mg, 0.0055 mmol), *t*-BuOH (0.048 mL, 0.5 mmol) and DIPEA (0.021 mL, 0.12 mmol) in PhMe (1 mL) with FCC (20% Et$_2$O in 40-60 petroleum ether) afforded ethyl (*R*) 4-{[(*tert*-butoxycarbonyl)amino]methyl}-2-fluoro-2-(4-chloromethylbenzoyl)pent-4-enoate (**79b**) as a white solid (21 mg, 50%). The product was recrystallized from toluene/CH$_2$Cl$_2$ to provide a colourless crystalline solid (>99% *ee*).

^{1}H NMR (400 MHz, CDCl$_3$): δ 7.97 (dd, *J* = 8.5, 1.5 Hz, 2H), 7.44 – 7.39 (m, 2H), 5.13 (s, 1H), 5.03 (s, 1H), 4.79 (br, 1H), 4.30 – 4.15 (m, 2H), 3.76 (d, *J* = 4.0 Hz, 2H), 3.13 (dd, *J* = 33.0, 15.0 Hz, 1H), 2.96 (dd, *J* = 18.5, 15.5 Hz, 1H), 1.43 (s, 9H), 1.19 (t, *J* = 7.0 Hz, 3H); **^{13}C NMR (101 MHz, CDCl$_3$)** δ 191.3 (d, *J* = 30.0 Hz), 167.1 (d, *J* = 26.0 Hz), 155.9, 140.7, 139.6, 132.0 (d, *J* = 3.5 Hz), 131.3 (d, *J* = 6.0 Hz), 129.1, 116.2, 100.0 (d, *J*= 200.0 Hz), 79.5, 62.9, 45.8, 38.2 (d, *J* = 20.5 Hz), 28.5, 14.1; **^{19}F NMR (377 MHz, CDCl$_3$)**: δ -157.7 (dd, *J* = 33.0, 19.0 Hz). **m.p**: 56.4-58.0°C. **HPLC** (Cellulose-1, hexane: ^{i}PrOH 90:10, flow rate 1.0 mL/min, λ = 254 nm, 25 °C) t$_R$(major) = 7.127 min, t$_R$(minor) = 17.703 min, *ee* = 81%; $[\alpha]_D^{22} = -30$ (*c* 1.0, CHCl$_3$).

ethyl (*R*) 4-{[(*tert*-butoxycarbonyl)amino]methyl}-2-fluoro-2-(4-nitrobenzoyl)pent-4-enoate (79c)[53]
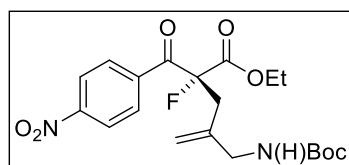
Following GPF with ethyl 2-fluoro-3-(4-chloromethylphenyl)-3-oxopropanoate (**78c**) (32 mg, 0.13 mmol), *tert*-butyl 5-methylene-2-oxo-1,3-oxazinane-3-carboxylate (**2a**) (22 mg, 0.1 mmol), Pd(dba)$_2$ (2.9 mg, 0.005 mmol) , *(R,R)*-Dach-phenyl Trost ligand (3.8 mg, 0.0055 mmol), *t*-BuOH (0.048 mL, 0.5 mmol) and DIPEA (0.021 mL, 0.12 mmol) in PhMe (1 mL) with FCC (gradient from 20-30% Et$_2$O in 40-60 petroleum ether) afforded ethyl (*R*) 4-{[(*tert*-

butoxycarbonyl)amino]methyl}-2-fluoro-2-(4-nitrobenzoyl)pent-4-enoate (**79c**) as an orange oil (32 mg, 77%).

^{1}H NMR (400 MHz, CDCl$_3$): δ 8.27 (d, *J* = 9.0 Hz, 2H), 8.17 (d, *J* = 9.0 Hz, 2H), 5.13 (s, 1H), 5.03 (s, 1H), 4.79 (br, 1H), 4.30 – 4.15 (m, 2H), 3.76 (d, *J* = 4.0 Hz, 2H), 3.13 (dd, *J* = 33.0, 15.0 Hz, 1H), 2.96 (dd, *J* = 18.5, 15.5 Hz, 1H), 1.43 (s, 9H), 1.19 (t, *J* = 7.0 Hz, 3H); **^{13}C NMR (101 MHz, CDCl$_3$)** δ 190.6 (d, *J* = 28.0 Hz), 166.3 (d, *J* = 26.0 Hz), 155.9, 150.7, 139.4, 138.9 (d, *J* = 106.5 Hz), 131.0 (d, *J* = 6.0 Hz), 123.9, 116.4, 100.2 (d, *J* = 200.0 Hz), 79.5, 62.9, 45.8, 38.2 (d, *J* = 20.5 Hz), 28.5, 14.1; **^{19}F NMR (377 MHz, CDCl$_3$)**: δ -158.3 (dd, *J* = 32.0, 20.5 Hz). **HPLC** (Cellulose-2, hexane: ^{i}PrOH 90:10, flow rate 1.0 mL/min, λ = 254 nm, 25 °C) t_R(major) = 15.393 min, t_R(minor) = 18.277 min, *ee* = 80%.

ethyl (*R*) 4-{[(*tert*-butoxycarbonyl)amino]methyl}-2-fluoro-2-(4-trifluoromethylbenzoyl)pent-4-enoate (79d)[53]

Following GPF with ethyl 2-fluoro-3-(4-trifluoromethylphenyl)-3-oxopropanoate (**78d**) (37 mg, 0.13 mmol), *tert*-butyl 5-methylene-2-oxo-1,3-oxazinane-3-carboxylate (**2a**) (22 mg, 0.1 mmol), Pd(dba)$_2$ (2.9 mg, 0.005 mmol), *(R,R)*-Dach-phenyl Trost ligand (3.8 mg, 0.0055 mmol), *t*-BuOH (0.048 mL, 0.5 mmol) and DIPEA (0.021 mL, 0.12 mmol) in PhMe (1 mL) with FCC (gradient from 20-30% Et$_2$O in 40-60 petroleum ether) afforded ethyl (*R*) 4-{[(*tert*-butoxycarbonyl)amino]methyl}-2-fluoro-2-(4-trifluoromethylbenzoyl)pent-4-enoate (**79d**) as a pale yellow oil (37 mg, 82%).

^{1}H NMR (400 MHz, CDCl$_3$): δ 8.13 (d, *J* = 8.0 Hz, 2H), 7.71 (d, *J* = 8.0 Hz, 2H), 5.14 (s, 1H), 5.03 (s, 1H), 4.76 (br, 1H), 4.29 – 4.13 (m, 2H), 3.75 (d, *J* = 5.5 Hz, 1H), 3.13 (dd, *J* = 32.5, 15.5 Hz, 1H), 2.97 (dd, *J* = 19.5, 15.5 Hz, 1H), 1.42 (s, 9H), 1.21 (t, *J* = 7.0 Hz, 3H); **^{13}C NMR (101 MHz, CDCl$_3$)** δ 190.8 (d, *J* = 26.5 Hz), 166.6 (d, *J* = 26.0 Hz), 155.9, 139.6, 136.5, 135.2 (q, *J* = 33.0 Hz), 130.3 (d, *J* = 6.0 Hz), 125.8 (d, *J* = 3.5 Hz), 123.5 (q, *J* = 273.0 Hz), 116.3, 100.2 (d, *J* = 200.0 Hz), 79.5, 62.9, 45.8, 38.2 (d, *J* = 20.5 Hz), 28.5, 14.1; **^{19}F NMR (377 MHz, CDCl$_3$)**: δ -63.4 (s), -160.1 (dd, *J* = 32.5, 19.5 Hz). **HPLC** (Cellulose-2, hexane: ^{i}PrOH 90:10, flow rate 1.0 mL/min, λ = 254 nm, 25 °C) t_R(major) = 5.133 min, t_R(minor) = 6.020 min, *ee* = 81%.

ethyl (*R*) 4-{[(*tert*-butoxycarbonyl)amino]methyl}-2-fluoro-2-(4-methoxybenzoyl)pent-4-enoate (79e)[53]
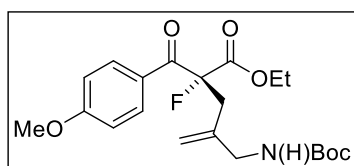
Following GPF with ethyl 2-fluoro-3-(4-methoxyphenyl)-3-oxopropanoate (**78e**) (32 mg, 0.13 mmol), *tert*-butyl 5-methylene-2-oxo-1,3-oxazinane-3-carboxylate (**2a**) (22 mg, 0.1 mmol), Pd(dba)$_2$ (2.9 mg, 0.005 mmol), *(R,R)*-Dach-phenyl Trost ligand (3.8 mg, 0.0055 mmol), *t*-BuOH (0.048 mL, 0.5 mmol) and DIPEA (0.021 mL, 0.12 mmol) in PhMe (1 mL) with FCC (gradient from 20-30% Et$_2$O in 40-60 petroleum ether) afforded ethyl (*R*) 4-{[(*tert*-butoxycarbonyl)amino]methyl}-2-fluoro-2-(4-methoxybenzoyl)pent-4-enoate (**79e**) as an orange oil (27 mg, 68%).

1H NMR (400 MHz, CDCl$_3$): **1H NMR (400 MHz, CDCl$_3$):** δ 8.06 (dd, *J* = 9.0, 1.5 Hz, 2H), 6.91 (d, *J* = 9.0 Hz, 2H), 5.14 (s, 1H), 5.03 (s, 1H), 4.76 (br, 1H), 4.29 – 4.13 (m, 2H), 3.87 (s, 3H), 3.75 (d, *J* = 5.5 Hz, 2H), 3.13 (dd, *J* = 32.5, 15.5 Hz, 1H), 2.97 (dd, *J* = 19.5, 15.5 Hz, 1H), 1.42 (s, 9H), 1.21 (t, *J* = 7.0 Hz, 3H); **13C NMR (101 MHz, CDCl$_3$)** δ 189.4 (d, *J* = 25.0 Hz), 167.4 (d, *J* = 26.0 Hz), 164.3, 155.9, 139.9, 132.5 (d, *J* = 6.0 Hz), 126.5 (d, *J* = 3.5 Hz), 116.0, 114.1, 100.0 (d, *J* = 200.5 Hz), 79.5, 62.7, 55.6, 45.8, 38.2 (d, *J* = 20.5 Hz), 28.5, 14.1; **19F NMR (377 MHz, CDCl$_3$):** δ -156.9 (dd, *J* = 33.8, 18.0 Hz). **HPLC** (Cellulose-1, hexane: ^{i}PrOH 90:10, flow rate 1.0 mL/min, λ = 254 nm, 25 °C) t_R(major) = 9.847 min, t_R(minor) = 14.267 min, *ee* = 74%.

ethyl (*R*) 4-{[(*tert*-butoxycarbonyl)amino]methyl}-2-fluoro-2-(4-methylbenzoyl)pent-4-enoate (79f)[53]
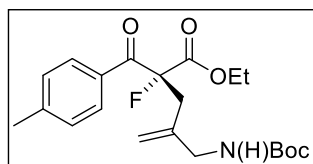
Following GPF with ethyl 2-fluoro-3-(4-methylphenyl)-3-oxopropanoate (**78f**) (30 mg, 0.13 mmol), *tert*-butyl 5-methylene-2-oxo-1,3-oxazinane-3-carboxylate (**2a**) (22 mg, 0.1 mmol), Pd(dba)$_2$ (2.9 mg, 0.005 mmol) , *(R,R)*-Dach-phenyl Trost ligand (3.8 mg, 0.0055 mmol), *t*-BuOH (0.048 mL, 0.5 mmol) and DIPEA (0.021 mL, 0.12 mmol) in PhMe (1 mL) with FCC (gradient from 20-30% Et$_2$O in 40-60 petroleum ether) afforded ethyl (*R*) 4-{[(*tert*-butoxycarbonyl)amino]methyl}-2-fluoro-2-(4-methylbenzoyl)pent-4-enoate (**79f**) as a white solid (18 mg, 47%). The product was recrystallized from toluene/CH$_2$Cl$_2$ to provide a colourless crystalline solid (96% *ee*).

¹H NMR (400 MHz, CDCl₃): δ 7.94 (dd, J = 8.0 1.5 Hz, 2H), 7.25 (d, J = 8.0 Hz, 2H), 5.14 (s, 1H), 5.03 (s, 1H), 4.78 (br, 1H), 4.30 – 4.16 (m, 2H), 3.77 (s, 2H), 3.13 (dd, J = 33.5, 15.5 Hz, 1H), 2.95 (dd, J = 18.0, 15.5 Hz, 1H), 2.40 (s, 3H), 1.43 (s, 9H), 1.19 (t, J = 7.0 Hz, 3H); **¹³C NMR (101 MHz, CDCl₃)** δ 190.7 (d, J = 25.5 Hz), 167.2 (d, J = 26.0 Hz), 155.9, 145.3, 139.9, 131.2 (d, J = 3.5 Hz), 130.1 (d, J = 5.5 Hz), 129.5, 116.0, 99.9 (d, J = 200.5 Hz), 79.5, 62.8, 45.8, 38.2 (d, J = 20.5 Hz), 28.5, 21.9, 14.1; **¹⁹F NMR (377 MHz, CDCl₃)**: δ -157.3 (dd, J = 33.5, 18.5 Hz). **m.p:** 72.5-74.6°C. **HPLC** (Cellulose-2, hexane: ⁱPrOH 90:10, flow rate 1.0 mL/min, λ = 254 nm, 25 °C) t_R(major) = 9.873 min, t_R(minor) = 11.433 min, ee = 77%; $[\alpha]_D^{22} = -30$ (c 1.0, CHCl₃).

ethyl (R)-4-(((tert-butoxycarbonyl)amino)methyl)-2-fluoro-2-(2-methylbenzoyl)pent-4-enoate (79g)[53]
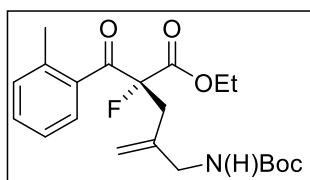
Following GPF with ethyl 2-fluoro-3-(2-methylphenyl)-3-oxopropanoate (**78 g**) (30 mg, 0.13 mmol), *tert*-butyl 5-methylene-2-oxo-1,3-oxazinane-3-carboxylate (**2a**) (22 mg, 0.1 mmol), Pd(dba)₂ (2.9 mg, 0.005 mmol), *(R,R)*-Dach-phenyl Trost ligand (3.8 mg, 0.0055 mmol), *t*-BuOH (0.048 mL, 0.5 mmol) and DIPEA (0.021 mL, 0.12 mmol) in PhMe (1 mL) with FCC (gradient from 20-30% Et₂O in 40-60 petroleum ether) afforded ethyl (*R*) 4-{[(*tert*-butoxycarbonyl)amino]methyl}-2-fluoro-2-(2-methylbenzoyl)pent-4-enoate (**79g**) as a white solid (20 mg, 83%).

¹H NMR (400 MHz, CDCl₃): δ 7.67 (dd, J = 7.5, 3.0 Hz, 1H), 7.38 (td, J = 7.5, 1.0 Hz, 1H), 7.32 – 7.21 (m, 2H) 5.13 (s, 1H), 5.05 (s, 1H), 4.77 (br, 1H), 4.25 (q, J = 7.0, 2.0 Hz, 2H), 3.73 (d, J = 5.5 Hz, 2H), 3.14 – 2.95 (m, 2H), 2.41 (s, 3H), 1.43 (s, 9H), 1.24 (t, J = 7.0 Hz, 3H); **¹³C NMR (101 MHz, CDCl₃)** δ 195.4 (d, J = 26.5 Hz), 166.8 (d, J = 26.0 Hz), 155.9, 139.8, 139.3, 134.3 (d, J =3.0 Hz), 132.1, 132.0, 129.0 (d, J = 9.0 Hz), 125.5, 116.1, 100.3 (d, J = 202.0 Hz), 79.5, 62.9, 45.8, 38.6 (d, J = 20.5 Hz), 28.5, 20.9, 14.1; **¹⁹F NMR (377 MHz, CDCl₃)**: δ -158.1 (dd, J = 29.0, 22.0 Hz). **HPLC** (Cellulose-1, hexane: ⁱPrOH 90:10, flow rate 1.0 mL/min, λ = 254 nm, 25 °C) t_R(major) = 5.497 min, t_R(minor) = 6.563 min, ee = 86%.

ethyl (*R*) 4-(((*tert*-butoxycarbonyl)amino)methyl)-2-fluoro-2-(furan-2-carbonyl)pent-4-enoate (79h)
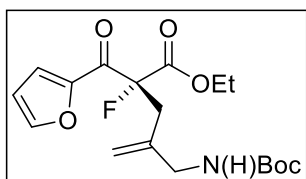
Following GPF with ethyl 2-fluoro-3-oxo-3-(furan-2-yl)propanoate (**78h**) (26 mg, 0.13 mmol), *tert*-butyl 5-methylene-2-oxo-1,3-oxazinane-3-carboxylate (**2a**) (22 mg, 0.1 mmol), Pd(dba)$_2$ (2.9 mg, 0.005 mmol), *(R,R)*-Dach-phenyl Trost ligand (3.8 mg, 0.0055 mmol), *t*-BuOH (0.048 mL, 0.5 mmol) and DIPEA (0.021 mL, 0.12 mmol) in PhMe (1 mL) with FCC (gradient from 30-40% Et$_2$O in 40-60 petroleum ether) afforded ethyl (*R*) 4-(((*tert*-butoxycarbonyl)amino)methyl)-2-fluoro-2-(furan-2-carbonyl)pent-4-enoate (**79h**) as a yellow oil (29 mg, 80%).

^{1}H NMR (400 MHz, CDCl$_3$): δ 7.69 (br, 1H), 7.50 (t, *J* = 3.5 Hz, 1H), 6.57 (dd, *J* = 3.5, 1.5 Hz, 1H), 5.12 (s, 1H), 5.04 (s, 1H), 4.75 (br, 1H), 4.29 – 4.17 (m, 2H), 3.74 (d, *J* = 5.5 Hz, 2H), 3.10 (dd, *J* = 31.5, 15.5 Hz, 1H), 2.95 (dd, *J* = 20.5, 15.5 Hz, 1H), 1.43 (s, 9H), 1.23 (t, *J* = 7.0 Hz, 3H); **^{13}C NMR (101 MHz, CDCl$_3$)** δ 179.4 (d, *J* = 26.5 Hz), 166.3 (d, *J* = 26.5 Hz), 156.9, 149.0 (d, *J* = 3.5 Hz), 148.5, 139.5, 122.8 (d, *J* = 11.0 Hz), 116.2, 112.8(d, *J* = 1.5 Hz), 99.2 (d, *J* = 200.0 Hz), 79.6, 62.9, 45.8, 37.5 (d, *J* = 20.0 Hz), 28.5, 14.1; **^{19}F NMR (377 MHz, CDCl$_3$)**: δ -160.9 (dd, *J* = 30.5, 22.0 Hz); **FTIR:** ν$_{max}$/cm^{-1} (neat) 2979, 1756, 1689, 1512, 1461, 1366, 1249, 1169, 1028, 905, 862, 773 cm^{-1}; **HRMS (ESI$^+$):** calculated for C$_{18}$H$_{24}$FNO$_6$Na (ES$^+$)(+Na$^+$): 392.1485. Found: 392.1472. **HPLC** (Cellulose-1, hexane: ^{i}PrOH 90:10, flow rate 1.0 mL/min, λ = 254 nm, 25 °C) t$_R$(major) = 10.737 min, t$_R$(minor) = 13.723 min, *ee* = 76%.

ethyl (*R*) 2-(2-naphthoyl)-4-(((*tert*-butoxycarbonyl)amino)methyl)-2-fluoropent-4-enoate (79i)[53]
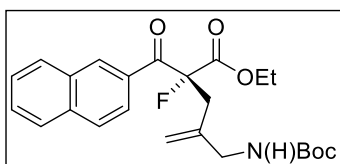
Following GPF with ethyl 2-fluoro-3-(naphthalen-2-yl)-3-oxopropanoate (**78i**) (34 mg, 0.13 mmol), *tert*-butyl 5-methylene-2-oxo-1,3-oxazinane-3-carboxylate (**2a**) (22 mg, 0.1 mmol), Pd(dba)$_2$ (2.9 mg, 0.005 mmol), *(R,R)*-Dach-phenyl Trost ligand (3.8 mg, 0.0055 mmol), *t*-BuOH (0.048 mL, 0.5 mmol) and DIPEA (0.021 mL, 0.12 mmol) in PhMe (1 mL) with FCC (gradient from 15-25% Et$_2$O in 40-60 petroleum ether) afforded ethyl (*R*) 2-(2-naphthoyl)-4-(((*tert*-butoxycarbonyl)amino)methyl)-2-fluoropent-4-enoate (**79i**) as a white solid

(33 mg, 80%). The product was recrystallized from toluene/CH$_2$Cl$_2$ to provide a colourless crystalline solid (>99% *ee*).

^{1}H NMR (400 MHz, CDCl$_3$) δ 8.65 (s, 1H), 8.03 (dt, *J* = 8.5, 1.5 Hz, 1H), 7.97 (d, *J* = 8.0 Hz, 1H), 7.87 (t, *J* = 8.5 Hz, 2H), 7.65 – 7.59 (m, 1H), 7.58 – 7.52 (m, 1H), 5.16 (s, 1H), 5.07 (s, 1H), 4.79 (br, 1H), 4.34 – 4.15 (m, 2H), 3.80 (br, 2H), 3.29 – 2.97 (m, 2H), 1.44 (s, 9H), 1.20 (t, *J* = 7.0 Hz, 3H); **^{13}C NMR (101 MHz, CDCl$_3$)** δ 191.0 (d, *J* = 25.5 Hz), 167.2 (d, *J* = 26.0 Hz), 155.9, 139.9, 136.0, 132.4, 132.3, 131.0 (2C), 130.3, 129.3, 128.6, 127.8, 127.1, 124.9 (d, *J* = 3.0 Hz), 116.1, 100.2 (d, *J* = 200.5 Hz), 62.9, 45.8, 38.3 (d, *J* = 20.5 Hz), 28.5, 14.1; **^{19}F NMR (377 MHz, CDCl$_3$)**: δ -156.7 (dd, *J* = 33.5, 18.5 Hz). **m.p:** 98.6-99.6°C. **HPLC** (Cellulose-2, hexane: ^{i}PrOH 90:10, flow rate 1.0 mL/min, λ = 254 nm, 25 °C) t$_R$(major) = 9.787 min, t$_R$(minor) = 11.630 min, *ee* = 82%; $[\alpha]_D^{22} = -30$ (*c* 1.0, CHCl$_3$).

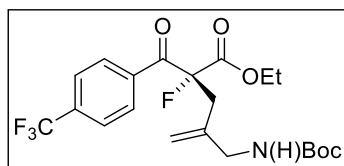**ethyl (*R*)-2-acetyl-4-(((tert-butoxycarbonyl)amino)methyl)-2-fluoropent-4-enoate (79j)**[53]
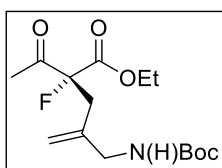
Following GPF with ethyl 2-fluoro-3-oxobutanoate (**79j**) (18 mg, 0.13 mmol), *tert*-butyl 5-methylene-2-oxo-1,3-oxazinane-3-carboxylate (**2a**) (22 mg, 0.1 mmol), Pd(dba)$_2$ (2.9 mg, 0.005 mmol), *(R,R)*-Dach-phenyl Trost ligand (3.8 mg, 0.0055 mmol), *t*-BuOH (0.048 mL, 0.5 mmol) and DIPEA (0.021 mL, 0.12 mmol) in PhMe (1 mL) with FCC (gradient from 20-30% Et$_2$O in 40-60 petroleum ether) afforded ethyl (*R*)-2-acetyl-4-(((tert-butoxycarbonyl)amino)methyl)-2-fluoropent-4-enoate (**79j**) as a colourless oil(21 mg, 65%).

^{1}H NMR (400 MHz, CDCl$_3$) δ 5.10 (s, 1H), 4.99 (s, 1H), 4.73 (br, 1H), 4.24 (q, *J* = 7.0 Hz, 2H), 3.77 – 3.62 (m, 2H), 2.94 – 2.73 (m, 2H), 2.29 (d, *J* = 5.0 Hz, 3H), 1.43 (s, 9H), 1.28 (t, *J* = 7.0 Hz, 3H); **^{13}C NMR (101 MHz, CDCl$_3$)** δ 201.5 (d, *J* = 29.5 Hz), 165.8 (d, *J* = 25.5 Hz), 155.9, 139.5, 115.8, 100.4 (d, *J* = 200.0 Hz), 79.6, 62.9, 45.8, 37.4 (d, *J* = 20.0 Hz), 28.5, 26.0, 14.1; **^{19}F NMR (377 MHz, CDCl$_3$)**: δ -163.6 – -163.7 (m);. **HPLC** (Cellulose-1, hexane: ^{i}PrOH 95:5, flow rate 1.0 mL/min, λ = 205 nm, 25 °C) t$_R$(major) = 11.583 min, t$_R$(minor) = 14.563 min, *ee* = 61%.

tert-butyl (*R*) 2-benzoyl-4-(((*tert*-butoxycarbonyl)amino)methyl)-2-fluoropent-4-enoate (90a)
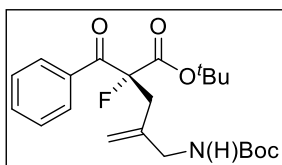
Following the General Procedure F with *tert*-butyl 2-fluoro-3-oxo-3-phenylpropanoate (**89a**) (31 mg, 0.13 mmol), *tert*-butyl 5-methylene-2-oxo-1,3-oxazinane-3-carboxylate (**2a**) (22 mg, 0.1 mmol), Pd(dba)$_2$ (2.9 mg, 0.005 mmol), *(R,R)*-Dach-phenyl Trost ligand (3.8 mg, 0.0055 mmol), *t*-BuOH (0.048 mL, 0.5 mmol) and DIPEA (0.021 mL, 0.12 mmol) in PhMe (1 mL) with FCC (gradient from 15-25% Et$_2$O in 40-60 petroleum ether) afforded *tert*-butyl (*R*) 2-benzoyl-4-(((*tert*-butoxycarbonyl)amino)methyl)-2-fluoropent-4-enoate (**90a**) as a yellow oil (30 mg, 75%).

^{1}H NMR (400 MHz, CDCl$_3$) δ 8.02 (d, *J* = 8.0 Hz, 2H) , 7.58 (t, *J* = 7.5 Hz, 1H), 7.44 (t, *J* = 8.0 Hz, 2H), 5.15 (s, 1H), 5.05 (s, 1H), 4.79 (br, 1H), 3.78 (d, *J* = 4.0 Hz, 2H), 3.09 (dd, *J* = 34.0, 15.5 Hz, 1H), 2.94 (dd, *J* = 18.0, 15.5 Hz, 1H), 1.44 (s, 9H), 1.36 (s, 9H); **^{13}C NMR (101 MHz, CDCl$_3$)** δ 191.4 (d, *J* = 26.0 Hz), 165.8 (d, *J* = 25.5 Hz), 156.9, 139.9, 133.9, 133.7 (d, *J* = 7.5 Hz), 129.8 (d, *J* = 4.0 Hz), 128.7, 116.1, 99.4 (d, *J* = 200.0 Hz), 84.6, 79.5, 45.7, 38.1 (d, *J* = 21.0 Hz), 28.5, 27.9; **^{19}F NMR (377 MHz, CDCl$_3$)**: δ -156.2 (dd, *J* = 33.8, 18.0 Hz). **FTIR:** ν$_{max}$/cm^{-1} (neat) 2979, 2929, 1707, 1512, 1422, 1366, 1223, 1155, 1059, 908, 839, 697; **HRMS (ESI$^+$):** calculated for C$_{22}$H$_{30}$FNO$_5$Na (ES$^+$)(+Na$^+$): 430.2006. Found: 430.2009. **HPLC** (Cellulose-1, hexane: ^{i}PrOH 99.5:0.5, flow rate 1.0 mL/min, λ = 254 nm, 25 °C) t$_R$(major) =32.000 min, t$_R$(minor) = 34.937 min, *ee* = 90%.

tert-butyl (*R*) 4-(((*tert*-butoxycarbonyl)amino)methyl)-2-(4-chlorobenzoyl)-2-fluoropent-4-enoate (90b)
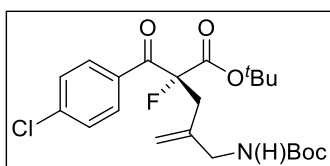
Following the General Procedure F with *tert*-butyl 3-(4-chlorophenyl)-2-fluoro-3-oxopropanoate (**89b**) (35 mg, 0.13 mmol), *tert*-butyl 5-methylene-2-oxo-1,3-oxazinane-3-carboxylate (**2a**) (22 mg, 0.1 mmol), Pd(dba)$_2$ (2.9 mg, 0.005 mmol), *(R,R)*-Dach-phenyl Trost ligand (3.8 mg, 0.0055 mmol), t-BuOH (0.048 mL, 0.5 mmol) and DIPEA (0.021 mL, 0.12 mmol) in PhMe (1 mL) with FCC (gradient from 10-15% Et$_2$O in 40-60 petroleum ether) afforded *tert*-butyl (*R*) 4-(((*tert*-butoxycarbonyl)amino)methyl)-2-(4-chlorobenzoyl)-2-fluoropent-4-enoate (**90b**) as a yellow oil (32 mg, 72%).

^{1}H NMR (400 MHz, CDCl$_3$) ^{1}H NMR (400 MHz, CDCl$_3$): δ 7.98 (dd, *J* = 8.5, 1.5 Hz, 2H), 7.41 (d, *J* = 8.5 Hz, 2H), 5.13 (s, 1H), 5.03 (s, 1H), 4.79 (br, 1H), 3.76 (d, *J* = 5.0 Hz, 2H), 3.07 (dd, *J* = 34.0, 15.5 Hz,

1H), 2.90 (dd, J = 18.0, 15.5 Hz, 1H), 1.42 (s, 9H), 1.36 (s, 9H) ; **13C NMR (101 MHz, CDCl3)** δ 190.4 (d, J = 26.0 Hz), 165.9 (d, J = 25.5 Hz), 156.1, 140.8, 140.1, 132.3, 131.5 (d, J = 5.5 Hz), 129.3, 116.3, 99.6 (d, J = 199.0 Hz), 85.0, 79.7, 45.9, 38.2 (d, J = 20.5 Hz), 28.7, 28.0; **19F NMR (377 MHz, CDCl3)**: δ -156.3 (dd, J = 34.0, 18.5 Hz). **FTIR:** v_{max}/cm^{-1} (neat) 2924, 1750, 1460, 1379, 908, 725; **HRMS (ESI$^+$):** calculated for $C_{22}H_{29}{}^{35}ClFNO_5Na$ (ES$^+$)(+Na$^+$): 464.1616. Found: 464.2206. **HPLC** (Cellulose-1, hexane: ^{i}PrOH 95.0:5.0, flow rate 1.0 mL/min, λ = 254 nm, 25 °C) t_R(major) = 5.997 min, t_R(minor) =7.533 min, *ee* = 91%.

tert-butyl (*R*) 4-(((*tert*-butoxycarbonyl)amino)methyl)-2-fluoro-2-(4-nitrobenzoyl)pent-4-enoate (90c)
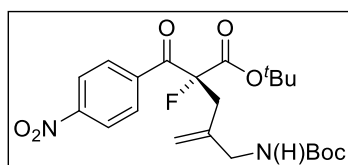
Following the General Procedure F with *tert*-butyl 2-fluoro-3-oxo-3-phenylpropanoate (**89c**) (37 mg, 0.13 mmol), *tert*-butyl 5-methylene-2-oxo-1,3-oxazinane-3-carboxylate (**2a**) (22 mg, 0.1 mmol), Pd(dba)$_2$ (2.9 mg, 0.005 mmol), *(R,R)*-Dach-phenyl Trost ligand (3.8 mg, 0.0055 mmol), *t*-BuOH (0.048 mL, 0.5 mmol) and DIPEA (0.021 mL, 0.12 mmol) in PhMe (1 mL) with FCC (20% Et$_2$O in 40-60 petroleum ether) afforded *tert*-butyl (*R*) 4-(((*tert*-butoxycarbonyl)amino)methyl)-2-fluoro-2-(4-nitrobenzoyl)pent-4-enoate (**90c**) as a yellow oil (35 mg, 80%).

1H NMR (400 MHz, CDCl3) δ 8.29 (d, J = 9.0 Hz, 2H) , 8.19 (dd, J = 9.0, 1.0 Hz, 2H), δ 5.16 (s, 1H), 5.06 (s, 1H), 4.76 (br, 1H), 3.76 (d, J = 5.5 Hz, 2H), 3.10 (dd, J = 32.5, 15.5 Hz, 1H), 2.94 (dd, J = 19.5, 15.5 Hz, 1H), 1.43 (s, 9H), 1.38 (s, 9H)**; 13C NMR (101 MHz, CDCl3)** δ 190.7 (d, J = 27.0 Hz), 165.2 (d, J = 25.5 Hz), 156.9, 150.7, 139.6, 138.5 (d, J = 3.5 Hz), 130.9 (d, J = 5.5 Hz), 123.8, 116.3, 99.7 (d, J = 199.0 Hz), 84.6, 79.5, 45.7, 37.9 (d, J = 20.5 Hz), 28.5, 27.9; **19F NMR (377 MHz, CDCl3)**: δ -156.9 (dd, J = 32.5, 19.5 Hz). **FTIR:** v_{max}/cm^{-1} (neat) 3020, 1717, 1529, 1370, 1214, 1153, 747, 668; **HRMS (ESI$^+$):** calculated for $C_{22}H_{29}FN_2O_7Na$ (ES$^+$)(+Na$^+$): 475.1851. Found: 475.1866. **HPLC** (Cellulose-1, hexane: ^{i}PrOH 97.0:3.0, flow rate 1.0 mL/min, λ = 254 nm, 25 °C) t_R(major) = 22.683 min, t_R(minor) = 26.023 min, *ee* = 91%.

### *tert*-butyl (*R*) 4-(((*tert*-butoxycarbonyl)amino)methyl)-2-fluoro-2-(4-(trifluoromethyl)benzoyl)pent-4-enoate (90d)
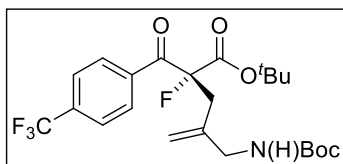
Following the General Procedure F with *tert*-butyl 2-fluoro-3-oxo-3-(4-(trifluoromethyl)phenyl)propanoate (**89d**) (40 mg, 0.13 mmol), *tert*-butyl 5-methylene-2-oxo-1,3-oxazinane-3-carboxylate (22 mg, 0.1 mmol), Pd(dba)$_2$ (2.9 mg, 0.005 mmol) , *(R,R)*-Dach-phenyl Trost ligand (3.8 mg, 0.0055 mmol), t-BuOH (0.048 mL, 0.5 mmol) and DIPEA (0.021 mL, 0.12 mmol) in PhMe (1 mL) with FCC (15% Et$_2$O in 40-60 petroleum ether) afforded *tert*-butyl (*R*) 4-(((*tert*-butoxycarbonyl)amino)methyl)-2-fluoro-2-(4-(trifluoromethyl)benzoyl)pent-4-enoate (**90d**) as a yellow oil (39 mg, 83%).

^{1}H NMR (400 MHz, CDCl$_3$) ^{1}H NMR (400 MHz, CDCl$_3$): δ 8.14 (d, *J* = 8.0 Hz, 2H), 7.72 (d, *J* = 8.0 Hz, 2H), 5.15 (s, 1H), 5.06 (s, 1H), 4.76 (br, 1H), 3.77 (d, *J* = 5.0 Hz, 2H), 3.08 (dd, *J* = 33.0, 15.5 Hz, 1H), 2.94 (dd, *J* = 19.0, 15.5 Hz, 1H), 1.44 (s, 9H), 1.38 (s, 9H); **^{13}C NMR (101 MHz, CDCl$_3$)** δ 190.9 (d, *J* = 26.5 Hz), 165.5 (d, *J* = 24.5 Hz), 155.9, 139.7, 136.7, 135.1 (q, *J* = 33.5 Hz), 130.2 (d, *J* = 5.0 Hz), 125.7 (d, *J* = 3.5 Hz), 123.6 (d, *J* = 274.0 Hz), 116.3, 99.6 (d, *J* = 199.5 Hz), 85.1, 79.6, 45.7, 38.0 (d, *J* = 20.6 Hz), 28.5, 27.9; **^{19}F NMR (377 MHz, CDCl$_3$)**: δ -63.3 (s), -156.8 (dd, J = 33.0, 19.0 Hz). **FTIR:** v_{max}/cm^{-1} (neat) 2980, 1754, 1704, 1512, 1411, 1327, 1131, 1065, 858, 759; **HRMS (ESI$^+$):** calculated for C$_{23}$H$_{29}$F$_4$NO$_5$Na (ES$^+$)(+Na$^+$): 475.1889. Found: 498.1874. **HPLC** (Cellulose-1, hexane: ^{i}PrOH 97.0:3.0, flow rate 1.0 mL/min, λ = 254 nm, 25 °C) t$_R$(major) =7.260 min, t$_R$(minor) = 9.993 min, ee = 90%.

tert-butyl (*R*) 4-(((*tert*-butoxycarbonyl)amino)methyl)-2-fluoro-2-(4-methoxybenzoyl)pent-4-enoate (90e)
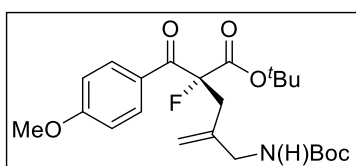
Following the General Procedure F with *tert*-butyl 2-fluoro-3-(4-methoxyphenyl)-3-oxopropanoate (**89e**) (35 mg, 0.13 mmol), *tert*-butyl 5-methylene-2-oxo-1,3-oxazinane-3-carboxylate (**2a**) (22 mg, 0.1 mmol), Pd(dba)$_2$ (2.9 mg, 0.005 mmol), *(R,R)*-Dach-phenyl Trost ligand (3.8 mg, 0.0055 mmol), *t*-BuOH (0.048 mL, 0.5 mmol) and DIPEA (0.021 mL, 0.12 mmol) in PhMe (1 mL) with FCC (10% EtOAc in 40-60 petroleum ether) afforded *tert*-butyl (*R*) 4-(((*tert*-butoxycarbonyl)amino)methyl)-2-fluoro-2-(4-methoxybenzoyl)pent-4-enoate (**90e**) as a yellow oil (22 mg, 51%).

¹H NMR (400 MHz, CDCl₃) ¹H NMR (400 MHz, CDCl₃): δ 8.04 (dd, J = 9.0, 1.5 Hz, 2H), 6.90 (d, J = 9.0 Hz, 2H), 5.13 (s, 1H), 5.04 (s, 1H), 4.82 (br, 1H), 3.86 (s, 3H), 3.77 (s, 2H), 3.08 (dd, J = 34.5, 15.5 Hz, 1H), 2.95 – 2.85 (m, 1H), 1.42 (s, 9H), 1.35 (s, 9H) ; **¹³C NMR (101 MHz, CDCl₃)** δ 189.7 (d, J = 25.0 Hz), 166.5 (d, J = 26.0 Hz), 164.4, 156.1, 140.2, 132.6 (d, J = 5.5 Hz), 126.9 (d, J = 3.5 Hz), 116.1, 114.1, 99.6 (d, J = 199.5 Hz), 84.6, 79.6, 56.8, 45.9, 38.3 (d, J = 20.5 Hz), 28.7, 28.1 ; **¹⁹F NMR (377 MHz, CDCl₃)**: δ -155.6 (dd, J = 34.5, 17.5 Hz). **FTIR:** v_{max}/cm⁻¹ (neat) 3004, 1710, 1420, 1359, 1221, 1092, 736; **HRMS (ESI⁺):** calculated for $C_{23}H_{32}FNO_6Na$ (ES⁺)(+Na⁺): 460.2111. Found: 460.2127. **HPLC** (Cellulose-2, hexane: ᶦPrOH 93.0:7.0, flow rate 1.0 mL/min, λ = 254 nm, 25 °C) t_R(major) =15.123 min, t_R(minor) =18.953 min, *ee* = 84%.

ethyl 2-acetyl-4-{[(*tert*-butoxycarbonyl)amino]methyl}-2-fluoropent-4-enoate (90f)
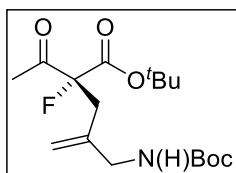
Following the General Procedure with *tert*-butyl 2-fluoro-3-oxobutanoate (**89f**) (23 mg, 0.13 mmol), *tert*-butyl 5-methylene-2-oxo-1,3-oxazinane-3-carboxylate (**2a**) (22 mg, 0.1 mmol), Pd(dba)₂ (2.9 mg, 0.005 mmol), *(R,R)*-Dach-phenyl Trost ligand (3.8 mg, 0.0055 mmol), *t*-BuOH (0.048 mL, 0.5 mmol) and DIPEA (0.021 mL, 0.12 mmol) in PhMe (1 mL) with FCC (20% Et₂O in 40-60 petroleum ether) afforded ethyl 2-acetyl-4-{[(*tert*-butoxycarbonyl)amino]methyl}-2-fluoropent-4-enoate (**90f**) as a colourless oil (27 mg, 79%).

¹H NMR (400 MHz, CDCl₃) δ 5.08 (s, 1H), 4.98 (s, 1H), 4.76 (br, 1H), 3.85 – 3.41 (m, 2H), 2.85 (dd, J = 27.5, 15.5 Hz, 1H), 2.71 (dd, J = 27.5, 15.5 Hz, 3H), 2.25 (s, 3H), 1.44 (s, 9H), 1.41 (s, 9H); **¹³C NMR (101 MHz, CDCl₃)** δ 201.9 (d, J = 30.2 Hz), 164.9 (d, J = 25.4 Hz), 156.1, 139.9, 115.8, 100.4 (d, J = 199.0 Hz), 84.9, 79.7, 46.0, 37.3 (d, J = 20.0 Hz), 28.7, 28.1, 26.0; **¹⁹F NMR (377 MHz, CDCl₃):** δ -162.4 – -162.5(m). **FTIR: v_{max}/cm⁻¹ (neat)** 2924, 1723, 1505, 1368, 1250, 1156, 910, 734; **HRMS (ESI⁺):** calculated for $C_{17}H_{28}FNO_5Na$ (ES⁺)(+Na⁺): 368.1849. Found: 368.1926. **HPLC** (Cellulose-2, hexane: ᶦPrOH 90:10, flow rate 1.0 mL/min, λ = 205 nm, 25 °C) t_R(major) = 5.643 min, t_R(minor) = 6.197 min, *ee* = 81%.

Interconversion of ethyl to *tert*-butyl ester (79e→90e): Evidence for homochirality across the ester substrates.
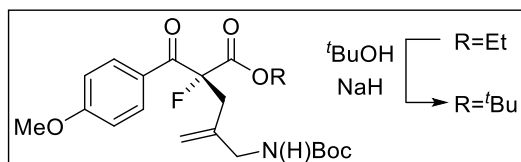
NaH (60% dispersion in mineral oil, 0.008 g, 0.20 mmol) and *t*-BuOH (2 mL) were added successfully to ethyl (*R*) 4-{[(*tert*-butoxycarbonyl)amino]methyl}-2-fluoro-2-(4-methoxybenzoyl)pent-4-enoate (**79e**) (33 mg, 0.078 mmol), The resulting mixture was refluxed overnight. *t*BuOH was removed by vacuum and the mixture was purified by FCC (15% Et$_2$O in petroleum ether) afforded *tert*-butyl (*R*) 4-(((*tert*-butoxycarbonyl)amino)methyl)-2-fluoro-2-(4-methoxybenzoyl)pent-4-enoate (**90e**) as a yellow oil (7 mg, 20%). This compound showed identical spectroscopic data and the same major enantiomer as **90e**.

Scale Up Experiment
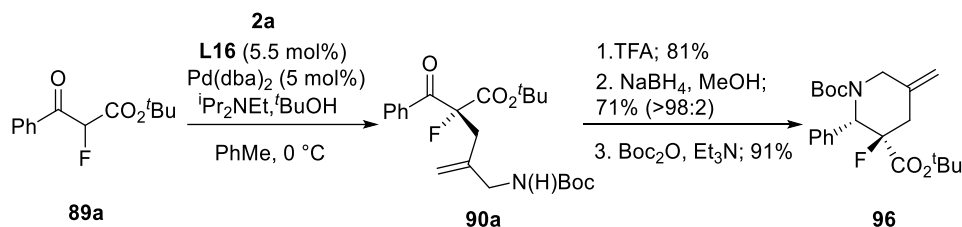
A flame-dried 250 mL round bottom flask was charged with Pd(dba)$_2$ (144 mg, 5 mol%), (*R,R*)-Dach-phenyl Trost ligand (190 mg, 5.5 mol%), *t*-BuOH (2.4 mL, 25 mmol) and DIPEA (1.0 mL, 6 mmol) and *tert*-butyl 5-methylene-2-oxo-1,3-oxazinane-3-carboxylate **2a** (1.06 g, 5 mmol) under nitrogen. Anhydrous PhMe (25.0 mL) was then added and the mixture stirred at 0 °C for 20 minutes. A solution of *tert*-butyl 2-fluoro-3-oxo-3-phenylpropanoate **89a** (1.54 g, 6.5 mmol) in PhMe (25.0 mL) was then added and the reaction stirred at 0 °C overnight. The reaction was then concentrated under vacuum and purified by flash silica column chromatography (15% Et$_2$O in petroleum ether). The collected intermediate **90a** was then dissolved in CH$_2$Cl$_2$ (86.0 mL) and TFA (16.4 mL, 50 equiv.) was added to the mixture. After stirring at room temperature for 30 minutes, the mixture was basified to pH 8 using sat. NaHCO$_3$ before extraction with CH$_2$Cl$_2$. The combined organic layers were then dried over anhydrous magnesium sulfate and concentrated under vacuum to afford *tert*-butyl 3-fluoro-5-methylene-2-phenyl-3,4,5,6-tetrahydropyridine-3-carboxylate as a yellow oil (1.03 g, 71% yield over two steps). To a solution of *tert*-butyl 3-fluoro-5-methylene-2-phenyl-3,4,5,6-tetrahydropyridine-3-carboxylate **91** (1.03 g, 3.55 mmol) in MeOH (17.8 mL) under

nitrogen at 0 °C was added NaBH$_4$ (0.537 mg, 14.2 mmol) and the resulting mixture warmed to room temperature and stirred overnight. The reaction was then diluted with NaHCO$_3$ and extracted with EtOAc. The combined organic layers were dried over anhydrous MgSO$_4$, concentrated under vacuum and the residue purified by FCC (20% EtOAc in 40-60 petroleum ether) to afford *tert*-butyl (2*S*,3*R*)-3-fluoro-5-methylene-2-phenylpiperidine-3-carboxylate (**93**) as a yellow oil (0.734 g, 71%). To a solution of (2*S*,3*R*)-3-fluoro-5-methylene-2-phenylpiperidine-3-carboxylate (**93**, 0.734 g, 2.52 mmol) in THF (14.8 mL) under nitrogen was added Et$_3$N (0.80 mL, 5.54 mmol) and di-*tert*-butyl dicarbonate (1.21 g, 5.54 mmol) and the resulting mixture stirred at room temperature overnight. The reaction was then diluted with H$_2$O and extracted with CH$_2$Cl$_2$. The combined organic layers were then dried over anhydrous MgSO$_4$, concentrated under vacuum and purified by FCC (4% EtOAc in 40-60 petroleum ether) to afford di-*tert*-butyl (2*S*,3*R*)-3-fluoro-5-methylene-2-phenylpiperidine-1,3-dicarboxylate (**96**) as a colourless oil (0.898 g, 46% yield over four steps). The product showed satisfactory spectroscopic data (vide infra).

tert-butyl (*R*)-3-fluoro-5-methylene-2-phenyl-3,4,5,6-tetrahydropyridine-3-carboxylate (91)
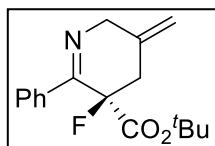
¹H NMR (400 MHz, CDCl$_3$) δ 7.71 – 7.65 (m, 2H), 7.42 – 7.31 (m, 3H), 5.08 (s, 1H), 5.01 (s, 1H), 4.63 (dd, *J* = 20.5, 5.5 Hz, 1H), 4.50 (dd, *J* = 20.5, 5.5 Hz, 1H), 2.95 – 2.78 (m, 2H), 1.25 (s, 9H). **¹³C NMR (101 MHz, CDCl$_3$)** δ 168.0 (d, *J* = 27.0 Hz), 161.0 (d, *J* = 18.5 Hz), 137.4, 136.9 (d, *J* = 3.5 Hz), 130.0, 128.4, 127.4 (d, *J* = 2.5 Hz), 112.4, 90.6 (d, *J* = 195.0 Hz), 84.0, 56.1, 39.5 (d, *J* = 24.1 Hz), 27.8; **¹⁹F NMR (377 MHz, CDCl$_3$):** δ -146.0 – -146.2 (m) **FTIR:** ν$_{max}$/cm^{-1} (neat) 2978, 1749, 1636, 1447, 1369, 1321, 1260, 1076, 733, 704cm^{-1}; **HRMS (ESI⁺):** calculated for: C$_{17}$H$_{21}$FNO$_2$ (ES⁺)(+H⁺): 290.1556. Found: 290.1569.

di-tert-butyl (2*S*,3*R*)-3-fluoro-5-methylene-2-phenylpiperidine-1,3-dicarboxylate (96)
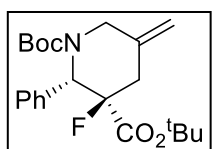
¹H NMR (400 MHz, CDCl$_3$) δ 7.41 – 7.12 (m, 5H), 5.42 (br, 1H), 5.07 (s, 1H), 4.95 (s, 1H), 4.43 (br, 1H), 3.82 (br, 1H), 3.12 (dd, *J* = 43.0 16.0 Hz, 1H), 2.76 (br, 1H), 1.34 (s, 9H), 1.17 (s, 9H); **¹³C NMR (101 MHz, CDCl$_3$)** δ 167.1 (d, *J* = 24.0 Hz), 154.9, 141.1, 137.0, 128.7, 128.5, 128.2, 113.9, 94.8 (d, *J* = 185.5 Hz), 83.2, 80.5, 61.3, 45.7, 34.8 (d, *J* = 88.0 Hz), 28.4, 27.5; **¹⁹F NMR (377 MHz, CDCl$_3$)** δ -144.6 (br), -145.6 (br); **FTIR:** ν$_{max}$/cm^{-1} (neat) 2977, 2932, 1740, 1694, 1455, 1392, 1367, 1284, 1251, 1156, 1106, 1061, 972,

894, 839, 765, 700; **HRMS (ESI+):** calculated for $C_{22}H_{30}FNO_4Na$ (ES+)(+Na$^+$): 414.2057. Found: 414.2079.

tert-butyl (2*S*,3*R*)- 3-fluoro-3-(hydroxymethyl)-5-methylene-2-phenylpiperidine-1-carboxylate (97)
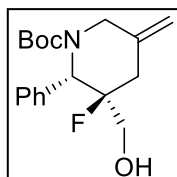
To a suspension of LiAlH$_4$ (7.6 mg, 0.2 mmol) in THF (2 mL) under nitrogen was added di-*tert*-butyl 3-fluoro-5-methylene-2-phenylpiperidine-1,3-dicarboxylate (96) (78 mg, 0.2 mmol) in THF (2 mL) and the resulting mixture stirred at room temperature for 22 hours. Et$_2$O (1.3 mL) was added to the resulting mixture at 0 °C and H$_2$O (0.026 mL) was then added dropwise and the reaction stirred for 15 minutes at room temperature before the addition of anhydrous MgSO$_4$. After 15 minutes the reaction mixture was filtered through celite and the volatiles removed under vacuum. Purification by FCC (20% EtOAc in 40-60 petroleum ether) afforded *tert*-butyl (2*S*,3*R*)-3-fluoro-3-(hydroxymethyl)-5-methylene-2-phenylpiperidine-1-carboxylate (97) as a colourless oil (36 mg, 56%; >98:2).

¹H NMR (400 MHz, CDCl₃): δ 7.43-7.30 (m, 5H), 5.37 (br, 1H), 5.22 (s, 1H), 5.02 (s, 1H), 4.42 (d, *J* = 15.0 Hz, 1H), 4.26 (d, *J* = 15.0 Hz, 1H), 3.51 (d, *J* = 6.0 Hz, 1H), 3.46 (d, *J* = 6.0 Hz, 1H), 2.65 (q, *J* = 16.0 Hz, 1H), 2.51 (d, *J* = 16.0 Hz, 1H) 1.93 (br, 1H), 1.33 (s, 9H); **¹³C NMR (101 MHz, CDCl₃):** δ 154.9, 141.1, 137.0, 129.2, 128.9, 128.4, 114.0, 97.5 (d, *J* = 176.0 Hz), 80.6, 66.2 (d, *J* = 21.5 Hz), 60.7, 47.2, 33.7 (d, *J* = 22.5 Hz), 28.7; **¹⁹F NMR (377 MHz, CDCl₃)** δ -154.1 (dd, *J* = 33.0, 19.5 Hz); **FTIR:** v$_{max}$/cm^{-1} (neat) 3445, 2926, 1676, 1457, 1378, 1162, 1053, 889 cm^{-1}; **HRMS (ESI+):** calculated for $C_{18}H_{24}FNO_3Na$ (ES+)(+Na$^+$): 344.1638. Found: 344.1661. **HPLC** (Cellulose-1, hexane: ^{i}PrOH 98.0:2.0, flow rate 1.0 mL/min, λ = 254 nm, 25 °C) t$_R$(major) = 23.890 min, t$_R$(minor) =30.800 min, *ee* = 91%.

di-*tert*-butyl (6S,7R)-7-fluoro-6-phenyl-1-oxa-5-azaspiro[2.5]octane-5,7-dicarboxylate (98)
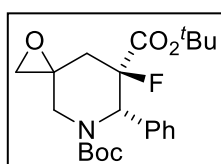
To a solution of di-*tert*-butyl 3-fluoro-5-methylene-2-phenylpiperidine-1,3-dicarboxylate (96) (58 mg, 0.15 mmol) in CH$_2$Cl$_2$ (4.5 mL) was added the solution of *m*-CPBA in CH$_2$Cl$_2$ (0.75 mL) dropwise at 0 °C under N$_2$. The resulting mixture was stirred at room temperature for 20 hours. The mixture was quenched by Na$_2$S$_2$O$_5$ and sat. NaHCO$_3$ and stirred for 10 minutes before extraction with CH$_2$Cl$_2$ (3 x 15 mL). The

combined organic layers were dried over MgSO$_4$, concentrated under vacuum and purified by FCC (10%-20% Et$_2$OAc in 40-60 petroleum ether) to afford di-*tert*-butyl (*6S,7R*)-7-fluoro-6-phenyl-1-oxa-5-azaspiro[2.5]octane-5,7-dicarboxylate (**98**) (39 mg, 64%; 3:2 mixture of diastereomers). The diastereomers could be isolated individually after careful chromatography allowing their isolation as a colourless oil and white solid, respectively. **FTIR:** ν$_{max}$/cm^{-1} (neat) 2978, 2932, 1741, 1699, 1395, 1369, 1312, 1289, 1253, 1157, 1099, 893, 808, 754, 701; **HRMS (ESI+):** calculated for C$_{22}$H$_{30}$F$_3$NO$_4$Na (ES+)(+Na$^+$): 430.2006. Found: 430.2036.

Major isomer

^{1}H NMR (400 MHz, CDCl$_3$) δ 7.49-7.30 (m, 5H), 5.84-5.54 (m, 1H), 3.69 (br 1H), 3.43 (br, 1H), 3.00 (d, *J* = 15.5 Hz, 1H), 2.89 (d, *J* = 15.5 Hz, 1H), 2.80 (br, 1H), 2.09 – 1.97 (m, 1H), 1.45 (s, 9H), 1.23 (s, 9H); **^{13}C NMR (101 MHz, CDCl$_3$) :** δ 166.7 (d, *J* = 23.0 Hz), 155.0, 136.0, 129.0, 128.9, 128.7, 96.0 (d, *J* = 183.0 Hz), 83.8, 81.2, 61.5, 55.9, 44.8, 35.2 (br), 30.0, 28.6, 27.7; **^{19}F NMR (377 MHz, CDCl$_3$)** δ-144.2 (br), -145.3 (br).

Minor Isomer

^{1}H NMR (400 MHz, CDCl$_3$) δ 7.35 (br, 5H), 5.68 (br, 1H), 3.74 (br, 1H), 3.61 (br, 1H), 3.03 (dd, *J* = 43.0, 16.0 Hz, 1H), 2.78 (d, *J* = 4.0 Hz, 1H), 2.74 (d, *J* = 4.0 Hz, 1H), 2.01 – 1.89 (m, 1H), 1.45 (s, 9H), 1.24 (s, 9H); **^{13}C NMR (101 MHz, CDCl$_3$)** 167.1 (d, *J* = 23.0 Hz), 156.3, 136.3, 128.9, 128.8, 128.6, 94.4 (d, *J* = 186.5 Hz), 83.6, 81.2, 60.9, 49.4, 45.6, 34.5 (br), 30.0, 28.6, 27.7; **^{19}F NMR (377 MHz, CDCl$_3$)** δ-145.2(br), -146.4 (br).

di-*tert*-butyl (*6S,7R*)-1,1,7-trifluoro-6-phenyl-5-azaspiro[2.5]octane-5,7-dicarboxylate (99)
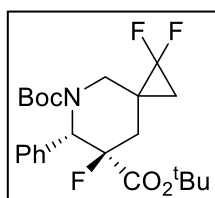
TMSCF$_3$ (0.037 mL, 0.25 mmol) and NaI (0.008 g, 0.05 mmol) were added in one portion to a solution containing di-*tert*-butyl 3-fluoro-5-methylene-2-phenylpiperidine-1,3-dicarboxylate (**96**) (39 mg, 0.1mmol) in THF (2 mL). The resulting mixture was heated at reflux for 4 hours. After 4 hours, additional TMSCF$_3$ (0.037 mL, 0.25 mmol) was added and the resulting mixture was heated at reflux overnight. The residue was dissolved in CH$_2$Cl$_2$, washed with water, sodium thiosulfate (0.1 M), brine, dried over Na$_2$SO$_4$, filtered, and the solvent was removed under reduced pressure. The residue was

diluted with H$_2$O (5 mL) and Na$_2$S$_2$O$_3$ (sat) and extracted with CH$_2$Cl$_2$ (3 x 5 mL). The combined organic layers were then extracted with brine (15 mL) dried over anhydrous MgSO$_4$, concentrated under vacuum and purified by FCC (20% Et$_2$O in 40-60 petroleum ether) to afford di-*tert*-butyl (*6S,7R*)-1,1,7-trifluoro-6-phenyl-5-azaspiro[2.5]octane-5,7-dicarboxylate (**99**) as a colourless solid (22 mg, 50%; 4:1 mixture of diastereomers). Each diastereomer was isolated as a mixture of rotamers. **FTIR:** v_{max}/cm^{-1} (neat) 2979, 2929, 1739, 1694, 1476, 1456, 1412, 1393, 1368, 1312, 1274, 1254, 1207, 1154, 1071, 1003, 972, 894, 839, 754, 700; **HRMS (ESI+):** calculated for C$_{23}$H$_{30}$F$_3$NO$_4$Na (ES+)(+Na$^+$): 464.2025. Found: 464.2047.

Major isomer

^{1}H NMR (400 MHz, CDCl$_3$) δ 7.43 – 7.28 (m, 5H), 5.91 (br, 0.5H), 5.60 (br, 0.5H), 3.86 (br, 0.5H), 3.69 (br, 0.5H), 3.15 (br, 1H), 2.91 – 2.72 (m, 1H), 1.95 (br, 1H), 1.44 (s, 9H), 1.26-1.19 (m, 11H); **^{13}C NMR (101 MHz, CDCl$_3$) :** δ 167.2 (d, J = 22.5 Hz), 156.4, 136.1, 129.1, 128.9, 128.7, 114.3 (t, J = 288.0 Hz), 94.2 (d, J = 184.5 Hz), 83.8, 81.2, 61.7, 41.3, 30.9, 29.9, 28.6, 27.7, 20.8; **^{19}F NMR (377 MHz, CDCl$_3$)** δ -138.4--138.9 (m, 1F CF$_2$), -140.3--140.9 (m, 1F CF$_2$),-146.9--148.0 (m, 1F)

Minor Isomer

^{1}H NMR (400 MHz, CDCl$_3$) δ 7.38 – 7.32 (m, 5H), 5.91 (br, 0.5H), 5.52 (br, 0.5H), 4.00 (br, 0.5H), 3.84 (br, 0.5H), 3.27 (br, 1H), 2.90 – 2.57 (m, 1H), 2.17 (br, 1H), 1.45 (s, 9H), 1.26-1.21 (m, 11H); **^{13}C NMR (101 MHz, CDCl$_3$)** δ 167.3 (d, J = 23.0 Hz), 154.8, 136.4, 129.1, 128.9, 128.6, 114.3 (t, J = 288.0 Hz), 93.1 (d, J = 181.0 Hz) 83.6, 81.2, 60.9, 40.7 (d, J = 52.5 Hz), 30.6, 30.0, 28.6, 27.7, 19.4; **^{19}F NMR (377 MHz, CDCl$_3$)** δ-137.2—137.9 (m, 1F CF$_2$), -140.0—140.8 (m, 1F CF$_2$), -149.2—150.5 (m, 1F).

di-*tert*-butyl (2*S*,3*R*)-3-fluoro-5-(hydroxymethyl)-2-phenylpiperidine-1,3-dicarboxylate (101)

Borane Reduction method:
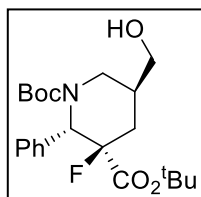
To a solution of BH$_3$·THF complex (1.0 M in THF, 2.25 ml, 2.25 mmol) was added di-*tert*-butyl 3-fluoro-5-methylene-2-phenylpiperidine-1,3-dicarboxylate (**96**) (0.058 g, 0.15 mmol) in THF (0.75 ml) dropwise at 0 °C under N$_2$. The resulting mixture was stirred at room temperature for 20 h and quenched with 3.0 mL

of 2 M aqueous NaOH solution (dropwise) and 0.90 mL of 30% aqueous H_2O_2 solution. After stirring

for 1.5 hours, the aqueous layer was extracted with diethyl ether (3 x 15 mL). The combined

organic layers were dried over $MgSO_4$, concentrated under vacuum and purified by FCC (20%

Et_2OAc in 40-60 petroleum ether) to afford di-*tert*-butyl (2*S*,3*R*)-3-fluoro-5-(hydroxymethyl)-2-

phenylpiperidine-1,3-dicarboxylate as a colourless oil (35 mg, 58%; 5:1 mixture of diastereomers).

The product was isolated as a mixture of rotamers. ^{1}H NMR (400 MHz, CDCl$_3$) (Major diastereomer):

δ 7.42 – 7.27 (m, 5H), 5.79-5.62 (m, 1H), 4.05 (d, J = 14.5 Hz, 1H), 3.81-3.78 (m, 1H), 3.55 (br, 1H),

2.99 (dd, J = 14.5, 2.5 Hz, 1H), 2.60 (ddd, J = 49.5, 16.0, 6.5 Hz, 1H), 2.22-2.09 (m, 2H), 1.50 (s, 9H),

1.17 (s,9H); ^{13}C NMR (101 MHz, CDCl3) δ 167.6, 167 4, 136.0 (d, J = 10.5 Hz), 128.8, 128.7, 128.5,

94.8 (d, J = 181.0 Hz), 83.2, 81.3, 64.2 (d, J = 219.0 Hz), 60.9, 37.8, 34.9, 29.6 (d, J = 22.5 Hz), 28.7,

27.6; ^{19}F NMR (377 MHz, CDCl3) δ -145.6 – -146.0 (m), -146.9 – -147.1 (m). FTIR: vmax/cm^{-1} (neat)

3450, 2921, 1740, 1674, 1369, 1161, 738 cm^{-1}; HRMS (ESI+): calculated for $C_{22}H_{32}FNO_5Na$

(ES+)(+Na+): 432.2162 Found: 432.2182.

9-BBN Reduction method:
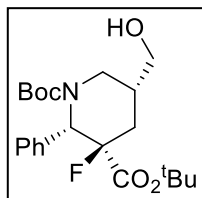
To a solution of 9-BBN (0.5 M in THF, 4.5 ml, 2.25 mmol), di-*tert*-butyl 3-fluoro-5-methylene-2-phenylpiperidine-1,3-dicarboxylate (**96**) (0.058g, 0.15 mmol) in THF (0.75 ml) was added dropwise at 0 °C under N_2. The resulting mixture was stirred at room temperature for 20 h and quenched with 3.0 mL of 2 M aqueous

NaOH solution (dropwise) and 0.90 mL of 30% aqueous H_2O_2 solution. After stirring for 1.5 hours,

the aqueous layer was extracted with diethyl ether (3 x 15 mL). The combined organic layers were

dried over $MgSO_4$, concentrated under vacuum, and purified by FCC (20% Et_2OAc in 40-60

petroleum ether) to afford di-*tert*-butyl (2*S*,3*R*)-3-fluoro-5-(hydroxymethyl)-2-phenylpiperidine-

1,3-dicarboxylate as a colorless oil (35 mg, 58%; 1:2 mixture of diastereomers). The product was

isolated as a mixture of rotamers. Spectra are too complex to allow clean assignments but are

displayed.

2-(dimethyl-λ^4-sulfaneylidene)-1-phenylethan-1-one (102a)[80]
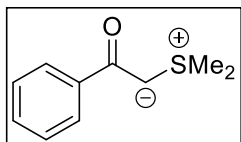
Following the General Procedure G with 2-bromoacetophenone (1.99 g, 10 mmol), dimethyl sulfide (0.745 g, 12 mmol) in acetone (20 mL). NaOH (2.0 g, 50 mmol) in H_2O (33 mL) was added to the generated sulfonium salt in CH_2Cl_2 (33 mL), which afforded 2-(dimethyl-λ^4-sulfaneylidene)-1-phenylethan-1-one (**102a**) as a yellow solid (0.93 g, 51%).

^{1}H NMR (400 MHz, CDCl$_3$): δ 7.53 – 7.51 (m, 2H), 7.11 – 6.98 (m, 3H), 4.04 (s, 1H), 2.52 (s, 6H); **^{13}C NMR (101 MHz, CDCl$_3$)**: δ 181.6, 140.6, 129.0, 127.5, 125.9, 53.1, 28.2.

2-(dimethyl-λ^4-sulfaneylidene)-1-(*p*-tolyl)ethan-1-one (102b)[80]

Following the General Procedure G with 2-bromo-4'-methylacetophenone (2.13 g, 10 mmol), dimethyl sulfide (0.745 g, 12 mmol) in acetone (20 mL). NaOH (2.0 g, 50 mmol) in H_2O (33 mL) was added to the generated sulfonium salt in CH_2Cl_2 (33 mL), afforded 2-(dimethyl-λ^4-sulfaneylidene)-1-(*p*-tolyl)ethan-1-one (**102b**) as a yellow solid (1.10 g, 57%).

^{1}H NMR (400 MHz, CDCl$_3$): δ 7.66 (d, *J* = 8.0 Hz, 2H), 7.13 (d, *J* = 8.0 Hz, 2H), 4.27 (s, 1H), 2.95 (s, 6H), 2.33 (s, 3H). **^{13}C NMR (101 MHz, CDCl$_3$)**: δ 183.5, 139.8, 138.5, 128.9, 126.6, 50.4, 28.9, 21.6.

2-(dimethyl-λ^4-sulfaneylidene)-1-(4-methoxyphenyl)ethan-1-one (102c)[80]
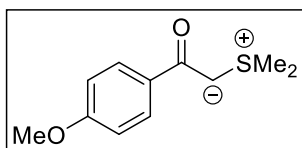
Following the General Procedure G with 2-bromo-1-(4-methoxyphenyl)ethan-1-one (2.29 g, 10 mmol), dimethyl sulfide (0.745 g, 12 mmol) in acetone (20 mL). NaOH (2.0 g, 50 mmol) in H_2O (33 mL) was added to the generated sulfonium salt in CH_2Cl_2 (33 mL), afforded 2-(dimethyl-λ4-sulfaneylidene)-1-(4-methoxyphenyl)ethan-1-one (**102c**) as a yellow solid (0.744 g, 36%).

^{1}H NMR (400 MHz, CDCl$_3$): δ 7.73 (d, *J* = 9.0 Hz, 2H), 6.83 (d, *J* = 9.0 Hz, 2H), 4.24 (s, 1H), 3.79 (s, 3H), 2.96 (s, 6H). **^{13}C NMR (101 MHz, CDCl$_3$):** δ 183.0, 161.1, 134.0, 128.2, 113.3, 55.5, 50.0, 28.9.

2-(dimethyl-λ^4-sulfaneylidene)-1-(4-(trifluoromethyl)phenyl)ethan-1-one (102d)[81]
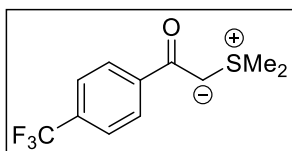
Following the General Procedure G with 2-bromo-1-(4-(trifluoromethyl)phenyl)ethan-1-one (2.67 g, 10 mmol), dimethyl sulfide (0.745 g, 12 mmol) in acetone (20 mL). NaOH (2.0 g, 50 mmol) in H_2O (33 mL) was added to the generated l sulfonium salt in CH_2Cl_2 (33 mL), afforded 2-(dimethyl-λ^4-sulfaneylidene)-1-(4-(trifluoromethyl)phenyl)ethan-1-one (**102d**) as a yellow solid (1.18 g, 48%).

^{1}H NMR (400 MHz, CDCl$_3$): δ 7.84 (d, J = 8.0 Hz, 2H), 7.57 (d, J = 8.0 Hz, 2H), 4.32 (s, 1H), 2.97 (s, 6H); **^{19}F NMR (376 MHz, CDCl$_3$):** δ -62.5; **^{13}C NMR (101 MHz, CDCl$_3$):** δ 181.6, 144.5, 131.3 (q, J = 31.5 Hz), 126.9, 125.4, 124.5 (q, J = 272.5 Hz), 52.7, 28.5.

2-(dimethyl-λ^4-sulfaneylidene)-1-(4-chlorophenyl)-ethan-1-one (102e)[81]
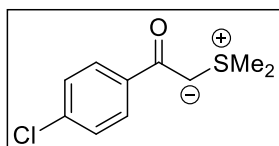
Following the General Procedure G with 2-bromo-1-(4-chlorophenyl)ethan-1-one (2.33 g, 10 mmol), dimethyl sulfide (0.745 g, 12 mmol) in acetone (20 mL). NaOH (2.0 g, 50 mmol) in H_2O (33 mL) was added to the generated sulfonium salt in CH_2Cl_2 (33 mL), afforded 1-(4-chlorophenyl)-2-(dimethyl-λ^4-sulfaneylidene)ethan-1-one (**102e**) as an orange solid (1.60 g, 74%).

^{1}H NMR (400 MHz, CDCl$_3$): δ 7.78 – 7.67 (m, 2H), 7.37 – 7.26 (m, 2H), 4.28 (s, 1H), 2.97 (s, 6H); **^{13}C NMR (101 MHz, CDCl$_3$):** δ 181.7, 139.6, 135.5, 128.2, 128.0, 51.7, 28.6.

2-(dimethyl-λ^4-sulfaneylidene)-1-(4-fluorophenyl)ethan-1-one (102f)[81]
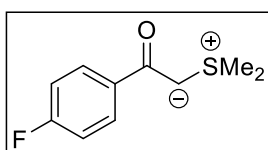
Following the General Procedure G with 2-bromo-1-(4-fluorophenyl)ethan-1-one (2.17 g, 10 mmol), dimethyl sulfide (0.745 g, 12 mmol) in acetone (20 mL). NaOH (2.0 g, 50 mmol) in H_2O (33 mL) was added to the generated l sulfonium salt in CH_2Cl_2 (33 mL), afforded 2-(dimethyl-λ^4-sulfaneylidene)-1-(4-fluorophenyl)ethan-1-one (**102f**) as an orange solid (1.04 g, 53%).

^{1}H NMR (400 MHz, CDCl$_3$): δ 7.76 – 7.73 (m, 2H), 7.01 – 6.96 (m, 2H), 4.24 (s, 1H), 2.96 (s, 6H); **^{19}F NMR (377 MHz, CDCl$_3$):** δ -112.3; **^{13}C NMR (101 MHz, CDCl$_3$):** δ 182.2, 164.0 (d, J = 248.0 Hz), 137.4, 128.6 (d, J = 8.5 Hz), 114.9 (d, J = 21.5 Hz), 51.0, 28.8.

4-(2-(dimethyl-l^4-sulfaneylidene)acetyl)benzonitrile (102h)[81]
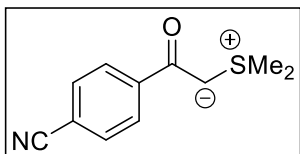
Following the General Procedure B with 4-(2-bromoacetyl)benzonitrile (2.24 g, 10 mmol), dimethyl sulfide (0.745 g, 12 mmol) in acetone (20 mL). NaOH (2.0 g, 50 mmol) in H_2O (33 mL) was added to the generated l sulfonium salt in CH_2Cl_2 (33 mL), afforded 4-(2-(dimethyl-l^4-sulfaneylidene)acetyl)benzonitrile (**102h**) a pale yellow solid (0.493 g, 24%).

^{1}H NMR (400 MHz, CDCl$_3$): δ7.76 (d, J = 8.0 Hz, 2H), 7.54 (d, J = 8.0 Hz, 2H), 4.28 (s, 1H), 2.91 (s, 6H); **^{13}C NMR (101 MHz, CDCl$_3$):** δ 180.4, 145.2, 131.9, 127.1, 119.1, 112.6, 54.0, 28.0.

2-(dimethyl-l^4-sulfaneylidene)-1-(2-methoxyphenyl)ethan-1-one (102i)[80]
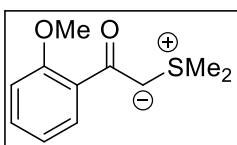
Following the General Procedure B with 2-bromo-1-(2-methoxyphenyl)ethan-1-one (2.29 g, 10 mmol), dimethyl sulfide (0.745 g, 12 mmol) in acetone (20 mL). NaOH (2.0 g, 50 mmol) in H_2O (33 mL) was added to the generated sulfonium salt in CH_2Cl_2 (33 mL), afforded 2-(dimethyl-λ^4-sulfaneylidene)-1-(2-methoxyphenyl)ethan-1-one (**102i**) as a yellow oil (345 mg, 34%).

^{1}H NMR (400 MHz, CDCl$_3$): δ 7.47 (d, J = 7.0 Hz, 1H), 6.99 (t, J = 7.0 Hz, 1H), 6.67 (t, J = 7.0 Hz, 1H), 6.60 (d, J = 8.0 Hz, 1H), 4.14 (s, 1H), 3.54 (s, 2H), 2.57 (s, 6H); **^{13}C NMR (101 MHz, CDCl$_3$):** δ 181.6, 157.1, 131.1, 130.0, 129.7, 120.5, 111.5, 56.3, 55.8, 28.9.

2-(dimethyl-λ^4-sulfaneylidene)-1-(3-methoxyphenyl)ethan-1-one (102j)[82]
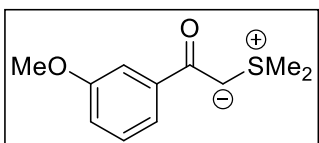
Following the General Procedure B with 2-bromo-1-(3-methoxyphenyl)ethan-1-one (2.29 g, 10 mmol), dimethyl sulfide (0.745 g, 12 mmol) in acetone (20 mL). NaOH (2.0 g, 50 mmol) in H_2O (33 mL) was added to the generated sulfonium salt in CH_2Cl_2 (33 mL), afforded 2-(dimethyl-λ^4-sulfaneylidene)-1-(3-methoxyphenyl)ethan-1-one (**102j**) as an orange oil (1.53 g, 73%).

^{1}H NMR (400 MHz, CDCl$_3$): δ 7.42-7.71 (m, 1H), 7.34-7.30 (m, 1H), 7.26-7.22 (m, 1H), 6.93-6.91 (m, 1H), 4.34 (s, 1H), 3.84 (s, 3H), 2.99 (s, 6H); **^{13}C NMR (101 MHz, CDCl$_3$):** δ 183.1, 159.7, 142.7, 129.1, 119.1, 116.4, 111.2, 55.6, 51.6, 28.7.

2-(dimethyl-λ^4-sulfaneylidene)-1-(3-fluorophenyl)ethan-1-one (102k)[83]
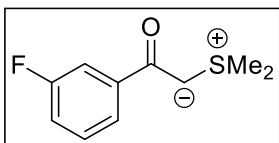
Following the General Procedure B with 2-bromo-1-(3-fluorophenyl)ethan-1-one (2.17 g, 10 mmol), dimethyl sulfide (0.745g, 12 mmol) in acetone (20 mL). NaOH (2.0 g, 50 mmol) in H_2O (33 mL) was added to the generated sulfonium salt in CH_2Cl_2 (33 mL), afforded 2-(dimethyl-λ^4-sulfaneylidene)-1-(3-fluorophenyl)ethan-1-one (**102k**) as an orange oil (1.52 g, 77%).

^{1}H NMR (400 MHz, CDCl$_3$): δ 7.55-7.53 (m, 1H), 7.50-7.47 (m, 1H), 7.33-7.27 (m, 1H), 7.07-7.02 (m, 1H), 4.31 (s, 1H), 2.99 (s, 6H); **^{19}F NMR (377 MHz, CDCl$_3$):** δ -113.8 – -114.0 (m); **^{13}C NMR (101 MHz, CDCl$_3$)**: δ 181.7, 163.0 (d, J = 245.0 Hz), 143.8, 129.6 (d, J = 8.0 Hz), 122.2 (d, J = 2.0 Hz), 116.5 (d, J = 22.0 Hz), 113.5 (d, J = 22.0 Hz), 52.0, 28.6.

2-(dimethyl-λ^4-sulfaneylidene)-1-(naphthalen-2-yl)ethan-1-one (102l)[80]
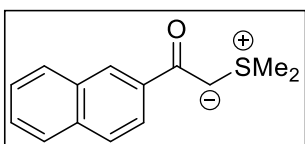
Following the General Procedure G with 2-bromo-1-(naphthalen-2-yl)ethan-1-one (2.49 g, 10 mmol), dimethyl sulfide (0.745 g, 12 mmol) in acetone (20 mL). NaOH (2.0 g, 50 mmol) in H_2O (33 mL) was added to the generated sulfonium salt in CH_2Cl_2 (33 mL), afforded 2-(dimethyl-λ^4-sulfaneylidene)-1-(naphthalen-2-yl)ethan-1-one (**102l**) as an orange solid (1.13 g, 49%).

^{1}H NMR (400 MHz, CDCl$_3$): δ 8.32-8.28 (m, 1H), 7.92 – 7.84 (m, 2H), 7.82-7.78 (m, 2H), 7.49 – 7.42 (m, 2H), 4.45 (s, 1H), 2.99 (s, 6H); **^{13}C NMR (101 MHz, CDCl$_3$):** δ 183.2, 138.5, 134.9, 133.3, 129.2, 127.8, 127.7, 126.7, 126.3, 126.2, 124.5, 51.7, 28.8.

2-(dimethyl-λ^4-sulfaneylidene)-1-(thiophen-2-yl)ethan-1-one (102m)[80]
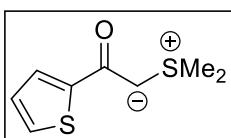
Following the General Procedure G with 2-bromo-1-(thiophen-2-yl)ethan-1-one (2.05 g, 10 mmol), dimethyl sulfide (0.745 g, 12 mmol) in acetone (20 mL). NaOH (2.0 g, 50 mmol) in H_2O (33 mL) was added to the generated sulfonium salt in CH_2Cl_2 (33 mL), afforded 2-(dimethyl-λ^4-sulfaneylidene)-1-(thiophen-2-yl)ethan-1-one (**102m**) as a white solid (1.10 g, 59%).

¹H NMR (400 MHz, CDCl₃): δ 7.36 (d, *J* = 3.0 Hz, 1H), 7.28 (d, *J* = 5.0 Hz, 1H), 6.98 (dd, *J* = 5.0, 3.0 Hz, 1H), 4.22 (s, 1H), 2.99 (s, 6H); **¹³C NMR (101 MHz, CDCl₃):** δ 176.9, 147.9, 127.5 (2 carbons), 125.6, 50.0, 28.9.
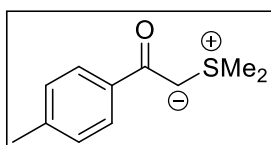
1-(dimethyl-l⁴-sulfaneylidene)-3,3-dimethylbutan-2-one (102n) [80]
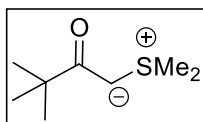
Following the General Procedure G with bromo pinacolone (1.79 g, 10 mmol), dimethyl sulfide (0.745 g, 12 mmol) in acetone (20 mL). NaOH (2.0 g, 50 mmol) in H₂O (33 mL) was added to the generated sulfonium salt in CH₂Cl₂ (33 mL), afforded 1-(dimethyl-l⁴-sulfaneylidene)-3,3-dimethylbutan-2-one (**102n**) as a white solid (0.248 g, 16%).

¹H NMR (400 MHz, CDCl₃): δ 3.70 (s, 1H), 2.80 (s, 6H), 1.06 (s, 9H); **¹³C NMR (101 MHz, CDCl₃):** δ 198.3, 48.5, 40.7, 29.0, 28.6.

ethyl 2-(diphenyl-λ⁴-sulfaneylidene)acetate (108)[84]
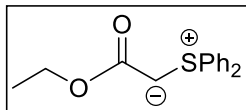
Following the General Procedure H with ethyl 2-bromoacetate (1.67 g, 10 mmol), diphenyl sulfide (3.72 g, 20 mmol), silver tetrafluoroborate (1.94 g, 10 mmol) in CHCl₃ (20 mL) after chromatography (gradient from 4-6% MeOH in CH₂Cl₂) afforded (2-ethoxy-2-oxoethyl) diphenyl sulfonium tetrafluoroborate as white solid (2.76 g, 77%). NaH (0.32 g, 8 mmol, 60 wt% in mineral oil) and (2-ethoxy-2-oxoethyl) diphenyl sulfonium tetrafluoroborate (1.44 g, 4 mmol) in anhydrous THF (25 mL), afforded ethyl 2-(diphenyl-λ⁴-sulfaneylidene)acetate (**108**) as a sticky pale yellow oil (1.08 g, 99%).

¹H NMR (400 MHz, CDCl₃): δ 7.57-7.45 (m, 10H), 4.10 (q, *J* = 7.0 Hz, 2H), 3.47-3.22 (br, 1H), 1.25 (t, *J* = 7.0 Hz, 3H); **¹³C NMR (101 MHz, CDCl₃):** δ 170.4, 136.7, 131.1, 130.0, 128.3, 58.9, 36.2, 15.3.

1-(diphenyl-λ⁴-sulfaneylidene)butan-2-one (109)
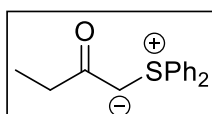
Following the General Procedure H with 1-bromobutan-2-one (1.51 g, 10 mmol), diphenyl sulfide (3.72 g, 20 mmol), silver tetrafluoroborate (1.94 g, 10 mmol) in CHCl₃ (20 mL) after chromatography (gradient from 2-4% MeOH in CH₂Cl₂) afforded (2-oxobutyl)diphenylsulfonium tetrafluoroborate as yellow oil (2.58

g, 75%). NaH (0.32g, 8 mmol, 60 wt% in mineral oil) and (2-oxobutyl)diphenylsulfonium tetrafluoroborate (1.37 g, 4 mmol) in anhydrous THF (25 mL), afforded 1-(diphenyl-λ^4-sulfaneylidene)butan-2-one (**109**) as a sticky yellow oil (1.01 g, 99%).

^{1}H NMR (400 MHz, CDCl$_3$): δ 7.55-7.44 (m, 10H), 4.08 (s, 1H), 2.29 (q, *J* = 7.5 Hz, 2H), 1.17 (t, *J* = 7.5 Hz, 3H); **^{13}C NMR (101 MHz, CDCl$_3$):** δ 191.7, 135.3, 131.4, 130.1, 128.7, 55.7, 34.3, 11.8; **FTIR: v_{max}/cm^{-1} (neat):** 3054, 1783, 1264, 895, 732, 704; **HRMS (ESI$^+$):** calculated for C$_{16}$H$_{17}$OS (ES$^+$)(+H$^+$): 257.1000, found: 257.1000.

2-(diphenyl-λ^4-sulfaneylidene)-1-(4-nitrophenyl)ethan-1-one (111)[85]
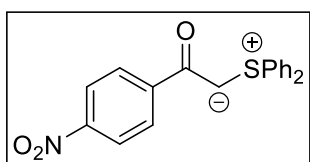
Following the General Procedure H with 1-bromobutan-2-one (2.44 g, 10 mmol), diphenyl sulfide (3.72 g, 20 mmol), silver tetrafluoroborate (1.94 g, 10 mmol) in CHCl$_3$(20 mL) after chromatography (gradient from 2-5% MeOH in CH$_2$Cl$_2$) afforded (2-(4-nitrophenyl)-2-oxoethyl)diphenylsulfonium tetrafluoroborate as an orange solid (2.82 g, 65%). NaH (0.32 g, 8 mmol, 60 wt% in mineral oil) and (2-oxobutyl) diphenyl sulfonium tetrafluoroborate (1.75 g, 4 mmol) in anhydrous THF (25 mL), afforded 1-(diphenyl-λ^4-sulfaneylidene)butan-2-one (**111**) as a yellow oil (0.293 g, 21%).

^{1}H NMR (400 MHz, CDCl$_3$): δ 8.19 (d, *J* = 9.0 Hz, 2H), 8.04 (d, *J* = 9.0 Hz, 2H), 7.64-7.51 (m, 10H), 4.87 (s, 1H); **^{13}C NMR (101 MHz, CDCl$_3$):** δ 60.4, 123.4, 127.3, 128.4, 130.4, 131.6, 133.7, 146.6, 148.6, 178.9.

(*S*)-3-(2-(diphenyl-λ^4-sulfaneylidene)acetyl)-4-isopropyloxazolidin-2-one (112)
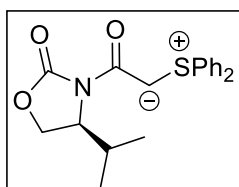
Following the General Procedure H with (*S*)-3-(2-bromoacetyl)-4-isopropyloxazolidin-2-one (2.50 g, 10 mmol), diphenyl sulfide (3.72 g, 20 mmol), silver tetrafluoroborate (1.94 g, 10 mmol) in CHCl$_3$ (20 mL) after chromatography (2% MeOH in CH$_2$Cl$_2$) afforded (*S*)-(2-(4isopropyl-2-oxooxazolidin-3-yl)-2-oxoethyl)diphenylsulfonium tetrafluoroborate as yellow solid (3.41 g, 77%). NaH (0.32 g, 8 mmol, 60 wt% in mineral oil) and (2-ethoxy-2-oxoethyl) diphenyl sulfonium

tetrafluoroborate (1.77 g, 4 mmol) in anhydrous THF (25 mL), afforded (*S*)-3-(2-(diphenyl-λ^4-sulfaneylidene)acetyl)-4-isopropyloxazolidin-2-one (**112**) as a sticky orange oil (1.40 g, 99%).

^{1}H NMR (400 MHz, CDCl$_3$): δ 7.61-7.40 (m, 10H), 5.19 (s, 1H), 4.52 (dt, *J* = 8.5. 3.5 Hz, 1H), 4.21 (dd, *J* = 9.0, 3.0 Hz, 1H), 4.13 (dd, *J* = 9.0, 3.0 Hz, 1H), 2.50 – 2.36 (m, 1H), 0.91 (d, *J* = 6.5 Hz, 3H), 0.89 (d, *J* = 6.5 Hz, 3H); **^{13}C NMR (101 MHz, CDCl$_3$):** δ 163.8, 155.6, 135.5, 131.4, 130.2, 128.8, 63.3, 58.9, 29.7, 18.4, 15.2;   **FTIR: v_{max}/cm^{-1} (neat):** 2962, 1748, 1596, 1573, 1350, 1195, 1065, 745, 689; **HRMS (ESI$^+$):**   calculated for C$_{20}$H$_{23}$NO$_3$S (ES$^+$)(+H$^+$): 356.1242, found: 356.1328.

(4-methylene-1-tosylpyrrolidin-2-yl)(phenyl)methanone (103a)
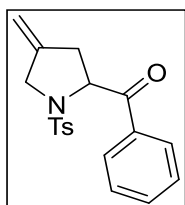
Following the General Procedure I with 2-(dimethyl-λ^4-sulfaneylidene)-1-phenylethan-1-one (**102a**) (54 mg, 0.3 mmol), 5-methylene-3-tosyl-1,3-oxazinan-2-one (**2b**) (27 mg, 0.1 mmol), *N,N*-diisopropyldibenzo[d,f][1,3,2]dioxaphosphepin-6-amine (1.7 mg, 0.0055 mmol), [(η^3-C$_3$H$_5$)PdCl]$_2$ (0.98 mg, 0.0025 mol) in CH$_2$Cl$_2$ (1 mL) after chromatography (10% EtOAc in 40-60 petroleum ether) afforded (4-methylene-1-tosylpyrrolidin-2-yl)(phenyl)methanone (**103a**) as a white solid (21 mg, 75%).

^{1}H NMR (400 MHz, CDCl$_3$): δ 7.96 (d, *J* = 8.0 Hz, 2H), 7.72 (d, *J* = 8.0 Hz, 2H), 7.63 – 7.57 (m, 1H), 7.52 – 7.46 (m, 2H), 7.29 (d, *J* = 7.5 Hz, 2H), 5.50 (dd, *J* = 9.5, 3.0 Hz, 1H), 5.00 – 4.96 (m, 1H), 4.96 – 4.91 (m, 1H), 4.15 (d, *J* = 13.5 Hz, 1H), 4.06 (d, *J* = 13.5 Hz, 1H), 2.92 (dd, *J* = 15.5, 9.5 Hz, 1H), 2.59 (dd, *J* = 15.5, 1.0 Hz, 1H), 2.42 (s, 3H); **^{13}C NMR (101 MHz, CDCl$_3$):** δ 196.8, 144.1, 142.4, 136.1, 134.7, 133.9, 129.9,129.1, 129.0, 127.9, 109.1 63.3, 52.3, 37.1, 21.9; **FTIR: v_{max}/cm^{-1} (neat):** 3061, 2923, 2851, 1662, 1596, 1447, 1329, 1218, 1159, 1094, 1015, 664, 558; **HRMS (ESI$^+$):** calculated for C$_{19}$H$_{20}$NO$_3$S (ES$^+$)(+H$^+$): 342.1165, found: 342.1168.

(4-methylene-1-((4-nitrophenyl)sulfonyl)pyrrolidin-2-yl)(phenyl)methanone (104)

Following the General Procedure I with 2-(dimethyl-λ^4-sulfaneylidene)-1-phenylethan-1-one (**102a**) (27 mg, 0.15 mmol), 5-methylene-3-((4-nitrophenyl)sulfonyl)-1,3-oxazinan-2-one (**2c**) (30 mg, 0.1 mmol), *N,N*-diisopropyldibenzo[d,f][1,3,2]dioxaphosphepin-6-amine (1.7 mg, 0.0055

140

mmol), [(η³-C₃H₅)PdCl]₂ (0.98 mg, 0.0025 mol) in CH₂Cl₂ (1 mL) after chromatography (10% EtOAc in 40-60 petroleum ether) afforded (4-methylene-1-((4-nitrophenyl)sulfonyl)pyrrolidin-2-yl)(phenyl)methanone (**104**) as a yellow solid (23 mg, 61%).

¹H NMR (400 MHz, CDCl₃): δ 8.34 (d, *J* = 9.0 Hz, 2H), 7.99 (d, *J* = 9.0 Hz, 2H), 7.89 (d, *J* = 7.5 Hz, 2H), 7.67 – 7.59 (m, 1H), 7.55 – 7.45 (m, 2H), 5.68 (dd, *J* = 9.5, 2.5 Hz, 1H), 5.07 – 5.00 (m, 1H), 5.00 – 4.96 (m, 1H), 4.30 (d, *J* = 13.0 Hz, 1H), 4.05 (d, *J* = 13.0 Hz, 1H), 3.13 (dd, *J* = 14.5, 11.0 Hz, 1H), 2.61 (d, *J* = 15.5 Hz, 1H); **¹³C NMR (101 MHz, CDCl₃):** δ 196.3, 150.2, 145.1, 141.6, 134.4, 134.2, 129.3, 129.0, 128.9, 124.5, 110.0, 63.9, 52.2, 37.6; **FTIR: ν_max/cm⁻¹ (neat):** 3061, 2919, 2851, 1695, 1529, 1350, 1216, 1166, 1100, 738, 617; **HRMS (ESI⁺):** calculated for $C_{18}H_{17}N_2O_5S$ (ES⁺)(+H⁺): 373.0858, found: 373.0860.

(4-methylene-1-(methylsulfonyl)pyrrolidin-2-yl)(phenyl)methanone (105)
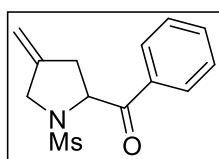
Following the General Procedure I with 2-(dimethyl-λ⁴-sulfaneylidene)-1-phenylethan-1-one (**102a**) (27 mg, 0.15 mmol), 5-methylene-3-(methylsulfonyl)-1,3-oxazinan-2-one (**2d**) (19 mg, 0.1 mmol), *N,N*-diisopropyldibenzo[d,f][1,3,2]dioxaphosphepin-6-amine (1.7 mg, 0.0055 mmol), [(η³-C₃H₅)PdCl]₂ (0.98 mg, 0.0025 mol) in CH₂Cl₂ (1 mL) after chromatography (35% Et₂O in 40-60 petroleum ether) afforded (4-methylene-1-(methylsulfonyl)pyrrolidin-2-yl)(phenyl)methanone (**105**) as a yellow oil (16 mg, 61%).

¹H NMR (400 MHz, CDCl₃): δ 8.01 – 7.86 (m, 2H), 7.68 – 7.57 (m, 1H), 7.53 – 7.45 (m, 2H), 5.63 (dd, *J* = 10.0, 2.5 Hz, 1H), 5.10 – 5.03 (m, 1H), 5.04 – 4.96 (m, 1H), 4.33 – 4.23 (m, 1H), 4.18 – 4.07 (m, 1H), 3.19 (dd, *J* = 15.0, 10.5 Hz, 1H), 3.03 (s, 3H), 2.63 (d, *J* = 15.0 Hz, 1H); **¹³C NMR (101 MHz, CDCl₃):** δ 197.6, 142.3, 134.3, 134.3, 129.3, 129.0, 109.4, 64.0, 51.9, 39.8, 37.6; **FTIR: ν_max/cm⁻¹ (neat):** 3105, 2926 1694, 1528, 1349, 1215, 1165, 1101, 738, 616; **HRMS (ESI⁺):** calculated for $C_{13}H_{15}NOS$ (ES⁺)(+Na⁺): 288.0670, found: 288.0666.

(4-methylene-1-tosylpyrrolidin-2-yl)(p-tolyl)methanone (103b)

Following the General Procedure I with 2-(dimethyl-λ^4-sulfaneylidene)-1-(*p*-tolyl)ethan-1-one (**102b**) (29 mg, 0.15 mmol), 5-methylene-3-tosyl-1,3-oxazinan-2-one (**2b**) (27 mg, 0.1 mmol), *N,N*-diisopropyldibenzo[d,f][1,3,2]dioxaphosphepin-6-amine (1.7 mg, 0.0055 mmol), [(η^3-C$_3$H$_5$)PdCl]$_2$ (0.98 mg, 0.0025 mol) in CH$_2$Cl$_2$ (1 mL) after chromatography (7.5% EtOAc in 40-60 petroleum ether) afforded (4-methylene-1-tosylpyrrolidin-2-yl)(*p*-tolyl)methanone (**103b**) as a white solid (21 mg, 75%).

^{1}H NMR (400 MHz, CDCl$_3$): δ 7.88 (d, *J* = 8.0 Hz, 2H), 7.74 (d, *J* = 8.0 Hz, 2H), 7.36 − 7.25 (m, 4H), 5.51 (dd, *J* = 9.5, 3.0 Hz, 1H), 5.00-4.98 (m, 1H), 4.98 − 4.92 (m, 1H), 4.17 (d, *J* = 13.5 Hz, 1H), 4.09 (d, *J* = 13.5 Hz, 1H), 2.93 (dd, *J* = 15.5, 9.5 Hz, 1H), 2.59 (d, *J* = 15.5 Hz, 1H), 2.44 (s, 6H); **^{13}C NMR (101 MHz, CDCl$_3$)**: δ 196.4, 144.9, 143.9, 142.8, 136.1, 132.2, 129.9, 129.8, 129.1, 127.9, 109.0, 63.2, 52.3, 37.3, 22.1, 21.9; **FTIR: v_{max}/cm^{-1} (neat):** 2920, 2851, 1690, 1606, 1343, 1158, 1097, 664, 588, 547 ; **HRMS (ESI$^+$):** calculated for C$_{20}$H$_{22}$NO$_3$S (ES$^+$)(+H$^+$): 356.1320., found: 356.1315.

(4-methoxyphenyl)(4-methylene-1-tosylpyrrolidin-2-yl)methanone (103c)

Following the General Procedure I with 2-(dimethyl-λ^4-sulfaneylidene)-1-(4-methoxyphenyl)ethan-1-one (**102c**) (32 mg, 0.15 mmol), 5-methylene-3-tosyl-1,3-oxazinan-2-one (**2b**) (27 mg, 0.1 mmol), *N,N*-diisopropyldibenzo[d,f][1,3,2]dioxaphosphepin-6-amine (1.7 mg, 0.0055 mmol), [(η^3-C$_3$H$_5$)PdCl]$_2$ (0.98 mg, 0.0025 mol) in CH$_2$Cl$_2$ (1 mL) after chromatography (10% EtOAc in 40-60 petroleum ether) afforded (4-methoxyphenyl)(4-methylene-1-tosylpyrrolidin-2-yl)methanone (**103c**) as a white solid (26 mg, 70%).

^{1}H NMR (400 MHz, CDCl$_3$): δ 7.98 (d, *J* = 9.0 Hz, 2H), 7.74 (d, *J* = 8.0 Hz, 2H), 7.31 (d, *J* = 8.0 Hz, 2H), 6.97 (d, *J* = 9.0 Hz, 2H), 5.48 (dd, *J* = 9.5, 3.0 Hz, 1H), 5.00-4.98 (m, 1H), 4.96 − 4.92 (m, 1H), 4.17 (d, *J* = 13.5 Hz, 1H), 4.08 (d, *J* = 13.5 Hz, 1H), 3.90 (s, 3H), 2.90 (dd, *J* = 15.5, 9.5 Hz, 1H), 2.60 (d, *J* = 15.5 Hz, 1H), 2.44 (s, 3H); **^{13}C NMR (101 MHz, CDCl$_3$):** δ 195.3, 164.2, 143.9, 142.9, 136.0, 131.4, 129.9, 127.9, 127.8, 114.3, 108.8, 62.9, 55.9, 52.3, 37.3, 21.9; **FTIR: v_{max}/cm^{-1} (neat):** 2920, 2851, 1600, 1161, 1260, 1097, 666, 588 ; **HRMS (ESI$^+$):** calculated for C$_{20}$H$_{22}$NO$_4$S (ES$^+$)(+H$^+$): 372.1270, found: 372.1274.

(4-methylene-1-tosylpyrrolidin-2-yl)(4-(trifluoromethyl)phenyl)methanone (103d)

Following the General Procedure I with 2-(dimethyl-λ^4-sulfaneylidene)-1-(4-(trifluoromethyl)phenyl)ethan-1-one (**102d**) (74 mg, 0.3 mmol), 5-methylene-3-tosyl-1,3-oxazinan-2-one (**2b**) (27 mg, 0.1 mmol), *N,N*-diisopropyldibenzo[d,f][1,3,2]dioxaphosphepin-6-amine (1.7 mg, 0.0055 mmol), [(η^3-C$_3$H$_5$)PdCl]$_2$ (0.98 mg, 0.0025 mol) in CH$_2$Cl$_2$ (1 mL) after chromatography (7.5% EtOAc in 40-60 petroleum ether) afforded (4-methylene-1-tosylpyrrolidin-2-yl)(4-(trifluoromethyl)phenyl)methanone (**103d**) as a yellow solid (32 mg, 79%).

^{1}H NMR (400 MHz, CDCl$_3$): δ 8.21 – 8.05 (m, 2H), 7.77 (d, *J* = 8.0 Hz, 2H), 7.74 (d, *J* = 8.0 Hz, 2H), 7.33 (d, *J* = 8.0 Hz, 2H), 5.41 (dd, J = 9.5, 3.5 Hz, 1H), 5.03 (s, 1H), 4.99 (s, 1H), 4.14 (d, *J* = 14.0 Hz, 1H), 4.08 (d, *J* = 14.0 Hz, 1H), 2.91 (dd, J = 16.0, 9.5 Hz, 1H), 2.71 – 2.56 (m, 1H), 2.46 (s, 3H); **^{19}F NMR (377 MHz, CDCl$_3$):** δ -63.2; **^{13}C NMR (101 MHz, CDCl$_3$):** δ 196.3, 144.3, 142.2, 137.6, 135.4, 135.1 (q, *J* = 33.0 Hz), 130.1, 129.5, 128.0, 126.2, 123.8 (q, *J* = 272.5 Hz), 109.5, 63.8, 52.4, 36.7, 21.9; **FTIR: v_{max}/cm^{-1} (neat):** 2917, 2850, 1702, 1326, 1161, 1067, 589; **HRMS (ESI$^+$):** calculated for C$_{20}$H$_{19}$F$_3$NO$_3$S (ES$^+$)(+H$^+$): 410.1038, found: 410.1044.

(4-chlorophenyl)(4-methylene-1-tosylpyrrolidin-2-yl)methanone (103e)

Following the General Procedure I with 1-(4-chlorophenyl)-2-(dimethyl-λ^4-sulfaneylidene)ethan-1-one (**102e**) (32 mg, 0.15 mmol), 5-methylene-3-tosyl-1,3-oxazinan-2-one (**2b**) (27 mg, 0.1 mmol), *N,N*-diisopropyldibenzo[d,f][1,3,2]dioxaphosphepin-6-amine (1.7 mg, 0.0055 mmol), [(η^3-C$_3$H$_5$)PdCl]$_2$ (0.98 mg, 0.0025 mol) in CH$_2$Cl$_2$ (1 mL) after chromatography (7.5% EtOAc in 40-60 petroleum ether) afforded (4-chlorophenyl)(4-methylene-1-tosylpyrrolidin-2-yl)methanone (**103e**) as a yellow solid (32 mg, 79%).

^{1}H NMR (400 MHz, CDCl$_3$): δ 7.95 (d, *J* = 7.0 Hz, 2H), 7.73 (d, *J* = 7.0 Hz, 2H), 7.48 (d, *J* = 7.0 Hz, 2H), 7.32 (d, *J* =7.0 Hz, 2H), 5.40 (d, *J* = 7.0 Hz, 1H), 5.00 (s, 1H), 4.96 (s, 1H), 4.13 (d, *J* = 13.0 Hz, 1H), 4.07 (d, *J* = 13.0 Hz, 1H), 2.99 – 2.79 (m, 1H), 2.61 (d, *J* = 15.5 Hz, 1H), 2.45 (s, 3H); **^{13}C NMR (101 MHz, CDCl$_3$):** δ 195.8, 144.1, 142.4, 140.5, 135.6, 133.1, 130.5, 130.0, 129.5, 127.9, 109.2, 63.4,

52.3, 36.9, 21.9; **FTIR: v_{max}/cm^{-1} (neat):** 2920, 2851, 1695, 1589, 1343, 1158, 1092, 663, 558; **HRMS (ESI$^+$):** calculated for $C_{19}H_{19}{}^{35}ClNO_3S$ (ES$^+$)(+H$^+$): 376.0774, found: 376.0784.
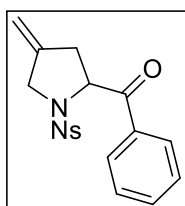
(4-fluorophenyl)(4-methylene-1-tosylpyrrolidin-2-yl)methanone (103f)
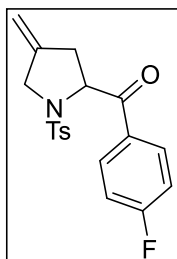
Following the General Procedure I with 2-(dimethyl-λ^4-sulfaneylidene)-1-(4-fluorophenyl)ethan-1-one (**102f**) (30 mg, 0.15 mmol), 5-methylene-3-tosyl-1,3-oxazinan-2-one (**2b**) (27 mg, 0.1 mmol), *N,N*-diisopropyldibenzo[d,f][1,3,2]dioxaphosphepin-6-amine (1.7 mg, 0.0055 mmol), [(η^3-C$_3$H$_5$)PdCl]$_2$ (0.98 mg, 0.0025 mol) in CH$_2$Cl$_2$ (1 mL) after chromatography (7.5% EtOAc in 40-60 petroleum ether) afforded (4-fluorophenyl)(4-methylene-1-tosylpyrrolidin-2-yl)methanone (**103f**) as a yellow solid (22 mg, 60%).

^{1}H NMR (400 MHz, CDCl$_3$): δ 8.02 (dd, *J* = 8.5, 5.5 Hz, 2H), 7.71 (d, *J* = 8.0 Hz, 2H), 7.30 (d, *J* = 8.0 Hz, 2H), 7.18-7.13 (m, 2H), 5.41 (dd, *J* = 9.5, 3.0 Hz, 1H), 4.98 (s, 1H), 4.94 (s, 1H), 4.12 (d, *J* = 14.0 Hz, 1H), 4.05 (d, *J* = 14.0 Hz, 1H), 2.93 – 2.82 (m, 1H), 2.59 (d, *J* = 15.5 Hz, 1H), 2.43 (s, 3H); **^{19}F NMR (376 MHz, CDCl$_3$):** δ -103.9 – -104.0 (m); **^{13}C NMR (101 MHz, CDCl$_3$):** δ 195.5, 167.6, 165.1, 144.1, 142.6, 135.7, 131.8, 130.0, 128.0, 116.3 (d, *J* = 22.0 Hz), 109.2, 63.3, 52.3, 37.0, 21.9. **FTIR: v_{max}/cm^{-1} (neat):** 2919, 2851, 1701, 1588, 1345, 1260, 1161, 750, 651, 589; **HRMS (ESI$^+$):** calculated for $C_{19}H_{19}FNO_3S$ (ES$^+$)(+H$^+$): 360.1070, found: 360.1067.

4-(4-methylene-1-tosylpyrrolidine-2-carbonyl)benzonitrile (103h)
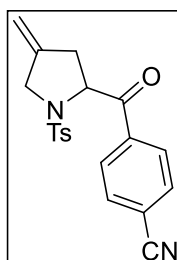
Following the General Procedure I with 2-(dimethyl-λ^4-sulfaneylidene)-1-(4-fluorophenyl)ethan-1-one (**102h**) (62 mg, 0.30 mmol), 5-methylene-3-tosyl-1,3-oxazinan-2-one (**2b**) (27 mg, 0.1 mmol), *N,N*-diisopropyldibenzo[d,f][1,3,2]dioxaphosphepin-6-amine (1.7 mg, 0.0055 mmol), [(η^3-C$_3$H$_5$)PdCl]$_2$ (0.98 mg, 0.0025 mol) in CH$_2$Cl$_2$ (1 mL) after chromatography (20% Et$_2$O in 40-60 petroleum ether) afforded 4-(4-methylene-1-tosylpyrrolidine-2-carbonyl)benzonitrile (**103h**) as a yellow oil (10 mg, 27%). A clean ^{13}C NMR spectrum could not be obtained and so this compound was characterized by ^{1}H NMR, FTIR and mass spectroscopy only.

¹H NMR (400 MHz, CDCl₃): δ 8.10 (d, J = 8.5 Hz, 2H), 7.79 (d, J = 8.5 Hz, 2H), 7.71 (d, J = 8.0 Hz, 2H), 7.32 (d, J = 8.0 Hz, 2H), 5.29 (dd, J = 9.5, 4.0 Hz, 1H), 5.04-4.99 (m, 1H), 4.99-4.95 (m, 1H), 4.10-4.03 (m, 2H), 2.86 (dd, J = 16.0, 9.5 Hz, 1H), 2.62 (dd, J = 16.0, 1.5 Hz, 1H), 2.44 (s, 3H); **FTIR: v_{max}/cm⁻¹ (neat):** 2929, 2232, 1705, 1160, 734, 664, 589; **HRMS (ESI⁺):** calculated for $C_{20}H_{18}N_2O_3SNa(ES^+)(+Na^+)$: 389.0936, found: 389.0935.

(2-methoxyphenyl)(4-methylene-1-tosylpyrrolidin-2-yl)methanone (103i)
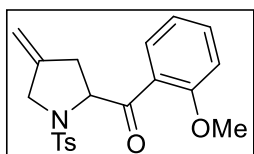
Following the General Procedure I with 2-(dimethyl-λ^4-sulfaneylidene)-1-(2-methoxyphenyl)ethan-1-one (**102i**) (64 mg, 0.30 mmol), 5-methylene-3-tosyl-1,3-oxazinan-2-one (**2b**) (27 mg, 0.1 mmol), *N,N*-diisopropyldibenzo[d,f][1,3,2]dioxaphosphepin-6-amine (1.7 mg, 0.0055 mmol), [(η³-C₃H₅)PdCl]₂ (0.98 mg, 0.0025 mol) in CH₂Cl₂ (1 mL) after chromatography (gradient from 20% Et₂O in 40-60 petroleum ether) afforded (2-methoxyphenyl)(4-methylene-1-tosylpyrrolidin-2-yl)methanone (**103i**) as a yellow oil (9.7 mg, 26%).

¹H NMR (400 MHz, CDCl₃): δ 7.71 (d, J = 8.0 Hz, 2H), 7.57 – 7.45 (m, 2H), 7.28 (d, J = 8.0 Hz, 2H), 7.06 – 6.92 (m, 2H), 5.59 (dd, J = 9.5, 2.0 Hz, 1H), 5.02 – 4.92 (m, 1H), 4.92 – 4.84 (m, 1H), 4.18 (d, J = 14.0 Hz, 1H), 4.03 (d, J = 14.0 Hz, 1H), 3.93 (s, 3H), 2.90 (dd, J = 15.0, 10.5 Hz, 1H), 2.55 (d, J = 15.0 Hz,1H), 2.42 (s, 3H); **¹³C NMR (101 MHz, CDCl₃):** δ 198.4, 159.2, 143.6, 143.3, 136.7, 134.8, 131.7, 129.8, 127.8, 125.5, 121.39, 112.1, 108.6, 67.01, 56.0, 52.6, 37.0, 21.9; **FTIR: v_{max}/cm⁻¹ (neat):** 2924, 2851, 1681, 1598, 1286, 1160, 1097, 666, 588; **HRMS (ESI⁺): calculated for $C_{20}H_{22}NO_4S$ (ES⁺)(+H⁺):** 372.1270, found: 372.1274.
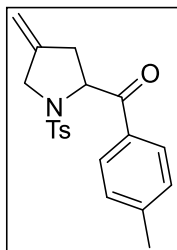
(3-methoxyphenyl)(4-methylene-1-tosylpyrrolidin-2-yl)methanone (103j)
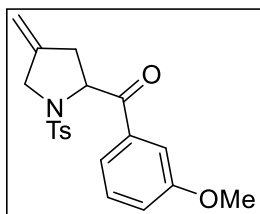
Following the General Procedure I with 2-(dimethyl-λ^4-sulfaneylidene)-1-(3-methoxyphenyl)ethan-1-one (**102j**) (32 mg, 0.15 mmol), 5-methylene-3-tosyl-1,3-oxazinan-2-one (**2b**) (27 mg, 0.1 mmol), *N,N*-diisopropyldibenzo[d,f][1,3,2]dioxaphosphepin-6-amine (1.7 mg, 0.0055 mmol), [(η³-C₃H₅)PdCl]₂ (0.98 mg, 0.0025 mol) in CH₂Cl₂ (1 mL) after chromatography (gradient

from 25-30% Et$_2$O in 40-60 petroleum ether) afforded (4-fluorophenyl)(4-methylene-1-tosylpyrrolidin-2-yl)methanone (**103j**) as a yellow oil (22 mg, 60%).

^{1}H NMR (400 MHz, CDCl$_3$): δ 7.72 (d, *J* = 8.0 Hz, 2H), 7.54 (d, *J* = 8.0 Hz, 1H), 7.48-7.47 (m, 1H), 7.41-7.17 (m, 1H), 7.30 (d, *J* = 8.0 Hz, 2H), 7.14 (dd, *J* = 8.0, 2.0 Hz, 1H), 5.48 (dd, *J* = 9.5, 3.0 Hz, 1H), 4.98 (s, 1H), 4.93 (s, 1H), 4.15 (d, *J* = 13.5 Hz, 1H), 4.06 (d, *J* = 13.5 Hz, 1H), 3.85 (s, 3H), 2.96 – 2.83 (m, 1H), 2.59 (d, *J* = 15.5 Hz, 1H), 2.43 (s, 3H); **^{13}C NMR (101 MHz, CDCl$_3$):** δ 196.7, 160.2, 143.9, 142.6, 136.1, (x2C), 130.0, 129.9, 127.9, 121.4, 120. 5, 113.3, 109.0, 63.4, 55.8, 52.5, 37.2, 21.9; **FTIR: v$_{max}$/cm^{-1} (neat):** 2920, 2851, 1701, 1600, 1260,1161, 1097, 666, 588; **HRMS (ESI$^+$): calculated for C$_{20}$H$_{22}$NO$_4$S (ES$^+$)(+H$^+$):** 372.1270, found: 372.1274.

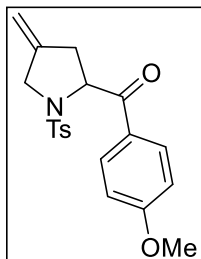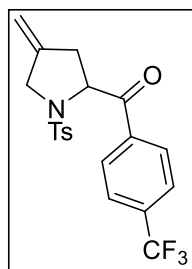**(3-fluorophenyl)(4-methylene-1-tosylpyrrolidin-2-yl)methanone (103k)**
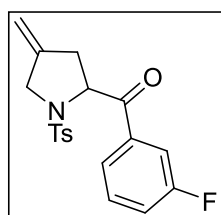
Following the General Procedure I with 2-(dimethyl-λ^4-sulfaneylidene)-1-(3-fluorophenyl)ethan-1-one (**102k**) (30 mg, 0.15 mmol), 5-methylene-3-tosyl-1,3-oxazinan-2-one (**2b**) (27 mg, 0.1 mmol), *N,N*-diisopropyldibenzo[d,f][1,3,2]dioxaphosphepin-6-amine (1.7 mg, 0.0055 mmol), [(η^3-C$_3$H$_5$)PdCl]$_2$ (0.98 mg, 0.0025 mol) in CH$_2$Cl$_2$ (1 mL) after chromatography (30% Et$_2$O in 40-60 petroleum ether) afforded (3-fluorophenyl)(4-methylene-1-tosylpyrrolidin-2-yl)methanone (**103k**) as a yellow oil (23 mg, 64%).

^{1}H NMR (400 MHz, CDCl$_3$): δ 7.79 (d, *J* = 7.5 Hz, 1H), 7.74 (d, *J* = 8.0 Hz, 2H), 7.66 (d, *J* = 9.0 Hz, 1H), 7.50 (td, *J* = 8.0, 5.5 Hz, 1H), 7.34-7.31 (m, 3H), 5.42 (dd, *J* = 9.5, 3.0 Hz, 1H), 5.01 (s, 1H), 4.97 (s, 1H), 4.15 (d, *J* = 13.0 Hz, 1H), 4.08 (d, *J* = 13.0 Hz, 1H), 2.93 (dd, *J* = 15.0, 10.5 Hz, 1H), 2.61 (d, *J* = 15.0 Hz, 1H), 2.45 (s, 3H); **^{19}F NMR (376 MHz, CDCl$_3$):** δ -111.06 – 111.12 (m); **^{13}C NMR (101 MHz, CDCl$_3$):** δ 195.7, 164.4, 161.8, 144.2, 142.4, 135.6, 130.9 (d, *J* = 7.5 Hz), 130.0, 127.9, 124.8 (d, *J* = 3.0 Hz), 121.0 (d, *J* = 21.5 Hz), 115.8 (d, *J* = 22.5 Hz), 109.4, 63.4, 52.2, 36.7, 21.9; **FTIR: v$_{max}$/cm^{-1} (neat):** 2919, 2851, 1701, 1588, 1345, 1260, 1161, 750, 651, 589; **HRMS (ESI$^+$):** calculated for C$_{19}$H$_{19}$FNO$_3$S (ES$^+$)(+H$^+$): 360.1070, found: 360.1067.

(4-methylene-1-tosylpyrrolidin-2-yl)(naphthalen-1-yl)methanone (103l)
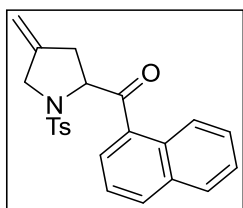
Following the General Procedure I with 2-(dimethyl-λ^4-sulfaneylidene)-1-(naphthalen-2-yl)ethan-1-one (**102l**) (30 mg, 0.15 mmol), 5-methylene-3-tosyl-1,3-oxazinan-2-one (**2b**) (27 mg, 0.1 mmol), *N,N*-diisopropyldibenzo[d,f][1,3,2]dioxaphosphepin-6-amine (1.7 mg, 0.0055 mmol), [(η^3-C$_3$H$_5$)PdCl]$_2$ (0.98 mg, 0.0025 mol) in CH$_2$Cl$_2$ (1 mL) after chromatography (10% EtOAc in 40-60 petroleum ether) afforded (4-methylene-1-tosylpyrrolidin-2-yl)(naphthalen-1-yl)methanone (**103l**) as a yellow oil (23 mg, 57%).

^{1}H NMR (400 MHz, CDCl$_3$): δ 8.52 (s, 1H), 7.98 (d, *J* = 8.5 Hz, 2H), 7.94 – 7.87 (m, 2H), 7.74 (d, *J* = 8.0 Hz, 2H), 7.60 (dt, *J* = 15.0, 7.0 Hz, 2H), 7.29 (d, *J* = 8.0 Hz, 2H), 5.68 (dd, *J* = 9.5, 3.0 Hz, 1H), 5.00 (s, 1H), 4.95 (s, 1H), 4.21 (d, *J* = 13.5 Hz, 1H), 4.11 (d, *J* = 13.5 Hz, 1H), 2.99 (dd, *J* = 16.0, 9.5 Hz, 1H), 2.66 (d, *J* = 16.0 Hz, 1H), 2.42 (s, 3H); **^{13}C NMR (101 MHz, CDCl$_3$):** δ 196.8, 143.8, 142.8, 136.1, 132.8, 132.1, 130.9, 130.0 (x2C), 129.9, 129.2, 129.1, 128.1, 127.9, 127.3, 124.4, 108.9, 63.4, 52.3, 37.4, 21.9; **FTIR: v_{max}/cm^{-1} (neat):** 2919, 2851, 1690, 1597, 1345, 1277, 1160, 763, 665, 589; **HRMS (ESI$^+$):** calculated for C$_{23}$H$_{22}$NO$_3$S (ES$^+$)(+H$^+$): 392.1320, found: 392.1317.

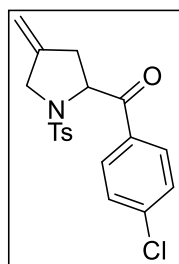**(4-methylene-1-tosylpyrrolidin-2-yl)(thiophen-2-yl)methanone (103m)**
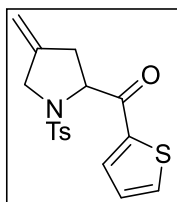
Following the General Procedure I with 2-(dimethyl-λ^4-sulfaneylidene)-1-(thiophen-2-yl)ethan-1-one (**102m**) (26 mg, 0.3 mmol), 5-methylene-3-tosyl-1,3-oxazinan-2-one (**2b**) (27 mg, 0.1 mmol), *N,N*-diisopropyldibenzo[d,f][1,3,2]dioxaphosphepin-6-amine (1.7 mg, 0.0055 mmol), [(η^3-C$_3$H$_5$)PdCl]$_2$ (0.98 mg, 0.0025 mol) in CH$_2$Cl$_2$ (1 mL) after chromatography (10% EtOAc in 40-60 petroleum ether) afforded (4-methylene-1-tosylpyrrolidin-2-yl)(thiophen-2-yl)methanone (**103m**) as a yellow oil (21 mg, 60%).

^{1}H NMR (400 MHz, CDCl$_3$): δ 7.93 (d, *J* = 3.5 Hz, 1H), 7.73 – 7.69 (m, 3H), 7.30 (d, *J* = 8.0 Hz, 2H), 7.17 (t, *J* = 4.5 Hz, 1H), 5.11 (dd, *J* = 9.0, 4.0 Hz, 1H), 4.98 (s, 1H), 4.95 (s, 1H), 4.09 (s, 2H), 2.84 (dd, *J* = 15.5, 9.5 Hz, 1H), 2.68 (d, *J* = 15.5 Hz, 1H), 2.43 (s, 3H); **^{13}C NMR (101 MHz, CDCl$_3$):** δ 190.2, 144.2, 142.4, 140.9, 135.1, 135.06, 133.8, 130.0, 128.6, 128.1, 109.3, 64.4, 52.8, 37.3, 22.4; **FTIR: v_{max}/cm^{-1} (neat):** 3092, 2924, 1668, 1413, 1343, 1158, 1095, 665, 588, 548; **HRMS (ESI$^+$):** calculated for C$_{17}$H$_{28}$NO$_3$S$_2$ (ES$^+$)(+H$^+$): 348.0728, found: 348.0722.

2,2-dimethyl-1-(4-methylene-1-tosylpyrrolidin-2-yl)propan-1-one (103n)
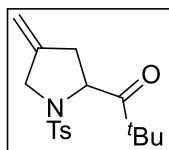
Following the General Procedure I with 2-(dimethyl-λ^4-sulfaneylidene)-1-(thiophen-2-yl)ethan-1-one (**102n**) (48 mg, 0.30 mmol), 5-methylene-3-tosyl-1,3-oxazinan-2-one (**2b**) (27 mg, 0.1 mmol), *N,N*-diisopropyldibenzo[d,f][1,3,2]dioxaphosphepin-6-amine (1.7 mg, 0.0055 mmol), [(η^3-C$_3$H$_5$)PdCl]$_2$ (0.98 mg, 0.0025 mol) in CH$_2$Cl$_2$ (1 mL) after chromatography (7.5% EtOAc in 40-60 petroleum ether) afforded 2,2-dimethyl-1-(4-methylene-1-tosylpyrrolidin-2-yl)propan-1-one (**103n**) as a yellow oil (6 mg, 18%). A clean ^{13}C NMR spectrum could not be obtained and so this compound was characterized by ^{1}H NMR, FTIR and mass spectroscopy only.

^{1}H NMR (400 MHz, CDCl$_3$): δ 7.70 (d, *J* = 8.0 Hz, 2H), 7.30 (d, *J* = 8.0 Hz, 2H), 5.04 (dd, *J* = 9.5, 3.5 Hz, 1H), 4.98 – 4.94 (m, 1H), 4.94 – 4.90 (m, 1H), 4.10 (d, *J* = 13.5 Hz, 1H), 4.04 (d, *J* = 13.5 Hz, 1H), 2.76 (dd, *J* = 15.5, 9.5 Hz, 1H), 2.42 (s, 3H), 2.34 (d, *J* = 15.5 Hz, 1H), 1.20 (s, 9H); **FTIR: v$_{max}$/cm^{-1} (neat):** 3054, 2969, 1714, 1528, 1348, 1164, 1100, 1061, 736, 618; **HRMS (ESI$^+$):** calculated for C$_{17}$H$_{23}$NO$_3$SNa (ES$^+$)(+Na$^+$): 344.1296, found: 344.1298.

ethyl 4-methylene-1-tosylpyrrolidine-2-carboxylate (103o)
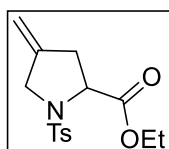
Following the General Procedure J with ethyl 2-(diphenyl-λ^4-sulfaneylidene)acetate (**108**) (54 mg, 0.2 mmol), 5-methylene-3-tosyl-1,3-oxazinan-2-one (**2b**) (27 mg, 0.1 mmol), *N,N*-diisopropyldibenzo[d,f][1,3,2]dioxaphosphepin-6-amine (3.5 mg, 0.011 mmol), [(η^3-C$_3$H$_5$)PdCl]$_2$ (1.83 mg, 0.005 mol) in CH$_2$Cl$_2$ (1 mL) after chromatography (20% Et$_2$O in 40-60 petroleum ether) afforded ethyl 4-methylene-1-tosylpyrrolidine-2-carboxylate (**103o**) as a yellow oil (20 mg, 65%).

^{1}H NMR (400 MHz, CDCl$_3$): δ 7.74 (d, *J* = 8.0 Hz, 2H), 7.31 (d, *J* = 8.0 Hz, 2H), 4.98 – 4.97 (m, 1H), 4.96 – 4.95 (m, 1H), 4.45 (dd, *J* = 9.0, 3.5 Hz, 1H), 4.19 – 4.04 (m, 2H), 4.02 (s, 2H), 2.77 (dd, *J* = 15.5, 9.0 Hz, 1H), 2.61 (d, *J* = 15.5 Hz, 1H), 2.42 (s, 3H), 1.22 (t, *J* = 7.0 Hz, 3H); **^{13}C NMR (101 MHz, CDCl$_3$):** δ 171.7, 144.0, 142.5, 135.7, 130.0, 128.0, 108.7, 61.6, 60.9, 52.1, 37.4, 22.0, 14.4; **FTIR: v$_{max}$/cm^{-1} (neat):** 2920, 2850, 1742, 1463, 1350, 1163, 1097, 665, 589, 549; **HRMS (ESI$^+$):** calculated for C$_{15}$H$_{20}$NO$_4$S (ES$^+$)(+H$^+$): 310.1113, found: 310.1113.

1-(4-methylene-1-tosylpyrrolidin-2-yl)propan-1-one (110)
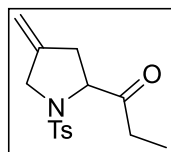
Following the General Procedure J with 1-(diphenyl-λ^4-sulfaneylidene)butan-2-one (**109**) (51 mg, 0.2 mmol), 5-methylene-3-tosyl-1,3-oxazinan-2-one (**2b**) (27 mg, 0.1 mmol), *N,N*-diisopropyldibenzo[d,f][1,3,2]dioxaphosphepin-6-amine (3.5 mg, 0.011 mmol), [(η^3-C$_3$H$_5$)PdCl]$_2$ (1.83 mg, 0.005 mol) in CH$_2$Cl$_2$ (1 mL) after chromatography (60% Et$_2$O in 40-60 petroleum ether) afforded 1-(4-methylene-1-tosylpyrrolidin-2-yl)propan-1-one (**110**) as a yellow oil (17 mg, 55%).

^{1}H NMR (400 MHz, CDCl$_3$) : δ 7.71 (d, *J* = 8.0 Hz, 2H), 7.33 (d, *J* = 8.0 Hz, 2H), 4.94 – 4.93 (m, 1H), 4.93 – 4.92 (m, 1H), 4.20 (dd, *J* = 9.5, 4.0 Hz, 1H), 4.04 (d, *J* = 14.0 Hz, 1H), 3.89 (d, *J* = 14.0 Hz, 1H), 2.95-2.84 (m, 1H), 2.66 – 2.39 (m, 6H), 1.07 (t, *J* = 7.0 Hz, 3H); ^{13}C NMR (101 MHz, CDCl$_3$) δ 210.6, 144.5, 142.2, 134.0, 130.2, 128.0, 109.1, 67.3, 52.9, 35.4, 31.9, 21.9, 7.6; **FTIR: v$_{max}$/cm^{-1} (neat):** 3054, 2993, 1722, 1264, 1162, 1097, 896, 733, 704; **HRMS (ESI$^+$):** calculated for C$_{15}$H$_{20}$NO$_3$S (ES$^+$)(+H$^+$): 294.1164, found: 294.1165.

## 4-methylene-2-(4-nitrophenyl)-1-tosylpyrrolidine (103g)
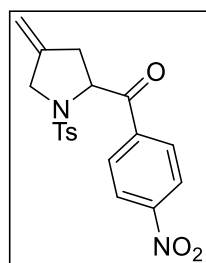
Following the General Procedure J with 2-(diphenyl-λ^4-sulfaneylidene)-1-(4-nitrophenyl)ethan-1-one (**111**) (70 mg, 0.2 mmol), 5-methylene-3-tosyl-1,3-oxazinan-2-one (**2b**) (27 mg, 0.1 mmol), *N,N*-diisopropyldibenzo[d,f][1,3,2]dioxaphosphepin-6-amine (3.5 mg, 0.011 mmol), [(η^3-C$_3$H$_5$)PdCl]$_2$ (1.83 mg, 0.005 mol) in CH$_2$Cl$_2$ (1 mL) at 50 after chromatography (30% Et$_2$O in 40-60 petroleum ether) afforded 4-methylene-2-(4-nitrophenyl)-1-tosylpyrrolidine (**103g**) as a yellow oil (17 mg, 45%).

^{1}H NMR (400 MHz, CDCl$_3$): δ 8.35 (d, J = 8.5 Hz, 2H), 8.20 (d, J = 8.5 Hz, 2H), 7.74 (d, J = 8.0 Hz, 2H), 7.35 (d, J = 8.0 Hz, 2H), 5.32 (dd, J = 9.5, 4.0 Hz, 1H), 5.04 (s, 1H), 5.00 (s, 1H), 4.09 (br, 2H), 2.89 (dd, J = 16.0, 9.5 Hz, 1H), 2.67 (d, J = 16.0 Hz, 1H), 2.46 (s, 3H); **^{13}C NMR (101 MHz, CDCl$_3$):** δ 196.1, 150.9, 144.4, 141.9, 139.3, 134.9, 130.2, 130.2, 128.0, 124.3, 109.8, 64.1, 52.4, 36.4, 21.9; ; **FTIR: v$_{max}$/cm^{-1} (neat):** 2921, 2856, 1703, 1525, 1346, 1160, 1096, 665, 588, 548; **HRMS (ESI$^+$):** calculated for C$_{19}$H$_{18}$N$_2$O$_5$SNa (ES$^+$)(+Na$^+$): 409.0939, found: 409.0839.

(S)-4-isopropyl-3-((R)-4-methylene-1-tosylpyrrolidine-2-carbonyl)oxazolidin-2-one (113)
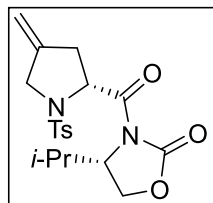
Following the General Procedure J with (S)-3-(2-(diphenyl-λ^4-sulfaneylidene)acetyl)-4-isopropyloxazolidin-2-one (**112**) (71 mg, 0.2 mmol), 5-methylene-3-tosyl-1,3-oxazinan-2-one (**2b**) (27 mg, 0.1 mmol), N,N-diisopropyldibenzo[d,f][1,3,2]dioxaphosphepin-6-amine (3.5 mg, 0.011 mmol), [(η^3-C$_3$H$_5$)PdCl]$_2$ (1.83 mg, 0.005 mol) in CH$_2$Cl$_2$ (1 mL) after chromatography (40% Et$_2$O in 40-60 petroleum ether) afforded (S)-4-isopropyl-3-((R)-4-methylene-1-tosylpyrrolidine-2-carbonyl)oxazolidin-2-one (**113**) as a yellow oil (25 mg, 65%; >19:1 dr).

^{1}H NMR (400 MHz, CDCl$_3$): δ 7.77 (d, J = 8.0 Hz, 2H), 7.34 (d, J = 8.0 Hz, 2H), 5.67 (dd, J = 9.0, 3.5 Hz, 1H), 4.99 – 4.98 (m, 1H), 4.97 – 4.96 (m, 1H), 4.49 (dt, J = 6.5. 3.5 Hz, 1H), 4.21 (dd, J = 9.0, 3.0 Hz, 1H), 4.28 (dd, J = 9.0, 3.0 Hz, 1H), 4.15 (d, J = 14.0 Hz, 1H), 3.98 (d, J = 14.0 Hz, 1H), 2.95 (dd, J = 17.0, 10.0 Hz, 1H), 2.52 (d, J = 15.0 Hz, 1H), 2.45 (s, 3H), 2.39 – 2.31 (m, 1H), 0.92 (d, J = 7.0 Hz, 3H), 0.88 (d, J = 7.0 Hz, 3H); **^{13}C NMR (101 MHz, CDCl$_3$):** δ 171.2, 154.4, 143.9, 142.3, 136.0, 130.1, 127.7, 109.1, 64.7, 60.9, 58.7, 52.3, 38.1, 28.9, 21.9, 18.1, 15.2; **FTIR: v$_{max}$/cm^{-1} (neat):**2962, 2922, 1776, 1713, 1389, 1343, 1160, 1096, 815**; HRMS (ESI$^+$):** calculated for C$_{19}$H$_{25}$N$_2$O$_5$S (ES$^+$)(+H$^+$): 393.1484, found: 393.1389.

Gram scale synthesis of compound (103o)
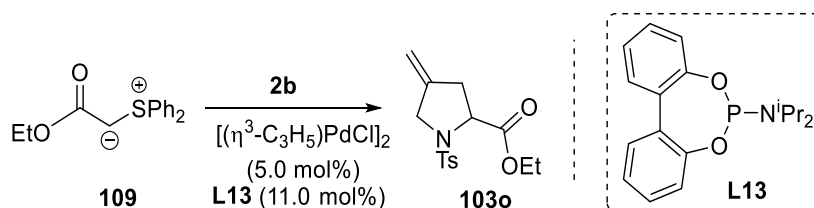
A flame-dried 50 mL round bottomed flask was charged 5-methylene-3-tosyl-1,3-oxazinan-2-one (**2b**) (1.34 g, 5.0 mmol), N,N-diisopropyldibenzo[d,f][1,3,2]dioxaphosphepin-6-amine (**L13**) (0.081 g, 0.275 mmol) and [(η^3-C$_3$H$_5$)PdCl]$_2$ (0.041 g 0.125 mmol) under nitrogen. Anhydrous CH$_2$Cl$_2$ (5 mL) was then added, and the mixture stirred at rt for 15 minutes. Ethyl 2-(diphenyl-λ^4-sulfaneylidene)acetate (**109**) (2.04 g, 7.5 mmol) in CH$_2$Cl$_2$ (5 mL) was added and the reaction mixture was stirred overnight at rt. A further portion of N,N-

diisopropyldibenzo[d,f][1,3,2]dioxaphosphepin-6-amine (**L13**) (0.081 g, 0.275 mmol), [(η^3-C$_3$H$_5$)PdCl]$_2$ (0.041 g 0.125 mmol) and ethyl 2-(diphenyl-λ^4-sulfaneylidene)acetate (**109**) (0.68 g, 2.5 mmol) were added and the reaction mixture was stirred for another 2 h at rt. The resulting mixture was then concentrated under vacuum and purified by flash column chromatography (20% Et$_2$O in 40-60 petroleum ether) to afford ethyl 4-methylene-1-tosylpyrrolidine-2-carboxylate (**103o**) as a yellow oil (1.24 g, 80%).

diethyl 5-tosyl-5-azaspiro[2.4]heptane-1,6-dicarboxylate (131)
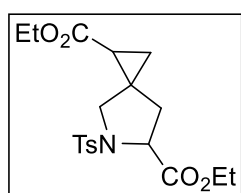
To a solution of ethyl 4-methylene-1-tosylpyrrolidine-2-carboxylate (**103o**) (30 mg, 0.10 mmol) and Rh$_2$(OAc)$_4$ (0.0008 g, 1.6 mol%) in refluxing CH$_2$Cl$_2$ (1.0 mL) was added ethyl diazoacetate (contains >13% w/w CH$_2$Cl$_2$, 0.02 mL) dropwise. The reaction mixture was stirred at refluxing conditions until **103o** was consumed. The reaction mixture was concentrated under vacuum and purified by chromatography (40% Et$_2$O in 40-60 petroleum ether) to afford diethyl 5-tosyl-5-azaspiro[2.4]heptane-1,6-dicarboxylate (**131**) as a colourless oil (18.4 mg, 47%)

^{1}H NMR (400 MHz, CDCl$_3$): δ 7.83 – 7.65 (m, 2H), 7.35 – 7.27 (m, 2H), 4.30 – 4.00 (m, 5H), 3.61 – 3.45 (m, 1H), 3.45 – 3.27 (m, 1H), 2.43 (s, 3H), 2.33 – 2.20 (m, 1H), 2.17 – 1.97 (m, 1H), 1.28 – 1.22 (m, 8H); **^{13}C NMR (101 MHz, CDCl$_3$):** δ 171.5, 171.4, 143.8, 135.2, 129.9, 127.6, 61.5, 60.7, 60.1, 55.8 (d, J = 28.5 Hz), 51.3 (d, J = 28.5 Hz), 34.3 (d, J = 113.0 Hz), 22.3 (d, J = 94.5 Hz), 20.9 (d, J = 72.5 Hz), 18.1 (d, J = 88.0 Hz), 14.3, 14.1; **FTIR: v_{max}/cm^{-1} (neat):** 3055, 2985, 1726, 1264, 1161, 1096, 1030, 896; **HRMS (ESI$^+$):** calculated for C$_{19}$H$_{26}$NO$_6$S (ES$^+$)(+H$^+$): 396.1403, found: 396.1490.

ethyl 1,1-difluoro-5-tosyl-5-azaspiro[2.4]heptane-6-carboxylate (133)
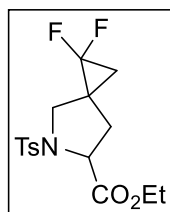
TMSCF$_3$ (0.037 mL, 0.25 mmol) and NaI (8 mg, 0.05 mmol) were added in one portion to a solution containing ethyl 4-methylene-1-tosylpyrrolidine-2-carboxylate (**103o**) (30 mg, 0.10 mmol) in THF (2 mL). The resulting mixture was heated at reflux for 4 hours. After 4 hours, additional TMSCF$_3$ (0.037 mL, 0.25 mmol) was added and the resulting mixture was heated at reflux overnight. The reaction mixture was concentrated under vacuum and purified by chromatography (20% Et$_2$O in 40-60 petroleum

ether) to afford ethyl 1,1-difluoro-5-tosyl-5-azaspiro[2.4]heptane-6-carboxylate (**133**) as a yellow solid (7.0 mg, 20%; 3:2 mixture of diastereomers).

^{1}H NMR (400 MHz, CDCl$_3$): δ 7.74 (d, *J* = 7.5 Hz, 2H), 7.33 (d, *J* = 7.5 Hz, 2H), 4.54 (d, *J* = 8.0 Hz, 0.4H), 4.41 (dd, *J* = 8.0, 4.5 Hz, 0.6 H), 4.26 – 3.94 (m, 2H), 3.66 (d, *J* = 10.0 Hz, 0.6H), 3.58 (d, *J* = 10.0 Hz, 0.4H), 3.55 – 3.43 (m, 1H), 2.43 (s, 3H), 2.39 – 2.22 (m, 1H), 2.12 – 1.91 (m, 1H), 1.33-1.29 (m, 2H), 1.25 – 1.15 (m, 3H); **^{19}F NMR (376 MHz, CDCl$_3$):** δ -136.14 – -138.56 (m), -138.8 (m); **^{13}C NMR (101 MHz, CDCl$_3$)**: δ 171.3, 171.0, 144.4, 144.2, 135.8, 135.1, 130.14, 130.05, 127.8, 127.7, 112.1 (d, *J* = 10.0 Hz), 109.3 , 62.0, 61.4, 61.0, 50.8, 49.6, 34.3, 33.8, 30.0, 21.9, 20.5 (t, *J* = 10.5 Hz), 17.5 (t, *J* = 10.5Hz) 14.4, 14.1; **FTIR: v$_{max}$/cm^{-1} (neat):** 3058, 2924, 1739, 1265, 1162, 906, 728; **HRMS (ESI$^+$):** calculated for C$_{16}$H$_{20}$F$_2$NO$_4$S (ES$^+$)(+H$^+$): 360.1003, found: 360.1079.

ethyl 4-(propan-2-ylidene)-1-tosylpyrrolidine-2-carboxylate (134)
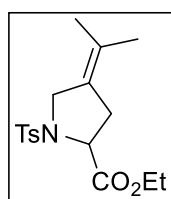
To a solution of ethyl 4-methylene-1-tosylpyrrolidine-2-carboxylate (**103o**) (31 mg, 0.1 mmol) and 2-methyl-2-butene (0.5 mL) in DCE (1 mL) under nitrogen was added Ti(O^{i}Pr)$_4$ (9.5 mg, 0.03 mmol). After 15 mins, the 2nd generation Hoveyda-Grubbs catalyst (7 mg, 0.01 mmol) was added and the resulting mixture was heated at 50 °C overnight. After cooling, the mixture was evaporated under vacuum and purified by column chromatography (30% Et$_2$O in 40-60 petroleum ether) to afford **e**thyl 4-(propan-2-ylidene)-1-tosylpyrrolidine-2-carboxylate (**134**) as a yellow oil (24 mg, 84%).

^{1}H NMR (400 MHz, CDCl$_3$): δ 7.74 (d, *J* = 8.0 Hz, 2H), 7.30 (d, *J* = 8.0 Hz, 2H), 4.40 (dd, *J* = 9.0, 4.0 Hz, 1H), 4.13-4.07 (m, 2H), 4.02 (d, *J* = 14.0 Hz, 1H), 3.93 (d, *J* = 14.0 Hz, 1H), 2.77 (dd, *J* = 15.5, 9.0 Hz, 1H), 2.66 (d, *J* = 15.5 Hz, 1H), 2.42 (s, 3H), 1.56 (s, 6H), 1.22 (t, *J* = 7.0 Hz, 3H); **^{13}C NMR (101 MHz, CDCl$_3$):** δ 172.0, 143.9, 135.6, 129.9, 127.9, 126.2, 125.5, 61.6, 61.1, 50.3, 34.6, 21.8, 21.3, 21.1, 14.3; **FTIR: v$_{max}$/cm^{-1} (neat):** 2988, 2917, 1737, 1347, 1161, 1094, 1031, 815; **HRMS (ESI$^+$):** calculated for C$_{17}$H$_{24}$NO$_4$S (ES$^+$)(+H$^+$): 338.1426, found: 338.1425.

ethyl 4-oxo-1-tosylpyrrolidine-2-carboxylate (136)
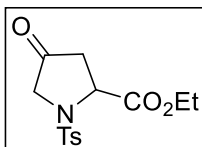
To a solution of ethyl 4-methylene-1-tosylpyrrolidine-2-carboxylate (**103o**) (31 mg, 0.1 mmol) dissolved in MeCN/CH$_2$Cl$_2$/H$_2$O (1:1:2 v/v/v, 2.0 mL) was added RuCl$_3$ (6.2 mg, 0.03 mmol) and the reaction mixture was stirred at 0 °C for 30 mins. Then NaIO4 (171 mg, 0.8 mmol) was added, and the reaction mixture was stirred at room temperate. After 4 hours, the resulting mixture was extracted with CH$_2$Cl$_2$ and the combined organic portions were washed with brine and dried with MgSO$_4$. The mixture was evaporated under high vacuum and purified by column chromatography (50% Et$_2$O in 40-60 petroleum ether) to afford ethyl 4-oxo-1-tosylpyrrolidine-2-carboxylate (**136**) as a white solid (19 mg, 61%).

1H NMR (400 MHz, CDCl$_3$): δ 7.73 (d, *J* = 8.0 Hz, 2H), 7.34 (d, *J* = 8.0 Hz, 2H), 4.76 (dd, *J* = 9.5, 2.5 Hz, 1H), 4.11 – 3.99 (m, 2H), 3.84 (d, *J* = 17.4 Hz, 1H), 3.77 (d, *J* = 17.5 Hz, 1H)2.77 (dd, *J* = 18.0, 9.5 Hz, 1H), 2.55 (dd, *J* = 18.0, 1.5 Hz, 1H), 2.44 (s, 3H), 1.19 (t, *J* = 7.1 Hz, 3H); **13C NMR (101 MHz, CDCl$_3$):** δ 206.7, 170.8, 145.0, 135.0, 130.3, 128.1, 62.2, 57.9, 52.9, 41.9, 21.9, 14.2; **FTIR: v$_{max}$/cm^{-1} (neat):** 2987, 2923, 1768, 1743, 1350, 1264, 729, 712; **HRMS (ESI$^+$):** calculated for C$_{14}$H$_{14}$NO$_5$SNa (ES$^+$)(+Na$^+$): 334.0725, Found: 334.0723

(4-methylene-1-tosylpyrrolidin-2-yl)methanol (138)
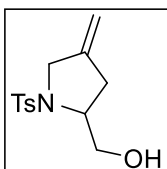
To a suspension of LiAlH$_4$ (4.5 mg, 0.12 mmol) in THF (1 mL) under nitrogen was added ethyl 4-methylene-1-tosylpyrrolidine-2-carboxylate (**103o**) (31 mg, 0.1 mmol) in THF (1 mL) and the resulting mixture stirred at 0 °C for 1 hour. H$_2$O (0.6 mL) was then added dropwise and the reaction stirred for 15 minutes at 0 °C before the addition of anhydrous MgSO$_4$. After 15 minutes the reaction mixture was filtered through celite and the volatiles removed under vacuum. Purification by column chromatography (50% Et$_2$O in 40-60 petroleum ether) afforded (4-methylene-1-tosylpyrrolidin-2-yl)methanol (**138**) as a colourless oil (18 mg, 69%).

1H NMR (400 MHz, CDCl$_3$): δ 7.73 (d, *J* = 7.5 Hz, 2H), 7.33 (d, *J* = 7.5 Hz, 2H), 4.94-4.88 (m, 2H), 4.03 (d, *J* = 14.5 Hz, 1H), 3.88 (d, *J* = 14.5 Hz, 1H), 3.83 – 3.63 (m, 1H), 3.66-3.57 (m, 2H), 2.57 (br, OH), 2.43 (s, 3H), 2.34-2.27 (m, 2H); **13C NMR (101 MHz, CDCl$_3$):** δ 144.1, 142.9, 134.2, 130.2, 127.9, 108.5, 65.3, 62.1, 53.4, 35.1, 21.9; **FTIR: v$_{max}$/cm^{-1} (neat):** 3061, 2989, 1264, 734, 704; **HRMS (ESI$^+$):** calculated for C$_{13}$H$_{18}$NO$_3$S (ES$^+$)(+H$^+$): 268.1007, found: 268.0999.

(*R*)-2-(((*tert*-butyldimethylsilyl)oxy)methyl)-4-methylene-1-tosylpyrrolidine (153)
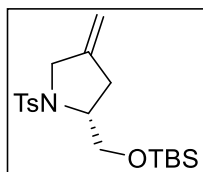
To a solution of (*R*)-(4-methylene-1-tosylpyrrolidin-2-yl)methanol (**151**) (26.7 mg, 0.1 mmol) in CH_2Cl_2 (2 mL) under nitrogen was added imidazole (7.5 mg, 0.11 mmol) and *tert*-butyldimethylsilyl chloride (16.6 mg, 0.11 mmol). The reaction mixture was stirred at room temperature overnight. The resulting mixture was quenched with NH_4Cl and extracted with EtOAc. The organic portion was washed with brine and dried with $MgSO_4$ and the solvent removed in vacuo. Purification by column chromatography (10% Et_2O in 40-60 petroleum ether) afforded (*R*)-2-(((tert-butyldimethylsilyl)oxy)methyl)-4-methylene-1-tosylpyrrolidine (**153**) as a colourless oil (15 mg, 82%).

^{1}H NMR (400 MHz, CDCl$_3$): δ 7.71 (d, *J* = 8.0 Hz, 2H), 7.29 (d, *J* = 8.0 Hz, 2H), 4.89 (br, 2H), 3.94 – 3.80 (m, 3H), 3.76 (dd, *J* =10.0, 4.0 Hz, 1H), 3.45 (dd, *J* = 10.0, 8.5 Hz, 1H), 2.44 (d, *J* = 15.5 Hz, 1H), 2.41 (s, 3H), 2.20 (dd, *J* = 15.5, 8.5 Hz, 1H), 0.86 (s, 9H), 0.04 (s, 3H), 0.03 (s, 3H); **^{13}C NMR (101 MHz, CDCl$_3$):** δ 144.0, 143.8, 135.4, 130.0, 127.6, 108.2, 65.5, 61.2, 52.9, 34.7, 26.1, 21.8, 18.4, -5.27; **FTIR: v_{max}/cm^{-1} (neat):** 3052, 2863, 1265, 733, 704; **HRMS (ESI$^+$):** calculated for $C_{19}H_{32}NO_3SSi$ (ES$^+$)(+H$^+$): 382.1872, found: 382.1871.

tert-butyl(*R*)-2-(((*tert*-butyldimethylsilyl)oxy)methyl)-4-methylenepyrrolidine-1-carboxylate (154)[86]
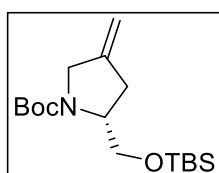
To a solution of (*R*)-2-(((*tert*-butyldimethylsilyl)oxy)methyl)-4-methylene-1-tosylpyrrolidine **153** (152 mg, 0.40 mmol) in MeOH (20.0 mL) under nitrogen was added magnesium turnings (677 mg, 27.88 mmol). The reaction mixture was ultrasonicated at 60 °C for 6 h, and sat. NH_4Cl was added to quench the reaction. The mixture was extracted with CH_2Cl_2, dried over $MgSO_4$ and the volatiles removed under vacuum. To a solution of the crude product in CH_2Cl_2 (2.0 mL) under nitrogen was added di-*tert*-butyl dicarbonate (175 mg, 0.80 mmol) portionwise, followed by 4-(dimethylamino)pyridine (4.8 mg, 0.04 mmol) and TEA (0.12 mL, 0.55 mmol) at 0 °C. The reaction mixture was slowly warmed to room temperature and stirred overnight. The resulting mixture was concentrated under vacuum and purified by column chromatography (5% Et_2O in 40-60 petroleum

ether) to afford *tert*-butyl (*R*)-2-(((*tert*-butyldimethylsilyl)oxy)methyl)-4-methylenepyrrolidine-1-carboxylate (**154**) as a colourless oil (52 mg, 40%; 3:2 mixture of rotamers).

¹H NMR (400 MHz, CDCl₃): δ 4.96-4.90 (m, 2H), 4.08-3.92 (m, 2H), 3.83 (br, 0.6H), 3.79 (br, 0.4H), 3.62 (dd, *J* = 9.5, 3.0 Hz, 1H), 3.61 – 3.29 (m, 1H), 2.72-2.63 (m, 1H), 2.56 (d, *J* = 15.0 Hz, 1H) 1.45 (s, 9H), 0.86 (s, 9H), 0.02 (s, 6H); **¹³C NMR (101 MHz, CDCl₃):** δ 154.4, 107.5, 106.6, 79.8, 79.5, 63.8, 63.6, 58.7, 58.4, 51.8, 51.1, 35.2, 34.6, 28.9, 26.2, 18.5, -4.9; **HPLC** (Cellulose-2, hexane: ⁱPrOH 99.9:0.1, flow rate 1.0 mL/min, λ = 210 nm, 25 °C) t_R(major) = 11.960 min, t_R(minor) = 13.637 min, *ee* = 95%; ; $[\alpha]_D^{22} = +20$ (*c* 1.0, CHCl₃).

Appendix

NMR spectra for di-*tert*-butyl (**2S,3R**)-3-fluoro-5-(hydroxymethyl)-2-phenylpiperidine-1,3-dicarboxylate (**101**)

^{1}H NMR, CDCl$_3$, 400 MHz (borane reduction)
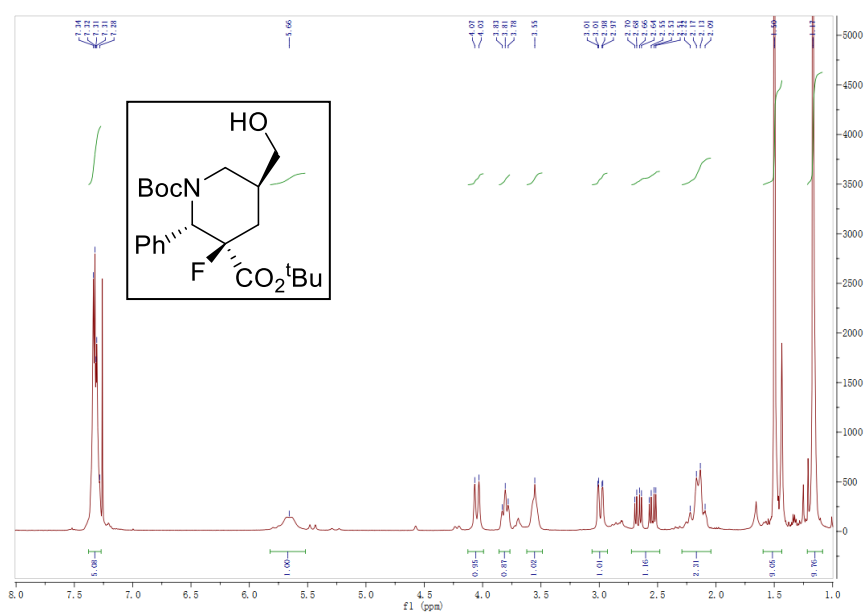
^{1}H NMR, CDCl$_3$, 400 MHz (9-BBN reduction)
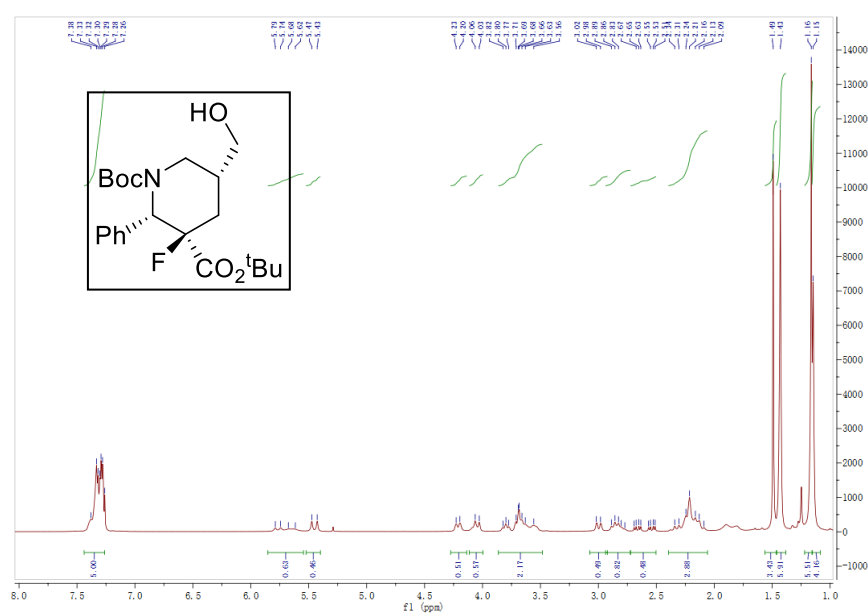
¹⁹F NMR, CDCl₃, 377 MHz (borane reduction)
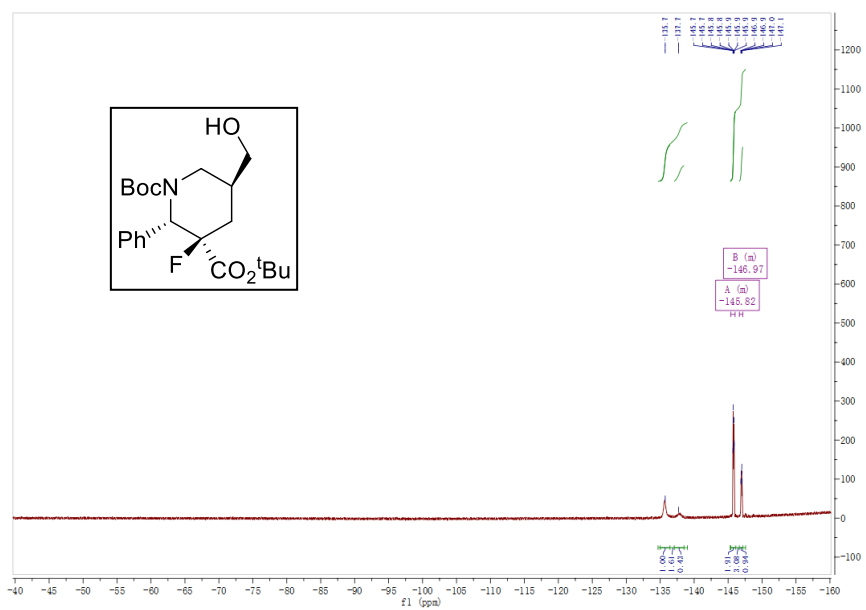
¹⁹F NMR, CDCl₃, 377 MHz (9-BBN reduction)
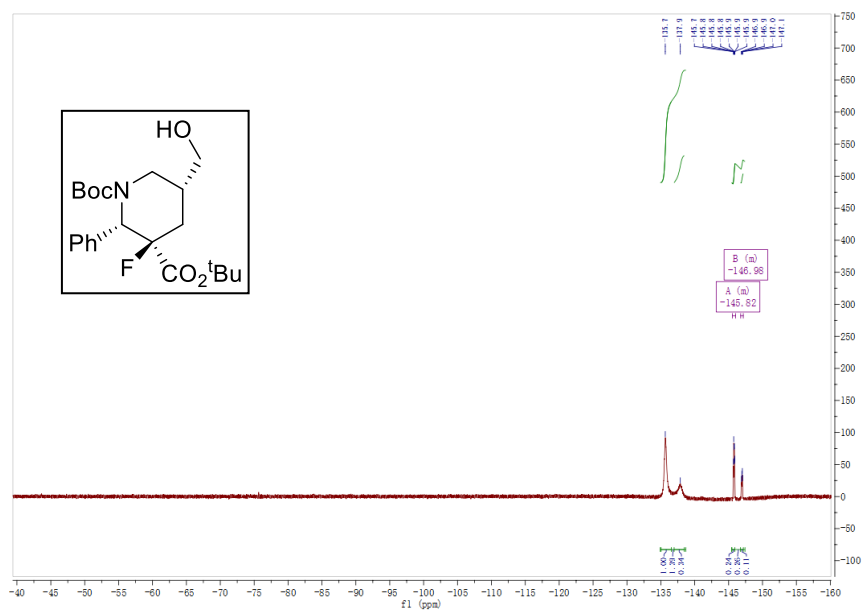
^{13}C NMR, CDCl$_3$, 101 MHz (borane reduction)
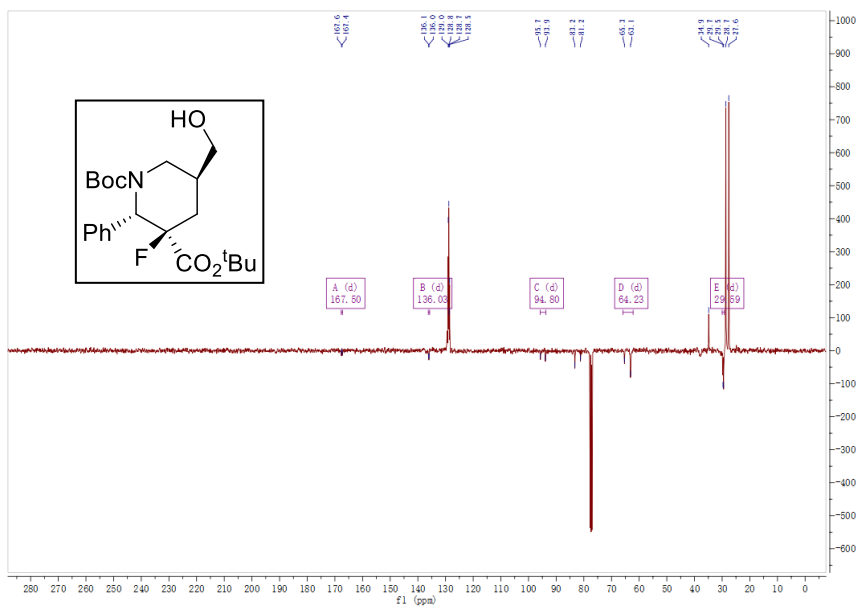
^{13}C NMR, CDCl$_3$, 101 MHz (9-BBN reduction)
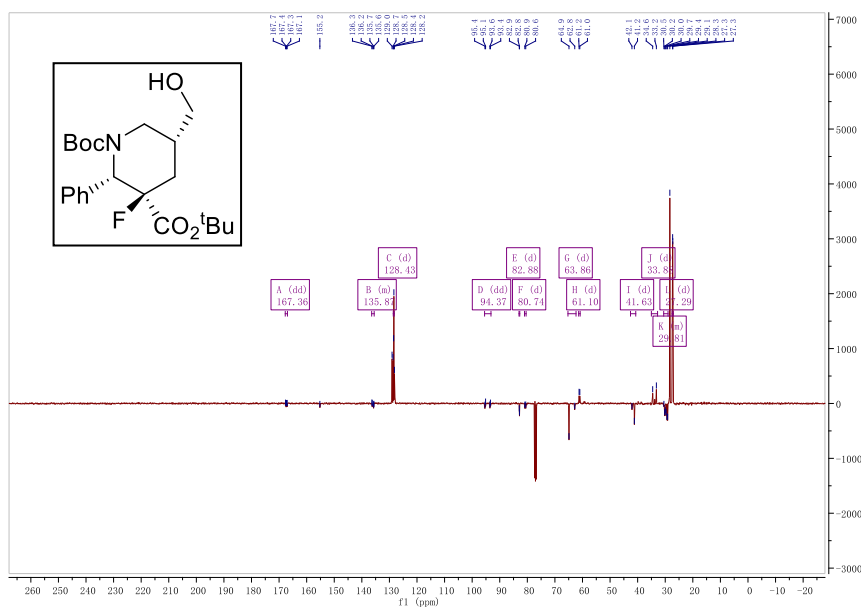
HPLC spectra
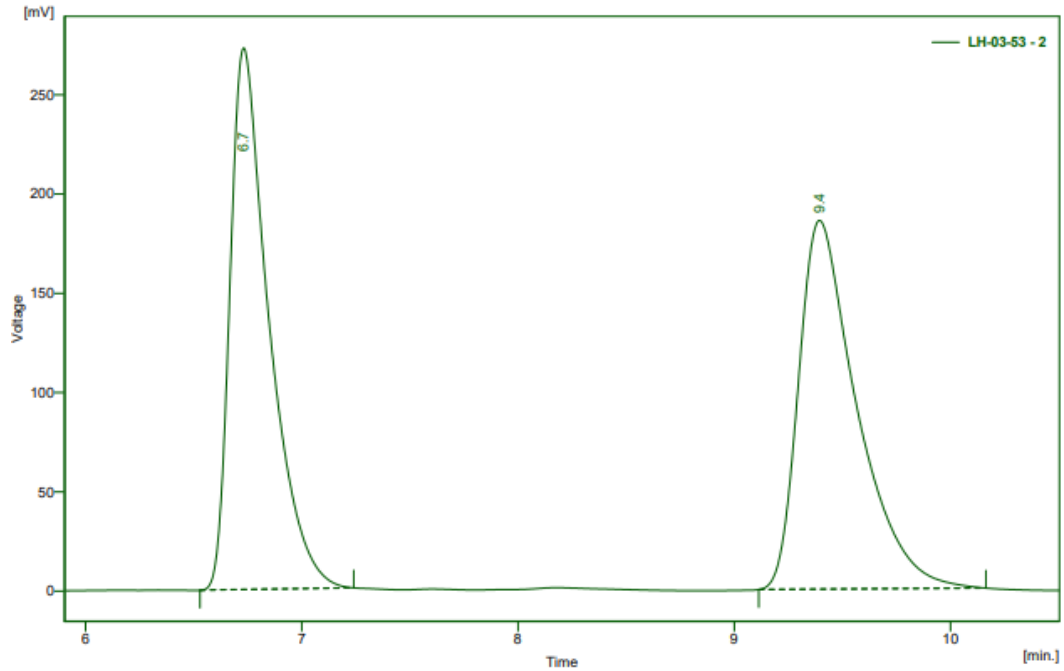
	Reten. Time [min]	Area [mV.s]	Height [mV]	Area [%]	Height [%]	W05 [min]
1	6.730	3413.484	272.845	49.6	59.5	0.19
2	9.393	3466.846	185.778	50.4	40.5	0.28
	Total	6880.329	458.623	100.0	100.0	
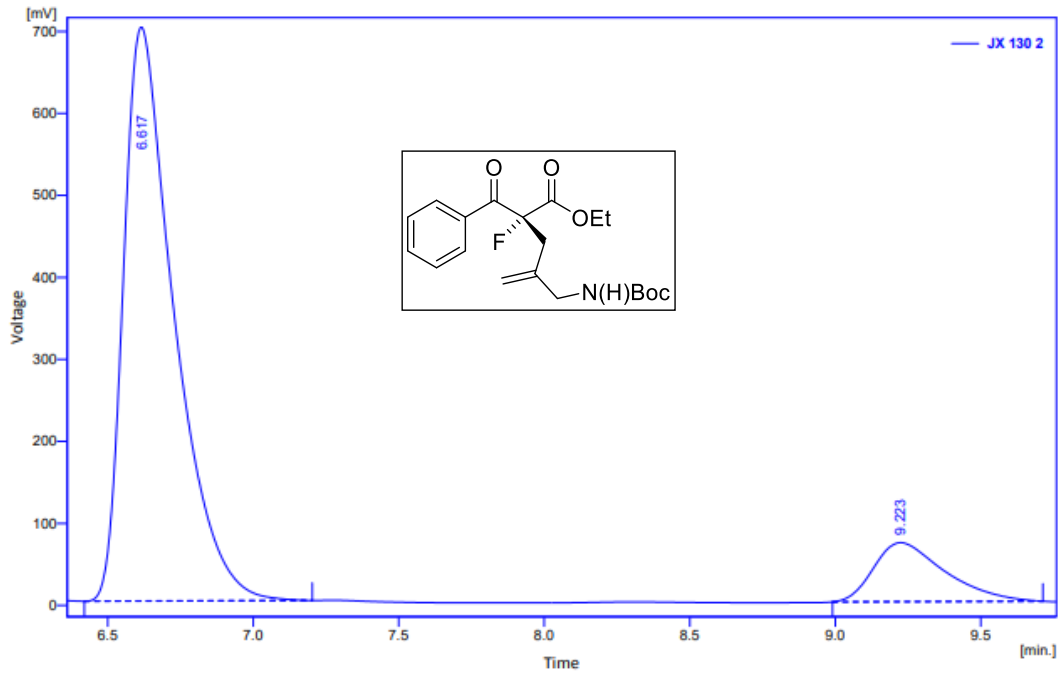
	Reten. Time [min]	Area [mV.s]	Height [mV]	Area [%]	Height [%]	W05 [min]
1	6.617	8457.831	699.950	87.4	90.7	0.18
2	9.223	1220.211	71.973	12.6	9.3	0.26
	Total	9678.042	771.923	100.0	100.0	

159

	Reten. Time [min]	Area [mV.s]	Height [mV]	Area [%]	Height [%]	W05 [min]
1	11.917	4818.220	154.491	50.1	52.0	0.51
2	13.193	4794.399	142.393	49.9	48.0	0.54
	Total	9612.619	296.885	100.0	100.0	

JX 134 08 12 21 crystal 2
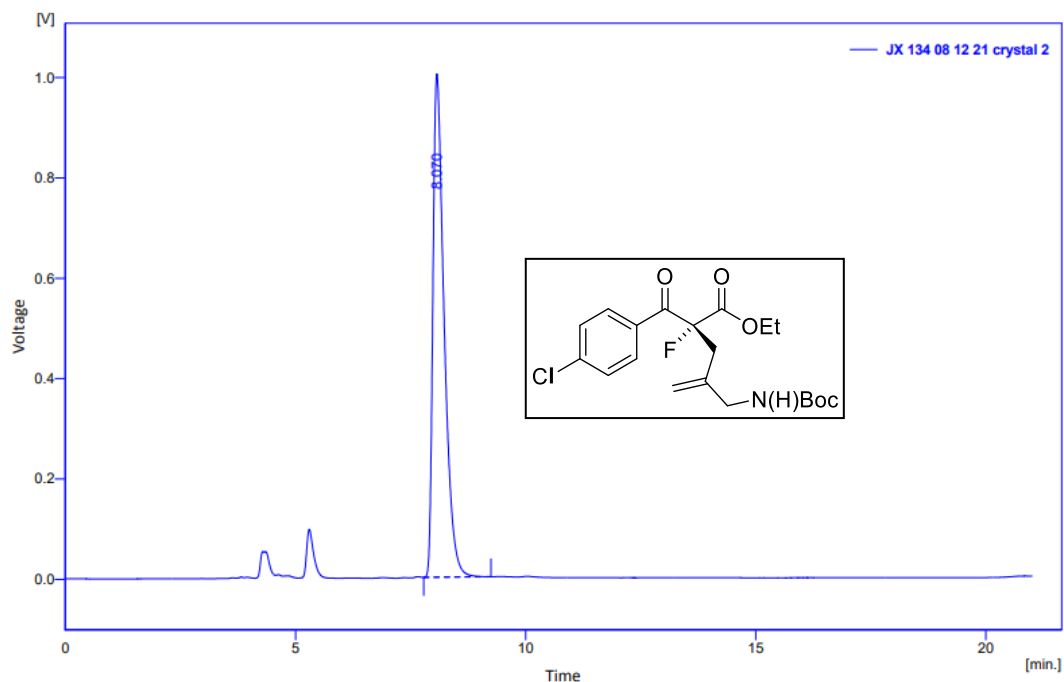
Result Table - Calculation Method Uncal

	Reten. Time [min]	Area [mV.s]	Height [mV]	Area [%]	Height [%]	W05 [min]
1	8.070	17049.277	1003.211	100.0	100.0	0.26
	Total	17049.277	1003.211	100.0	100.0	
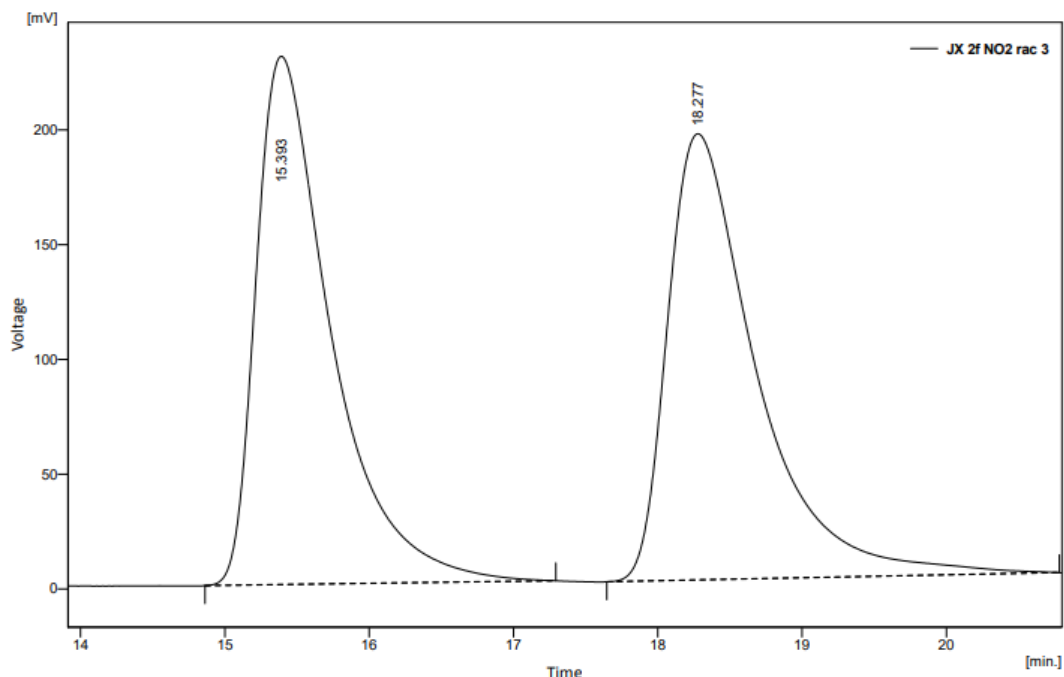
160

	Reten. Time [min]	Area [mV.s]	Height [mV]	Area [%]	Height [%]	W05 [min]
1	15.393	8322.978	230.171	49.9	54.2	0.53
2	18.277	8348.458	194.408	50.1	45.8	0.62
	Total	16671.436	424.580	100.0	100.0	
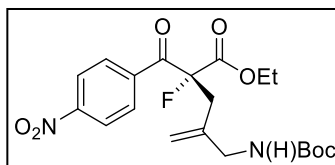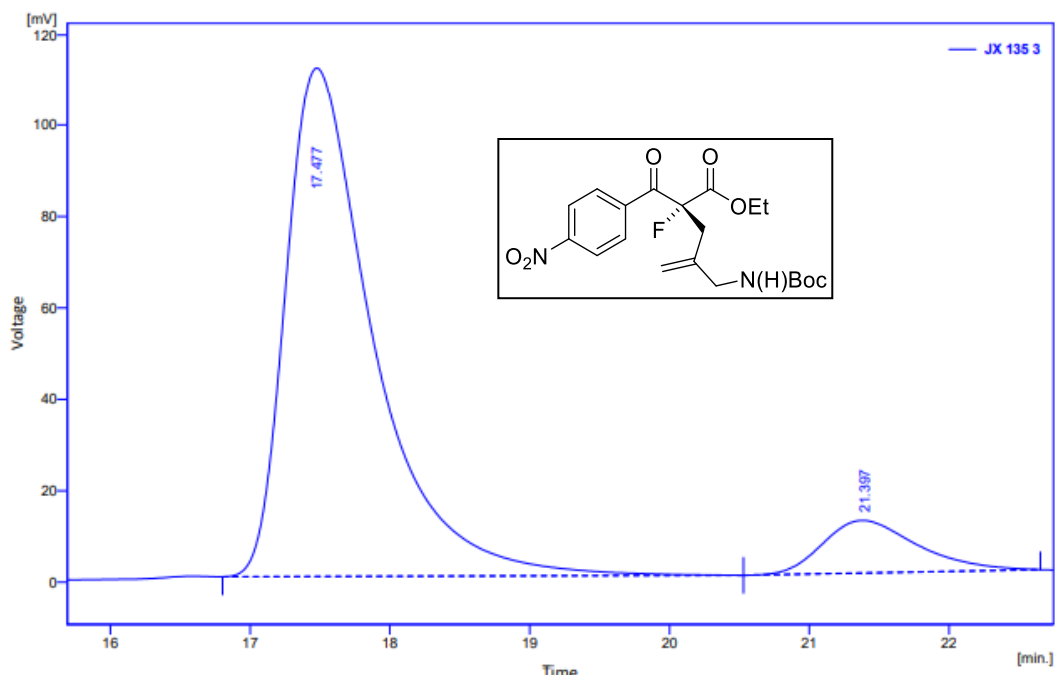
	Reten. Time [min]	Area [mV.s]	Height [mV]	Area [%]	Height [%]	W05 [min]
1	17.477	4851.648	111.547	90.0	90.7	0.62
2	21.397	541.185	11.495	10.0	9.3	0.73
	Total	5392.833	123.042	100.0	100.0	
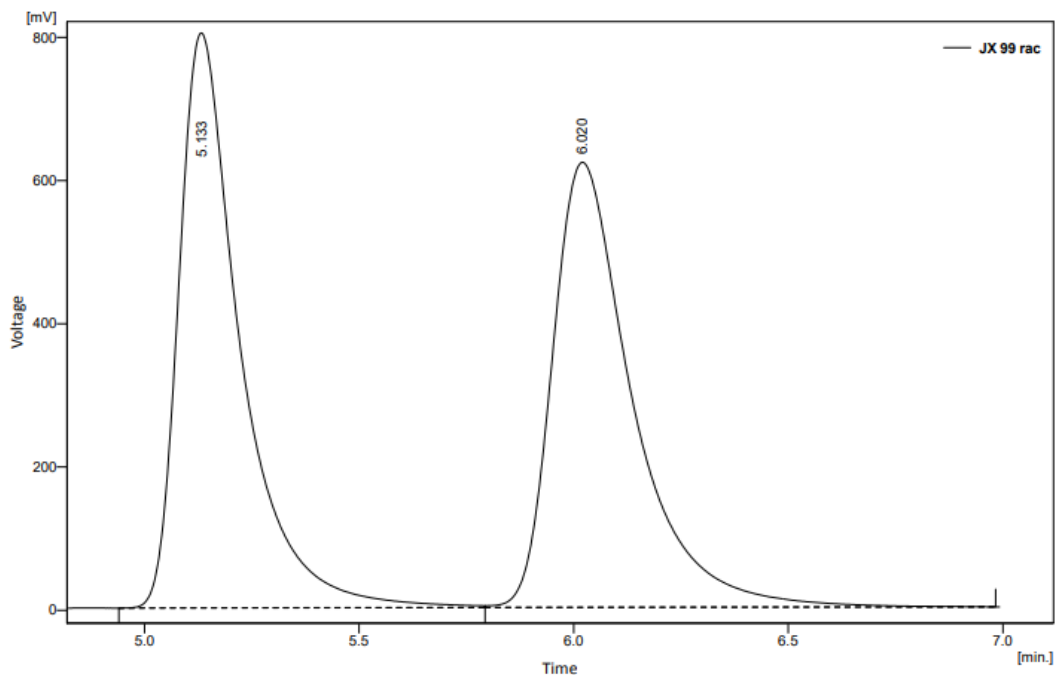
Result Table - Calculation Method Uncal

	Reten. Time [min]	Area [mV.s]	Height [mV]	Area [%]	Height [%]	W05 [min]
1	5.133	8032.259	803.050	49.9	56.4	0.14
2	6.020	8065.111	621.689	50.1	43.6	0.19
	Total	16097.371	1424.739	100.0	100.0	
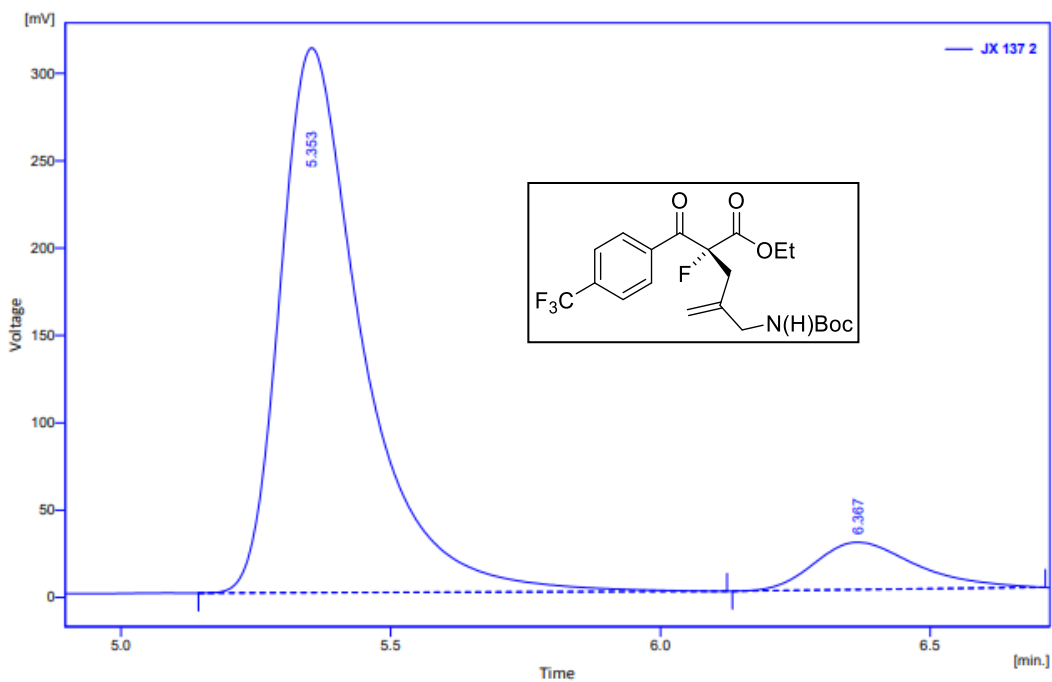
Result Table - Calculation Method Uncal

	Reten. Time [min]	Area [mV.s]	Height [mV]	Area [%]	Height [%]	W05 [min]
1	5.353	3315.628	311.866	90.3	92.0	0.15
2	6.367	356.404	27.152	9.7	8.0	0.20
	Total	3672.032	339.018	100.0	100.0	
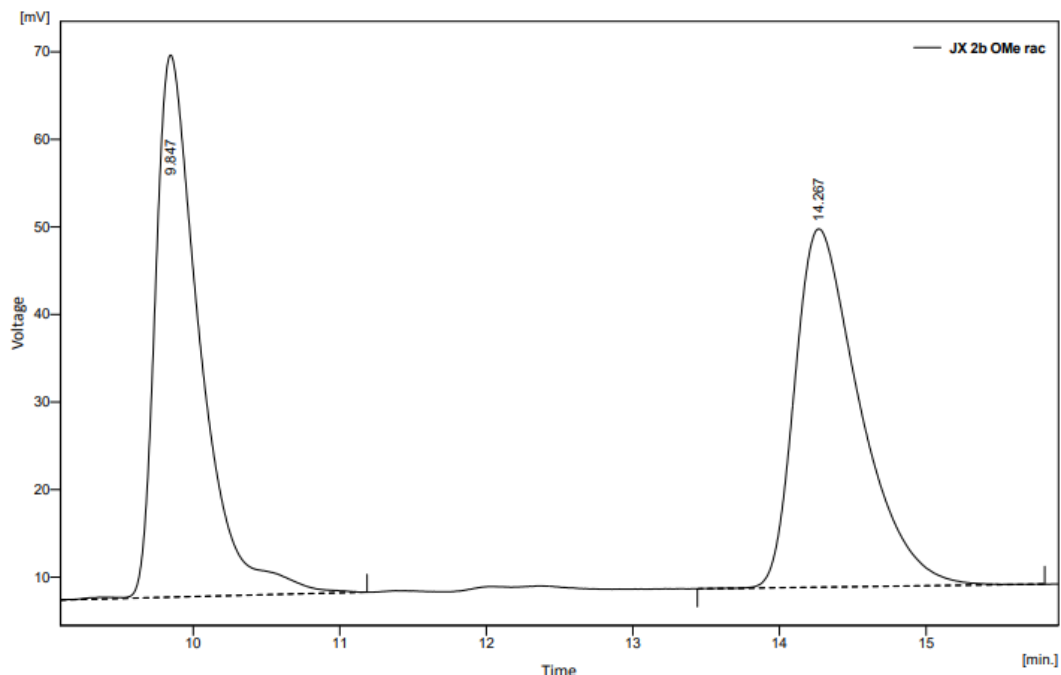
Result Table - Calculation Method Uncal

	Reten. Time [min]	Area [mV.s]	Height [mV]	Area [%]	Height [%]	W05 [min]
1	9.847	1298.282	61.911	50.8	60.2	0.30
2	14.267	1258.822	40.913	49.2	39.8	0.47
	Total	2557.104	102.824	100.0	100.0	
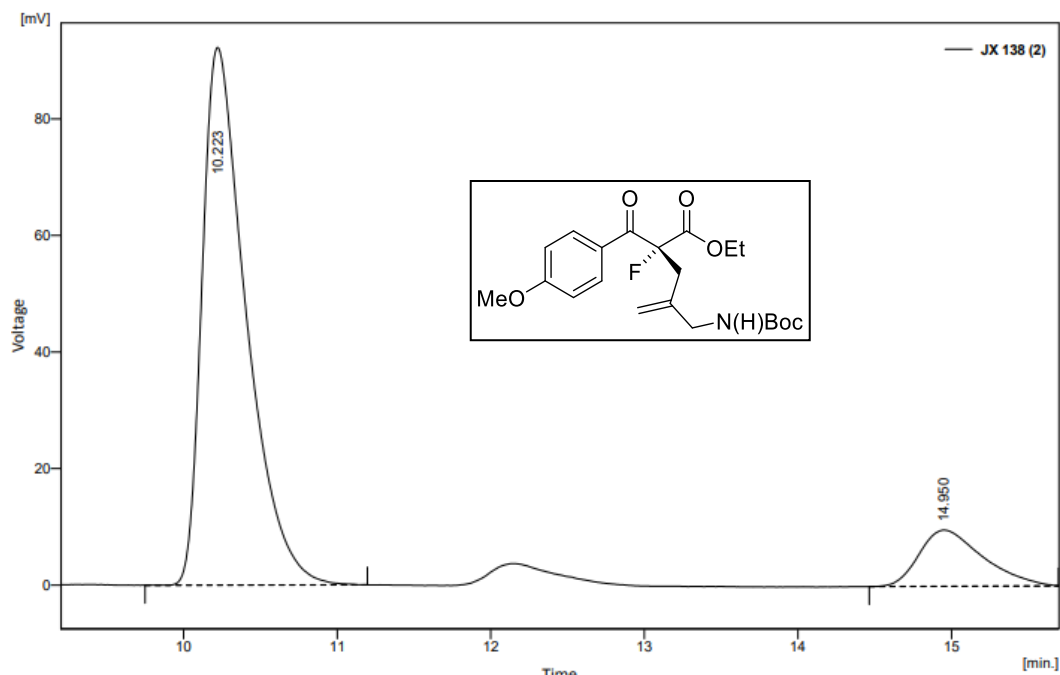
Result Table - Calculation Method Uncal

	Reten. Time [min]	Area [mV.s]	Height [mV]	Area [%]	Height [%]	W05 [min]
1	10.223	1837.814	92.243	86.9	90.5	0.30
2	14.950	278.039	9.658	13.1	9.5	0.45
	Total	2115.853	101.902	100.0	100.0	
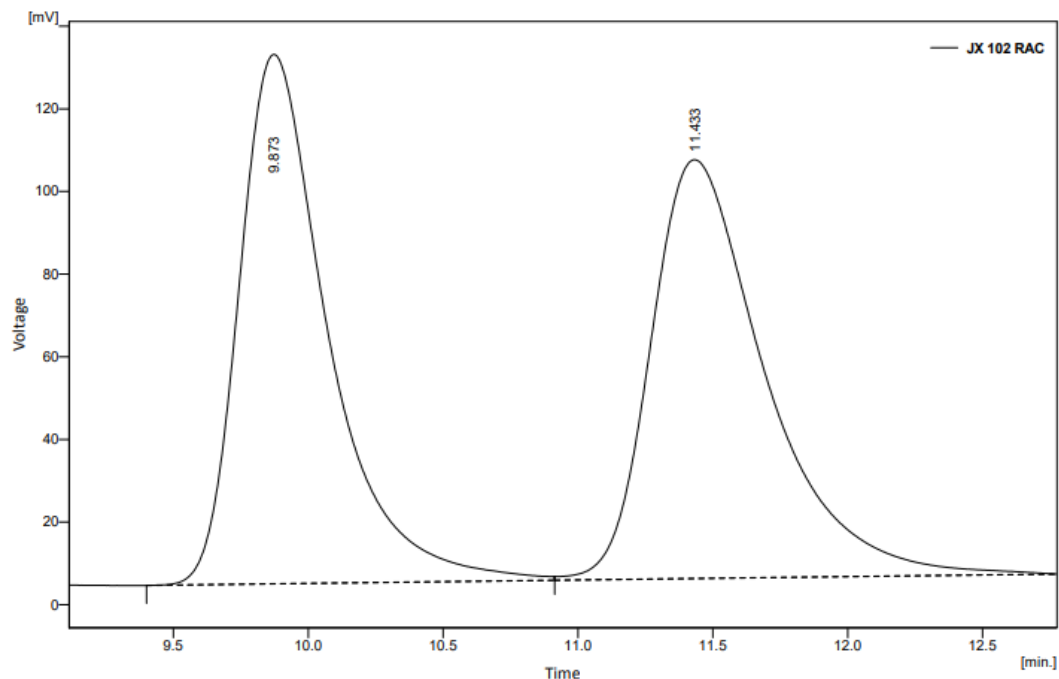
163

JX 102 RAC

Result Table - Calculation Method Uncal

	Reten. Time [min]	Area [mV.s]	Height [mV]	Area [%]	Height [%]	W05 [min]
1	9.873	2942.053	128.104	49.5	55.8	0.34
2	11.433	2996.364	101.368	50.5	44.2	0.44
	Total	5938.417	229.472	100.0	100.0	
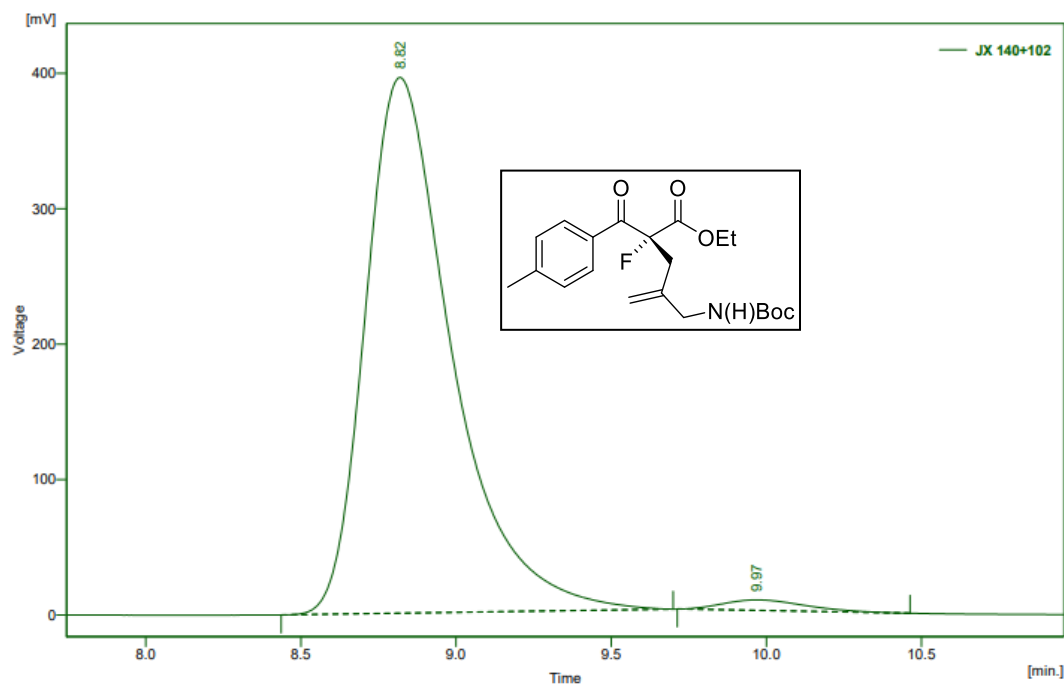
JX 140+102

Result Table - Calculation Method Uncal

	Reten. Time [min]	Area [mV.s]	Height [mV]	Area [%]	Height [%]	W05 [min]
1	8.820	7687.398	395.576	98.1	98.1	0.29
2	9.970	146.507	7.835	1.9	1.9	0.29
	Total	7833.905	403.411	100.0	100.0	
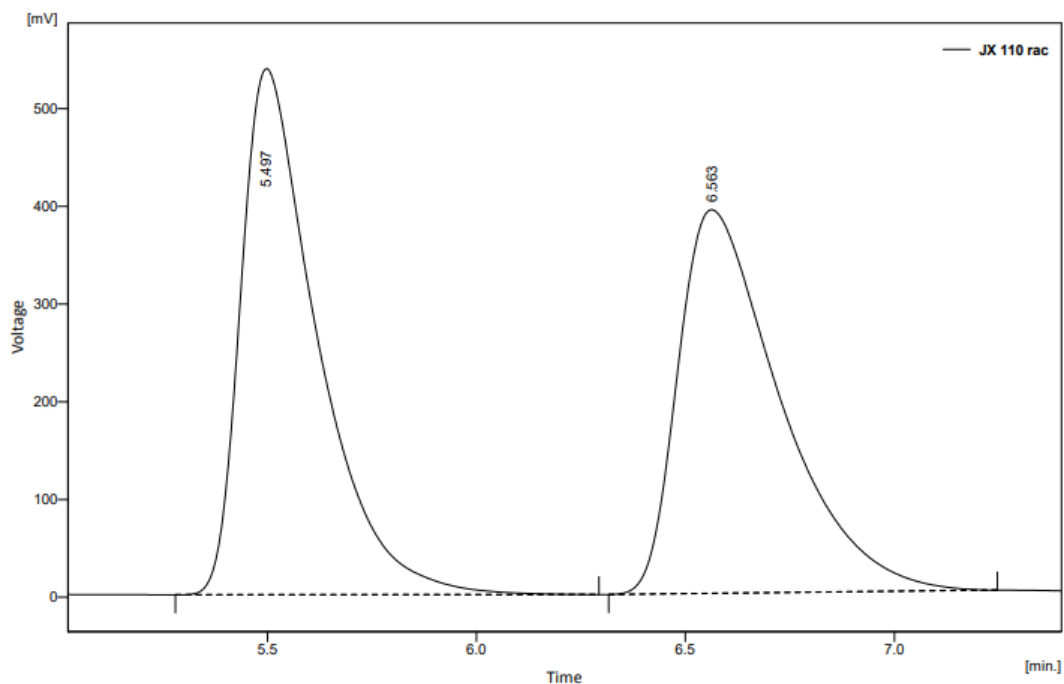
164

Result Table - Calculation Method Uncal

	Reten. Time [min]	Area [mV.s]	Height [mV]	Area [%]	Height [%]	W05 [min]
1	5.497	6858.209	538.620	50.7	57.8	0.19
2	6.563	6667.813	392.723	49.3	42.2	0.26
	Total	13526.022	931.343	100.0	100.0	
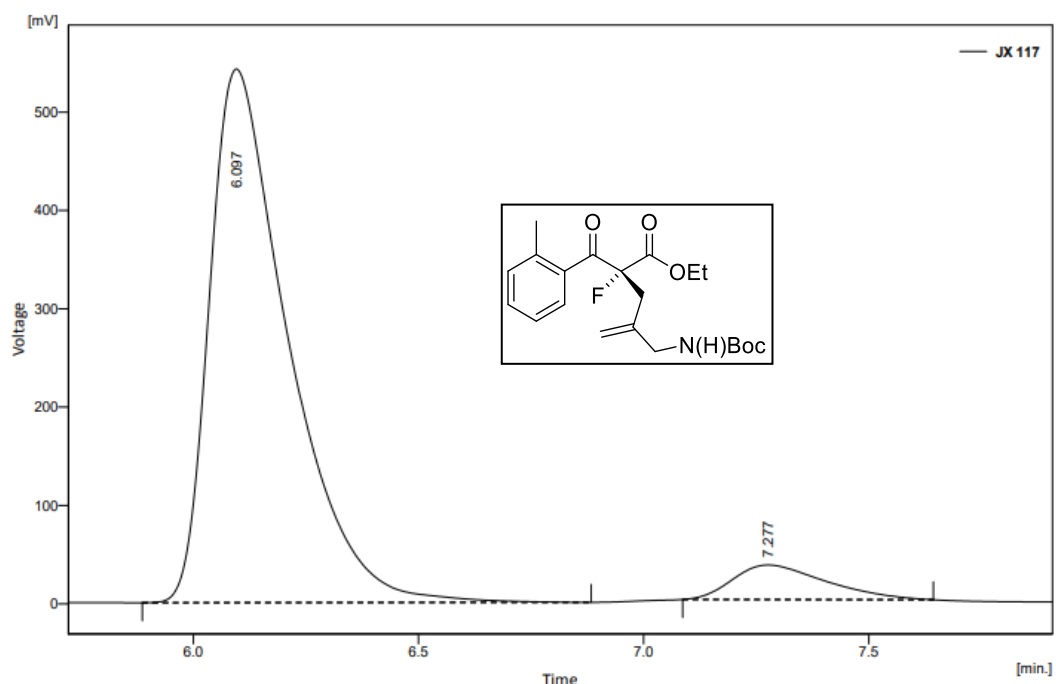
Result Table - Calculation Method Uncal

	Reten. Time [min]	Area [mV.s]	Height [mV]	Area [%]	Height [%]	W05 [min]
1	6.097	6574.472	542.660	92.9	93.9	0.18
2	7.277	504.736	35.129	7.1	6.1	0.23
	Total	7079.208	577.789	100.0	100.0	
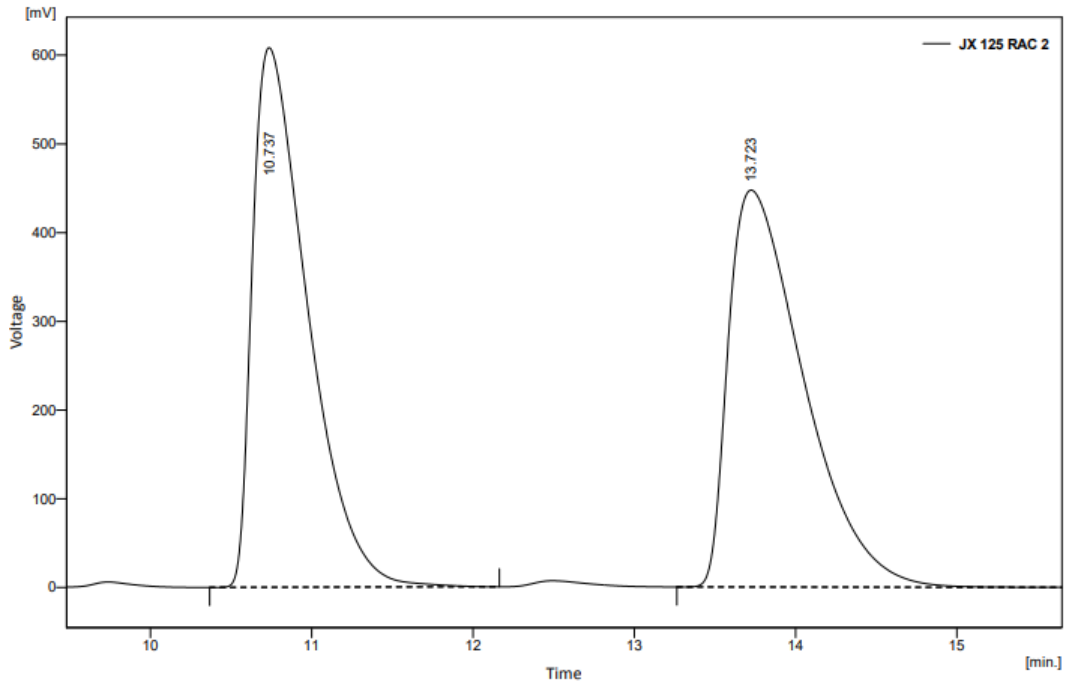
Result Table - Calculation Method Uncal

	Reten. Time [min]	Area [mV.s]	Height [mV]	Area [%]	Height [%]	W05 [min]
1	10.737	14496.283	608.395	49.9	57.6	0.37
2	13.723	14536.514	447.575	50.1	42.4	0.51
	Total	29032.797	1055.970	100.0	100.0	
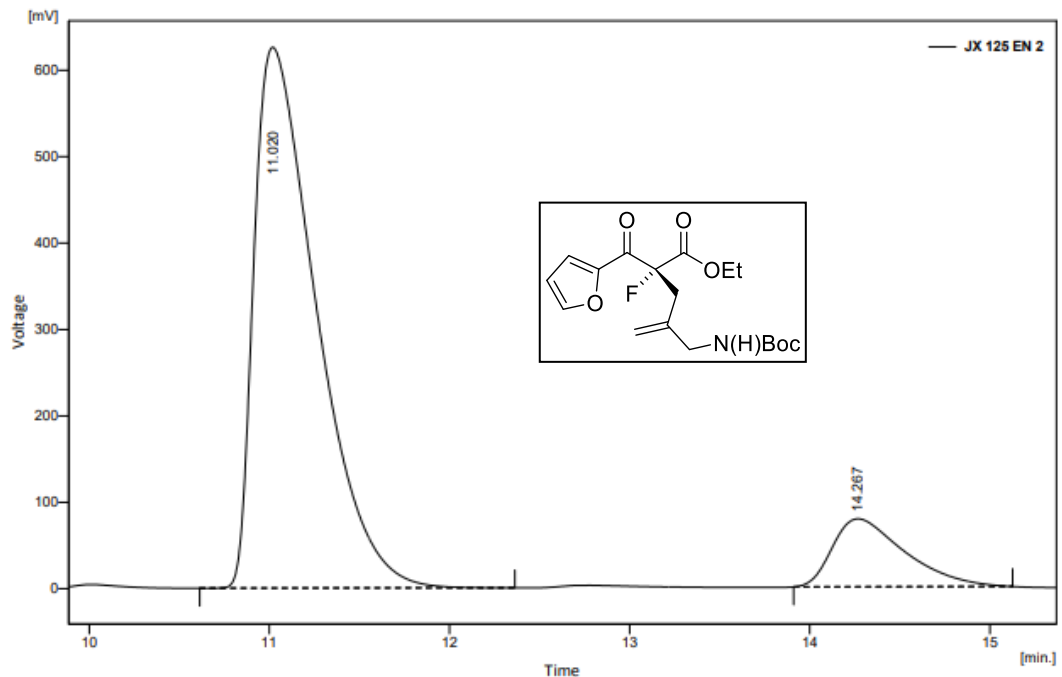
Result Table - Calculation Method Uncal

	Reten. Time [min]	Area [mV.s]	Height [mV]	Area [%]	Height [%]	W05 [min]
1	11.020	15007.810	625.905	87.3	88.8	0.37
2	14.267	2189.724	78.705	12.7	11.2	0.43
	Total	17197.533	704.610	100.0	100.0	
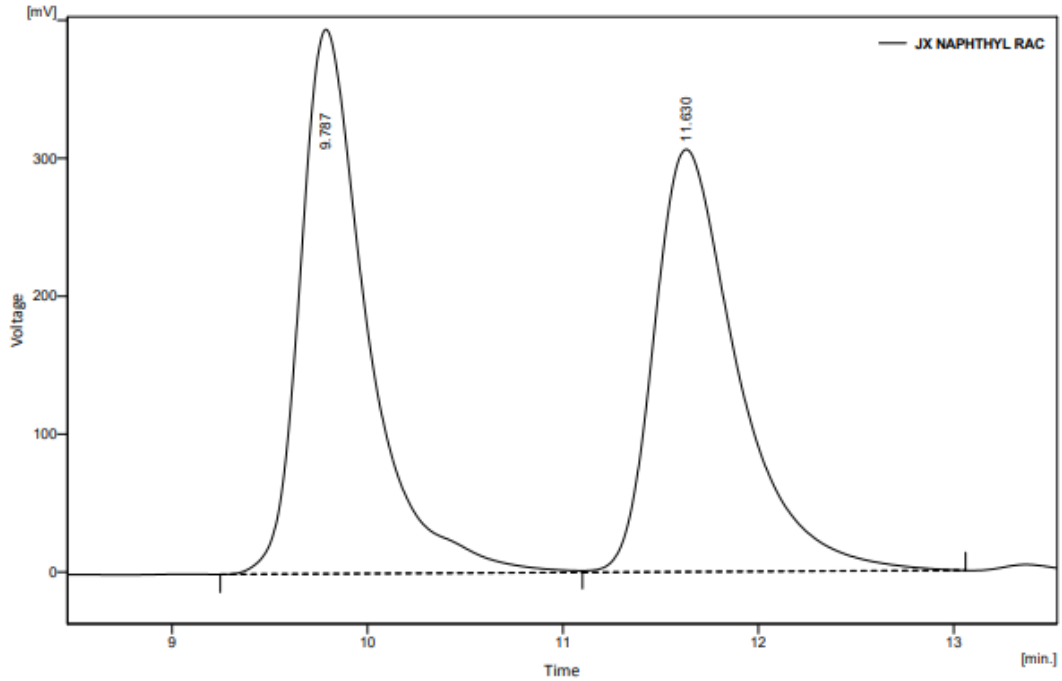
Result Table - Calculation Method Uncal

	Reten. Time [min]	Area [mV.s]	Height [mV]	Area [%]	Height [%]	W05 [min]
1	9.787	9433.867	394.619	50.9	56.3	0.34
2	11.630	9117.082	306.304	49.1	43.7	0.44
	Total	18550.949	700.923	100.0	100.0	
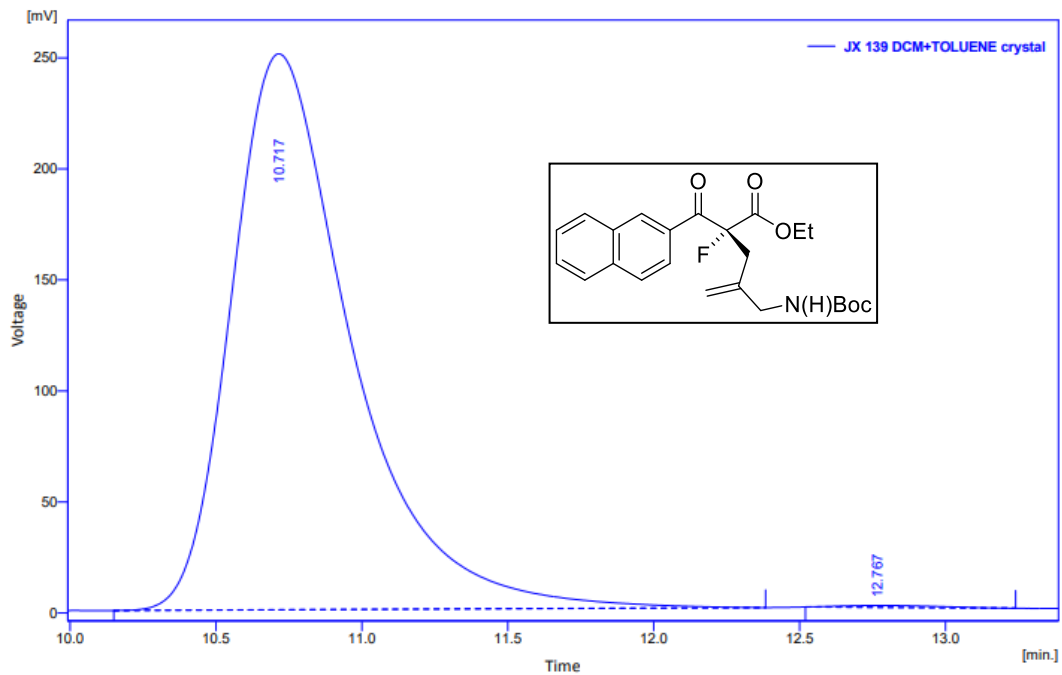
Result Table - Calculation Method Uncal

	Reten. Time [min]	Area [mV.s]	Height [mV]	Area [%]	Height [%]	W05 [min]
1	10.717	7203.743	250.347	99.7	99.6	0.42
2	12.767	21.833	0.901	0.3	0.4	0.38
	Total	7225.576	251.248	100.0	100.0	
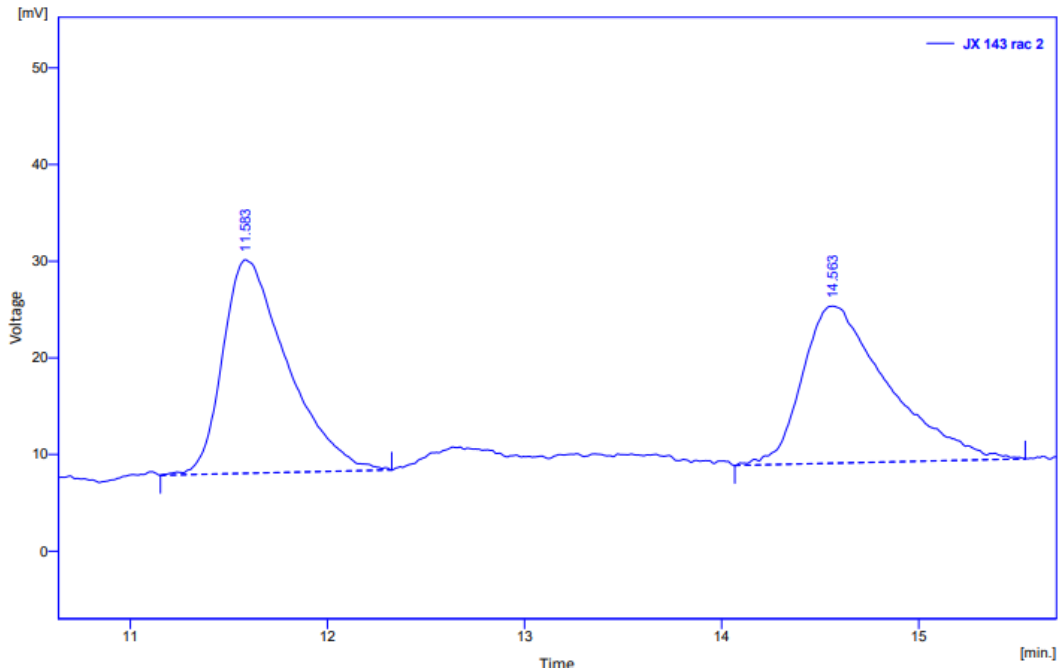
167

Result Table - Calculation Method Uncal

	Reten. Time [min]	Area [mV.s]	Height [mV]	Area [%]	Height [%]	W05 [min]
1	11.583	504.597	22.112	50.6	57.6	0.35
2	14.563	493.554	16.258	49.4	42.4	0.45
	Total	998.152	38.370	100.0	100.0	
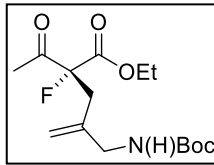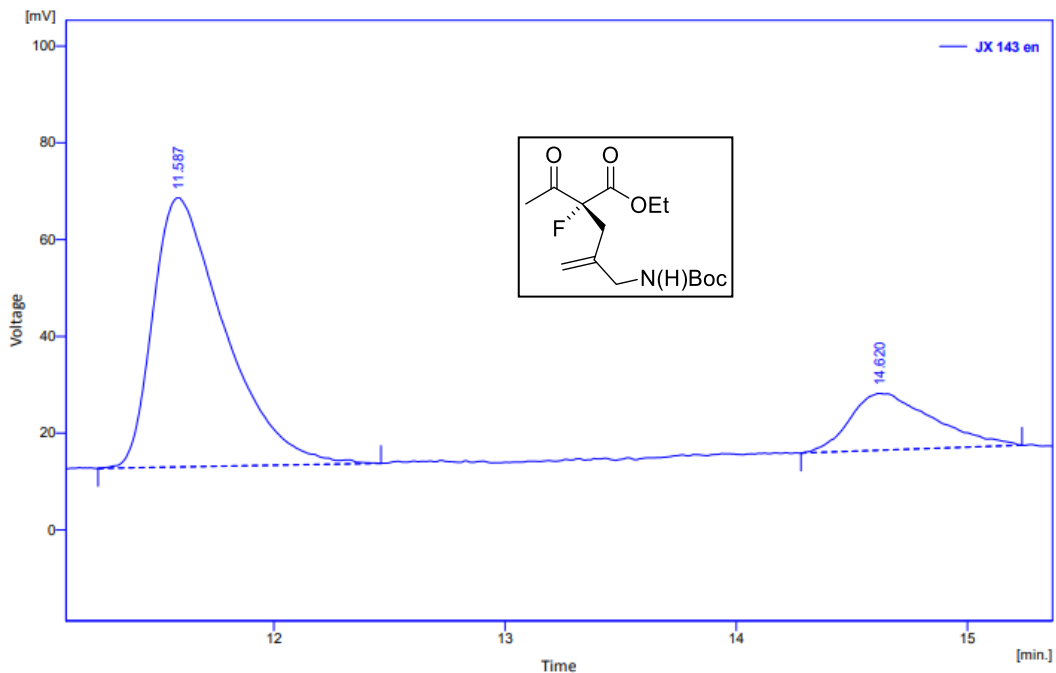
Result Table - Calculation Method Uncal

	Reten. Time [min]	Area [mV.s]	Height [mV]	Area [%]	Height [%]	W05 [min]
1	11.587	1205.905	55.701	80.3	82.5	0.33
2	14.620	295.157	11.775	19.7	17.5	0.40
	Total	1501.062	67.476	100.0	100.0	
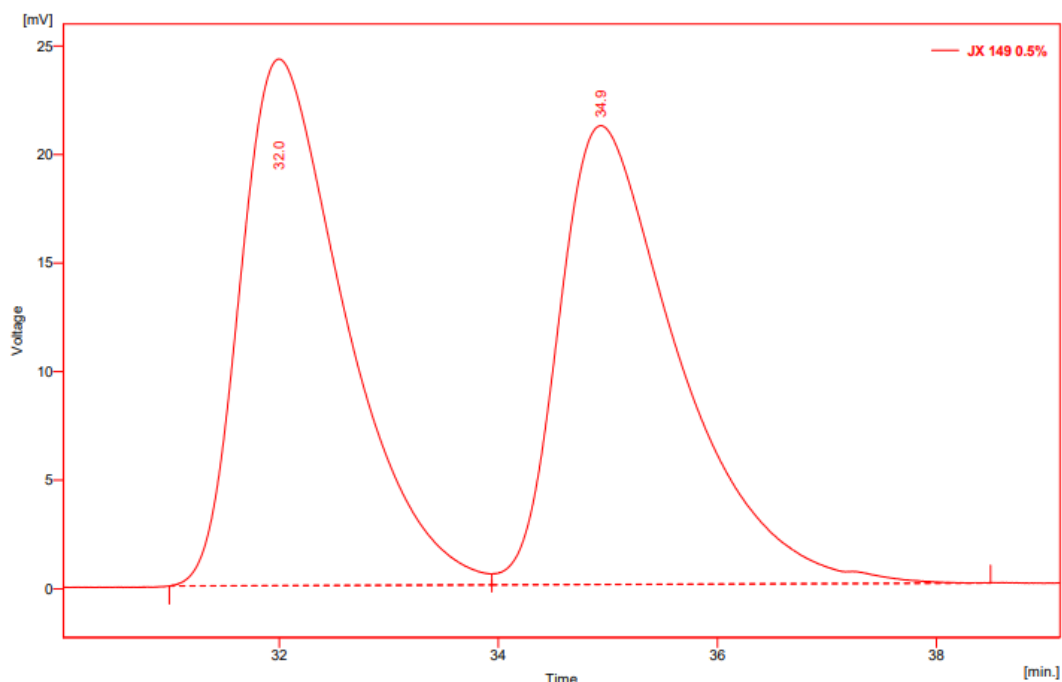
168

Result Table - Calculation Method Uncal

	Reten. Time [min]	Area [mV.s]	Height [mV]	Area [%]	Height [%]	W05 [min]
1	32.000	1615.333	24.253	50.0	53.4	1.01
2	34.937	1612.580	21.137	50.0	46.6	1.13
	Total	3227.913	45.390	100.0	100.0	
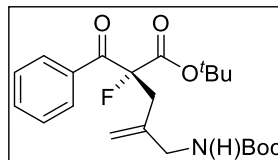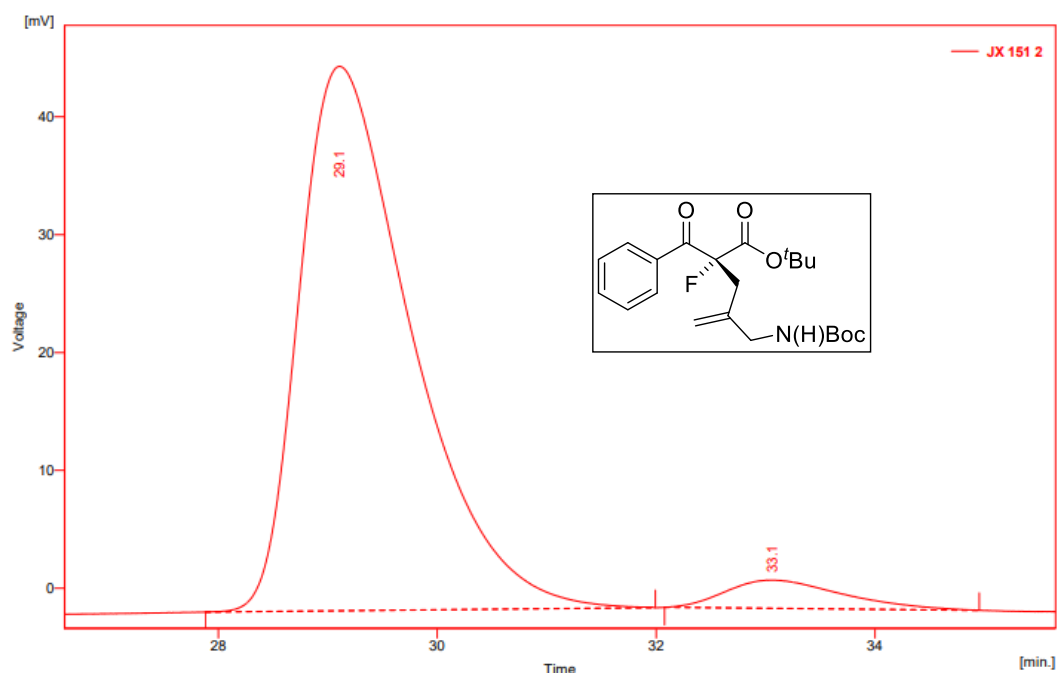
Result Table - Calculation Method Uncal

	Reten. Time [min]	Area [mV.s]	Height [mV]	Area [%]	Height [%]	W05 [min]
1	29.107	3290.714	46.206	94.9	95.1	1.09
2	33.060	178.537	2.403	5.1	4.9	1.14
	Total	3469.251	48.609	100.0	100.0	
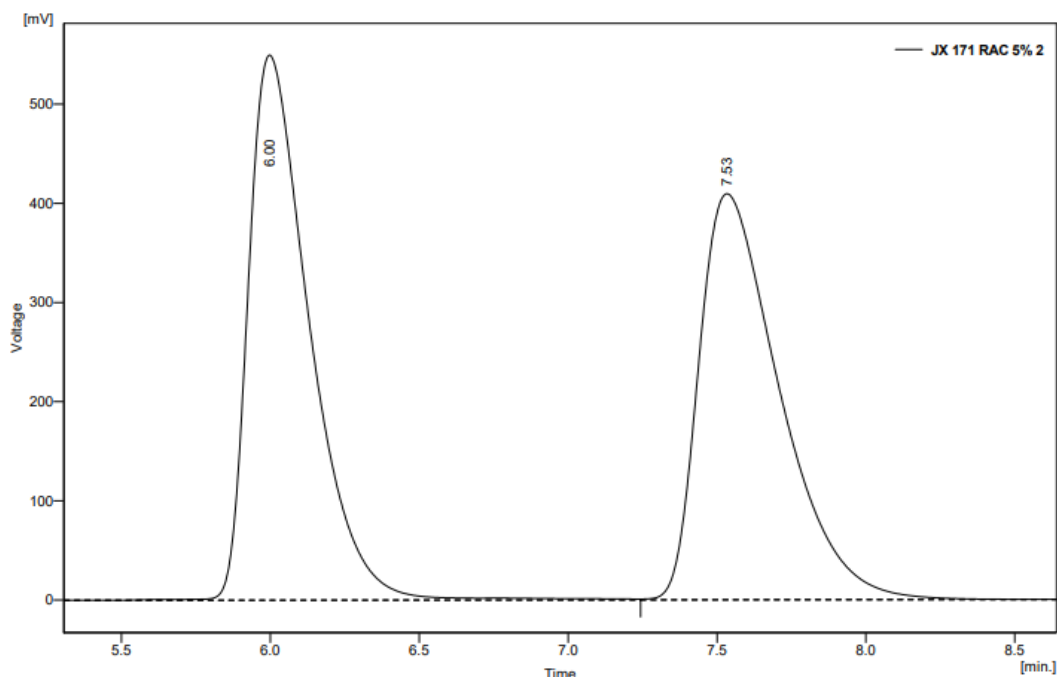
169

Result Table - Calculation Method Uncal

	Reten. Time [min]	Area [mV.s]	Height [mV]	Area [%]	Height [%]	W05 [min]
1	5.997	7847.601	549.837	50.4	57.3	0.22
2	7.533	7711.772	409.710	49.6	42.7	0.29
	Total	15559.373	959.547	100.0	100.0	
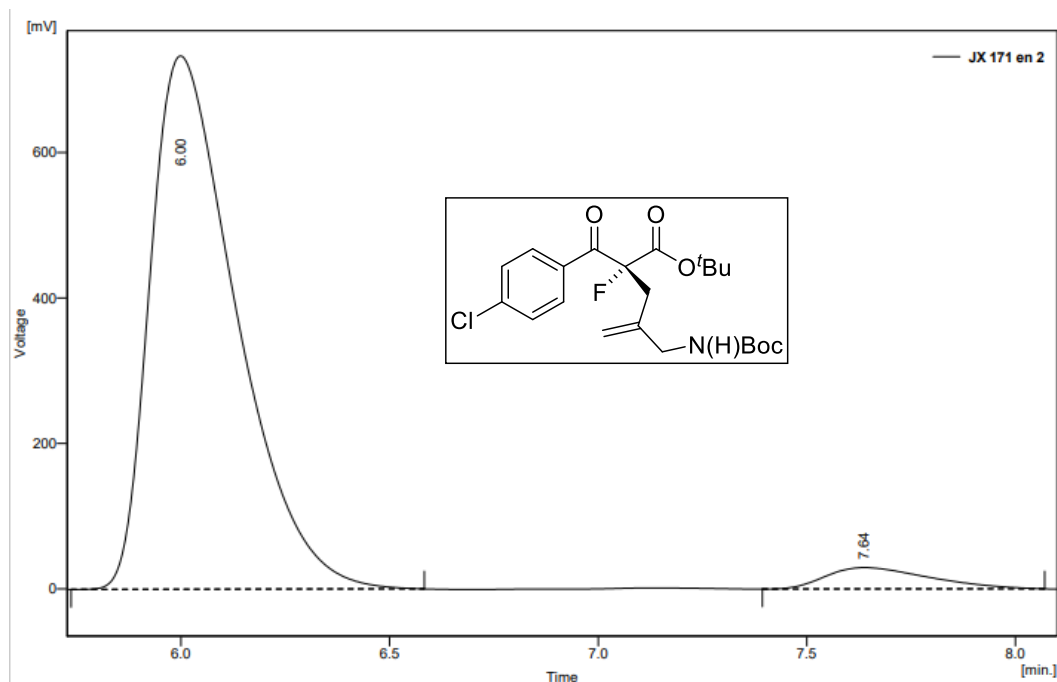
Result Table - Calculation Method Uncal

	Reten. Time [min]	Area [mV.s]	Height [mV]	Area [%]	Height [%]	W05 [min]
1	6.000	10542.544	733.410	95.4	96.1	0.22
2	7.637	509.796	29.493	4.6	3.9	0.28
	Total	11052.340	762.903	100.0	100.0	
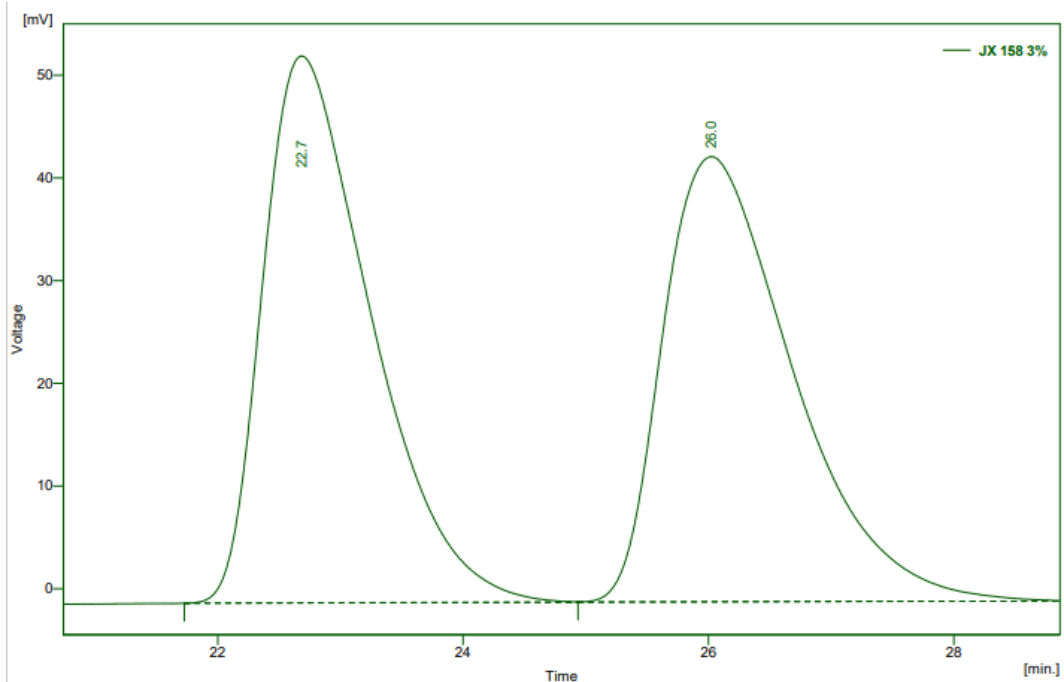
Result Table - Calculation Method Uncal

	Reten. Time [min]	Area [mV.s]	Height [mV]	Area [%]	Height [%]	W05 [min]
1	22.683	3264.334	53.264	50.5	55.1	0.95
2	26.023	3198.249	43.355	49.5	44.9	1.14
	Total	6462.583	96.619	100.0	100.0	
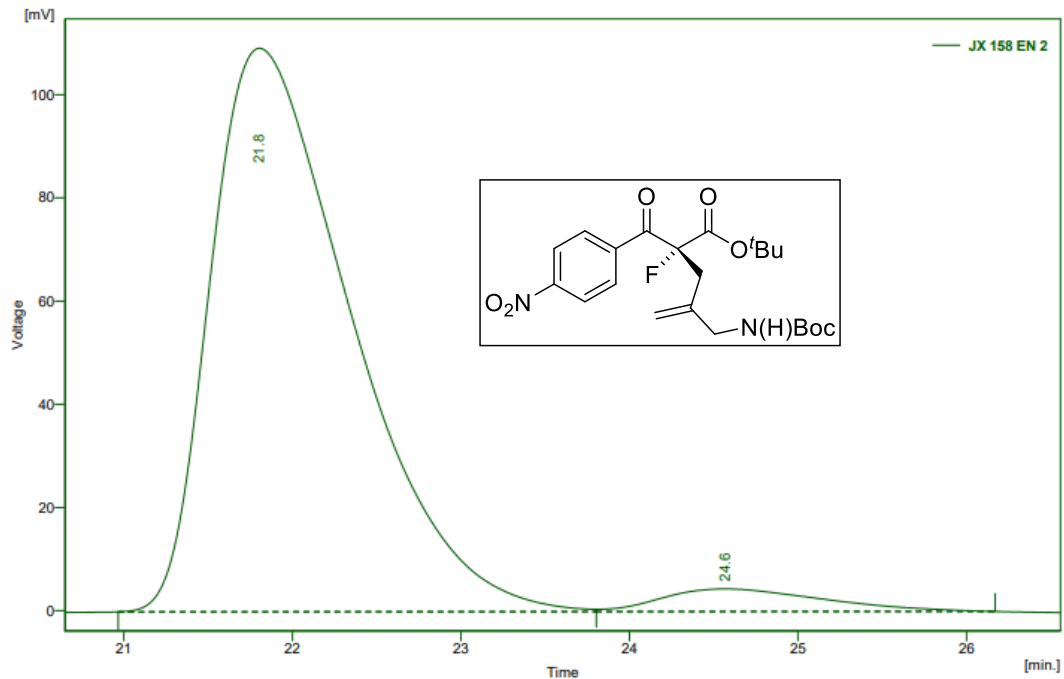
Result Table - Calculation Method Uncal

	Reten. Time [min]	Area [mV.s]	Height [mV]	Area [%]	Height [%]	W05 [min]
1	21.803	6332.865	109.243	95.6	96.1	0.90
2	24.567	294.796	4.416	4.4	3.9	1.06
	Total	6627.661	113.659	100.0	100.0	
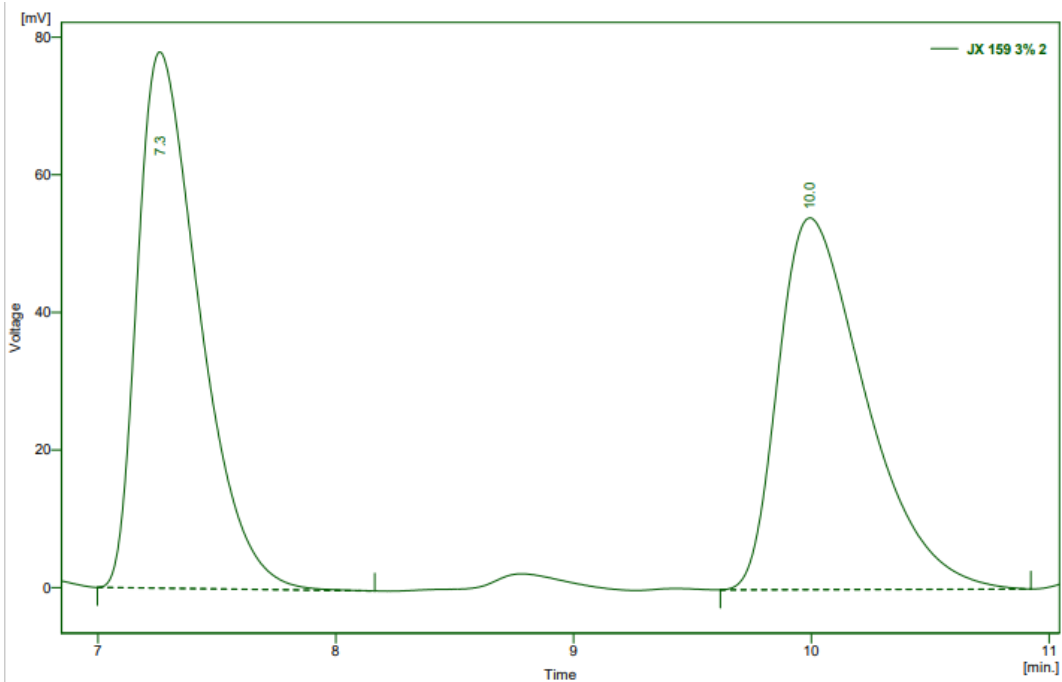
171

JX 159 3% 2

Result Table - Calculation Method Uncal

	Reten. Time [min]	Area [mV.s]	Height [mV]	Area [%]	Height [%]	W05 [min]
1	7.260	1408.234	77.951	50.5	59.1	0.28
2	9.993	1380.580	54.030	49.5	40.9	0.40
Total		2788.813	131.980	100.0	100.0	
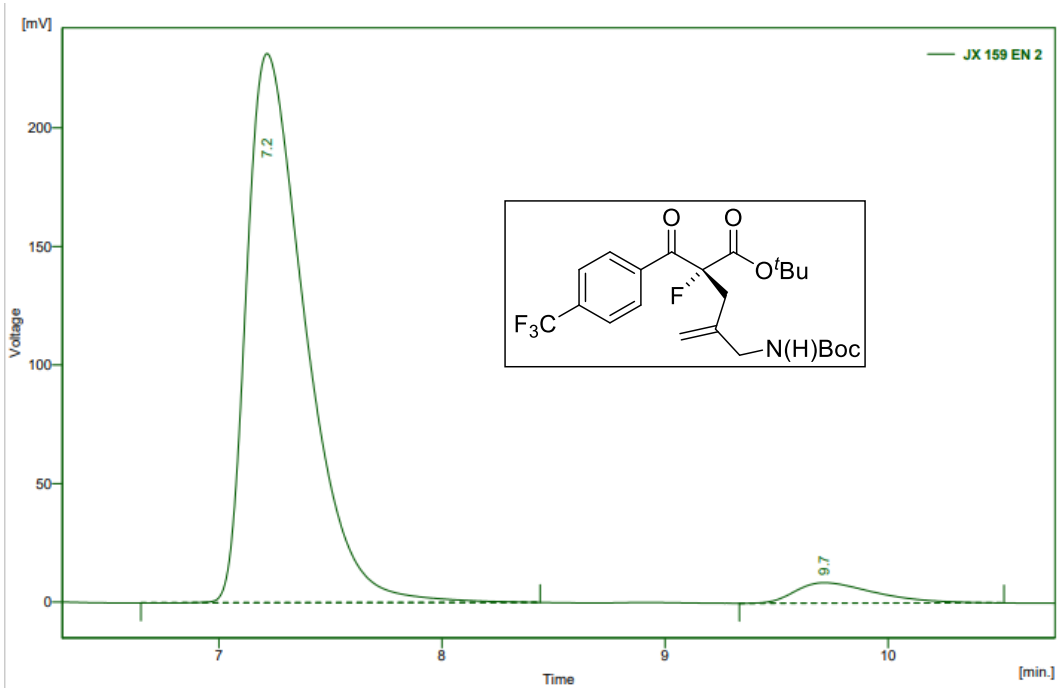
JX 159 EN 2

Result Table - Calculation Method Uncal

	Reten. Time [min]	Area [mV.s]	Height [mV]	Area [%]	Height [%]	W05 [min]
1	7.217	4237.319	231.637	95.2	96.4	0.28
2	9.713	215.174	8.645	4.8	3.6	0.39
Total		4452.493	240.282	100.0	100.0	
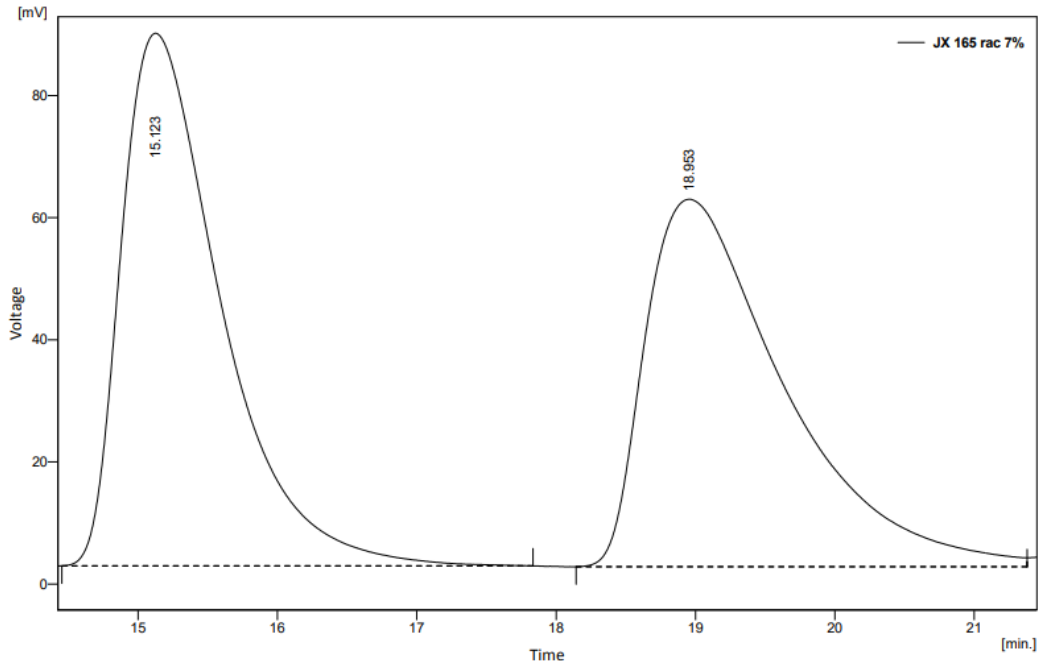
172

JX 165 rac 7%

Result Table - Calculation Method Uncal

	Reten. Time [min]	Area [mV.s]	Height [mV]	Area [%]	Height [%]	W05 [min]
1	15.123	4337.351	87.223	50.9	59.2	0.74
2	18.953	4178.458	60.180	49.1	40.8	1.04
Total		8515.810	147.403	100.0	100.0	
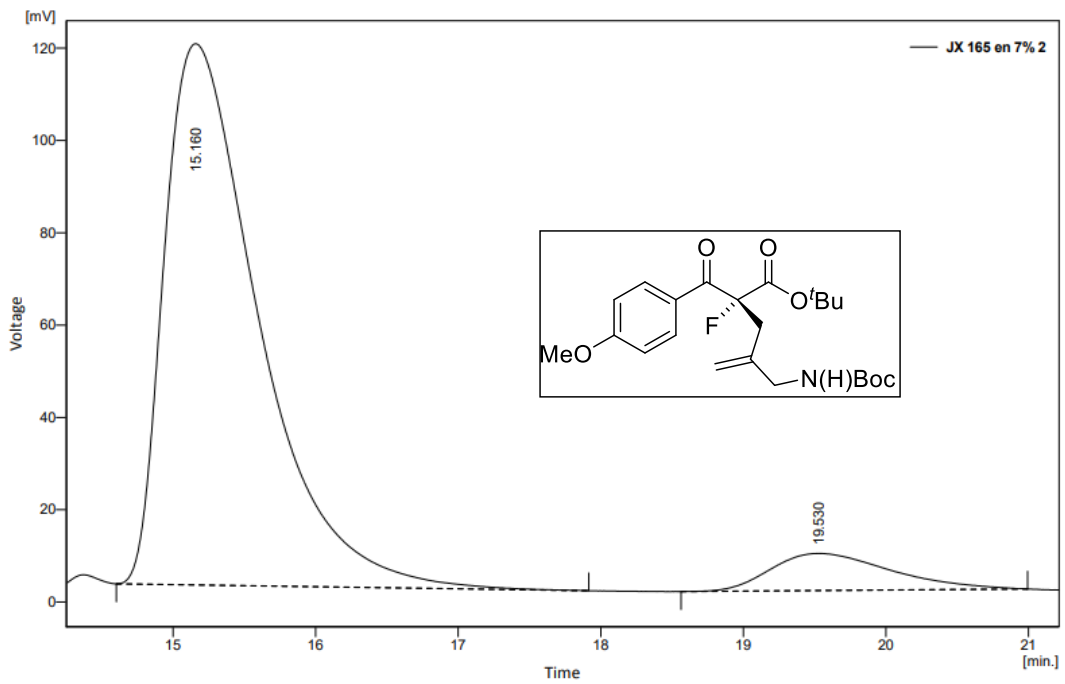
JX 165 en 7% 2

Result Table - Calculation Method Uncal

	Reten. Time [min]	Area [mV.s]	Height [mV]	Area [%]	Height [%]	W05 [min]
1	15.160	5392.299	117.261	92.0	93.6	0.69
2	19.530	471.202	8.045	8.0	6.4	0.92
Total		5863.501	125.306	100.0	100.0	
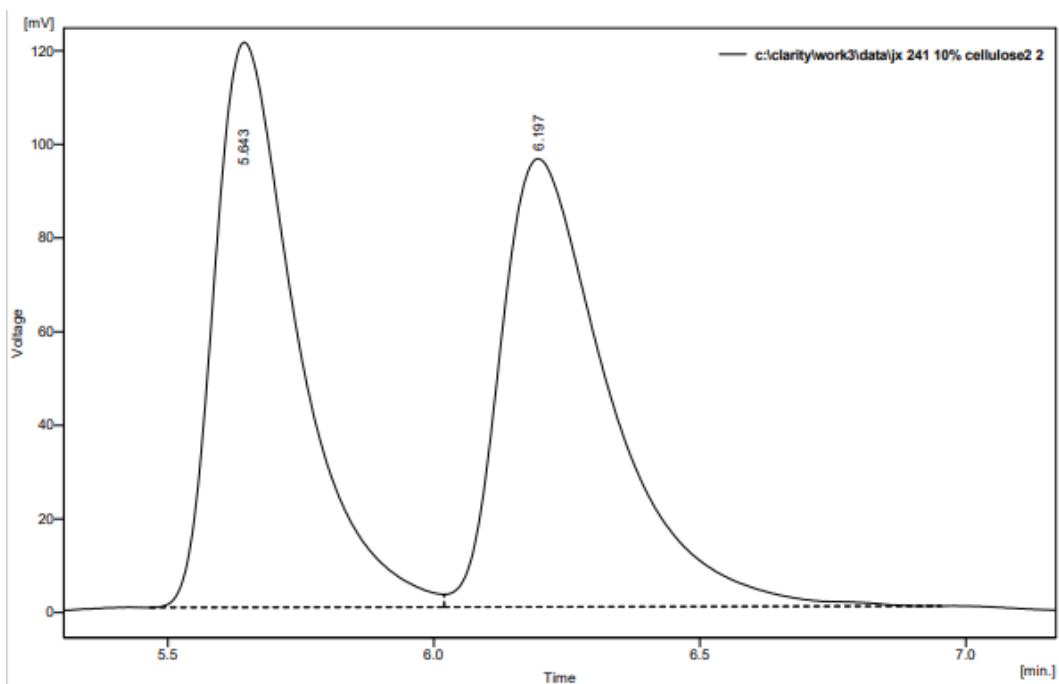
173

Result Table - Calculation Method Uncal

	Reten. Time [min]	Area [mV.s]	Height [mV]	Area [%]	Height [%]	W05 [min]
1	5.643	1647.220	150.948	49.2	55.8	0.16
2	6.197	1701.172	119.693	50.8	44.2	0.21
Total		3348.392	270.641	100.0	100.0	
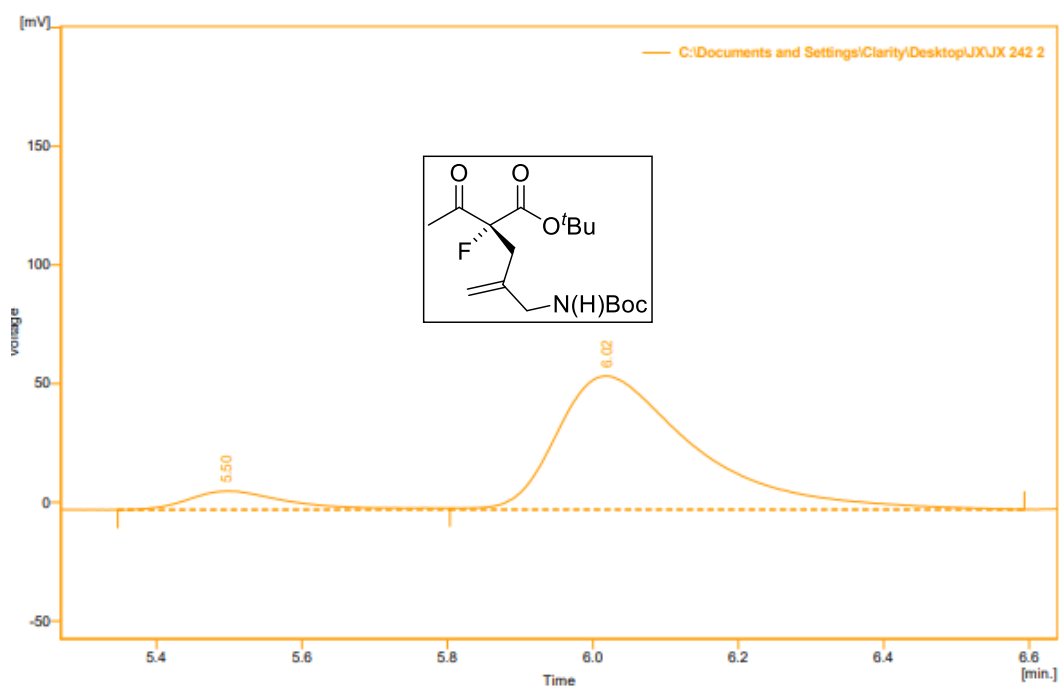
Result Table - Calculation Method Uncal

	Reten. Time [min]	Area [mV.s]	Height [mV]	Area [%]	Height [%]	W05 [min]
1	5.497	76.009	7.863	9.3	12.3	0.14
2	6.020	742.408	56.250	90.7	87.7	0.19
Total		818.417	64.114	100.0	100.0	
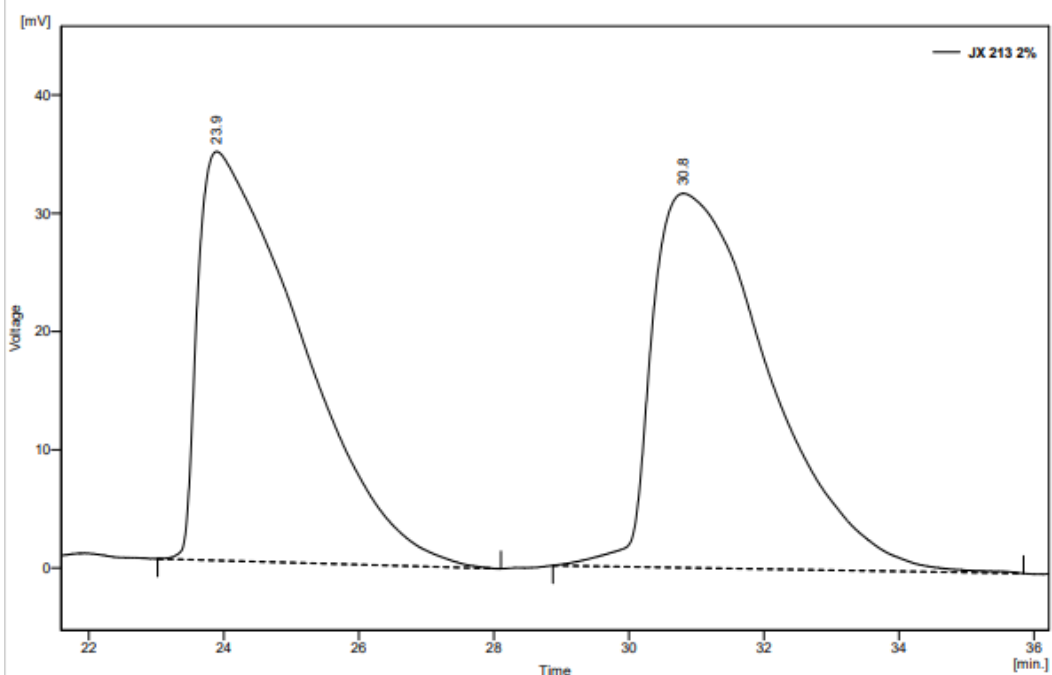
174

Result Table - Calculation Method Uncal

	Reten. Time [min]	Area [mV.s]	Height [mV]	Area [%]	Height [%]	W05 [min]
1	23.890	3678.455	34.598	49.1	52.2	1.68
2	30.800	3818.421	31.656	50.9	47.8	1.83
	Total	7496.876	66.255	100.0	100.0	
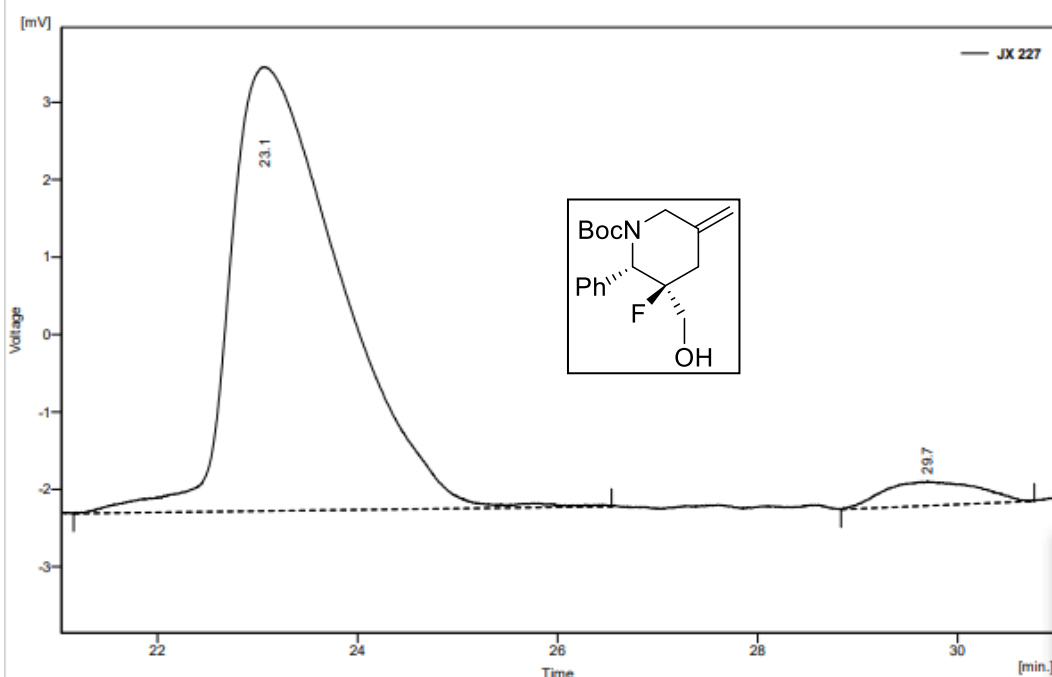
Result Table - Calculation Method Uncal

	Reten. Time [min]	Area [mV.s]	Height [mV]	Area [%]	Height [%]	W05 [min]
1	23.073	439.550	5.738	95.4	94.8	1.17
2	29.700	20.959	0.312	4.6	5.2	1.21
	Total	460.509	6.050	100.0	100.0	

175

	Reten. Time [min]	Area [mV.s]	Height [mV]	Area [%]	Height [%]	W05 [min]
1	11.917	4818.220	154.491	50.1	52.0	0.51
2	13.193	4794.399	142.393	49.9	48.0	0.54
	Total	9612.619	296.885	100.0	100.0	
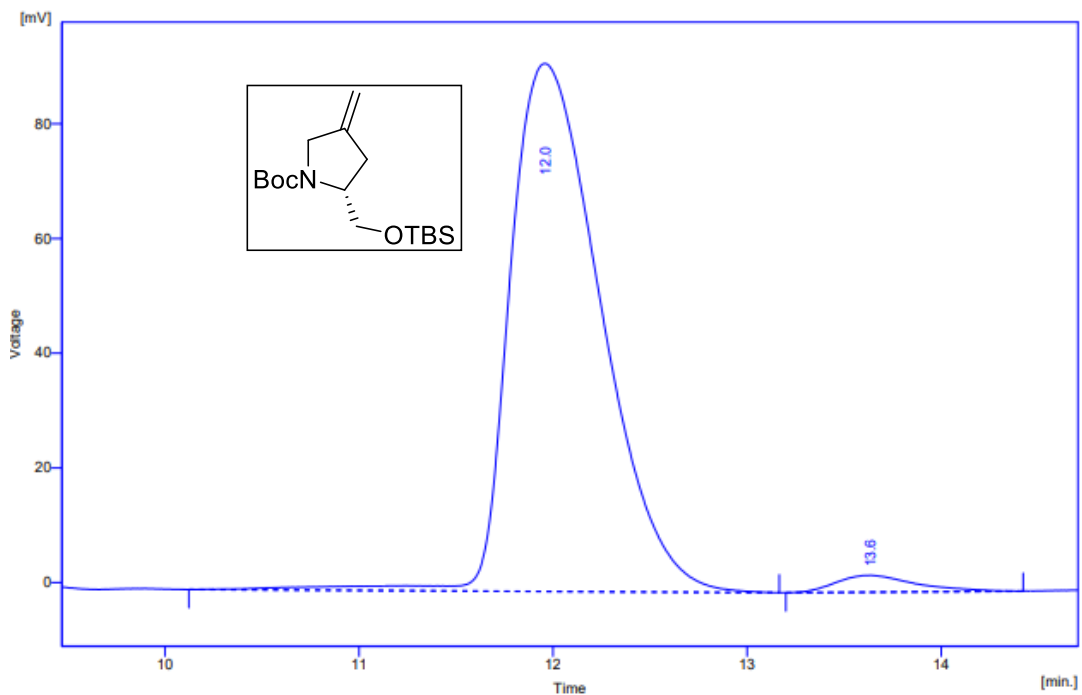
Result Table - Calculation Method Uncal

	Reten. Time [min]	Area [mV.s]	Height [mV]	Area [%]	Height [%]	W05 [min]
1	11.960	3000.966	92.031	97.3	96.9	0.51
2	13.637	84.261	2.952	2.7	3.1	0.43
	Total	3085.228	94.984	100.0	100.0	
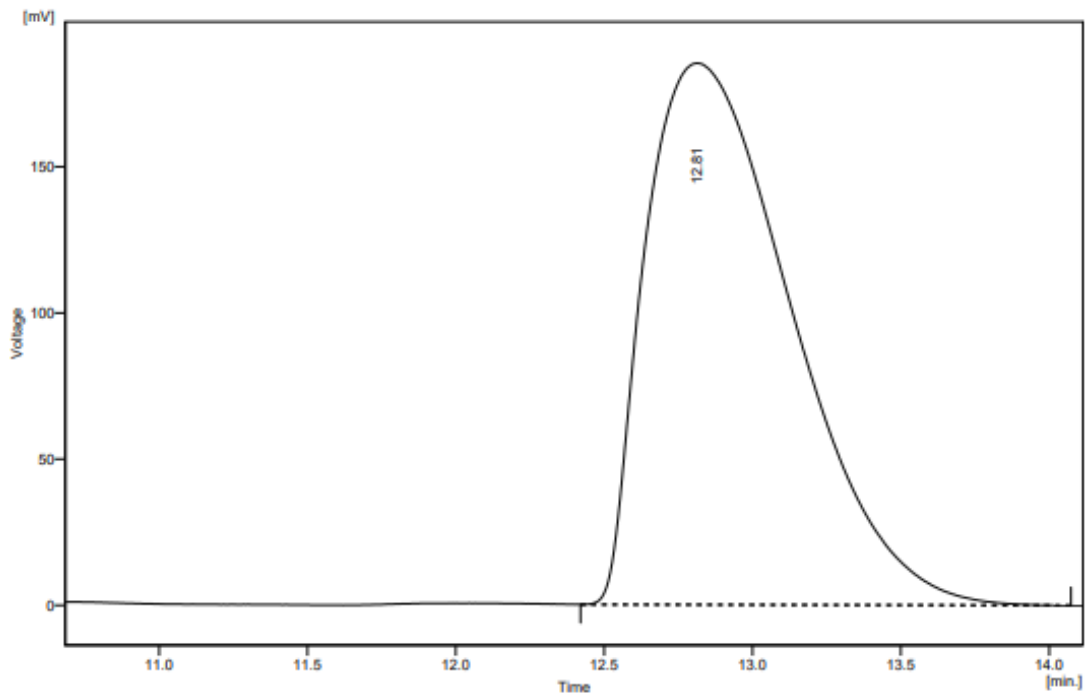
Result Table - Calculation Method Uncal

Commercial (*S*) isomer

	Reten. Time [min]	Area [mV.s]	Height [mV]	Area [%]	Height [%]	W05 [min]
1	12.813	6341.739	185.231	100.0	100.0	0.55
	Total	6341.739	185.231	100.0	100.0	

Mixture of commercial (S) isomer + **154**
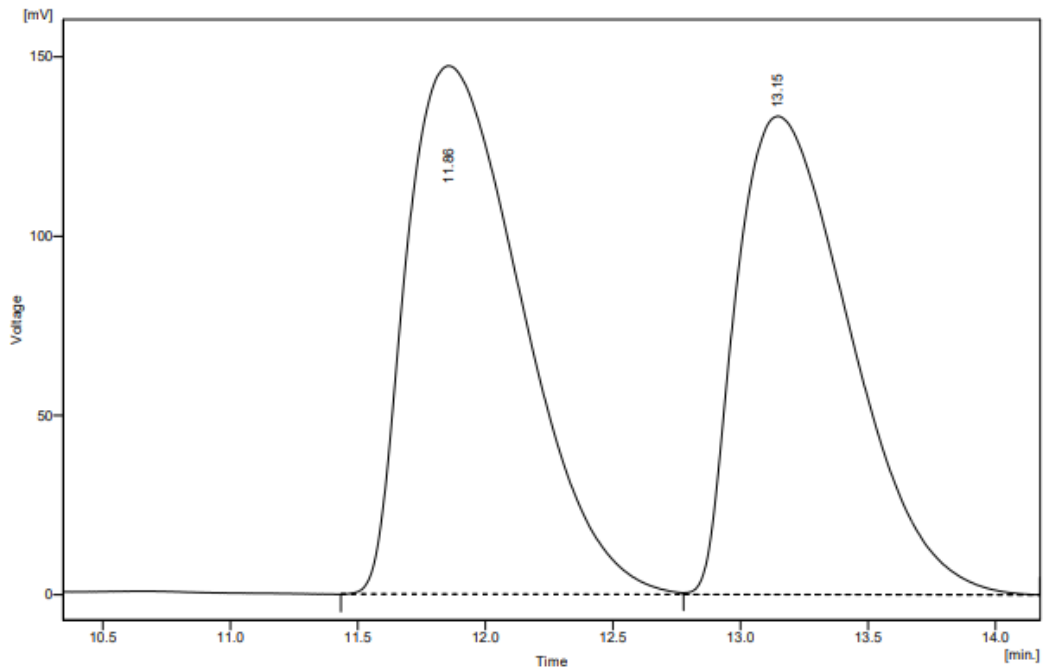
	Reten. Time [min]	Area [mV.s]	Height [mV]	Area [%]	Height [%]	W05 [min]
1	11.857	4629.961	147.357	52.8	52.5	0.51
2	13.147	4144.645	133.413	47.2	47.5	0.50
	Total	8774.607	280.769	100.0	100.0	

X-ray crystallographic analysis for compound 79b (CCDC 2170247)
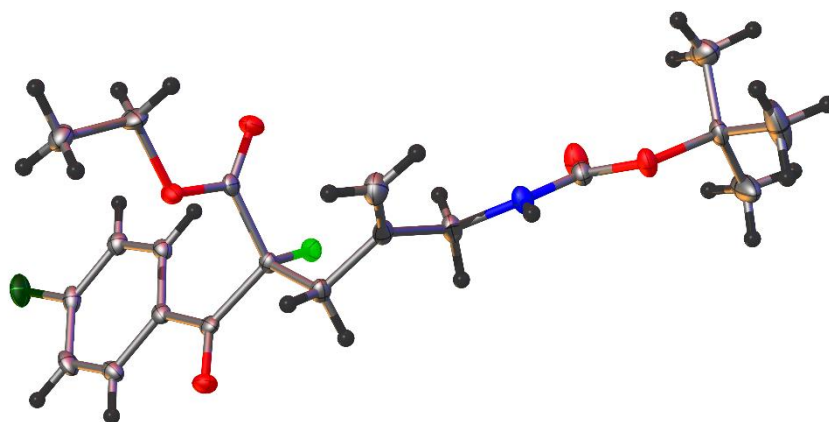
Table 1 Crystal data and structure refinement for 79b.

Identification code	OJH408s_0m
Empirical formula	$C_{20}H_{25}ClFNO_5$
Formula weight	413.86
Temperature/K	296.15
Crystal system	monoclinic
Space group	$P2_1$
a/Å	13.030(2)
b/Å	5.4670(9)
c/Å	14.728(3)
α/°	90
β/°	104.532(4)
γ/°	90
Volume/Å^3	1015.6(3)
Z	2
ρ_{calc}g/cm^3	1.353
μ/mm^{-1}	0.228
F(000)	436.0
Crystal size/mm^3	0.5 × 0.03 × 0.02
Radiation	MoKα (λ = 0.71073)
2Θ range for data collection/°	2.856 to 57.662
Index ranges	-17 ≤ h ≤ 17, -7 ≤ k ≤ 7, -19 ≤ l ≤ 19
Reflections collected	19372
Independent reflections	5281 [R_{int} = 0.0477, R_{sigma} = 0.0466]
Data/restraints/parameters	5281/1/261
Goodness-of-fit on F^2	1.029

Final R indexes [I>=2σ (I)] R_1 = 0.0369, wR_2 = 0.0777

Final R indexes [all data] R_1 = 0.0454, wR_2 = 0.0819

Largest diff. peak/hole / e Å^{-3} 0.32/-0.27

Flack parameter   0.04(3)

Table 2 Fractional Atomic Coordinates (×10^4) and Equivalent Isotropic Displacement Parameters (Å^2×10^3) for 79b. U_{eq} is defined as 1/3 of of the trace of the orthogonalised U_{IJ} tensor.

Atom	x	y	z	U(eq)
Cl1	4930.1(5)	-267.6(12)	9238.8(4)	26.58(15)
F1	3464.2(10)	3792(2)	4722.9(9)	16.4(3)
O1	4703.6(13)	8414(3)	6008.9(11)	19.2(4)
O2	1527.9(12)	4477(3)	4911.2(11)	19.5(4)
O3	2017.6(12)	7970(3)	5721.5(11)	16.2(3)
O4	2259.2(16)	2405(3)	1255.8(12)	29.7(4)
O5	1774.3(14)	5590(3)	227.6(11)	20.4(4)
N1	2233.2(17)	6349(4)	1749.5(14)	19.6(4)
C1	4705(2)	1704(5)	8286.1(16)	19.0(5)
C2	5350.0(19)	3732(5)	8313.7(16)	21.3(5)
C3	5166.0(18)	5271(4)	7544.2(16)	18.6(5)
C4	4334.0(16)	4797(5)	6750.7(14)	14.8(4)
C5	3696.5(18)	2745(4)	6736.9(15)	15.9(5)
C6	3883.3(19)	1187(5)	7505.9(16)	18.2(5)
C7	4169.0(17)	6581(4)	5957.6(15)	14.4(4)
C8	3287.3(17)	6111(4)	5044.7(15)	13.3(4)
C9	3348.7(19)	8012(4)	4306.6(15)	16.7(5)
C10	2524.6(19)	7757(4)	3381.5(15)	16.8(5)
C11	2754(2)	5834(4)	2726.4(16)	19.4(5)
C12	2169.7(18)	6039(4)	5211.5(15)	13.6(4)
C13	943.7(18)	8158(5)	5862.7(18)	22.7(5)
C14	926(2)	10253(5)	6516.7(17)	22.7(5)
C15	1686(2)	9218(5)	3175.7(18)	25.0(6)
C16	2104.5(18)	4575(5)	1088.7(15)	18.5(5)
C17	1547.6(19)	4054(5)	-623.4(16)	20.1(5)
C18	657(2)	2267(6)	-618(2)	31.7(6)
C19	1162(3)	5916(6)	-1394(2)	48.1(9)
C20	2533(2)	2770(7)	-718(2)	41.0(8)

Table 3 Anisotropic Displacement Parameters (Å²×10³) for 79b. The Anisotropic displacement factor exponent takes the form: -2π²[h²a*²U₁₁+2hka*b*U₁₂+…].

Atom	U_{11}	U_{22}	U_{33}	U_{23}	U_{13}	U_{12}
Cl1	35.7(3)	27.6(3)	14.5(3)	3.4(2)	2.7(2)	11.3(3)
F1	20.2(7)	11.9(6)	18.1(7)	-3.5(5)	6.7(5)	-0.3(5)
O1	16.5(8)	19.3(9)	22.1(9)	-3.3(7)	5.3(7)	-5.9(7)
O2	15.7(8)	20.8(9)	20.5(8)	-2.2(7)	1.7(6)	-4.5(7)
O3	12.1(8)	18.5(8)	18.1(8)	-4.1(7)	3.8(6)	0.9(7)
O4	47.9(12)	20.5(10)	18.7(9)	0.1(7)	4.9(8)	3.1(9)
O5	28.4(9)	19.3(9)	12.5(8)	-1.9(6)	3.2(7)	-2.0(7)
N1	25.5(11)	17.6(11)	14.1(10)	0.2(8)	2.2(8)	0.3(9)
C1	22.8(12)	20.7(12)	13.6(11)	-0.6(9)	4.5(9)	9.0(10)
C2	17.3(12)	27.7(13)	15.3(11)	-5.2(10)	-2.5(9)	6.1(10)
C3	15.5(11)	19.9(13)	19.5(11)	-6.1(9)	2.4(9)	-0.1(9)
C4	11.8(10)	17.6(10)	15.0(10)	-2.7(10)	3.4(8)	2.9(10)
C5	14.4(11)	18.0(11)	14.4(11)	-1.8(9)	2.2(8)	2.1(9)
C6	18.4(11)	18.8(12)	18.0(11)	-0.9(9)	5.6(9)	3.2(10)
C7	11.2(10)	16.9(11)	16.5(11)	-3.5(9)	5.9(8)	1.2(9)
C8	16.4(11)	10.8(10)	13.4(10)	-2.0(8)	4.8(8)	-0.8(9)
C9	21.2(12)	14.8(11)	15.2(11)	-0.5(9)	6.5(9)	-3.1(9)
C10	21.9(12)	15.7(11)	13.9(11)	1.4(9)	6.5(9)	-2.5(10)
C11	23.7(12)	20.0(12)	13.8(11)	-1.0(9)	3.2(9)	2.6(10)
C12	15.9(11)	15.1(11)	9.0(10)	1.5(8)	1.7(8)	0.9(9)
C13	12.2(11)	29.0(14)	27.9(13)	-4.8(11)	7.0(9)	1.7(10)
C14	19.7(12)	27.8(14)	22.5(12)	-1.3(10)	8.9(9)	3.4(10)
C15	29.1(14)	27.4(15)	19.1(12)	1.4(10)	7.1(10)	4.5(11)
C16	18.2(11)	21.8(12)	15.2(10)	-1.5(10)	3.6(8)	0.3(11)
C17	24.1(13)	23.4(13)	11.7(10)	-4.2(9)	2.7(9)	-2.5(10)
C18	27.3(15)	37.0(16)	32.2(15)	-11.9(12)	10.1(12)	-6.5(13)
C19	87(3)	31.6(17)	16.6(14)	-2.4(12)	-3.0(15)	-9.8(18)
C20	22.9(14)	69(2)	31.0(15)	-24.5(16)	6.2(12)	-1.3(15)

Table 4 Bond Lengths for 79b.

Atom	Atom	Length/Å	Atom	Atom	Length/Å
Cl1	C1	1.735(2)	C3	C4	1.404(3)
F1	C8	1.392(3)	C4	C5	1.393(3)
O1	C7	1.212(3)	C4	C7	1.495(3)
O2	C12	1.200(3)	C5	C6	1.389(3)
O3	C12	1.339(3)	C7	C8	1.555(3)

Table 4 Bond Lengths for 79b.

Atom	Atom	Length/Å	Atom	Atom	Length/Å
O3	C13	1.469(3)	C8	C9	1.521(3)
O4	C16	1.218(3)	C8	C12	1.537(3)
O5	C16	1.352(3)	C9	C10	1.515(3)
O5	C17	1.476(3)	C10	C11	1.507(3)
N1	C11	1.456(3)	C10	C15	1.326(4)
N1	C16	1.354(3)	C13	C14	1.500(3)
C1	C2	1.386(4)	C17	C18	1.518(4)
C1	C6	1.389(3)	C17	C19	1.513(4)
C2	C3	1.383(3)	C17	C20	1.500(4)

Table 5 Bond Angles for 79b.

Atom	Atom	Atom	Angle/˚	Atom	Atom	Atom	Angle/˚
C12	O3	C13	114.52(18)	C9	C8	C12	110.70(18)
C16	O5	C17	120.78(19)	C12	C8	C7	112.95(17)
C16	N1	C11	121.0(2)	C10	C9	C8	115.31(19)
C2	C1	Cl1	119.68(18)	C11	C10	C9	115.5(2)
C2	C1	C6	121.5(2)	C15	C10	C9	120.5(2)
C6	C1	Cl1	118.8(2)	C15	C10	C11	124.0(2)
C3	C2	C1	118.9(2)	N1	C11	C10	112.3(2)
C2	C3	C4	120.6(2)	O2	C12	O3	125.5(2)
C3	C4	C7	117.3(2)	O2	C12	C8	124.0(2)
C5	C4	C3	119.6(2)	O3	C12	C8	110.44(18)
C5	C4	C7	123.06(19)	O3	C13	C14	108.2(2)
C6	C5	C4	120.0(2)	O4	C16	O5	125.9(2)
C5	C6	C1	119.4(2)	O4	C16	N1	124.6(2)
O1	C7	C4	121.5(2)	O5	C16	N1	109.5(2)
O1	C7	C8	118.6(2)	O5	C17	C18	110.60(19)
C4	C7	C8	119.86(19)	O5	C17	C19	102.3(2)
F1	C8	C7	107.17(17)	O5	C17	C20	110.6(2)
F1	C8	C9	109.63(16)	C19	C17	C18	109.1(2)
F1	C8	C12	106.01(17)	C20	C17	C18	111.9(2)
C9	C8	C7	110.19(18)	C20	C17	C19	112.1(3)

Table 6 Hydrogen Bonds for 79b.

D	H	A	d(D-H)/Å	d(H-A)/Å	d(D-A)/Å	D-H-A/°
N1	H1	O4[1]	0.84(3)	2.56(3)	3.392(3)	173(3)
C9	H9A	F1[1]	0.97	2.30	3.215(3)	157.2
C13	H13B	O2[2]	0.97	2.57	3.217(3)	124.4
C14	H14C	O2[2]	0.96	2.80	3.384(3)	120.4

[1]+X,1+Y,+Z; [2]-X,1/2+Y,1-Z

Table 7 Torsion Angles for 79b.

A	B	C	D	Angle/˚	A	B	C	D	Angle/˚
Cl1	C1	C2	C3	179.36(18)	C7	C4	C5	C6	-178.8(2)
Cl1	C1	C6	C5	-179.76(17)	C7	C8	C9	C10	-179.77(19)
F1	C8	C9	C10	62.5(2)	C7	C8	C12	O2	-132.3(2)
F1	C8	C12	O2	-15.2(3)	C7	C8	C12	O3	48.6(2)
F1	C8	C12	O3	165.69(16)	C8	C9	C10	C11	-79.5(2)
O1	C7	C8	F1	125.8(2)	C8	C9	C10	C15	102.6(3)
O1	C7	C8	C9	6.6(3)	C9	C8	C12	O2	103.6(3)
O1	C7	C8	C12	-117.8(2)	C9	C8	C12	O3	-75.5(2)
C1	C2	C3	C4	0.5(3)	C9	C10	C11	N1	-155.1(2)
C2	C1	C6	C5	-0.5(3)	C11	N1	C16	O4	11.0(4)
C2	C3	C4	C5	-0.6(3)	C11	N1	C16	O5	-169.4(2)
C2	C3	C4	C7	178.5(2)	C12	O3	C13	C14	174.71(18)
C3	C4	C5	C6	0.2(3)	C12	C8	C9	C10	-54.1(3)
C3	C4	C7	O1	-2.8(3)	C13	O3	C12	O2	-3.2(3)
C3	C4	C7	C8	177.80(19)	C13	O3	C12	C8	175.91(19)
C4	C5	C6	C1	0.3(3)	C15	C10	C11	N1	22.7(3)
C4	C7	C8	F1	-54.7(2)	C16	O5	C17	C18	61.3(3)
C4	C7	C8	C9	-173.96(18)	C16	O5	C17	C19	177.4(2)
C4	C7	C8	C12	61.6(3)	C16	O5	C17	C20	-63.2(3)
C5	C4	C7	O1	176.3(2)	C16	N1	C11	C10	-162.3(2)
C5	C4	C7	C8	-3.1(3)	C17	O5	C16	O4	1.0(4)
C6	C1	C2	C3	0.1(3)	C17	O5	C16	N1	-178.57(19)

Table 8 Hydrogen Atom Coordinates ($\text{Å}\times10^4$) and Isotropic Displacement Parameters ($\text{Å}^2\times10^3$) for 79b.

Atom	x	y	z	U(eq)
H1	2190(20)	7820(60)	1582(19)	24(8)
H2	5897.71	4052.91	8840.96	26
H3	5596.74	6631.89	7552.49	22
H5	3145.81	2417.38	6212.66	19
H6	3461.95	-189.69	7498.57	22
H9A	3277.67	9621.25	4561.28	20
H9B	4046.4	7923.52	4186.38	20
H11A	3514.13	5741.91	2798.18	23
H11B	2518.32	4256.02	2896.83	23
H13A	756.59	6650.32	6129.36	27
H13B	434.34	8437.75	5267.26	27
H14A	1153.86	11717.85	6265.3	34
H14B	1395.2	9907.33	7117.99	34
H14C	218.72	10473.97	6585.4	34
H15A	1197.13	9090.03	2597.03	30
H15B	1587.28	10371.72	3610.02	30
H18A	917.09	986.69	-173.5	48
H18B	402.06	1573.06	-1231.79	48
H18C	88.89	3112.07	-444.16	48
H19A	554.86	6755.09	-1290.18	72
H19B	971.48	5098.03	-1989.74	72
H19C	1716.64	7074.81	-1391.5	72
H20A	3086.13	3948.2	-691.48	62
H20B	2390.31	1923.77	-1307.68	62
H20C	2753.53	1615.76	-215.55	62

Crystal structure determination of 79b

Crystal Data for $C_{20}H_{25}ClFNO_5$ (M =413.86 g/mol): monoclinic, space group $P2_1$ (no. 4), a = 13.030(2) Å, b = 5.4670(9) Å, c = 14.728(3) Å, β = 104.532(4)°, V = 1015.6(3) Å^3, Z = 2, T = 296.15 K, μ(MoKα) = 0.228 mm^{-1}, $Dcalc$ = 1.353 g/cm^3, 19372 reflections measured (2.856° ≤ 2Θ ≤ 57.662°), 5281 unique (R_{int} = 0.0477, R_{sigma} = 0.0466) which were used in all calculations. The final R_1 was 0.0369 (I > 2σ(I)) and wR_2 was 0.0819 (all data).

X-ray crystallographic analysis for compound 79f (CCDC 2170248)
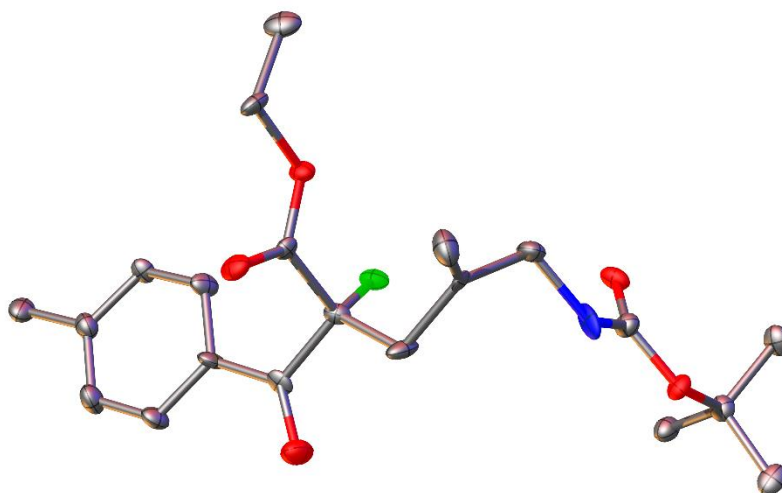
Table 1 Crystal data and structure refinement for 79f.

Identification code	OJH409v_0m
Empirical formula	$C_{21}H_{28}FNO_5$
Formula weight	393.44
Temperature/K	100.02
Crystal system	monoclinic
Space group	$P2_1$
a/Å	5.4499(6)
b/Å	8.2741(9)
c/Å	23.173(3)
α/°	90
β/°	93.304(5)
γ/°	90
Volume/Å^3	1043.2(2)
Z	2
ρ_{calc}g/cm^3	1.253
μ/mm^{-1}	0.786
F(000)	420.0
Crystal size/mm^3	0.179 × 0.082 × 0.053
Radiation	CuKα (λ = 1.54178)
2Θ range for data collection/°	3.82 to 133.504
Index ranges	-6 ≤ h ≤ 5, -9 ≤ k ≤ 9, -27 ≤ l ≤ 27
Reflections collected	18900
Independent reflections	3657 [R_{int} = 0.0541, R_{sigma} = 0.0362]
Data/restraints/parameters	3657/205/258

Goodness-of-fit on F^2 1.160

Final R indexes [I>=2σ (I)] R_1 = 0.1442, wR_2 = 0.3843

Final R indexes [all data] R_1 = 0.1463, wR_2 = 0.3850

Largest diff. peak/hole / e Å^{-3} 1.65/-0.82

Flack parameter   0.14(7)

Table 2 Fractional Atomic Coordinates (×10^4) and Equivalent Isotropic Displacement Parameters (Å^2×10^3) for 79f. U_{eq} is defined as 1/3 of of the trace of the orthogonalised U_{IJ} tensor.

Atom	x	y	z	U(eq)
F1	2588(15)	5050(10)	2771(4)	18.2(19)
O1	6900(20)	3131(15)	3506(5)	26(3)
O2	7150(20)	7509(13)	3453(5)	21(2)
O3	3560(20)	8049(12)	2971(5)	17(2)
O4	1132(19)	3412(13)	1110(5)	19(2)
O5	4302(19)	1843(12)	805(4)	16(2)
N1	5200(30)	4076(18)	1271(5)	24(3)
C1	1460(30)	4990(20)	5055(7)	21(3)
C2	3580(30)	4030(20)	5063(7)	25(3)
C3	4810(30)	3750(20)	4564(7)	20(3)
C4	4070(30)	4530(19)	4052(7)	18(3)
C5	1950(30)	5520(20)	4039(7)	20(3)
C6	650(30)	5707(19)	4535(6)	17(3)
C7	110(30)	5230(20)	5603(7)	24(3)
C8	5410(30)	4211(19)	3538(6)	15(3)
C9	5010(30)	5316(18)	2992(6)	14(3)
C10	6780(30)	4893(19)	2542(7)	21(3)
C11	6560(30)	6022(18)	2010(6)	14(3)
C12	4660(30)	5659(19)	1540(7)	21(3)
C13	5370(30)	7085(17)	3168(6)	13(3)
C14	3900(30)	9768(18)	3120(7)	18(3)
C15	1570(30)	10610(20)	2862(8)	26(4)
C16	7980(30)	7260(20)	1981(7)	27(4)
C17	3350(30)	3120(19)	1066(7)	17(3)
C18	2730(30)	515(19)	572(6)	18(3)
C19	4600(30)	-603(19)	327(7)	22(3)
C20	1030(30)	1170(20)	75(7)	23(3)
C21	1420(30)	-270(20)	1041(7)	22(3)

Table 3 Anisotropic Displacement Parameters (Å^2×10^3) for 79f. The Anisotropic displacement factor exponent takes the form: -2π^2[h^{2}a*^{2}U$_{11}$+2hka*b*U$_{12}$+…].

Atom	U$_{11}$	U$_{22}$	U$_{33}$	U$_{23}$	U$_{13}$	U$_{12}$
F1	15(4)	13(4)	26(4)	3(4)	-4(3)	-1(3)
O1	25(6)	26(6)	29(6)	3(5)	5(5)	8(5)
O2	20(5)	13(5)	29(6)	-6(4)	-3(4)	-2(4)
O3	19(5)	10(4)	21(5)	0(4)	-3(4)	-1(4)
O4	14(4)	17(6)	24(5)	4(4)	-8(4)	-4(4)
O5	16(5)	13(5)	20(5)	-6(4)	2(4)	-4(4)
N1	33(7)	24(6)	14(6)	0(5)	-12(5)	-16(6)
C1	24(7)	22(8)	17(6)	1(6)	-3(5)	-2(6)
C2	25(8)	34(9)	16(6)	3(6)	-1(5)	1(6)
C3	22(8)	21(8)	18(6)	9(6)	1(5)	3(6)
C4	19(7)	18(8)	19(6)	9(5)	1(5)	7(6)
C5	21(7)	22(8)	18(6)	8(6)	7(5)	3(6)
C6	10(6)	22(8)	18(6)	2(5)	-1(5)	-2(6)
C7	34(9)	18(9)	21(7)	4(6)	3(6)	1(7)
C8	6(6)	20(7)	18(6)	3(5)	-5(4)	-5(5)
C9	10(6)	13(6)	20(6)	3(5)	-1(4)	-2(5)
C10	25(8)	10(7)	28(7)	4(6)	12(6)	6(6)
C11	19(7)	13(6)	11(6)	-4(5)	4(5)	6(5)
C12	21(7)	18(7)	23(7)	2(6)	-4(6)	6(6)
C13	11(6)	12(6)	15(6)	-2(5)	5(4)	-1(4)
C14	21(7)	10(6)	23(7)	-3(6)	9(6)	2(5)
C15	23(8)	14(8)	42(9)	1(7)	1(7)	-4(6)
C16	34(9)	29(8)	17(8)	1(6)	-2(7)	-9(7)
C17	17(5)	15(6)	20(7)	-3(5)	-1(5)	-2(5)
C18	19(7)	16(7)	20(7)	-1(5)	0(5)	-5(5)
C19	23(8)	15(7)	29(8)	-4(6)	8(6)	-9(6)
C20	17(7)	29(9)	22(8)	-1(6)	-4(6)	-5(6)
C21	26(8)	17(8)	23(7)	0(6)	5(6)	0(6)

Table 4 Bond Lengths for 79f.

Atom	Atom	Length/Å	Atom	Atom	Length/Å
F1	C9	1.406(16)	C3	C4	1.39(2)
O1	C8	1.213(19)	C4	C5	1.41(2)
O2	C13	1.196(19)	C4	C8	1.46(2)
O3	C13	1.327(18)	C5	C6	1.40(2)

Table 4 Bond Lengths for 79f.

Atom	Atom	Length/Å	Atom	Atom	Length/Å
O3	C14	1.473(18)	C8	C9	1.566(19)
O4	C17	1.243(19)	C9	C10	1.50(2)
O5	C17	1.337(19)	C9	C13	1.53(2)
O5	C18	1.477(18)	C10	C11	1.55(2)
N1	C12	1.49(2)	C11	C12	1.49(2)
N1	C17	1.35(2)	C11	C16	1.29(2)
C1	C2	1.40(2)	C14	C15	1.54(2)
C1	C6	1.39(2)	C18	C19	1.51(2)
C1	C7	1.52(2)	C18	C20	1.53(2)
C2	C3	1.39(2)	C18	C21	1.48(2)

Table 5 Bond Angles for 79f.

Atom	Atom	Atom	Angle/°	Atom	Atom	Atom	Angle/°
C13	O3	C14	114.8(12)	C10	C9	C13	109.3(12)
C17	O5	C18	121.5(12)	C13	C9	C8	109.5(12)
C17	N1	C12	120.2(14)	C9	C10	C11	112.8(12)
C2	C1	C7	120.1(14)	C12	C11	C10	118.7(14)
C6	C1	C2	118.3(15)	C16	C11	C10	120.2(15)
C6	C1	C7	121.6(15)	C16	C11	C12	121.1(15)
C3	C2	C1	121.2(15)	N1	C12	C11	109.7(12)
C4	C3	C2	120.3(15)	O2	C13	O3	125.2(13)
C3	C4	C5	119.1(14)	O2	C13	C9	121.0(13)
C3	C4	C8	118.6(13)	O3	C13	C9	113.8(12)
C5	C4	C8	122.2(13)	O3	C14	C15	104.8(13)
C6	C5	C4	119.9(14)	O4	C17	O5	126.5(14)
C1	C6	C5	121.0(15)	O4	C17	N1	124.7(15)
O1	C8	C4	123.5(14)	O5	C17	N1	108.8(13)
O1	C8	C9	116.3(13)	O5	C18	C19	101.8(12)
C4	C8	C9	120.2(13)	O5	C18	C20	108.9(13)
F1	C9	C8	106.7(11)	O5	C18	C21	110.4(12)
F1	C9	C10	109.8(12)	C19	C18	C20	109.0(13)
F1	C9	C13	110.5(11)	C21	C18	C19	111.8(13)
C10	C9	C8	111.1(12)	C21	C18	C20	114.2(14)

Table 6 Torsion Angles for 79f.

A	B	C	D	Angle/°	A	B	C	D	Angle/°
F1	C9	C10	C11	65.7(16)	C8	C4	C5	C6	175.9(15)
F1	C9	C13	O2	167.4(13)	C8	C9	C10	C11	-176.6(12)
F1	C9	C13	O3	-13.2(16)	C8	C9	C13	O2	50.2(18)
O1	C8	C9	F1	114.3(14)	C8	C9	C13	O3	-130.4(12)
O1	C8	C9	C10	-5.3(19)	C9	C10	C11	C12	-84.3(17)
O1	C8	C9	C13	-126.1(14)	C9	C10	C11	C16	94.8(18)
C1	C2	C3	C4	5(3)	C10	C9	C13	O2	-71.8(18)
C2	C1	C6	C5	-3(2)	C10	C9	C13	O3	107.6(14)
C2	C3	C4	C5	-4(2)	C10	C11	C12	N1	-63.5(17)
C2	C3	C4	C8	179.9(16)	C12	N1	C17	O4	-4(2)
C3	C4	C5	C6	0(2)	C12	N1	C17	O5	174.9(12)
C3	C4	C8	O1	11(2)	C13	O3	C14	C15	-178.5(12)
C3	C4	C8	C9	-167.1(14)	C13	C9	C10	C11	-55.6(17)
C4	C5	C6	C1	3(2)	C14	O3	C13	O2	1(2)
C4	C8	C9	F1	-67.1(16)	C14	O3	C13	C9	-178.3(12)
C4	C8	C9	C10	173.3(13)	C16	C11	C12	N1	117.4(17)
C4	C8	C9	C13	52.4(17)	C17	O5	C18	C19	179.9(13)
C5	C4	C8	O1	-164.7(15)	C17	O5	C18	C20	64.9(17)
C5	C4	C8	C9	17(2)	C17	O5	C18	C21	-61.2(18)
C6	C1	C2	C3	-2(3)	C17	N1	C12	C11	147.0(14)
C7	C1	C2	C3	178.0(16)	C18	O5	C17	O4	-5(2)
C7	C1	C6	C5	177.9(15)	C18	O5	C17	N1	175.6(12)

Table 7 Hydrogen Atom Coordinates (Å×10⁴) and Isotropic Displacement Parameters (Å²×10³) for 79f.

Atom	x	y	z	U(eq)
H1	6732.01	3763.5	1245.78	29
H2	4183.63	3553.82	5416.88	30
H3	6165.09	3029.67	4572.36	24
H5	1426.82	6067.37	3692.26	24
H6	-822.37	6328.56	4517.95	20
H7A	1114.67	5882.08	5877.39	36
H7B	-210.76	4171.62	5775.22	36
H7C	-1456.69	5778.82	5509.25	36
H10A	6481.93	3765.4	2413.69	25
H10B	8480.27	4952.96	2717.65	25
H12A	3013.25	5623.14	1701.02	25

Table 7 Hydrogen Atom Coordinates (Å×10⁴) and Isotropic Displacement Parameters (Å²×10³) for 79f.

Atom	x	y	z	U(eq)
H12B	4644.35	6521.16	1243.97	25
H14A	5385.73	10207.35	2950.58	22
H14B	4057.82	9914.91	3544.91	22
H15A	1416.58	10411.12	2443.9	39
H15B	1686.03	11770.81	2934.63	39
H15C	127.21	10170.06	3041.15	39
H16A	7817.96	7961.8	1656.81	32
H16B	9178.75	7473.98	2285	32
H19A	5544.27	-10.84	48.56	33
H19B	3748.48	-1512.72	131.84	33
H19C	5710.21	-1010.46	640.75	33
H20A	-310.84	1787.35	233.9	35
H20B	342.67	265.72	-154.99	35
H20C	1967.39	1874.51	-170.92	35
H21A	2592.31	-489.89	1368.28	33
H21B	686.32	-1281.12	898.76	33
H21C	132.11	457.05	1164.79	33

Crystal structure determination of 79f

Crystal Data for $C_{21}H_{28}FNO_5$ (M =393.44 g/mol): monoclinic, space group $P2_1$ (no. 4), a = 5.4499(6) Å, b = 8.2741(9) Å, c = 23.173(3) Å, β = 93.304(5)°, V = 1043.2(2) Å³, Z = 2, T = 100.02 K, μ(CuKα) = 0.786 mm⁻¹, $Dcalc$ = 1.253 g/cm³, 18900 reflections measured (3.82° ≤ 2Θ ≤ 133.504°), 3657 unique (R_{int} = 0.0541, R_{sigma} = 0.0362) which were used in all calculations. The final R_1 was 0.1442 (I > 2σ(I)) and wR_2 was 0.3850 (all data).

# X-ray crystallographic analysis for compound 79i (CCDC 2170249)
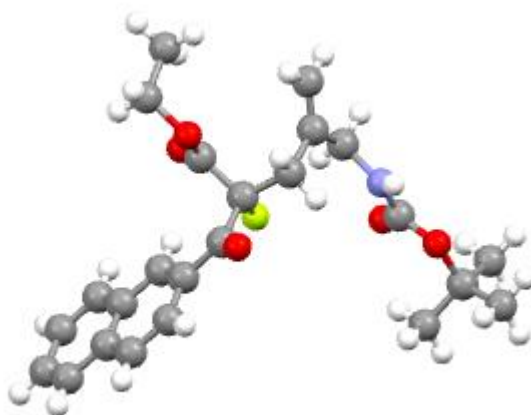
Table 1 Crystal data and structure refinement for 79i.

Identification code	OJH410v_2_0m
Empirical formula	$C_{24}H_{28}FNO_5$
Formula weight	429.47
Temperature/K	100.00
Crystal system	monoclinic
Space group	$P2_1$
a/Å	6.84040(10)
b/Å	10.0817(2)
c/Å	15.9492(3)
α/°	90
β/°	99.4250(10)
γ/°	90
Volume/Å³	1085.05(3)
Z	2
ρ_{calc}g/cm³	1.315
μ/mm⁻¹	0.805
F(000)	456.0
Crystal size/mm³	0.17 × 0.11 × 0.038
Radiation	CuKα (λ = 1.54178)
2Θ range for data collection/°	5.616 to 133.254
Index ranges	-8 ≤ h ≤ 8, -12 ≤ k ≤ 12, -18 ≤ l ≤ 18
Reflections collected	36222
Independent reflections	3825 [R_{int} = 0.0374, R_{sigma} = 0.0171]
Data/restraints/parameters	3825/1/284
Goodness-of-fit on F²	1.082

Final R indexes [I>=2σ (I)] $R_1 = 0.0250$, $wR_2 = 0.0615$

Final R indexes [all data] $R_1 = 0.0268$, $wR_2 = 0.0627$

Largest diff. peak/hole / e Å^{-3} 0.14/-0.21

Flack parameter   0.02(4)

Table 2 Fractional Atomic Coordinates (×10^4) and Equivalent Isotropic Displacement Parameters (Å^2×10^3) for 3i. U_{eq} is defined as 1/3 of the trace of the orthogonalised U_{IJ} tensor.

Atom	x	y	z	U(eq)
F1	3412.4(15)	4450.6(10)	7246.1(6)	17.5(2)
O1	5632(2)	4640.7(14)	9292.5(8)	22.4(3)
O2	746.6(19)	6284.8(13)	7420.5(9)	21.7(3)
O3	2748.2(19)	7215.6(13)	8522.3(8)	18.6(3)
O4	5898(2)	3578.0(14)	5315.5(9)	23.1(3)
O5	9117(2)	3326.8(13)	5976.4(8)	20.0(3)
N1	7424(2)	5066.7(16)	6280.0(10)	16.8(3)
C1	2600(3)	3515.7(19)	8878.6(12)	15.0(4)
C2	830(3)	3392.6(18)	8326.6(11)	14.8(4)
C3	-670(3)	2522.4(18)	8510.4(12)	15.0(4)
C4	-2495(3)	2379.2(19)	7953.3(12)	17.1(4)
C5	-3912(3)	1520(2)	8142.0(12)	19.9(4)
C6	-3569(3)	762(2)	8899.8(13)	22.0(4)
C7	-1817(3)	883(2)	9444.7(12)	20.8(4)
C8	-320(3)	1756.1(18)	9269.0(12)	16.5(4)
C9	1525(3)	1868.4(19)	9810.2(12)	17.8(4)
C10	2947(3)	2717.5(19)	9627.1(12)	17.3(4)
C11	4189(3)	4473.5(18)	8752.8(11)	15.7(4)
C12	3968(3)	5313.1(19)	7924.9(11)	14.4(4)
C13	5903(3)	6003.8(19)	7824.7(11)	15.4(4)
C14	5794(3)	6777.1(19)	7002.2(12)	16.0(4)
C15	5789(3)	6011(2)	6187.9(12)	17.0(4)
C16	2283(3)	6324.0(19)	7910.1(11)	15.4(4)
C17	1225(3)	8223(2)	8583.9(13)	22.5(4)
C18	1133(3)	9246(2)	7890.3(13)	24.7(4)
C19	5740(3)	8091(2)	6997.4(14)	22.6(4)
C20	7340(3)	3955.4(19)	5803.3(11)	15.7(4)
C21	9443(3)	2053(2)	5567.0(13)	20.7(4)
C22	11581(3)	1731(2)	5946.9(15)	30.5(5)
C23	8041(3)	1005(2)	5809.1(13)	25.8(5)
C24	9234(3)	2244(2)	4609.1(13)	25.7(5)

Table 3 Anisotropic Displacement Parameters (Å²×10³) for 79i. The Anisotropic displacement factor exponent takes the form: -2π²[h²a*²U₁₁+2hka*b*U₁₂+…].

Atom	U_{11}	U_{22}	U_{33}	U_{23}	U_{13}	U_{12}
F1	21.1(6)	17.0(5)	14.2(5)	-4.2(4)	2.2(4)	-4.5(4)
O1	22.3(7)	24.8(8)	17.7(7)	0.6(6)	-3.4(6)	-4.5(6)
O2	17.3(7)	18.8(7)	26.2(7)	1.7(6)	-4.9(6)	-1.9(5)
O3	19.7(7)	18.6(7)	17.5(6)	-2.9(6)	2.6(5)	3.4(6)
O4	19.9(7)	23.6(7)	24.0(7)	-7.1(6)	-1.6(6)	0.5(6)
O5	18.6(7)	19.0(7)	21.5(7)	-6.1(6)	0.4(5)	2.6(5)
N1	14.1(8)	18.5(8)	17.0(8)	-3.7(6)	0.1(6)	-0.4(6)
C1	17.7(9)	13.1(9)	14.9(9)	-1.4(7)	4.4(7)	1.5(7)
C2	18.7(9)	12.7(9)	13.4(8)	1.6(7)	3.7(7)	2.5(7)
C3	19.4(9)	11.8(9)	14.7(8)	-1.3(7)	5.1(7)	3.2(7)
C4	19.9(9)	15.0(9)	16.6(9)	0.1(7)	3.5(7)	2.2(8)
C5	18.2(10)	18.2(10)	23.2(10)	-2.5(8)	3.1(8)	-1.1(8)
C6	22.0(10)	20.5(10)	25.5(10)	1.2(8)	10.0(8)	-3.5(8)
C7	26.1(10)	18.4(10)	19.9(10)	1.9(8)	9.5(8)	-0.8(8)
C8	22.5(10)	13.1(9)	15.6(9)	-0.5(7)	7.9(7)	2.9(7)
C9	23.2(10)	17.7(9)	12.8(9)	2.0(7)	4.1(7)	4.5(8)
C10	18.1(9)	18.4(10)	15.0(9)	0.4(8)	1.1(7)	3.9(8)
C11	16.9(9)	14.6(9)	15.6(9)	-2.8(7)	2.6(7)	0.3(8)
C12	15.7(9)	14.7(9)	12.4(9)	-4.0(7)	1.0(7)	-2.8(7)
C13	14.0(9)	17.4(9)	14.8(9)	-2.4(8)	2.5(7)	-1.0(7)
C14	10.5(9)	19.0(10)	18.6(9)	-0.5(8)	2.6(7)	-1.4(7)
C15	17.8(9)	16.8(9)	16.5(9)	1.0(8)	3.0(7)	1.6(8)
C16	17.8(10)	15.0(9)	14.0(8)	2.6(7)	4.2(7)	-3.8(7)
C17	23.4(10)	21.3(11)	23.9(10)	-3.0(9)	7.6(8)	7.2(8)
C18	24.7(11)	18.8(10)	30.7(11)	-0.9(9)	4.7(8)	2.9(8)
C19	22.5(11)	19.6(11)	26.7(10)	-0.3(8)	7.2(8)	-1.7(8)
C20	17.4(9)	16.4(9)	13.7(8)	0.4(7)	3.6(7)	-0.8(8)
C21	22.1(10)	17.7(10)	22.2(10)	-6.5(8)	3.0(8)	4.1(8)
C22	26.2(11)	31.0(12)	33.0(12)	-7.6(10)	1.4(9)	8.4(9)
C23	33.3(12)	19.8(10)	24.4(10)	-0.3(9)	5.4(9)	1.4(9)
C24	27.5(11)	27.4(11)	23.3(10)	-5.3(9)	7.5(9)	2.4(9)

Table 4 Bond Lengths for 79i.

Atom	Atom	Length/Å	Atom	Atom	Length/Å
F1	C12	1.392(2)	C4	C5	1.370(3)

Table 4 Bond Lengths for 79i.

Atom	Atom	Length/Å	Atom	Atom	Length/Å
O1	C11	1.210(2)	C5	C6	1.416(3)
O2	C16	1.203(2)	C6	C7	1.366(3)
O3	C16	1.327(2)	C7	C8	1.413(3)
O3	C17	1.470(2)	C8	C9	1.412(3)
O4	C20	1.213(2)	C9	C10	1.363(3)
O5	C20	1.358(2)	C11	C12	1.555(3)
O5	C21	1.474(2)	C12	C13	1.527(2)
N1	C15	1.458(2)	C12	C16	1.536(3)
N1	C20	1.350(2)	C13	C14	1.517(3)
C1	C2	1.381(3)	C14	C15	1.511(3)
C1	C10	1.427(3)	C14	C19	1.325(3)
C1	C11	1.492(3)	C17	C18	1.506(3)
C2	C3	1.417(3)	C21	C22	1.523(3)
C3	C4	1.416(3)	C21	C23	1.519(3)
C3	C8	1.422(3)	C21	C24	1.523(3)

Table 5 Bond Angles for 79i.

Atom	Atom	Atom	Angle/°	Atom	Atom	Atom	Angle/°
C16	O3	C17	115.46(14)	F1	C12	C13	109.54(14)
C20	O5	C21	120.79(15)	F1	C12	C16	107.08(14)
C20	N1	C15	121.61(16)	C13	C12	C11	111.83(14)
C2	C1	C10	119.43(17)	C13	C12	C16	110.91(15)
C2	C1	C11	123.67(16)	C16	C12	C11	110.04(14)
C10	C1	C11	116.88(16)	C14	C13	C12	113.84(15)
C1	C2	C3	120.85(16)	C15	C14	C13	118.27(16)
C2	C3	C8	119.04(17)	C19	C14	C13	121.06(18)
C4	C3	C2	121.81(17)	C19	C14	C15	120.66(18)
C4	C3	C8	119.15(17)	N1	C15	C14	110.72(15)
C5	C4	C3	120.62(18)	O2	C16	O3	125.37(18)
C4	C5	C6	120.25(18)	O2	C16	C12	124.19(17)
C7	C6	C5	120.06(18)	O3	C16	C12	110.42(15)
C6	C7	C8	121.21(18)	O3	C17	C18	111.64(15)
C7	C8	C3	118.71(18)	O4	C20	O5	126.20(17)
C9	C8	C3	119.07(17)	O4	C20	N1	125.21(18)
C9	C8	C7	122.20(17)	N1	C20	O5	108.58(15)
C10	C9	C8	121.15(18)	O5	C21	C22	102.39(16)
C9	C10	C1	120.41(17)	O5	C21	C23	110.22(16)

Table 5 Bond Angles for 79i.

Atom	Atom	Atom	Angle/°	Atom	Atom	Atom	Angle/°
O1	C11	C1	121.44(17)	O5	C21	C24	109.74(16)
O1	C11	C12	118.86(16)	C23	C21	C22	110.84(18)
C1	C11	C12	119.66(15)	C23	C21	C24	112.54(17)
F1	C12	C11	107.26(14)	C24	C21	C22	110.64(17)

Table 6 Hydrogen Bonds for 79i.

D	H	A	d(D-H)/Å	d(H-A)/Å	d(D-A)/Å	D-H-A/°
N1	H1	O2[1]	0.88	2.10	2.937(2)	159.8

[1] 1+X,+Y,+Z

Table 7 Torsion Angles for 79i.

A	B	C	D	Angle/°	A	B	C	D	Angle/°
F1	C12	C13	C14	58.13(19)	C8	C9	C10	C1	-0.1(3)
F1	C12	C16	O2	4.0(2)	C10	C1	C2	C3	2.4(3)
F1	C12	C16	O3	-177.45(14)	C10	C1	C11	O1	-5.8(3)
O1	C11	C12	F1	134.28(17)	C10	C1	C11	C12	176.26(16)
O1	C11	C12	C13	14.2(2)	C11	C1	C2	C3	-175.98(17)
O1	C11	C12	C16	-109.57(19)	C11	C1	C10	C9	176.58(17)
C1	C2	C3	C4	-179.91(17)	C11	C12	C13	C14	176.89(15)
C1	C2	C3	C8	-0.9(3)	C11	C12	C16	O2	-112.23(19)
C1	C11	C12	F1	-47.7(2)	C11	C12	C16	O3	66.29(19)
C1	C11	C12	C13	-167.80(15)	C12	C13	C14	C15	-74.6(2)
C1	C11	C12	C16	68.5(2)	C12	C13	C14	C19	106.6(2)
C2	C1	C10	C9	-1.9(3)	C13	C12	C16	O2	123.50(19)
C2	C1	C11	O1	172.67(18)	C13	C12	C16	O3	-57.98(19)
C2	C1	C11	C12	-5.3(3)	C13	C14	C15	N1	-51.0(2)
C2	C3	C4	C5	179.29(17)	C15	N1	C20	O4	-6.1(3)
C2	C3	C8	C7	-179.51(17)	C15	N1	C20	O5	175.14(15)
C2	C3	C8	C9	-1.0(3)	C16	O3	C17	C18	-75.4(2)
C3	C4	C5	C6	0.0(3)	C16	C12	C13	C14	-59.86(19)
C3	C8	C9	C10	1.5(3)	C17	O3	C16	O2	-0.2(3)
C4	C3	C8	C7	-0.5(3)	C17	O3	C16	C12	-178.73(14)
C4	C3	C8	C9	177.98(17)	C19	C14	C15	N1	127.79(19)
C4	C5	C6	C7	-0.2(3)	C20	O5	C21	C22	-179.70(16)

Table 7 Torsion Angles for 79i.

A	B	C	D	Angle/˚	A	B	C	D	Angle/˚
C5	C6	C7	C8	0.0(3)	C20	O5	C21	C23	-61.7(2)
C6	C7	C8	C3	0.3(3)	C20	O5	C21	C24	62.8(2)
C6	C7	C8	C9	-178.11(18)	C20	N1	C15	C14	154.18(16)
C7	C8	C9	C10	179.95(18)	C21	O5	C20	O4	-0.7(3)
C8	C3	C4	C5	0.3(3)	C21	O5	C20	N1	178.03(15)

Table 8 Hydrogen Atom Coordinates (Å×10⁴) and Isotropic Displacement Parameters (Å²×10³) for 79i.

Atom	x	y	z	U(eq)
H1	8491.94	5224.82	6655.51	20
H2	615.18	3898.01	7817.08	18
H4	-2738.08	2883.82	7443.8	21
H5	-5130.57	1431.23	7763.12	24
H6	-4557.51	169.91	9029.17	26
H7	-1600.66	369.74	9951.11	25
H9	1779	1343.08	10310.68	21
H10	4178.19	2778.34	10000.23	21
H13A	6277.38	6618.35	8308.49	18
H13B	6961.06	5328.1	7850.92	18
H15A	4517.7	5530.39	6039.53	20
H15B	5910.79	6635.87	5720.33	20
H17A	1521.07	8667.78	9143.81	27
H17B	-82.49	7785.16	8544.85	27
H18A	770.32	8814.7	7335.89	37
H18B	2430.87	9670.96	7921.81	37
H18C	136.71	9916.84	7961.89	37
H19A	5698.81	8560.93	6478.4	27
H19B	5743.74	8563.76	7513.06	27
H22A	12458.44	2419.07	5783.13	46
H22B	11945.76	869.37	5734.22	46
H22C	11714.14	1698.97	6567.78	46
H23A	8233.03	917.64	6429.17	39
H23B	8316.53	153.06	5556.42	39
H23C	6669.78	1267.92	5598.05	39
H24A	7891.46	2554.58	4386.03	39
H24B	9473.84	1398.5	4340.55	39
H24C	10200.46	2902.37	4484.4	39

Crystal structure determination of 79i

Crystal Data for $C_{24}H_{28}FNO_5$ (M =429.47 g/mol): monoclinic, space group $P2_1$ (no. 4), a = 6.84040(10) Å, b = 10.0817(2) Å, c = 15.9492(3) Å, β = 99.4250(10)°, V = 1085.05(3) Å^3, Z = 2, T = 100.00 K, μ(CuKα) = 0.805 mm^{-1}, $Dcalc$ = 1.315 g/cm^3, 36222 reflections measured (5.616° ≤ 2Θ ≤ 133.254°), 3825 unique (R_{int} = 0.0374, R_{sigma} = 0.0171) which were used in all calculations. The final R_1 was 0.0250 (I > 2σ(I)) and wR_2 was 0.0627 (all data).

Reference

1. (a) Tietze, L. F., *Chem. Rev.* **1996**, *96*, 115-136; (b) Negishi, E.-i.; Coperet, C.; Ma, S.; Liou, S.-Y.; Liu, F., *Chem. Rev.* **1996**, *96*, 365-394.

2. (a) Vlaar, T.; Ruijter, E.; Orru, R. V. A., *Adv. Synth. Catal.* **2011**, *353*, 809-814;(b) Lu, L.-Q.; Chen, J.-R.; Xiao, W.-J., *Acc. Chem. Res*. **2012**, *45*, 1278-1293.

3. Trost, B. M.; Van Vranken, D. L., *Chem. Rev. 1996, 96*, 395-422.

4. Trost, B. M.; Schultz, J. E., *Synth*. **2019**, *51*, 1-30.

5. Clayden, J.; Greeves, N.; Warren, S., *Organic chemistry*, Oxford University Press, Oxford; New York, 2nd ed., 2012.

6. a) Trost, B. M.; Toste, F. D., *J. Am. Chem. Soc.* **1999**, *121*, 4545-4554; b) Trost, B. M.; Verhoeven, T. R., *J. Am. Chem. Soc*. **1980**,*102*, 4730-4743.

7. a) Shimizu, I.; Yamada, T.; Tsuji, J., *Tetrahedron Lett*. **1980**,*21*,3199–3202; b) Tsuda, T.; Chujo, Y.; Nishi, S.; Tawara, K.; Saegusa, T., *J. Am. Chem. Soc.* **1980**, *102*, 6381–6384.

8. a) Tsuji, J., *Tetrahedron*. **1986**, *42*, 4361–4401; b) Weaver, J. D.; Recio III, A.; Grenning, A. J.; Tunge, J. A., *Chem.Rev.* **2011**, *111*, 1846–1913; c) R. Shintani., *Bull. Chem. Soc. Jpn.* **2012**, *85*, 931–939.

9. You, Y.; Li, Q.; Zhang, Y. P.; Zhao, J. Q.; Wang, Z. H.; Yuan, W. C., *Chem. Cat. Chem.* **2022**, *14*, e202101887.

10. Our group previous and current work on the area of Pd DAAA for the synthesis of N-heterocyclic compounds: a) Allen, B. D. W.; Lakeland, C. P.; Harrity, J. P. A., *Chem. Eur. J.* **2016**, *22*, 13000-13003; b) Gao, W.; Han, J.; Greaves, S.; Harrity, J. P., *Org. Lett.* **2023**, *25*, 6555-6559; c) Elhajj, E.A. Confirmation Report, The University of Sheffield, **2022**.

11. Mao, B.; Xu, J.; Shi, W.; Wang, W.; Wu, Y.; Xiao, Y.; Guo, H., *Org. Biomol. Chem.* **2022**, *20*, 4086-4090.

12. Yuan, S.P.; Bao, Q.; Sun, T.J.; Zhao, J.Q.; Wang, Z.H.; You, Y.; Zhang, Y.P.; Zhou, M.Q.; W.C., *Org. Lett*. **2022**, *24*, 8348–8353.

13. Tian, Y.; Duan, M.; Liu, J.; Fu, S.; Dong, K.; Yue, H.; Hou, Y.; Zhao, Y., *Adv. Synth. Catal.* **2021**,*363*, 4461–4474.

14. a) Wang, C.; Li, Y.; Wu, Y.; Wang, Q.; Shi, W.; Yuan, C.; Zhou, L.; Xiao, Y.; Guo, H., *Org. Lett.* **2018**, *20*, 2880−2883; b) Qin, X.; Meng, F.; Wang, M.; Tu, S.; Hao, W.; Wang, J.; Jiang, B., *ACS Catal.* **2021**, *11*, 6951–6959.

15. Chen, B.H.; Liu, S.J.; Zhao, Q.; Hou, Q.; Yuan, J.L.; Zhan, G.; Yang, Q.Q.; Huang, W., *Chem. Commun*. **2023**, *59*, 1233–1236.

16. Bastos, M.M.; Costa, C.C.; Bezerra, T.C.; da Silva, F.D.C.; Boechat, N., *Eur. J. Med. Chem*. **2016**, *108*, 455–465.

17. Mei, G.J.; Bian, C.Y.; Li, G.H; Xu, S.L.; Zheng, W.Q.; Shi, F., *Org. Lett.* **2017**, *19*, 3219–3222.

18. a) Shintani, R.; Moriya, K.; Hayashi, T., *Chem Commun.* **2011**, *47*, 3057-3059; Explanation of the influence of electronic nature of ligand on reaction selectivity: b) Shintani, R.; Tsuji, T.; Park, S.; Hayashi, T., *J. Am. Chem. Soc.* **2010**, *132*, 21, 7508–7513; c) He, Z.; Zajdlik, A.; St. Denis, J.D.; Assem, N.; Yudin, A.K.; *J. Am. Chem. Soc.* **2012**, *134*, 9926–9929.

19. Mao, B.; Liu, H.; Yan, Z.; Xu, Y.; Xu, J.; Wang, W.; Wu, Y.; Guo, H., *Angew. Chem. Int. Ed.* **2020**, *59*, 11316 –11320.

20. Shintani, R.; Murakami, M.; Hayashi, T., *J. AM. CHEM. SOC.* **2007**, *129*, 12356-12357.

21. Shintani, R.; Murakami, M.; Tsuji, T.; Tanno, H; Hayashi, T., *Org. Lett.* **2009**, *11*, 5642–5645.

22. Zheng, Y.; Qin, T.; Zi, W., *J. Am. Chem. Soc.* **2021**, *143*, 1038–1045.

23. Yan, B.; Zuo, L.; Chang, X.; Liu, T.; Cui, M.; Liu, Y.; Sun, H; Chen, W; Guo, W., *Org. Lett.* **2021**, *23*, 351–357.

24. (a) Trost, B. M.; McEachern, E. J.; Toste, F. D., *J. Am. Chem. Soc.* **1998**, *120*, 12702-12703; (b) Trost, B. M.; McEachern, E. J., *J. Am. Chem. Soc.* **1999**, *121*, 8649-8650.

25. (a) Trost, B. M.; Murphy, D. J., *Organometallics* **1985**, *4*, 1143-1145; (b) Hayashi, T.; Ohno, A.; Lu, S.J.; Matsumoto, Y.; Fukuyo, E.; Yanaga, K., *J. Am. Chem. Soc*. **1994**, *116*, 4221-4226.

26. (a) Kudis, S.; Helmchen, G., *Angew. Chem., Int. Ed.* **1998**, *37*, 3047-3050; (b) Evans, D. A.; Campos, K. R.; Tedrow, J. S.; Michael, F. E.; Gagne, M. R., *J. Am. Chem. Soc.* **2000**, *122*, 7905-7920.

27. Trost, B. M.; Xu, J.; Schmidt, T., *J. Am. Chem. Soc.* **2009**, *131*, 18343–18357.

28. Trost, B. M.; Schroeder, G. M., *Chem. Eur. J.* **2005**, *11*, 174.

29. Butts, C. P.; Filali, E.; Lloyd-Jones, G. C.; Norrby, P. O.; Sale, D. A.; Schramm, Y., *J. Am. Chem. Soc.* **2009**, *131*, 9945–9957.

30. James, J.; Guiry, P. J., *ACS Catal.* **2017**, *7*, 1397–1402.

31. Wang, J., Che, C.M., Doyle, M.P. eds., *Transition metal-catalysed carbene transformations,* Wiley-VCH, Weinheim, **2022**.

32. Soam, P.; Kamboj, P.; Tyagi, V., *Asian J. Org. Chem.* **2022**, *11*, e202100570.

33. Green, S. P.; Wheelhouse, K. M.; Payne, A. D.; Hallett, J. P.; Miller, P. W.; Bull, J. A., *Org. Process Res. Dev.* **2020**, *24*, 67–84.

34. Li, M.M.; Wei, Y.; Liu, J.; Chen, H.W.; Lu, L.Q.; Xiao, W.J., *J. Am. Chem. Soc.* **2017**, *139*, 14707–14713.

35. Hao, J.; Xu, Y.; Xu, Z.; Zhang, Z.; Yang, W., *Org. Lett.* **2018**, *20*, 7888–7892.

36. Tucker, Z.D.; Hill, H.M.; Smith, A.L.; Ashfeld, B.L., *Org. Lett.* **2020**, *22*, 6605–6609.

37. Wang, B.C.; Rao, L.; Fang, K.X.; Qu, B.L.; Xiong, F.Y.; Feng, Y.; Tan, Y.; Lu, L.Q.; Xiao, W.J., *Angew. Chem.Int. Ed.* **2023**, *62,* e202301592.

38. Hu, M.; Wu, Z.; Yao, B.; Li, J.; Wu, W.; Jiang, H., *J. Org. Chem.* **2021**, *86*, 11545–11556.

39. Lu, Y.X.; Zhu, L.W.; Lv, T.K.; Chen, B.H., *Tetrahedron Lett.* **2022**, *105*, 154051.

40. Liu, W. B.; He, H.; Dai, L. X.; You, S. L., *Chem. Eur. J.* **2010**, *16*, 7376 – 7379.

41. (a) Toda, Y.; Sakamoto, T.; Komiyama, Y.; Kikuchi, A.; Suga, H., *ACS Catal.* **2017**, 7, 6150–6154; (b) Chen, T.; Gan, L.; Wang, R.; Deng, Y.; Peng, F.; Lautens, M.; Shao, Z. *Angew. Chem., Int. Ed.* **2019**, *58*, 15819– 15823.

42. Xu, S.; Huang, H.; Yan, Z.; Xiao, Q., *Org. Lett.* **2019**, *21*, 10018–10022.

43. a) Li, Y.; Wang, Q.; Yang, X.; Xie, F.; Li, X., *Org. Lett.* **2017**, *19*, 3410–3413; b) Li, X. G.; Sun, M.; Liu, K.; Jin, Q.; Liu, P. N. *Chem. Commun.* **2015**, *51*, 2380-2383.

44. Chen, T.; Ding, Z.; Guan, Y.; Zhang, R.; Yao, J.; Chen, Z., *Chem. Commun*. **2021**, *57*, 2665-2668.

45. a) Taylor, A. P.; Robinson, R. P.; Fobian, Y. M.; Blakemore, D. C.; Jones, L. H.; Fadeyi, O., *Org. Biomol. Chem.* **2016**, *14*, 6611– 6637; b) Vitaku, E.; Smith, D. T.; Njardarson, J. T., *J. Med. Chem*. **2014**, *57*, 10257-10274.

46. a) Cox, C.D.; Coleman, P.J.; Breslin, M.J.; Whitman, D.B.; Garbaccio, R.M.; Fraley, M.E.; Buser, C.A.; Walsh, E.S.; Hamilton, K.; Schaber, M.D.; Lobell, R.B., *J. Med. Chem*. **2008**, *51*, 4239–4252; b) Ibrahim, L.; DiazGranados, N.; Jolkovsky, L.; Brutsche, N.; Luckenbaugh, D.A.; Herring, W.J.; Potter, W.Z.; Zarate Jr, C.A., *Psychopharmacol*. **2012**, *32*, 551– 557; c) Curtis, N.R.; Davies, S.H.; Gray, M.; Leach, S.G.; McKie, R.A.; Vernon, L.E.; Walkington, A.J., *Org. Process Res. Dev.* **2015**, *19*, 865–871.

47. Koudih, R.; Gilbert, G.; Dhilly, M.; Abbas, A.; Barré, L.; Debruyne, D.; Sobrio, F., *Org. Biomol. Chem.*, **2012**, *10*, 8493-8500.

48. a) Kong, W.; Feige, P., de Haro, T.; Nevado, C., *Angew. Chem. Int. Ed.* **2013**, *52*, 2469-2473; b) Hou, C.; Chen, P.; Liu, G., *Angew. Chem. Int. Ed.* **2020**, *59*, 2735-2739.

49. Nairoukh, Z.; Wollenburg, M.; Schlepphorst, C.; Bergander, K.; Glorius, F., *Nature Chemistry* **2019**, *11*, 264-270.

50. Kim, K. Y.; Kim, B. C.; Lee, H. B.; Shin, H., *J. Org. Chem.* **2008**, *73*, 8106–8108.

51. PCT Int. Appl., WO2006113471A2, 2006.

52. Van Hende, E.; Verniest, G.; Thuring, J. W.; Macdonald, G.; Deroose, F.; De Kimpe, N., *Synlett*. **2009**, *11*, 1765-1768.

53. García-Vázquez, V.; Hoteite, L.; Lakeland, C. P.; Watson, D. W.; Harrity, J. P., *Org. Lett.* **2021**, *23*, 2811–2815.

54. Nakamura, M.; Hajra, A.; Endo, K.; Nakamura, E., *Angew. Chem., Int. Ed.* **2005**, *44*, 7248–7251.

55. Wang, W.; Shen, H.; Wan, X.L.; Chen, Q.Y.; Guo, Y., *J. Org. Chem.* **2014**, *79*, 6347–6353.

56. Trost, B. M.; Frederiksen, M. U., *Angew. Chem. Int. Ed.* **2005**,*44*, 308-310.

57. Hoteite, L.; PhD Thesis, The University of Sheffield, DATE.

58. (a) Racys, D.T.; Eastoe, J.; Norrby, P.O.; Grillo, I.; Rogers, S.E.; Lloyd-Jones, G.C., *Chem. Sci.* **2015**, *6*, 5793–5801; (b) Lloyd-Jones, G.C.; Stephen, S.C.; Fairlamb, I.J.; Martorell, A.; Dominguez, B.; Tomlin, P.M.; Murray, M.; Fernandez, J.M.; Jeffery, J.C.; Riis-Johannessen, T.; Guerziz, T., *Pure Appl. Chem.* **2004**, *76*, 589–601.

59. Zhao, H., *ACS Omega*. **2022**, *7*, 9080–9085.

60. (a) Downes, T.D.; Jones, S.P.; Klein, H.F.; Wheldon, M.C.; Atobe, M.; Bond, P.S.; Firth, J.D.; Chan, N.S.; Waddelove, L.; Hubbard, R.E.; Blakemore, D.C., *Chem. Eur. J.* **2020**, *26*, 8969–8975; (b) Kaur, A.; Prakash, R.; Pandey, S.K., *ChemistrySelect* **2018**, *3*, 105-107.

61. Kürti, L.; Czakó, B., *Strategic applications of named reactions in organic synthesis: background and detailed mechanisms,* Elsevier Academic Press, Amsterdam; Boston, 2005.

62. Sun, T. J.; Zhang, Y. P.; You, Y.; Zhao, J. Q.; Yin, J. Q.; Yuan, W. C., *Chem. Synth*. **2023**, *3*, 12.

63. Burtoloso, A. C.; Dias, R. M.; Leonarczyk, I. A., *Eur. J. Org. Chem.* **2013**, 23, 5005–5016.

64. (a) Lehn, J. M.; Wipff, G., *J. Am. Chem. Soc.* 1976, 98, 24, 7498–7505; (b) Bernardi, F.; Csizmadia, I.G.; Mangini, A.; Schlegel, H.B.; Whangbo, M.H.; Wolfe, S., *J. Am. Chem. Soc.* **1975**, *97*, 2209–2218; (c) Streitwieser, A., Jr.; Williams, J.E., *J. Am. Chem. Soc.* **1975**, *97*, 191–192; (d) Hoffmann, R.; Howell, J.M.; Muetterties, E.L., *J. Am. Chem. Soc.* **1972**, *94*, 3047–3058.

65. Unthank, M. G.; Hussain, N.; Aggarwal, V. K., *Angew. Chem. Int. Ed.* **2006**, *45*, 7066–7069.

66. Li, T.R.; Tan, F.; Lu, L.Q.; Wei, Y.; Wang, Y.N.; Liu, Y.Y.; Yang, Q.Q.; Chen, J.R.; Shi, D.Q.; Xiao, W.J., *Nat Commun*. **2014, 5,** 5500**.**

67. Punna, N.; Das, P.; Gouverneur, V.; Shibata, N., *Org. Lett.* **2018**, 20, 1526–1529.

68. Vitaku, E.; Smith, D. T.; Njardarson, J. T. *J. Med. Chem.* **2014**, *57*, 10257-10274.

69. Molinaro, C., Phillips, E.M., Xiang, B., Milczek, E., Shevlin, M., Balsells, J., Ceglia, S., Chen, J., Chen, L., Chen, Q. and Fei, Z., *J. Org. Chem.* **2019**, *84*, 8006-8018.

70. Cai, W.; Wu, J.; Zhang, H.; Jalani, H.B.; Li, G.; Lu, H., *J. Org. Chem.* **2019**, *84*, 10877–10891.

71. Mazón, A.; Nájera, C., *Tetrahedron: Asymmetry* **1997**, *8*, 1855– 1859.

72. Cai, W.; Wu, J.; Zhang, H.; Jalani, H. B.; Li, G.; Lu, H., *J. Org. Chem.* **2019**, *84*, 10877–10891.

73. Trost, B. M. *J. Am. Chem. Soc.* **1966**, *88*, 1587–1588.

74. Müller, P.; Fernandez, D.; Nury, P.; Rossier, J. C., *Helvetica Chimica Acta*. **1999**, *82*, 935-945.

75. Gordillo, P.G.; Aparicio, D.M.; Flores, M.; Mendoza, A.; Orea, L.; Juárez, J.R.; Huelgas, G.; Gnecco, D.; Terán, J.L., *Eur. J. Org. Chem*. **2013**, *25*, 5561–5565.

76. Allen, B. D. W.; PhD Thesis, The University of Sheffield, DATE.

77. (a) Mykhailiuk, P. K.; Afonin, S.; Palamarchuk, G. V.; Shishkin, O. V.; Ulrich, A. S.; Komarov, I. V., *Angew. Chem. Int. Ed.* **2008**, *47*, 5765–5767; (b) Kubyshkin, V.; Afonin, S.; Kara, S.; Budisa, N.; Mykhailiuk, P. K.; Ulrich, A. S., *Org. Biomol. Chem.* **2015**, *13*, 3171-3181.

78. PCT Int. Appl., WO2014025736A1, 2014.

79. Hamashima, Y.; Suzuki, T.; Takano, H.; Shimura, Y.; Tsuchiya, Y.; Moriya, K.-i.; Goto, T.; Sodeoka, M., *Tetrahedron* **2006**, *62*, 7168-7179.

80. K. Pagire, S.; Kumagai, N.; Shibasaki, M., *ACS Catal*. **2021**, *11*, 11597–11606.

81. Dong, J.; Du, H.; Xu, J., *RSC Adv.* **2019**, *9*, 25034–25038.

82. Ushakov, P. Y.; Khatuntseva, E. A.; Nelyubina, Y. V.; Tabolin, A. A.; Ioffe, S. L.; Sukhorukov, A. Y., *Adv. Synth. Catal.* **2019**, *361*, 5322–5327.

83. Pramanik, M. M.; Yuan, F.; Yan, D. M.; Xiao, W. J.; Chen, J. R., *Org. Lett.* **2020**, *22*, 2639–2644.

84. Müller, P.; Fernandez, D.; Nury, P.; Rossier, J. C., *Helv. Chim. Acta.* **1999**, *81*, 935-945.

85. Podrugina, T. A.; Alferova, V. A.; Mironov, A. V.; Matveeva, E. D.; Gleiter, R.; Zefirov, N. S., *Tetrahedron.* **2016**, *72*, 6955–6962.

86. Sardini, S. R.; Lambright, A. L.; Trammel, G. L.; Omer, H. M.; Liu, P.; Brown, M. K., *J. Am. Chem. Soc .***2019**, *141*, 9391–9400.